Facultad de Ciencias
Sede Bogotá

UNIVERSIDAD
NACIONAL
DE COLOMBIA

REVISTA COLOMBIANA DE CIENCIAS QUÍMICO-FARMACÉUTICAS

Universidad Nacional de Colombia
Facultad de Ciencias
Departamento de Farmacia

Rev. Colomb. Cienc. Quím. Farm., vol. 49(3), diciembre 2020

REVISTA COLOMBIANA DE CIENCIAS QUÍMICO-FARMACÉUTICAS
Universidad Nacional de Colombia, Facultad de Ciencias, Departamento de Farmacia.
ISSN 0034-7418, Fax: 3165060, Cra. 30 No. 45-03, Bogotá, D. C., Colombia.
Correo electrónico: *rcciquifa_fcbog@unal.edu.co*
http://www.revistas.unal.edu.co/index.php/rccquifa
http://www.scielo.org.co/scielo.php?script=sci_serial&pid=0034-7418&rep=
https://scholar.google.com/citations?user=TvBT68sAAAAJ&hl=es

Asistente editorial: Anyeli A. Rivera, B. A.
Edición, armada electrónica e impresión: Proceditor Ltda., Bogotá.
Teléfonos: 757 9200. Fax: ext. 102.
Correo electrónico: proceditor@yahoo.es

MISIÓN

La *Revista Colombiana de Ciencias Químico-Farmacéuticas* es un órgano de difusión en el cual se publican investigaciones científicas, comunicaciones técnicas y revisiones temáticas originales en las áreas de las ciencias farmacéuticas (véanse Normas para publicación). La revista está destinada principalmente a químicos farmacéuticos, químicos, ingenieros químicos, médicos cirujanos, médicos veterinarios, y a otros profesionales de las ciencias físicas y naturales, de la ingeniería y de las profesiones sanitarias relacionadas con el uso de medicamentos.

VISIÓN

En pro de la difusión de las investigaciones, los contenidos de la *Revista Colombiana de Ciencias Químico-Farmacéuticas* son de acceso libre, con ello se espera llegar a un número mayor de lectores, propiciando la consolidación de comunidades académicas. Además, se proyecta que los contenidos publicados contribuyan al desarrollo e innovación de las ciencias farmacéuticas.

ÉTICA

La responsabilidad de lo expresado en cada artículo es exclusiva de los autores y no representa ni compromete posiciones de la revista ni del cuerpo editorial. Los contenidos publicados pueden reproducirse siempre que se cite la fuente respectiva. Esta revista sigue los lineamientos del COPE (Committee on Publication Ethics), que pueden ser consultados en *http://publicationethics.org/*

Contenido

Mini-review article / *http://dx.doi.org/10.15446/rcciquifa.v49n3.91247*

Compounds isolated from *Bixa orellana*: evidence-based advances to treat infectious diseases

Roberval Nascimento Moraes Neto[1,2,3], Gabrielle Guedes Coutinho[1,2,3], Aline de Oliveira Rezende[1,2,3], Daniel de Brito Pontes[1], Rayana Larissa Pinheiro Soares Ferreira[1,3], Danilo de Araújo Morais[1,2], Rafaela Pontes Albuquerque[1,3], Lídio Gonçalves Lima-Neto[1], Luís Cláudio Nascimento da Silva[1,2], Cláudia Quintino da Rocha[4], Letícia Machado Gonçalves[5], Luís Ângelo Macedo Santiago[6], Renata Mondego-Oliveira[7], Rafael Cardoso Carvalho[1,3], Eduardo Martins de Sousa[1,2,3]*

[1]Laboratório de Imunologia e Microbiologia das Infecções Respiratórias, Programa de Mestrado em Biologia Microbiana, Universidade CEUMA, Maranhão, Brasil.

[2]Universidade CEUMA, Biomedicina, Maranhão, Brasil.

[3]Programa de Pós-Graduação em Ciências da Saúde, Universidade Federal do Maranhão, Brasil.

[4]Centro de Ciência e Tecnologia, Departamento de Química, Universidade Federal do Maranhão, Brasil.

[5]Programa de Pós-Graduação em Odontologia, Universidade CEUMA, Maranhão, Brasil.

[6]Programa de Pós-Graduação em Biodiversidade e Biotecnologia da Rede Bionorte, Maranhão, Brasil.

[7]Rede Nordeste de Biotecnologia, Programa, Universidade Federal do Maranhão, Maranhão, Brasil.

*Corresponding author: edmsousa@hotmail.com, ORCID: 0000-0002-2506-169X

Received: 4 October 2019

Revised: 10 June 2020

Accepted: 15 June 2020

Summary

Bixa orellana L. is a native plant from Brazil, but it is also present in other tropical countries such as Peru, Colombia, Ecuador, Mexico, Indonesia, India and East Africa. It is popularly known as Urucum in Brazil. This review shows the potential of bioactive compounds derived from *B. orellana* to treat infectious diseases due their antimicrobial and antioxidant properties. This plant is also related as an anti-inflammatory agent for treatment of pulmonary diseases, or even as eye drops for redness. Its leaves are used for treatment of snakebite, diarrhea, gonorrhea, hepatitis, gastritis, diuretic, antipyretic, and for skin disease. This popular knowledge has encouraged the identification of bioactive compounds in this plant. Compounds as β-cryptoxanthin, geranylgeraniol, lutein, procyanidin B2, procyanidin B3, ellagi-

tannin isomer and ellagic acid deoxyhexose have been described. These compounds inhibited pathogenic microorganisms such as bacteria, fungi, protozoan and viruses. In addition, some compounds with anti-inflammatory and antioxidant activities were also described. In this sense, *B. orellana* is a promising source of compounds that could be applied in antimicrobial therapy. This review work may help in the understanding and incentive of new research for antimicrobial discoveries using different *B. orellana* compounds.

Key words: Natural products, antimicrobial activity, human pathogens, phytochemical compounds.

Resumen

Compuestos aislados de *Bixa orellana*: avances basados en la evidencia para tratar enfermedades infecciosas

Bixa orellana L. es una planta nativa de Brasil, pero también está presente en otros países tropicales como Perú, Colombia, Ecuador, México, Indonesia, India y África Oriental. Es conocida popularmente como Urucum en Brasil. Esta revisión expone el potencial de los compuestos bioactivos derivados de *B. orellana* para tratar enfermedades debido a sus propiedades antimicrobianas y antioxidantes. Esta planta también está relacionada como un agente antiinflamatorio para el tratamiento de enfermedades pulmonares e incluso como gotas para los ojos para el enrojecimiento. Sus hojas se utilizan para el tratamiento de la mordedura de serpiente, diarrea, gonorrea, hepatitis, gastritis, diuréticos, antipiréticos y para enfermedades de la piel. Ese conocimiento popular ha fomentado la identificación de compuestos bioactivos en esa planta. Los compuestos β-criptoxantina, geranilgeraniol, luteína, procianidina B2, procianidina B3, isómero elagitanino y ácido elágico desoxihexosa inhibieron microorganismos patógenos como bacterias, hongos, protozoos y virus. En ese sentido, *B. orellana* es una fuente prometedora de compuestos que podrían aplicarse en la terapia antimicrobiana. Este trabajo de revisión puede ayudar a comprender e incentivar nuevas investigaciones para los descubrimientos de antimicrobianos que utilizan diferentes compuestos de *B. orellana*.

Palabras clave: Productos naturales, actividad antimicrobiana, patógenos humanos, compuestos fitoquímicos.

Introduction

Bixa orellana L. is a plant native to Brazil, but it is also present in other tropical countries such as Peru, Columbia, Ecuador, Mexico, Indonesia, India and East Africa [1-3]. It is popularly named as "Urucum" in Brazil and "Annatto in United States of America [2]. *B. orellana* is a tree that has between 3 and 10 meters of height, being more often found of 3 to 5 meters, has the thin trunk with approximately 30 cm of diameter with dark coloration. Its leaves have on average 15 cm in length, with 5 to 10 cm of width, fine with green coloration [4, 5].

The seeds measure around 0.3 to 0.5 cm in length with an approximate diameter of 0.3 cm and often they have a conical shape with an elongated base [5, 6]. Seeds are rich in carotenoids and are source of a natural dye with low toxicity [7, 8]. In this sense, the seeds are considered the most important commercial part of the plant due their industrial applications for production of fabrics and cosmetics [5, 9].

B. orellana is widely used in folk medicine to treat different pathologies. For example, the tea seeds are often used as a laxative, cardiac tonic, hypotensive, expectorant, antimicrobial agent and sometimes used as an anti-inflammatory formulation for treatment of pulmonary diseases such as bronchitis. Products derived from seeds is also used as eye drops for redness [2]. Its leaves are used for treatment of snakebite [10], diarrhea, gonorrhea, [11], hepatitis [2], gastritis [12], diuretic, antipyretic, and for skin problems [2]. These reports have encouraged other studies to provide scientific evidences to the ethnopharmacological knowledge and also in order to identify and isolate the active(s) substance(s).

Herein, we provided a review about the compounds with antimicrobial activity obtained from *B. orellana*. The articles were searched on Pubmed database (1998 to March 2019) scientific articles. Search terms were: '*B. orellana*', 'antimicrobial activity' and 'antibacterial'. An exhaustive literature search was performed, but only urucum extracts and isolated compounds with positive results were included. This review was made due to the recent increase in published articles regarding *B. orellana*, as well as the increase in the number of publications in this regard.

Compounds of seed with antimicrobial activity

The phytochemical compounds of the *B. orellana* seeds were described in the literature by Galindo-Cuspinera and Rankin (2005) [13]. After the discovery of these compounds they were studied for their antimicrobial activity [14-18]. The compounds of *B. orellana* seeds that exhibit some antimicrobial activity according to the literature are described below. The chemical structure of the compounds can be visualized in table 1.

Table 1. Antimicrobial activity of phytochemical compounds isolated from the seeds and leaves from *B. orellana* extract.

Part of the plant	Compound	Molecular structure	Antimicrobial activity	Reference
Seeds	Cryptoxanthin	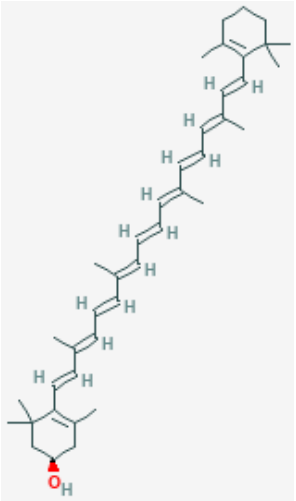	*Staphylococcus aureus, Staphylococcus epidermidis, Salmonella typhimurium, Proteus vulgaris*	Findlay and Patil [15]
	Geranylgeraniol	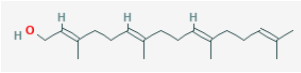	*Mycobacterium tuberculosis*	Vik *et al.* [16]
			Leishmania amazonensis	Lopes *et al.* [22] Vik *et al.* [16]
			Mycobacterium tuberculosis	Montero *et al.* [29]
	Lutein	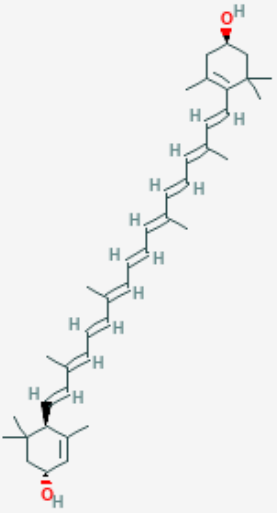	*Listeria monocytogenes,*	Liu *et al.* [17]
			Aspergillus niger, Trichophyton mentagrophytes, Candida albicans	Ragasa *et al.* [33]

(*Continued*)

Table 1. Antimicrobial activity of phytochemical compounds isolated from the seeds and leaves from *B. orellana* extract.

Part of the plant	Compound	Molecular structure	Antimicrobial activity	Reference
Leaves	Procyanidin B2	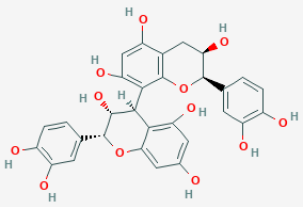	*Porphyromonas gingivalis*	Schmuch *et al.* [30]
			Influenza virus	Yang *et al.* [34] Lik *et al.* []
	Procyanidin B3	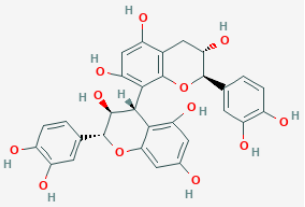	*Staphylococcus aureus*	Wang *et al.* [] Liu *et al.* [17]
	Ellagitannin isomer	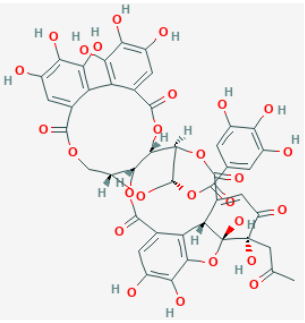	*Escherichia coli*	Voravuthikunchai *et al.* [31]
	Ellagic acid deoxyhexose	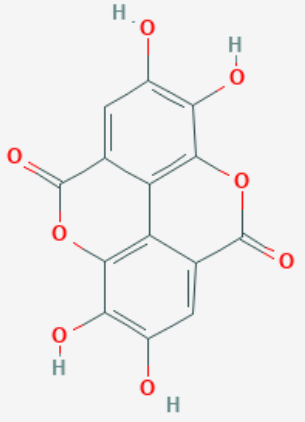	*Escherichia coli, Staphylococcus aureus, Pseudomonas aeruginosa*	Raga *et al.* [32]

Compounds of leaves with antimicrobial activity

The phytochemical profile of the leaves of *B. Orellana* was evaluated and it presented the following compounds: Procyanidin B-2, Procyanidin B-3, Granatin B, Neostrictinin, Ellagirannin isomer, kaempferol-3-O-β-D-6-(p-coumaroyl) glucopyranoside, ellagic acid glucoside, kaempferol-3-O-D-glucoside, ellagic acid deoxyhexose [19]. The following are listed which of these compounds present antimicrobial activity according to the literature. The chemical structure of the compounds can be visualized in table 1.

Activity against protozoan

Crude extract

Leishmaniasis is a neglected tropical disease caused by *Leishmania* protozoa. There is currently no vaccine against leishmaniasis, and chemotherapy remains the only effective control. Some research on plants has shown a successful approach to obtain new antileishmanial alternatives. Herein, the *in vitro* and *in vivo* effects of the essential oil from *B. orellana* seeds against *Leishmania amazonensis* were evaluated. The oil showed activity against intracellular amastigote form (IC50 = 8.5 μg/mL), while the cytotoxic concentration was sevenfold higher for the host cells. The ability of Bixa oil to control disease progression of established cutaneous leishmaniasis in BALB/c mice was demonstrated, after a treatment with 30 mg/kg by intraperitoneal administration over 14 days [20]. Other study performed with *Leishmania amazonenses* was demonstrated similar results[21].

Geranylgeraniol

Lopes *et al*., (2012) demonstrated the activity of geranylgeraniol, the major bioactive constituent from seeds of *B. orellana*, against *L. amazonensis*. Geranylgeraniol was identified through (1)H and (13)C nuclear magnetic resonance imaging and DEPT. The compound inhibited the promastigote and intracellular amastigote forms, with IC (50) of 11 ± 1.0 and 17.5 ± 0.7 μg/mL, respectively. This compound was also more toxic to parasites than to macrophages and did not cause lysis in human blood cells [22].

Activity against bacteria

Several studies provide scientific evidences about the action of *B. orellana* crude extracts against different bacteria. These extracts were obtained from both seeds [2, 23-26] and leaves [27], against bacteria of different species. Among the species of bacteria described in the literature are: methicillin-resistant *Staphylococcus aureus* (MRSA) [23, 25, 27]; *Bacillus cereus* [24,25]*; Escherichia coli* [24,27]; *Streptococcus thermophilus*, *Lactobacillus*

casei subsp. *casei*, *Lactococcus lactis*, *Paenibacillus polymyxa*; *Clostridium perfringens* [25]; *Bacillus subtilis*; *Streptococcus pyogenes*; *Salmonella typhi*; *Pseudomonas aeroginosa* [27]; *Mycobacterium abscessus* subsp. *massiliense* [19].

Crude extract

As mentioned above, the seeds of *B. orellana* is used to prepare tea and infusions for treatment of infections due their antimicrobial and anti-inflammatory activities [2]. In this sense, crude extracts and essential oils were targets of some studies to prove their pharmacological potential. The hydroalcoholic extract of *B. orellana* seeds was able to inhibit the growth of bacteria: *S. thermophilus*, *Lactobacillus casei* subsp. *casei*, *L. lactis*, and *P. polymyxa,* microorganisms of significance in food fermentation, food preservation, and human health [25].

Another research has also demonstrated the activity of the essential oil of *B. orellana* against other species of pathogenic bacteria. In this work the MIC of the hidroalcolic extract was evaluated, the different bacteria and their respective MICs are listed below: *B. cereus* (MIC: 0.08 μg/mL); *C. perfringens* (MIC: 0.31 μg/mL) [24]. In other study carried out in Nigeria, the antimicrobial activity of extract of *B. orellana* seeds and Piper Guinean fruit extract was evaluated, demonstrating antimicrobial activity against *Pseudomonas aeruginosa* UCH 655 strain at 5 mg/mL [26].

Research developed *in vitro* evaluating the antimicrobial activity of medicinal plants used in Colombia, showed the activity of the hydroalcoholic extract of seeds of *B. orellana* against bacteria causing non-nosocomial infections. These results demonstrate a minimum inhibitory concentration (MIC) was 0.8 μg/mL against *E. coli* and also a MIC was 0.2 μg/mL against *B. cereus*, which were lower than the values found for other plants tested in this study [24].

The high antimicrobial potential of extracts obtained from *B. orellana* promoted other research in order to endorse the biotechnological applications of them. An interesting work demonstrated *B. orellana* seeds powder could maintain the physicochemical properties of pork patties. This effect was related to the antioxidant and antimicrobial abilities of *B. orellana* seeds. The authors reported that the meat exposed to *B. orellana* seeds powder lower microbial counts for *Enterobacteriaceae* than control group. Therefore, *B. orellana* seed powder might be a good source of natural antioxidants for the production of meat products [28].

In other study, with tocotrienols from hydroalcoholic extract of *B. orellana* seeds was shown as an effective agent against MRSA in experimental infection model using BALB/c mice. In this work the bacteria were inoculated by subcutaneous injection, at

a concentration of $5x10^6$ CFU per animal. The results demonstrate a significant delay in the growth of MRSA in mice treated with *B. orellana* seed extract in contrast to the infected and untreated group [23]. The authors also reported the extract improved the *in vivo* activity of daptomycin in the treatment of MRSA infection [23].

The hydroalcoholic extract (BoHE) and the ethyl acetate fraction (BoEA) from *B. orellana* leaves also showed activity against pathogenic bacteria [19, 27]. The action of leaves extracts against infection by fast growing mycobacteria (RGM), specifically *Mycobacterium abscessus* subsp. *massiliense*. The MIC of the extract against *M. abscessus* was obtained resulting in 2.34 mg/mL for BoHE and 0.39 mg/mL for BoEA. When comparing the cytotoxicity also evaluated in this work, the result of the Selective Index of 19.8 for BoEA and 3.2 for BoHE was obtained. This shows an important antimicrobial activity for this mycobacterium [19].

Other studies using the ethanolic extract of the leaves of *B. orellana* were carried out with the purpose of evaluating the antimicrobial activity through observation of the colonies growth. These works demonstrated good activity of the extract against the bacteria: *B. subtilis*, *S. aureus*, *S. pyogenes*, *S. tythi*, *P. aeruginosa* and *E. coli* [27].

B-cryptoxanthin

Cryptoxanthin is not a unique compound of *B. orellana* seeds, it can also be found in other plant species, such as *Navicula delognei L.* [15]. The main activities of β-cryptoxanthin as described in figure 1a. The evaluations of the antimicrobial activity of cryptoxanthin from *N. delognei* were performed by the same author, and demonstrated an important antibacterial activity against *Staphylococcus aureus*, *Staphylococcus epidermidis*, *Salmonella typhimurium*, and *Proteus vulgaris* through the evaluation of zone of inhibition [15].

Geranylgeraniol

Geranylgeraniol is a compound of the terpenes family. This was evaluated for its antimicrobial activity against *Mycobacterium tuberculosis in vitro*. For this, their capacity to inhibit pathogen growth was evaluated, which resulted in a MIC of 1.56 μg/mL, showing its capacity as a growth inhibitor of *M. tuberculosis* [16]. Other studies shown that geranylgeraniol regulates negatively caspase-1 implication in the Th1 response against *Mycobacterium tuberculosis* [29].

Lutein

Lutein is a small natural molecule present in fruits and vegetables that demonstrates good activity as an inhibitor of listeriolysin-O-oligomerization (LLO), an important

virulence factor of the bacteria *Listeria monocytogenes*. It is *in vitro* and *in vivo* activity against *L. monocytogenes* bacteria was evaluated. The results demonstrate a significant reduction in bacterial growth as well as an important specificity for the bacteria, showing no toxicity to BALB/c mice [17].

Procyanidin B2

Procyanidin B2 is not a compost exclusive of *B. orellana* leaves, it is also present in other plant species, such as *Rumex acetosa* L. The antimicrobial activity of procyanidin B2 of *R. acetosa* was evaluated against *Porphyromonas gingivalis*, an important pathogen causing gingivitis as well as other systemic infections. The results demonstrate a bacteriostatic effect against the colonization of this bacterium, as well as the loss of the adhesion capacity of the bacteria in vitro [30].

Procyanidin B3

Procyanidin B3 is not a compound exclusive of *B. orellana* leaves. It is also present in the flowers of *Rhododendron formosanum*. Its bactericidal activity was evaluated against *S. aureus* infections. Their results showed a MIC of 4 μg/mL, in addition to an important antioxidant activity [17].

Ellagitannin isomer

Ellagitannin isomer is a compound present in several plant species, among them *B. orellana* leaves [19] and *Quercus infectoria* [31]. The antimicrobial activity of ellagitannin isomer was evaluated in mice infected with *E. coli*. The results of this study demonstrate an important reduction of the microbial load in comparison with the control group, as well as activity as renal protector [31].

Ellagic acid deoxyhexose

Ellagic acid deoxyhexose is a sesquiterpenes present in leaves of *B. orellana* that has activities of gastric, analgesic, hypoglycemic and antimicrobial protector, being proven to inhibit the growth of *E. coli*; *S. aureus* and *P. aeruginosa* [32].

Activity against fungi

Lutein

Blumea balsamifera leaves similar to *B. orellana* seeds also have Lutein in their composition. In evaluating the antifungal activity of *B. balsamifera* compounds, the fungistatic action of lutein resulted in low growth of *Aspergillus niger, Trichophyton mentagrophytes,* and *Candida albicans* [33].

Activity against viruses

Procyanidin B2

Influenza poses a particular risk of severe outcomes in the elderly, the very young and those with underlying diseases. Tea polyphenols are the natural phenolic compounds in teas, and principally consist of catechins, proanthocyanidins, flavonols, and the aflavins, which antiviral activities have been reported recently. Some studies shown a significantly damage in viral structures and antiviral activity of procyanidin B2 [34, 35].

Lutein

Despite the availability of an effective vaccine, the hepatitis B virus (HBV) infection and its treatment remains one of the foremost public health problems in the world. The anti-HBV activity of lutein *in vitro* was investigated. The antiviral activity of lutein was examined by detecting the levels of HBsAg, HBeAg and extracellular HBV DNA in stable HBV-producing human hepatoblastoma HepG2 2.2.15 cells. It was found that lutein effectively suppressed the secretion of HBsAg from HepG2 2.2.15 cells in a dose-dependent manner, and it also suppressed the amount of extracellular HBV DNA [36].

Anti-inflammatory and immunomodulation activity

Crude extract

Some studies shown an important anti-inflammatory activity against acute and chronic inflammations in rats. Acute inflammatory reactions induced in rats paws by carrageenan, histamine, serotonin, and bradykinin were all inhibited by the oral administration of 50 and 150 mg/Kg of *B. orellana* leaves extract. In the same study chronic inflammation was induced and treated with *B. orellana* extracts when administered 150 mg/Kg of extract [25]. It was confirmed four years later by Keong *et al.* [37], in their research was evaluated the anti-inflammatory effects of *B. orellana* in rats with edema induced by bradykynin. In that study *Bixa* leaf extract shown a significantly suppressed the inflammatory markers. The extract also decreased nitric oxide production, indicating that the anti-inflammatory effect may be related to a reduction in reactive oxygen species [37, 38]. The antioxidant and free radical scavenging activities of extracts of *Bixa* leaves were also demonstrated by several authors [38, 39].

Yong *et al.* evaluated the anti-inflammatory activities of aqueous extract of *B. orellana* leaves and its possible mechanisms in animal models. The anti-inflamatory activity of the extract was evaluated using serotonin-induced rat edema, increased peritoneal vascular permeability, and evaluation of leukocyte infiltrations. Was evaluated the nitric oxide (NO) production, as well the vascular growth endothelial growth factor

(VEGF). That research showed the anti-inflammatory activity of *B. orellana* extract, indicated by the suppression of increased vascular permeability and leukocyte infiltration. The authors concluded the inhibition of these inflammatory events are probably mediated via inhibition of NO and VEGF formation and release [40]

B-cryptoxanthin

The anti-inflammatory activity from cryptoxanthin was evaluated in mice with nonalcoholic steatohepatitis. That study evaluated the anti-inflammatory effects on lipopolysaccharide (LPS)-induced inflammation in mice. The results showed that significantly inhibited LPS-induced decreases in cell viability and in the percentage of apoptotic cells. The same study shown an up-regulation of tumor necrosis factor-α (TNF-α), interleukin-10 (IL-10), interleukin-6 (IL-6) and interleukin-1β (IL-1β) in Sertoli cells, and down-regulation of NF-kB resulting in suppression of inflammation [17].

Other studies shown an immunomodulation action, being a significantly increase IFN-g production and NK cytotoxic activity in human KHTG-1 natural killers (NK) cells [41] and KHYG-1 NK cells [42]. Studies performed in rabbits shown an important increase to $CD4^+$ lymphocytes count and humoral immunity [43].

The antioxidant activity of β-cryptoxanthin was evaluated in non-alcoholic fatty liver disease by several authors [44-47]. That's studies shown an important reduction in lipogenesis β-oxidation [48-50], and reduction in lipid peroxidation [48, 51] showing a protective response in steatohepatitis and cirrhosis. In addition that compound shown an influence in macrophage polarization, increasing the polarization for macrophages M2, and reducing the polarization for macrophages M1 [9]. For more information on the antioxidant activity of β-cryptoxanthin we recommended the review of Ni *et al.* [17].

Geranylgeraniol

The anti-inflammatory activity of geranylgeraniol was evaluated by Giriwono *et al*. In that study rats were fed a diet supplemented with or without geranylgeraniol for 10 days. Then, these animals were submitted to intraperitoneal injection of 0.5 mg/Kg LPS or vehicle. The results shown that animals with supplementation demonstrated a significantly suppression of NF-kB in liver. The authors concluded the supplementation with geranylgeraniol was sufficient to inhibit inflammation in liver [52, 53].

In other study, geranylgeraniol isolated from fruit oil of *Pterodon pubescens* was evaluated in rabbits. That shown a significantly inhibition of platelets aggregation induced by U-46619 and thrombin, associated with the fruit oil and geranylgeraniol suppression of prostaglandin E_2, and thromboxane A_2. That demonstrate the geranylgeraniol was involved in the metabolization by inhibiting the cyclooxygenase enzyme [54]. In a

study performed by Silva *et al.*, the evaluation of efficacy of encapsulated geranylgeraniol shown an important antioxidant activity [55]. The main activities of geranylgeraniol are described in figure 1b.

Lutein

In a study performed by Karakurt *et al.*, rats with induced retinal injury was submitted by treatment with lutein. In that study was observed a statistical significantly higher ($p<0.001$) reduction of IL-1β and TNF-α levels in animals submitted by lutein, in addition was observed the antioxidant activity [56, 57]. Some studies shown an anti-oxidant activity[58-60]. Other several studies shown that lutein was an important anti-inflammatory activity [58, 60-62].

Tan *et al.* investigated the effect of lutein against severe traumatic brain injury (STBI) and examined the mechanism of this protective effect. In that study was observed that a treatment with lutein effectively down-regulated the expression of NF-κB p65 and cyclooxygenase-2 (COX-2), intercellular adhesion molecule (ICAM)-1 protein, and upregulated nuclear factor erythroid 2 like 2 (Nrf-2) and endothelin-1 protein levels in STBI rats. These findings demonstrated that lutein protects against STBI, it has anti-inflammation and antioxidative effects and alters ICAM-1/Nrf-2 expression, which may be a novel therapeutic for STBI the clinic [18].

Other study evaluated the effects of lutein and conjugated linoleic acid (CLA) on growth performance and immune response of broiler chickens were evaluated in the presence and absence of Salmonella lipopolysaccharide (LPS) immune challenge. That study shown that CLA decreased broiler chicken growth performance, but lutein could prevent this negative effect (depending on CLA dose). Lutein had an anti-inflammatory effect, and a 2% CLA supplementation improved the humoral immune response [63]. The main activities of geranylgeraniol were described in figure 1c.

Procyanidin B2

Procyanidin B2 shown a significantly reduction in NF-kB and decrease of TNF-α, IL-6 and IL-10. Other studies shown a significantly antioxidant activity [64, 65].

Conclusion

Bixa orellana is a plant present in Latin America, mainly in tropical regions, with important antimicrobial capacity. It possesses activity against both gram-negative and gram-positive bacteria. In addition, to activity against BAAR bacteria such as *M. tuberculosis, M. abscessus* and human pathogenic bacteria. Therefore, it is an important

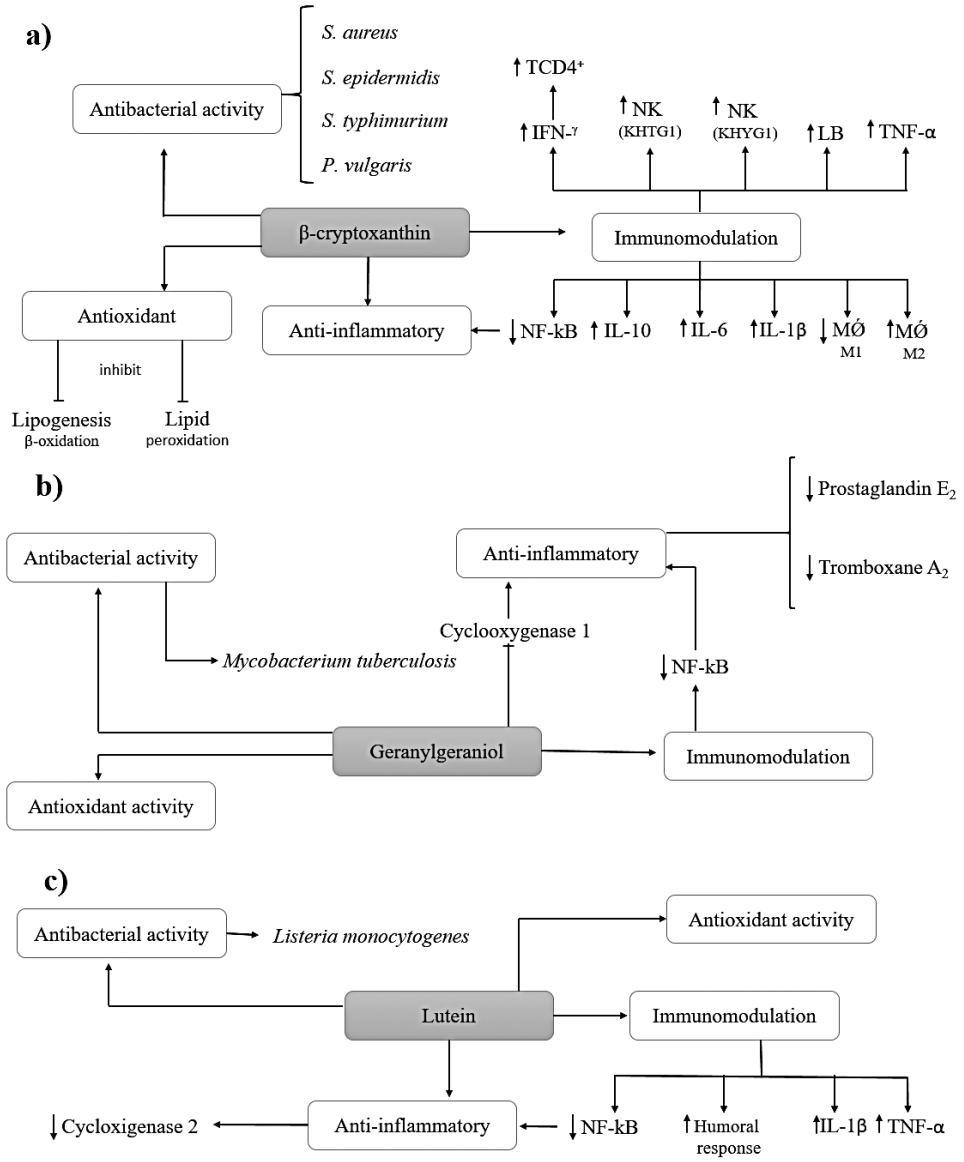

Figure 1. Compounds pharmacological activities: a) β-cryptoxanthin; b) geranylgeraniol; c) lutein.

target of future studies, since it can represent an important advance in the treatment of bacterial infections. This becomes important as it opens up the possibility of treating bacteria resistant to commercial antibiotics. We believe that this review work may help in the understanding and incentive of new research for antimicrobial discoveries using different *B. orellana* compounds. Facilitating scientific development.

Data availability

The data used to build graphs and figures to support the findings of this study are available from the corresponding author upon request.

Authors' contributions

Eduardo Martins de Sousa, Rafael Cardoso Carvalho, Cláudia Quintino da Rocha, Letícia Gonçalves Machado, Luís Cláudio Nascimento da Silva, and Lídio Gonçalves Lima Neto conceptualized and designed the study.

Roberval Nascimento Moraes Neto, Gabrielle Guedes Coutinho, Aline de Oliveira Rezende, Daniel de Brito Pontes, Rayana Larissa Pinheiro Soares Ferreira, Danilo de Araújo Morais, Rafaela Pontes Albuquerque, Lídio Gonçalves Lima-Neto, Cláudia Quintino da Rocha, Letícia Machado Gonçalves, Luís Cláudio Nascimento da Silva, Luís Ângelo Macedo Santiago, Renata Mondego-Oliveira, Rafael Cardoso Carvalho, and Eduardo Martins de Sousa wrote the manuscript.

Disclosure statement

No potential conflict of interest was reported by the authors.

Acknowledgments

This work received financial support from FAPEMA (BEPP-02529/18; CIDADES-05255/18; UNIVERSAL-01468/16; UNIVERSAL-01032/19) and Uni-CEUMA.

References

1. M.E.A. Elias, G. Schroth, J.L.V. Macedo, M.S.S. Mota, S.A. D'Angelo, Mineral nutrition, growth and yields of annatto trees (*Bixa orellana*) in agroforestry on an Amazonian Ferralsol, *Expl. Agric.*, **38**(3), 277-289 (2002).

2. D. de Araujo-Vilar, M.S. de Araujo-Vilar, T.F.A. de Lima e Moura, et al., Traditional uses, chemical constituents, and biological activities of *Bixa orellana* L.: a review, *Sci. World J.,* **2014**, 857292 (2014).

3. A.L. Prada, A.P.R. Bitencourt, J.R.R. Amado, R.A.S. Cruz, J.C.T. Carvalho, C.P. Fernandes, Development and characterization of *Cassia grandis* and *Bixa orellana* nanoformulations, *Curr. Top. Med. Chem.*, **16**(18), 2057-2065 (2016).

4. J. Revilla, *Plantas da Amazônia: Oportunidades Econômicas e Sustentáveis*, Programa de Desenvolvimento Empresarial e Tecnológico, Manaus, 2001.

5. D. Raddatz-Mota, L.J. Perez-Flores, F. Carrari, J.A. Mendoza-Espinoza, F. de Leon-Sanchez, L.L. Pinzon-Lopez, G. Godoy-Hernandez, F. Rivera-Cabrera, Achiote (*Bixa orellana* L.): a natural source of pigment and vitamin E, *J. Food Sci. Technol.*, **54**(6), 1729-1741 (2017).

6. F. Oliveira, G. Akisue, M.K. Akisue, *Farmacognosia*, Atheneu, São Paulo, 1991.

7. A.R.R. Bastos, J.G. Carvalho, R.P. Assis, A.B.C. Filho, Marcha de absorção de nutrientes em urucum (*Bixa orellana* L.) tipo cultivado piave vermelha em fase de viveiro, *Cerne*, **5**, 76-85 (1999).

8. G. Dequigiovanni, S.L.F. Ramos, A. Alves-Pereira, E.G. Fabri, D. Picanco-Rodrigues, C.R. Clement, P. Gepts, E.A. Veasey, Highly structured genetic diversity of *Bixa orellana* var. *urucurana*, the wild ancestor of annatto, in Brazilian Amazonia, *PLoS One*, **13**(6), e0198593 (2018).

9. R.P. Louro, L.J. Santiago, Development of carotenoid storage cells in *Bixa orellana* L. seed arils, *Protoplasma*, **253**(1), 77-86 (2016).

10. R. Otero, R. Fonnegra, S.L. Jimenez, *et al.*, Snakebites and ethnobotany in the northwest region of Colombia: Part I: traditional use of plants, *J. Ethnopharmacol.*, **71**(3), 493-504 (2000).

11. A. Caceres, H. Menendez, E. Mendez, *et al.*, Antigonorrhoeal activity of plants used in Guatemala for the treatment of sexually transmitted diseases, *J. Ethnopharmacol.*, **48**(2), 85-88 (1995).

12. D.L. Lentz, A.M. Clark, C.D. Hufford, *et al.*, Antimicrobial properties of Honduran medicinal plants, *J. Ethnopharmacol.*, **63**(3), 253-263 (1998).

13. V. Galindo-Cuspinera, S.A. Rankin, Bioautography and chemical characterization of antimicrobial compound(s) in commercial water-soluble annatto extracts, *J. Agric. Food Chem.*, **53**(7), 2524-2529 (2005).

14. S.J. Martin, S.E. Evan, Comparative modulation of levels of oxidative stress in the liver of anti-tuberculosis drug treated Wistar rats by vitamin B12, beta-carotene, and *Spirulina fusiformis*: Role of NF-kB, iNOS, IL-6, and IL-10, *J. Cell. Biochem.*, **118**(11), 3825-3833 (2017).

15. J.A. Findlay, A.D. Patil, Antibacterial constituents of the diatom *Navicula delognei*, *J. Nat. Prod.*, **47**(5), 815-818 (1984).

16. A. Vik, A. James, L.L. Gundersen, Screening of terpenes and derivatives for antimycobacterial activity: identification of geranylgeraniol and geranylgeranyl acetate as potent inhibitors of *Mycobacterium tuberculosis in vitro*, *Planta Med.*, **73**(13), 1410-1412 (2007).

17. B. Liu, Z. Teng, J. Wang, G. Lu, X. Deng, L. Li, Inhibition of listeriolysin O oligomerization by lutein prevents *Listeria monocytogenes* infection, *Fitoterapia*, **116**, 45-50 (2017).

18. B. Gökalsin, B. Aksoydan, B. Erman, N.C. Sesal, Reducing virulence and biofilm of *Pseudomonas aeruginosa* by potential quorum sensing inhibitor carotenoid: Zeaxanthin, *Microb. Ecol.*, **74**(2), 466-473 (2017).

19. J. Lima-Viana, A. Zagmignan, L.F. Lima-Lobato, *et al.*, Hydroalcoholic extract and ethyl acetate fraction of *Bixa orellana* leaves decrease the inflammatory response to *Mycobacterium abscessus* Subsp. massiliense, *Evid. Based Complement. Alternat. Med.*, **2018**, 6091934 (2018).

20. L. Monzote, M. Garcia, R. Scull, A. Cuellar, W.N. Setzer, Antileishmanial activity of the essential oil from *Bixa orellana*, *Phytother. Res.*, **28**(5), 753-758 (2014).

21. M. Garcia, L. Monzote, A.M. Montalvo-Alvarez, R. Scull-Lizama, Effect of *Bixa orellana* against *Leishmania amazonensis*, *Forschende Komplementärmedizin*, **18**(6), 351-353 (2011).

22. M.V. Lopes, V.C. Desoti, O. Caleare-Ade, T. Ueda-Nakamura, S.O. Silva, C.V. Nakamura, Mitochondria superoxide anion production contributes to geranylgeraniol-induced death in *Leishmania amazonensis*, *Evid. Based Complement. Alternat. Med.*, **2012**, 298320 (2012).

23. E. Pierpaoli, F. Orlando, O. Cirioni, O. Simonetti, A. Giacometti, M. Provinciali, Supplementation with tocotrienols from *Bixa orellana* improves the *in vivo* efficacy of daptomycin against methicillin-resistant *Staphylococcus aureus* in a mouse model of infected wound, *Phytomedicine*, **36**, 50-53 (2017).

24. J.J. Rojas, V.J. Ochoa, S.A. Ocampo, J.F. Munoz, Screening for antimicrobial activity of ten medicinal plants used in Colombian folkloric medicine: a possible alternative in the treatment of non-nosocomial infections, *BMC Complement. Altern. Med.*, **2006,** 6, 2 (2006).

25. V. Galindo-Cuspinera, D.C. Westhoff, S.A. Rankin, Antimicrobial properties of commercial annatto extracts against selected pathogenic, lactic acid, and spoilage microorganisms, *J. Food Prot.*, **66**(6), 1074-1078 (2003).

26. O.A. Oyedeji, B.A. Adeniyi, O. Ajayi, W.A. Konig, Essential oil composition of *Piper guineense* and its antimicrobial activity. Another chemotype from Nigeria, *Phytother. Res.*, **19**(4), 362-364 (2005).

27. T.C. Fleischer, E.P. Ameade, M.L. Mensah, I.K. Sawer, Antimicrobial activity of the leaves and seeds of *Bixa orellana*, *Fitoterapia*, **74**(1-2), 136-138 (2003).

28. T.V. Cuong, K.B. Chin, Effects of annatto (*Bixa orellana* L.) seeds powder on physicochemical properties, antioxidant and antimicrobial activities of pork patties during refrigerated storage, *Korean J. Food Sci. Anim. Resour.*, **36**(4), 476-486 (2016).

29. M.T. Montero, J. Matilla, E. Gomez-Mampaso, M.A. Lasuncion, Geranylgeraniol regulates negatively caspase-1 autoprocessing: implication in the Th1 response against *Mycobacterium tuberculosis*, *J. Immunol.*, **173**(8), 4936-4944 (2004).

30. J. Schmuch, B. Beckert, S. Brandt, G. Lohr, F. Hermann, T.J. Schmidt, T. Beikler, A. Hensel, Extract from *Rumex acetosa* L. for prophylaxis of periodontitis: inhibition of bacterial *in vitro* adhesion and of gingipains of *Porphyromonas gingivalis* by epicatechin-3-O-(4b°8)-epicatechin-3-O-gallate (procyanidin-B2-di-gallate), *PLoS One*, **10**(3), e0120130 (2015).

31. S.P. Voravuthikunchai, S. Suwalak, W. Mitranan, Ellagitannin from *Quercus infectoria* eradicates intestinal colonization and prevents renal injuries in mice infected with *Escherichia coli* O157:H7, *J. Med. Microbiol.*, **61**(10), 1366-1372 (2012).

32. D.D. Raga, R.A. Espiritu, C.C. Shen, C.Y. Ragasa, A bioactive sesquiterpene from *Bixa orellana*, *J. Nat. Med.*, **65**(1), 206-211 (2011).

33. C.Y. Ragasa, A.L. Co, J.A. Rideout, Antifungal metabolites from *Blumea balsamifera*, *Nat. Prod. Res.*, **19**(3), 231-237 (2005).

34. Z.F. Yang, L.P. Bai, W.B. Huang, X.Z. Li, S.S. Zhao, N.S. Zhong, Z.H. Jiang, Comparison of *in vitro* antiviral activity of tea polyphenols against influenza A and B viruses and structure-activity relationship analysis, *Fitoterapia*, **93**, 47-53 (2014).

35. D. Liu, J. Deng, S. Joshi, P. Liu, C. Zhang, Y. Yu, R. Zhang, D. Fan, H. Yang, D.H. D'Souza, Monomeric catechin and dimeric procyanidin B2 against human norovirus surrogates and their physicochemical interactions, *Food Microbiol.*, **76**, 346-353 (2018).

36. R. Pang, J.Y. Tao, S.L. Zhang, *et al.*, *In vitro* antiviral activity of lutein against hepatitis B virus, *Phytother. Res.*, **24**(11), 1627-1630 (2010).

37. Y. Yoke-Keong, A.K. Arifah, S. Sukardi, A.H. Roslida, M.N. Somchit, A. Zuraini, *Bixa orellana* leaves extract inhibits bradykinin-induced inflammation through suppression of nitric oxide production, *Med. Princ. Pract.*, **20**(2), 142-146 (2011).

38. S.J. Stohs, Safety and efficacy of *Bixa orellana* (achiote, annatto) leaf extracts, *Phytother. Res.*, **28**(7), 956-960 (2014).

39. O.A. Conrad, I.P. Dike, U. Agbara, *In vivo* antioxidant assessment of two anti-malarial plants-*Allamamda cathartica* and *Bixa orellana*, *Asian Pac. J. Trop. Biomed.*, **3**(5), 388-394 (2013).

40. Y.K. Yong, Z.A. Zakaria, A.A. Kadir, M.N. Somchit, G.E. Cheng-Lian, Z. Ahmad, Chemical constituents and antihistamine activity of *Bixa orellana* leaf extract, *BMC Complement. Altern. Med.*, **13**, 32 (2013).

41. K. Nagahama, N. Eto, T. Shimojo, T. Kondoh, K. Nakahara, Y. Sakakibara, K. Fukui, M. Suiko, Effect of kumquat (*Fortunella crassifolia*) pericarp on natural killer cell activity *in vitro* and *in vivo*, *Biosci. Biotechnol. Biochem.*, **79**(8), 1327-1336 (2015).

42. R. Terao, A. Murata, K. Sugamoto, *et al.*, Immunostimulatory effect of kumquat (*Fortunella crassifolia*) and its constituents, beta-cryptoxanthin and R-limonene, *Food Funct.*, **10**(1), 38-48 (2019).

43. S. Ghodratizadeh, G. Kanbak, M. Beyramzadeh, Z.G. Dikmen, S. Memarzadeh, R. Habibian, Effect of carotenoid beta-cryptoxanthin on cellular and humoral immune response in rabbit, *Vet. Res. Commun.*, **38**(1), 59-62 (2014).

44. Y. Ni, F. Zhuge, M. Nagashimada, T. Ota, Novel action of carotenoids on non-alcoholic fatty liver disease: macrophage polarization and liver homeostasis, *Nutrients*, **8**(7), 391 (2016).

45. K. Unno, S. Noda, Y. Kawasaki, K. Iguchi, H. Yamada, Possible gender difference in anti-stress effect of beta-cryptoxanthin, *Yakugaku Zasshi*, **136**(9), 1255-1262 (2016).

46. K. Unno, S. Noda, H. Nii, Y. Kawasaki, K. Iguchi, H. Yamada, Anti-stress effect of beta-cryptoxanthin in satsuma mandarin orange on females, *Biol. Pharm. Bull.*, **42**(8), 1402-1408 (2019).

47. K. Unno, M. Sugiura, K. Ogawa, *et al.*, Beta-cryptoxanthin, plentiful in Japanese mandarin orange, prevents age-related cognitive dysfunction and oxidative damage in senescence-accelerated mouse brain, *Biol. Pharm. Bull.*, **34**(3), 311-317 (2011).

48. B.J. Burri, M.R. La Frano, C. Zhu, Absorption, metabolism, and functions of beta-cryptoxanthin, *Nutr. Rev.*, **74**(2), 69-82 (2016).

49. B. Atlı, M. Yamaç, Z. Yıldız, O.S. Isikhuemnen, Enhanced production of lovastatin by *Omphalotus olearius* (DC.) Singer in solid state fermentation, *Rev. Iberoam. Micolog.*, **32**(4), 247-251 (2015).

50. J.S. Park, K.S. Cha, H.W. Lee, *et al.*, Predictive and protective role of high-density lipoprotein cholesterol in acute myocardial infarction, *Cardiol. J.*, **26**(2), 176-185 (2019).

51. M. Kobori, Y. Ni, Y. Takahashi, *et al.*, Beta-cryptoxanthin alleviates diet-induced nonalcoholic steatohepatitis by suppressing inflammatory gene expression in mice, *PLoS One*, **9**(5), e98294 (2014).

52. P.E. Giriwono, H. Shirakawa, Y. Ohsaki, *et al.*, Dietary supplementation with geranylgeraniol suppresses lipopolysaccharide-induced inflammation via inhibition of nuclear factor-kB activation in rats, *Eur. J. Nutr.*, **52**(3), 1191-1199 (2013).

53. P.E. Giriwono, H. Shirakawa, Y. Ohsaki, *et al.*, Geranylgeraniol suppresses the expression of IRAK1 and TRAF6 to inhibit NFkB activation in lipopolysaccharide-induced inflammatory responses in human macrophage-like cells, *Int. J. Mol. Sci.*, **20**(9), 2320 (2019).

54. N.O. Calixto, M.C. da Costa e Silva, C.R. Gayer, M.G. Coelho, M.C. Paes, A. Todeschini, Antiplatelet activity of geranylgeraniol isolated from *Pterodon pubescens* fruit oil is mediated by inhibition of cyclooxygenase-1, *Planta Med.*, **73**(5), 480-483 (2007).

55. E.K. Silva, G.L. Zabot, M.A. Bargas, M.A.A. Meireles, Microencapsulation of lipophilic bioactive compounds using prebiotic carbohydrates: Effect of the degree of inulin polymerization, *Carbohydr. Polym.*, **152**, 775-783 (2016).

56. Y. Karakurt, H. Suleyman, F. Keskin-Cimen, *et al.*, The effects of lutein on optic nerve injury induced by ethambutol and isoniazid: an experimental study, *Cutan. Ocul. Toxicol.*, **38**(2), 136-140 (2019).

57. Y. Karakurt, T. Ucak, N. Tasli, *et al.*, The effects of lutein on cisplatin-induced retinal injury: an experimental study, *Cutan. Ocul. Toxicol.*, **37**(4), 374-379 (2018).

58. E.L. Wils-Plotz, K.C. Klasing, Effects of immunomodulatory nutrients on growth performance and immune-related gene expression in layer chicks challenged with lipopolysaccharide, *Poultry Sci.*, **96**(3), 548-555 (2017).

59. A.N. Howard, D.I. Thurnham, Lutein and atherosclerosis: Belfast versus Toulouse revisited, *Med. Hypotheses*, **98**, 63-68 (2017).

60. Z. Montero-Lobato, M. Vazquez, F. Navarro, *et al.*, Chemically-induced production of anti-inflammatory molecules in microalgae, *Mar. Drugs*, **16**(12), 478 (2018).

61. D. Tan, X. Yu, M. Chen, J. Chen, J. Xu, Lutein protects against severe traumatic brain injury through antiinflammation and antioxidative effects via ICAM1/Nrf2, *Mol. Med. Rep.*, **16**(4), 4235-4240 (2017).

62. K.J. Chung, J.K. Lee, S.C. Lee, J.W. Park, D.J. Seo, *A new method for producing pravastatin precursor*, ml-236b. Google Patents, 1999.

63. M.L. Moraes, A.M. Ribeiro, E. Santin, K.C. Klasing, Effects of conjugated linoleic acid and lutein on the growth performance and immune response of broiler chickens, *Poultry Sci.*, **95**(2), 237-246 (2016).

64. H. Su, Y. Li, D. Hu, L. Xie, H. Ke, X. Zheng, W. Chen, Procyanidin B2 ameliorates free fatty acids-induced hepatic steatosis through regulating TFEB-mediated lysosomal pathway and redox state, *Free Radic. Biol. Med.*, **126**, 269-286 (2018).

65. T.C. Sutcliffe, A.N. Winter, N.C. Punessen, D.A. Linseman, Procyanidin B2 protects neurons from oxidative, nitrosative, and excitotoxic stress, *Antioxidants (Basel)*, **6**(4), 77 (2017).

How to cite this article

R.N. Moraes-Neto, G. Guedes-Coutinho, A. de Oliveira-Rezende, D. de Brito-Pontes, R.L. Pinheiro Soares-Ferreira, D. de Araújo-Morais, R. Pontes-Albuquerque, L. Gonçalves Lima-Neto, L.C. Nascimento da Silva, C. Quintino da Rocha, L. Machado-Gonçalves, L.Â. Macedo-Santiago, R. Mondego-Oliveira, R. Cardoso-Carvalho, E. Martins de Sousa, Compounds isolated from *Bixa orellana*: evidence-based advances to treat infectious diseases, *Rev. Colomb. Cienc. Quím. Farm.*, **49**(3), 581-601 (2020).

Artigo de pesquisa científica / *http://dx.doi.org/10.15446/rcciquifa.v49n3.91249*

Funcionalização do polietilenoglicol metil éter via reação de bromoacetilação: ativação, caracterização por MALDI-TOF e mecanismo de reação

Lídia Pereira B. Cordeiro[1], William Gustavo Lima[1], Ana Caroline Soares[1], Marcia Helena Borges[2], Maria Elena de Lima[1,3], Júlio César Moreira Brito[1,2*]

[1]Universidade Federal de Minas Gerais (UFMG), Belo Horizonte, MG, Brasil.

[2]Fundação Ezequiel Dias (FUNED), Rua Conde Pereira Carneiro, 80. Gameleira, Minas Gerais, 35501-293, Belo Horizonte, MG, Brasil.

[3]Instituto de Ensino e Pesquisa, Santa Casa-Belo Horizonte, MG, Brasil.

*Autor para correspondência: juliocmbrito@gmail.com,
ORCID: 0000-0003-2794-5680

Recebido: 3 de junho de 2020

Revisado: 11 de junho de 2020

Aceto: 15 de junho de 2020

Resumo

A PEGuilação, reação química de conjugação com a molécula de polietilenoglicol (PEG) ou polietilenoglicol metil éter (mPEG), tem sido amplamente aplicada pelas indústrias farmacêuticas como estratégia de melhoria das propriedades farmacocinéticas de compostos bioativos. O PEG é um polímero que possui um esqueleto de poliéter quimicamente inerte e que apresenta grupos hidroxilas (-OH) em suas extremidades. Assim, o PEG para tornar-se apto como reagente de conjugação deve ser ativado com um grupo funcional que seja reativo. Nesse sentido, a bromoacetilação apresenta-se como uma alternativa para a funcionalização do PEG. Portanto, nesse trabalho objetivamos descrever em detalhes os procedimentos e o mecanismo de reação envolvida na funcionalização do mPEG, através da reação de bromoacetilação. Além do mais, estudamos a aplicação do MALDI-ToF para a caracterização do produto ativado. Após a bromoacetilação, por um procedimento adaptado, obteve-se o bromoacetil-mPEG-éster, com rendimento bruto de 56,78%. Análises posteriores, por espectrometria de massas por MALDI-ToF, possibilitaram identificar e caracterizar o produto bromoacetilado. Entre as condições de reação, o controle de temperatura (-10 ºC a 0 ºC) mostrou-se eficaz favorecendo a adição nucleofílica essencial à bromoacetilação. Assim, concluímos que o controle da baixa temperatura reacional é um fator chave para o favorecimento da adição nucleofílica à carbonila e, portanto, essencial na obtenção do mPEG funcionalizado via bromoacetilação. Estudos posteriores serão necessários, no entanto, para confirmar se o mPEG esterificado, nessas condições, poderá ser utilizado na conjugação com moléculas de natureza proteica ou peptídica, por meio de substituição nucleofílica bimolecular.

Palavras-chaves: Polietilenoglicol (PEG), PEGuilação, bromoacetilação, adição nucleofílica.

Summary

Poly(ethylene glycol) methyl ether functionalization by bromoacetylation reaction: Activation, characterization by MALDI-TOF and reaction mechanism

PEGylation, a chemical reaction of conjugation with the polyethylene glycol molecule (PEG), has been widely applied by the pharmaceutical industries as a strategy to improve the pharmacokinetic properties of bioactive compounds. PEG is a polymer that has a chemically inert polyether backbone and hydroxyl groups (-OH) at its ends. Thus, PEG to become fit as a reagent for conjugation must be activated with a functional group that is reactive. In this sense, bromoacetylation presents itself as an alternative for the functionalization of PEG. Therefore, in this study we aim to describe in detail the procedures and reaction mechanism involved in the functionalization of mPEG through the bromoacetylation reaction. In addition, we used the spectrometric technique, by MALDI-ToF, for the characterization of the activated product. After applying an adapted bromoacetylation procedure, bromoacetyl-mPEG-ester was obtained with a yield of 56.78%. Subsequent analyzes of MALDI-ToF mass spectrometry were able to correctly identify and characterize the bromoacetylated product. Among the reaction conditions, temperature control (from -10 °C to 0 °C) was effective in favoring the essential nucleophilic addition to bromoacetylation. Thus, we conclude that the control of the low reaction temperature is a key factor in favoring the nucleophilic addition to carbonyl and, therefore, obtaining a favorable conversion to functionalized PEG via bromoacetylation. Further studies, however, will be necessary to confirm whether PEG esterified with these conditions can be used in conjunction with molecules of a protein or peptide nature by means of bimolecular nucleophilic substitution.

Keywords: polyethylene glycol (PEG), PEGylation, bromoacetylation, nucleophilic addition.

Resumen

Funcionalización de polietilenglicol metil éter mediante reacción de bromoacetilación: activación, caracterización por MALDI-TOF y mecanismo de reacción

La PEGilación, una reacción química de conjugación con la molécula de polietilenglicol (PEG), ha sido ampliamente aplicada por las industrias farmacéuticas como una estrategia para mejorar las propiedades farmacocinéticas de los compuestos

bioactivos. El PEG es un polímero formado por un esqueleto de poliéter químicamente inerte con grupos hidroxilo (-OH) en sus extremos. Por lo tanto, para usar el PEG como reactivo de conjugación debe activarse con un grupo funcional que sea reactivo. En este sentido, la bromoacetilación es una alternativa para la funcionalización de PEG. De esta manera, en este trabajo nuestro objetivo es describir en detalle los procedimientos y el mecanismo de reacción involucrados en la funcionalización de PEG a través de la reacción de bromoacetilación. Además, estudiamos la aplicación de MALDI-ToF para la caracterización del producto activado. Después de aplicar un procedimiento de bromoacetilación adaptado, se obtuvo bromoacetil-mPEG-éster con un rendimiento bruto de 56,78%. Los análisis posteriores de espectrometría de masas por MALDI-ToF pudieron identificar y caracterizar correctamente el producto bromoacetilado. Entre las condiciones de reacción, el control de la temperatura (desde -10 ºC hasta 0 ºC) fue eficaz para favorecer la adición nucleofílica esencial a la bromoacetilación. Así, concluimos que el control de la baja temperatura de reacción es un factor clave para favorecer la adición nucleofílica al carbonilo y, por lo tanto, esencial para obtener el mPEG funcionalizado mediante la bromoacetilación. Sin embargo, serán necesarios más estudios para confirmar si el mPEG esterificado en estas condiciones puede usarse junto con moléculas de naturaleza proteica o peptídica por medio de la sustitución nucleófila bimolecular.

Palabras clave: Polietilenglicol (PEG), pegilación, bromoacetilación, adición nucleofílica.

Introdução

A prospecção de novas moléculas com potencial efeito terapêutico, frente a diversas doenças na atualidade se faz necessária, em resposta à demanda por tratamentos mais inovadores, seguros e efetivos [1]. Assim, para que tais moléculas se viabilizem como fármacos, são necessárias etapas de avaliação de suas viabilidades de aplicação terapêutica, dentre as quais se destaca o delineamento farmacocinético, que aponta fatores associados à absorção, distribuição, metabolismo, excreção e toxicidade (ADMET) destes potenciais agentes terapêuticos [2]. Vale destacar que, grande parte das moléculas com atividade farmacológica promissora nos ensaios pré-clínicos falham em ensaios clínicos, muito em virtude de características farmacocinéticas inadequadas, como baixa estabilidade plasmática, rápida excreção e biodistribuição ineficaz [1-3]. Nesse contexto, com o intuito de superar as limitações farmacocinéticas de determinadas moléculas (como os peptídeos e proteínas), sistemas bioconjugados têm sido propostos. Esses sistemas empregam polímeros que, a exemplo do polietilenoglicol metil éter (mPEG-OH), resultam em aumento do tempo de meia-vida da molécula de interesse,

redução do seu *clearance* renal, melhora da solubilidade e proteção contra inativação proteolítica [2, 3].

O polietilenoglicol (PEG) foi muito difundido na indústria como aditivo na produção de papel, agente de controle de viscosidade e precipitação de proteínas, e excipiente de formulações medicamentosas. Porém, foi somente na década de 70 que se explorou a conjugação deste polímero anfifílico com proteínas, com o pioneirismo do estudo de Abuchowski e Davis (1977) que resultou na conjugação da albumina bovina sérica com o mPEG-OH. A partir de então, a técnica da PEGuilação passou a ser mais explorada na bioconjugação de peptídeos, proteínas e oligonucleotídeos. De fato, o sucesso da PEGuilação levou ao lançamento de moléculas bioativas conjugadas na clínica, como o caso do Oncaspar® (Pegaspargase) e Cimzia® (Certolizumab pegol), que são atualmente empregados na terapia da leucemia e artrite reumatóide, respectivamente.

A polimerização de unidades de oxietileno (-CH_2CH_2O) pode resultar na formação dos polímeros de polietilenoglicol (PEG) ou polietilenoglicol metil éter (mPEG) de diversos tamanhos. Os índices de polidispersão variam de 1,01 para polímeros de PEG com massa molar entre 2-10 kDa e 1,2 para polímeros de alta massa molar. Por se tratar de polímeros com unidades monoméricas óxido de etileno, cada unidade monomérica é capaz de coordenar a 3-5 moléculas de água, o que aumenta o volume hidrodinâmico do polímero de 10-15 vezes, retardando a excreção renal e prolongando a meia vida das moléculas conjugadas. A conjugação com tais polímeros também confere proteção frente à degradação química, redução da imunogenicidade, opsonização e agregação [2, 3].

Enquanto o PEG é um diol, *i.e.*, tem dois sítios de reação; o mPEG contém um grupo metoxila e um grupo hidroxila que corresponde ao sítio de reação e que deve estar devidamente ativado para servir de agente de PEGuilação (figura 1). Assim, para conjugação do mPEG com o potencial alvo é necessário que o polímero esteja funcionalizado com um grupo reativo ao fármaco. O presente trabalho descreve a obtenção do polímero bromoacetil-mPEG-éster via bromoacetilação, com potencial aplicabilidade na conjugação com peptídeos e proteínas por reação de substituição nucleofílica bimolecular (S_N2) [2-11].

Métodos

A funcionalização do polímero mPEG-OH via reação de bromoacetilação foi realizada conforme metodologia de Benincasa *et al.* [8], com modificações. Foram empregados 151 μL (0,3 mmol) de mPEG-OH (Sigma Aldrich®) de 550 Da, os quais foram solubilizados em 2,5 mL de tolueno seco (Synth®). O solvente foi evaporado sob vácuo, a 80 °C até formação de um filme marrom. Posteriormente, o sistema foi mantido sob

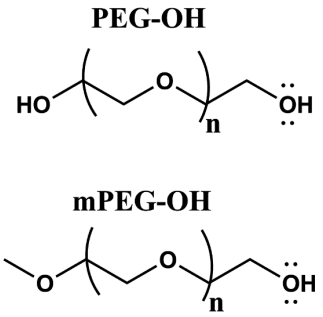

Figura 1. Estrutura química geral dos polímeros PEG-OH e mPEG-OH.

resfriamento a -10 °C, e em seguida foram adicionados 9 mL de diclorometano seco (DCM; Carlo Erba®) contendo 413 μL (2,5 mmol) de *N,N*-diisopropiletilamina (DIPEA; Sigma Aldrich®). A solução foi vigorosamente agitada por cerca de cinco minutos e, em seguida, foi adicionada sob gotejamento, solução contendo 413 μL (3 mmol) de brometo de bromoacetila ($BrCH_2COBr$; Sigma Aldrich®) em 2 mL de diclorometano seco. A seguir, a solução foi agitada por 15 minutos a –5 °C e depois por 1 hora à temperatura ambiente (figura 2) [3].

Após agitação à temperatura ambiente, 15 mL de isopropanol (Química Moderna®) foram adicionados e o diclorometano foi evaporado sob pressão. A solução em banho de gelo foi então submetida ao gotejamento de 10 mL de éter etílico (Dinâmica®) e mantida sob agitação em resfriamento durante 1 hora. Em seguida, o produto foi filtrado sob vácuo e submetido a duas lavagens com cada um dos seguintes solventes, sequencialmente: 5 mL de isopropanol gelado, 5 mL de isopropanol:éter etílico (1:1) e 5 mL de éter etílico. O resíduo restante foi dissolvido em 7 mL de acetonitrila (Honeywell®), precipitado em éter etílico gelado sob centrifugação a 6600 rpm por cinco minutos e secado sob fluxo de nitrogênio (figura 2). Finalmente, o produto obtido foi caracterizado por espectrometria de massas por ionização/dessorção assistida por laser e análise por tempo de voo (MALDI-ToF; Bruker Daltonics Autoflex SmartBeam, MA) em matriz de ácido sinapínico [3].

Resultados e discussão

Apesar de que atualmente se dispõem de diversos mPEG's funcionalizados comercialmente como o mPEG-succinato de succinimidila, mPEG-maleimidil, mPEG-carbonato de succinimidila, e mPEG-iodoacetamida, a ativação do mPEG *in house* ainda tem sido frequentemente empregada por indústrias químicas e farmacêuticas de todo o mundo. O procedimento adaptado de Benincasa *et al.* [8] e proposto nesse traba-

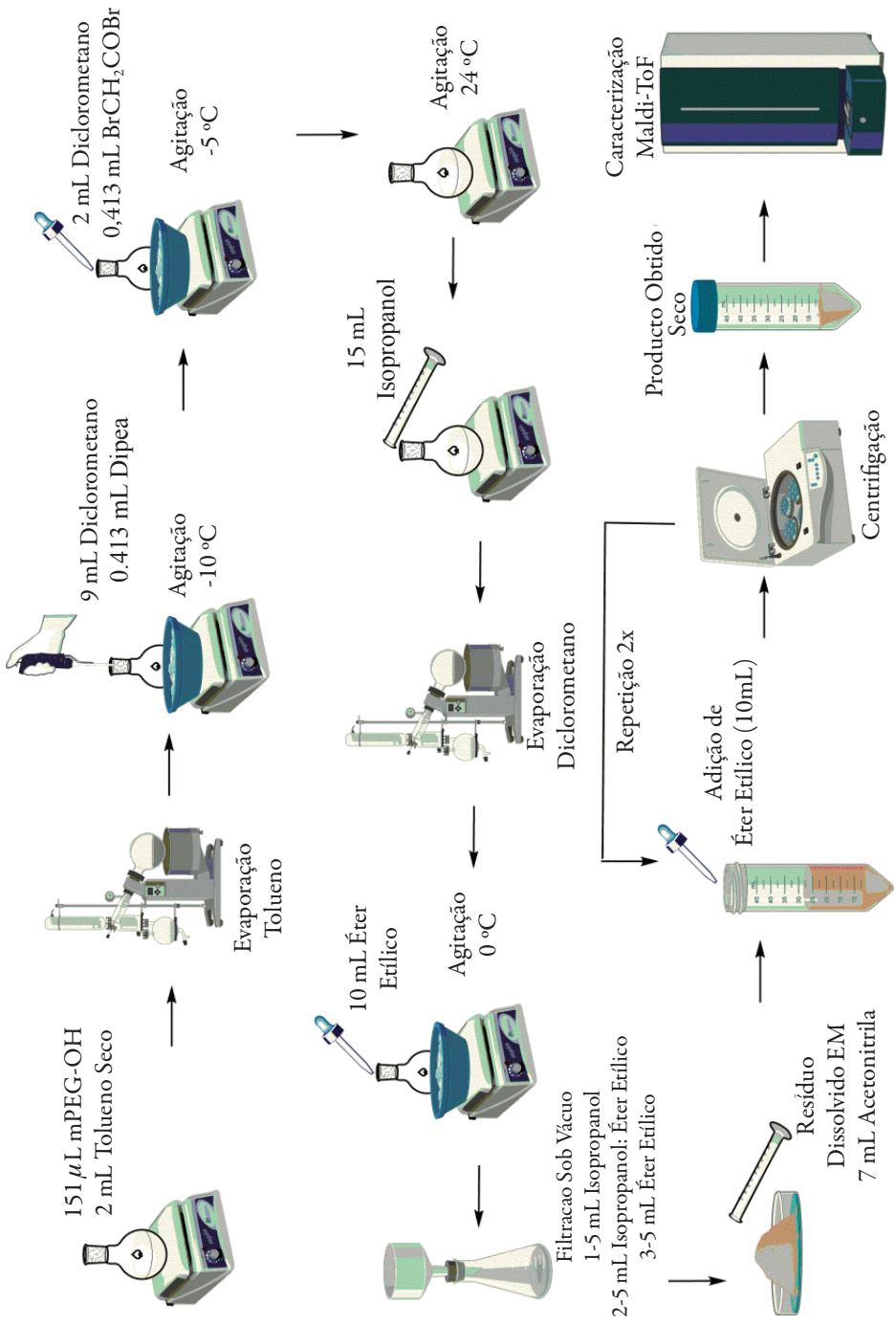

Figura 2. Representação esquemática do procedimento de bromoacetilação do mPEG-OH proposto nesse estudo.

lho foi eficaz na obtenção do produto bromoacetil-mPEG-éster (mPEG-Br). Macroscopicamente, o mPEG-Br foi obtido como um sólido cristalizado amorfo (figura 3) e um rendimento bruto de 56,78 %. A verificação da formação do mPEG-Br se deu pelo espectro de massas MALDI ToF, demonstrando um sinal intenso correspondente ao íon molecular com razão massa carga igual a 671,644 [M+H$^+$] (massa teórica 670 g.mol^{-1}). Outro aspecto que corrobora este resultado é a diferença característica de 44 unidades entre os picos adjacentes, correspondendo à unidade monomérica (oxietileno) do mPEG-OH (figura 4).

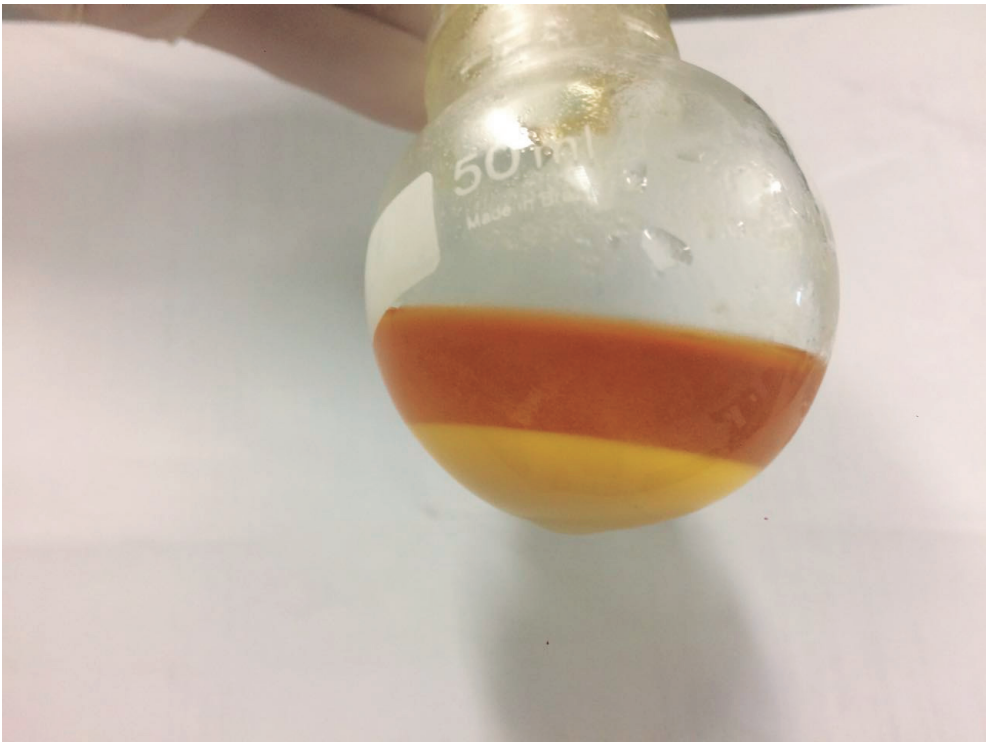

Figura 3. Produto amarronzado precipitado com éter etílico, obtido pela reação de bromoacetilação.

Benincasa *et al.* [8] utilizaram mPEG-OH 20 kDa e nesse trabalho foi funcionalizado mPEG-OH com massa 36 vezes menor (550 Da). Nesse sentido, para se obter o produto precipitado foram utilizados dois ciclos utilizando éter etílico gelado e centrifugação a 6600 rpm (figura 2), adaptações feitas à técnica de Benincasa *et al.* [8]. Esses dois ciclos favoreceram a obtenção do polímero funcionalizado, pois o choque térmico induziu a precipitação e a centrifugação possibilitou a concentração do produto funcionalizado [12].

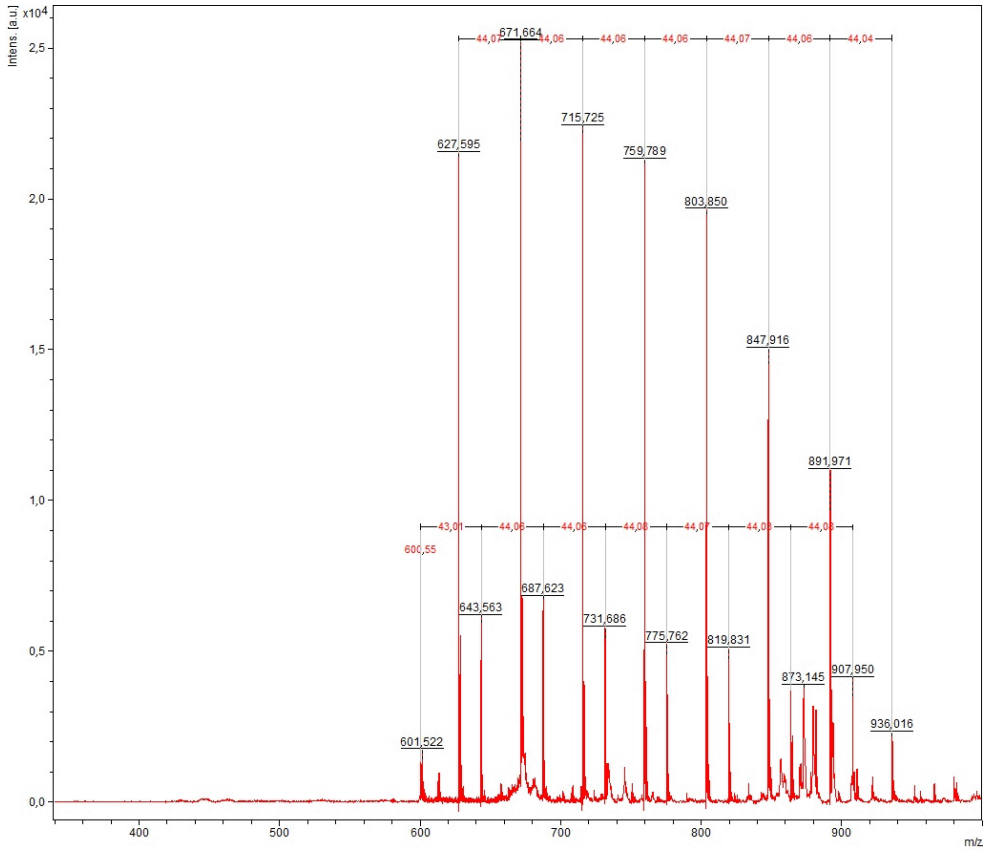

Figura 4. Espectro de massas obtido por técnica MALDI-ToF, evidenciando o sinal intenso correspondente ao íon molecular de massa carga 671,664 [M+H⁺], confirmativo da obtenção do produto de interesse (bromoacetil-mPEG-éster).

O brometo de bromoacetila tem dois sítios eletrofílicos susceptíveis ao ataque da hidroxila, a carbonila e o metileno, tal que as condições de reação empregadas favorecem a formação do produto esterificado [13, 14]. Considerando os mecanismos envolvidos nas duas possíveis reações, a etapa lenta da reação de adição à carbonila envolve um intermediário quaternário que mediante a saída do íon brometo leva à formação do produto esterificado [15]. Já na reação de substituição nucleofílica bimolecular, o mecanismo seria concertado com o ataque e simultânea saída do íon brometo, levando à formação do respectivo éter (figura 5).

Nesse estudo mostramos, através da proposição do mecanismo de reação, que o controle de baixa temperatura favorece a reação de adição nucleofílica à carbonila em detrimento da reação de substituição nucleofílica bimolecular (figura 5) [13]. Isso resulta

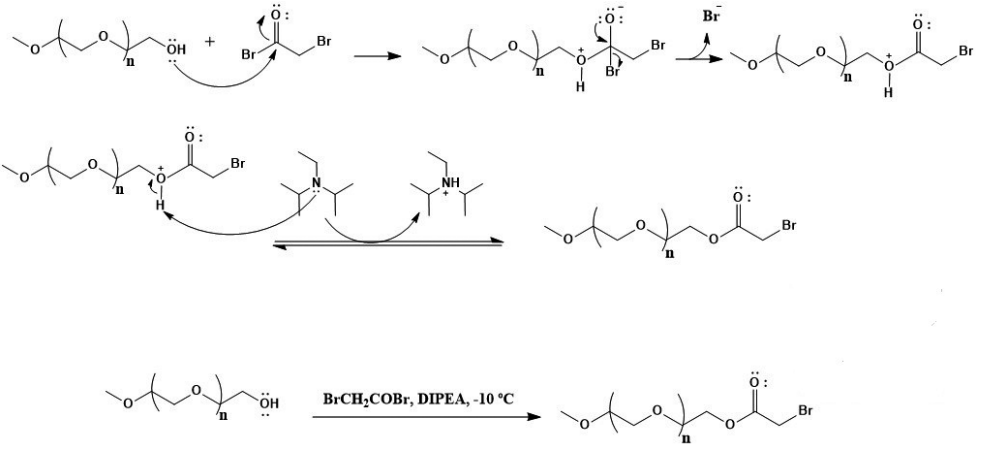

Figura 5. Mecanismo proposto da reação de bromoacetilação do mPEG-OH, evidenciando a formação do produto esterificado em etapa de precipitação com éter etílico gelado [14].

na disponibilidade do bromometil frente aos peptídeos e proteínas passíveis de reação, tendo em vista a susceptibilidade à reação com grupamentos nucleofílicos como sulfidrila (–SH) e amina ($–NH_2$) levando à formação de ligação covalente estável com biomoléculas.

Uma vez que a reatividade do polímero mPEG-OH frente a peptídeos e proteínas depende da funcionalização da hidroxila com grupos eletrofílicos, o mPEG-Br destaca-se como um produto funcionalizado que pode ser empregado na conjugação com peptídeos e proteínas. A susceptibilidade dessas biomoléculas à conjugação com o mPEG-Br se dá pelo fato de que peptídeos e proteínas têm resíduos de aminoácidos contendo grupamentos nucleofílicos como -OH, $-NH_2$, -SH, os quais são passíveis de reagirem com os grupos eletrofílicos presentes. Entretanto, vale destacar que para a reação de PEGuilação ocorrer normalmente, as reatividades dos grupamentos eletrofílico e nucleofílico devem ser compatíveis em termos reacionais com o pH, a temperatura, a concentração salina, e condições termodinamicamente favoráveis. Sendo assim, a ativação do PEG não deve ser considerada isoladamente durante a conjugação com as biomoléculas [2].

Conclusão

Com esse trabalho concluímos que, a exposição do mPEG ao brometo de bromoacetila ($BrCH_2COBr$) em meio básico anidro, possibilita, mediante o controle de temperatura (-10 °C a 0 °C), a correta bromoacetilação do mPEG. Posteriormente, mostramos

que o espectro de massas do MALDI-ToF foi capaz de caracterizar com eficiência o bromoacetil-mPEG-éster e que o controle da baixa temperatura reacional é essencial à obtenção do produto de interesse. Estudos adicionais deverão confirmar se o PEG esterificado nessas condições, poderá ser utilizado na conjugação com moléculas de natureza proteica ou peptídica por meio de substituição nucleofílica bimolecular. Assim, esse trabalho destaca as etapas e mecanismos envolvidos na ativação do mPEG por bromoacetilação, o que pode contribuir no desenvolvimento biofarmacêutico e melhora das propriedades terapêuticas de moléculas promissoras.

Agradecimentos

Agradecemos a Vivian Pena da Fundação Ezequiel Dias pelo auxílio técnico; Waleska Stephanie da Cruz Nizer de Carleton University, Ottawa, Ontario, Canadá; José Maria Muñoz Lopez da Universidade Federal de Minas Gerais. W.G.L. agradece à Coordenação de Aperfeiçoamento de Pessoal de Nível Superior (CAPES) pela bolsa de doutorado. Ao CNPq e Fapemig pelo financiamento da pesquisa.

Conformidade com os padrões éticos

Financiamento: CNPq e a Fapemig para a compra de reagentes.

Aprovação ética: este artigo não contém estudos com participantes humanos ou animais realizados por qualquer um dos autores, dispensando, portanto, aprovação por um comitê de ética.

Contribuição dos autores: todos os autores contribuíram para o desenvolvimento, análise, redação e revisão deste artigo.

Conflito de interesse

Todos os autores relatam que não têm nenhum conflito de interesse.

Referências

1. S. Pushpakom, F. Iorio, P.A. Eyers, K.J. Escott, S. Hopper, A. Wells, A. Doig, T. Guilliams, J. Latimer, C. McNamee, A. Norris, P. Sanseau, D. Cavalla, M. Pirmohamed, Drug repurposing: progress, challenges and recommendations, *Nature Reviews Drug Discovery*, **18**(1), 41-58 (2019).

2. F.M. Veronese, *PEGylated Protein Drugs: Basic Science and Clinical Applications*, Birkhäuser, 2009, Vol. 1, p.14-27.

3. F.M. Veronese, Peptide, and protein PEGylation: a review of problems and solutions, *Biomaterials*, **22**(5), 405-417 (2001).

4. A. Abuchowski, T.V. Es, N.C. Palczuk, F.F. Davis, Alteration of immunological properties of bovine serum albumin by covalent attachment of polyethylene glycol, *The Journal of Biological Chemistry*, **252**(11), 3578-3581 (1977).

5. M. Hamidi, A. Azadi, P. Rafiei, Pharmacokinetic consequences of PEGylation, *Drug Delivery*, **13**(6), 399-409 (2006).

6. M.J. Roberts, M.D. Bentley, J.M. Harris, Chemistry for peptide and protein PEGylation, *Advanced Drug Delivery Reviews*, **54**(4), 459-476 (2002).

7. C.J. Fee, J.M.V. Alstine, PEG-proteins: Reaction engineering and separation issues, *Chemical Engineering Science*, **61**(3), 924-939 (2006).

8. M. Benincasa, S. Zahariev, C. Pelillo, A. Milan, R. Gennaro, M. Scocchi, PEGylation of the peptide Bac7(1-35) reduces renal clearance while retaining antibacterial activity and bacterial cell penetration capacity, *European Journal of Medicinal Chemistry*, **95**, 210-219 (2015).

9. I.W. Hamley, PEG-peptide conjugates, *Biomacromolecules*, **15**(5), 1543-1559 (2014).

10. J.M. Harris, R.B. Chess, Effect of PEGylation on pharmaceuticals, *Nature Reviews Drug Discovery*, **2**(3), 214-221 (2003).

11. P.L. Turecek, M.J. Bossard, F. Schoetens, I.A. Ivens, PEGylation of biopharmaceuticals: A review of chemistry and nonclinical safety information of approved drugs, *Journal of Pharmaceutical Sciences*, **105**(2), 460-475 (2016).

12. S. Lee, X. Tong, F. Yang, Effects of the poly(ethylene glycol) hydrogel crosslinking mechanism on protein release, *Biomaterials Science*, **4**(3), 405-411 (2016).

13. D.F. Schneider, M.S. Viljoen, Bromoacetyl bromide: a versatile and selective cleaving agent for ethers and acetals, *Synthetic Communications*, **32**(5), 721-728 (2002).

14. M. Li, Z. Tang, H. Sun, J. Ding, W. Song, X. Chen, pH, and reduction dual-responsive nanogel cross-linked by quaternization reaction for enhanced cellular internalization and intracellular drug delivery, *Polymer Chemistry*, **4**, 1199-1207 (2013).

15. J. Clayden, N. Greeves, S. Warren, *Organic Chemistry*, 2 ed., Oxford University Press, New York, Vol. 1, 2012.

Como citar este artigo

L. Pereira B. Cordeiro, W.G. Lima, A.C. Soares, M.H. Borges, M.E. de Lima, J.C. M. Brito, Funcionalização do polietilenoglicol metil éter via reação de bromoacetilação: Ativação, Caracterização por MALDI-TOF e mecanismo de reação, *Rev. Colomb. Cienc. Quím. Farm.*, **49**(3), 602-613 (2020).

Technological research article / *http://dx.doi.org/10.15446/rcciquifa.v49n3.91251*

Drying kinetics of *Bixa orellana* Labil (annatto) leaves and the influence of temperature on the physicochemical and biological properties of its essential oil

Gustavo Oliveira Everton[1]*, Everton Holanda Sales[1], Nilton Silva Costa Mafra[1], Rebecca Jemima Araújo[1], Paulo Sérgio Santos Júnior[1], Paulo Victor Serra Rosa[1], Ana Patrícia Matos Pereira[1], Franscristhiany Silva Souza[2], Caritas de Jesus Silva Mendonca[2], Fernando Carvalho Silva[2], Paulo Roberto Barros Gomes[3], Victor Elias Mouchrek Filho[1]

[1]Laboratório de Pesquisa e Aplicação de Óleos Essenciais (LOEPAV-UFMA), Universidade Federal do Maranhão, São Luís, Maranhão, Brasil.

[2]Núcleo de Combustíveis, Catálise e Ambiental (NCCA-UFMA), Universidade Federal do Maranhão, São Luís, Maranhão, Brasil.

[3]Instituto Federal do Pará, São Luís, Maranhão, Brasil.

*Corresponding author: gustavooliveiraeverton@gmail.com

Received: 10 April 2020

Revised: 16 June 2020

Accepted: 18 June 2020

Summary

Bixa orellana L. is widely used as a dye, and other properties are still little studied, especially in relation to leaves. This article evaluates how drying *B. orellana* L. influences the properties of essential oils (EOs) extracted from their leaves. The collected plant material was submitted to convective air-drying oven at temperatures of 35, 45 and 55 °C. Chemical profiles were determined by Gas Chromatography-Mass Spectrometry (GC-MS). Mathematical models were applied to represent the drying process and statistical analysis performed using Statistica 10 software. The EO's were obtained through the hydrodistillation technique with verification of physicochemical properties and antimicrobial activity by the Disc Diffusion Method. For the toxicity test, the bioassay was applied to *Artemia salina*. Through the results obtained it was possible to determine that the mathematical model of Verma was the one that best fitted the experimental data. Significant differences in the properties of EO's were observed. The temperature of 45 °C allowed obtaining the best EO yield, still presenting the most efficient antimicrobial activity. This study states through the activities analyzed that the drying temperature influences the physicochemical and biological properties of the EO's, thus requiring studies such as this one that evaluate the best mathematical model to predict drying as well as the specific temperatures that influence the properties of the product obtained.

Key words: Essential oil, kinetic, antimicrobial, *B. orellana* L.

Resumen

Cinética de secado de las hojas de *Bixa orellana* Labil (annatto) e influencia de la temperatura sobre las propiedades fisicoquímicas y biológicas de su aceite esencial

Bixa orellana L. es ampliamente utilizado como un tinte y tiene otras propiedades que han sido poco estudiadas, especialmente en relación con las hojas. Este artículo evalúa cómo el secado B. orellana L. influye en las propiedades de los aceites esenciales (EOs) extraídos de sus hojas. El material vegetal recogido se sometió al horno de secado por aire convectivo a temperaturas de 35, 45 y 55 °C. Los perfiles químicos fueron determinados por GC-MS. Se aplicaron modelos matemáticos para representar el proceso de secado y el análisis estadístico realizado utilizando el *software* Statistica 10. Las EO se obtuvieron a través de la técnica de hidrodestilación con verificación de propiedades fisicoquímicas y actividad antimicrobiana. Para el ensayo de toxicidad se aplicó el bioensayo a *Artemia salina*. A través de los resultados obtenidos fue posible determinar el modelo matemático que se ajustaba mejor. Se observaron diferencias significativas en las propiedades de los EO. La temperatura de 45 °C permitió obtener el mejor rendimiento de EO, porque la actividad antimicrobiana fue más eficiente. Este estudio afirma a través de las actividades analizadas que la temperatura de secado influye en las propiedades fisicoquímicas y biológicas de las EO. Estudios como este evalúan el mejor modelo matemático para predecir el secado, así como las temperaturas específicas que influyen en las propiedades del producto obtenido.

Palabras clave: Aceite esencial, cinético, antimicrobiano, *B. orellana* L.

Introduction

Medicinal plants are one of the oldest forms used for the treatment of diseases, due to the healing properties of substances present in certain species [1]. A plant is considered as medicinal when it has active substances that provoke in the human body reactions that can range from cure to disease relaxation. Medicinal plants have a promising world market in the face of growing demand [2].

However, there is a lack of studies that is reflected in the frequent lack of quality of the product offered, making it commercially less competitive [3]. The medicinal plant of the species *B. orellana* L., family Bixaceae, produces fruits called annatto, whose popular name originates from the Tupi word "uruku", which means "red". It is a shrub

originating in Central or South America, more specifically from the Amazon region, which grows spontaneously from Guyana to Bahia [4].

In this sense, aiming at postharvest quality, including the durability of the compounds, it is important that *B. orellana* L. has its water content reduced soon after harvest. Drying, therefore, is one of the fundamental stages of post-harvest, being directly linked to the quality of medicinal plants. In the case of medicinal plants in which they have the presence of essential oils (EOs), drying has a direct influence on sensitive components [5].

Drying and storage are fundamental steps among the post-harvest processes for obtaining quality products, which are the basis for the manufacture of herbal medicines. Drying is a complex procedure due to the structure and composition of the material, the transport phenomena involved and the biological variability. The drying rate depends on variables such as temperature, speed, relative humidity of the drying air and product characteristics. Thus, mathematical modeling and simulation of this process are useful tools to deal with its complexity and obtain adequate operating conditions [6, 7].

Therefore, the positive and negative effects of the drying process depend on the conditions and according to the sensitivity of the chemical substances, which can be lost by volatilization, as is the case of Eos [8, 9]. In order to obtain greater knowledge about the effect of drying on the chemical composition of medicinal plants, it is necessary to make use of specific analyses. In the case of EO, it is regularly recommended to use the gas chromatography system coupled to the mass spectrum (GC/MS), in order to identify substances derived from secondary metabolism [10, 11]. Therefore, it is of fundamental importance to know the sensitivity of the active ingredient of plants and the adequacy of drying conditions to their quality in the final product.

In addition, EO's are used in topical formulations. Because they have antimicrobial action, they can inhibit bacterial growth and promote the wound healing process, providing a better alternative to treatment [12]. EOs extracted from medicinal plants have been widely used successfully in research aimed at controlling phytopathogens. It presents as secondary metabolites with naturally volatile substances that interact with each other, forming classes of compounds with microbial potential, especially terpenes, monoterpenes, sesquiterpenes, aromatic compounds, phenols, aldehydes, ketones, alcohols and esters [13, 14].

These various combinations of chemical constituents presented by EOs can control food oxidation and bacteria that have consistently high resistance to antimicrobial agents such as *Salmonella cholerasuis*, *Listeria monocytogenes*, *Staphylococcus aureus* and *Escherichia coli*. Although the EO's represent an interesting possibility for the preservation of food, it is necessary to know its antibacterial and antioxidant properties [15,

16]. In this context, this work aimed to evaluate in an unprecedented way the influence of drying air temperature, as well as to adjust and statistically model the drying curves of the leaf, in addition, to estimate the yield and toxicity of the EO of the leaf by *B. orellana*.

Materials and methods

Collection of plant material

The fresh leaves of *B. orellana* L. to perform the drying kinetics were collected in the Herbarium Ático Seabra of the Federal University of Maranhão under the register of n° 00815, in the city of São Luís-MA in July 2019. The leaves were collected manually in the morning, presenting water content in 54.16%. The material was transported in thermal packaging to the Laboratory of Research and Application of Essential Oils of the Federal University of Maranhão (UFMA) for screening, determination of water content and drying in a digital greenhouse of convective air FANEM 520.

The collected leaves were analyzed in the laboratory and selected for visual aspects, using only undamaged plant material. Manual cuts were made, with caution in the standardization of the cuts. The cuts were performed transversely in parts of a maximum of 5 cm in length and 2 cm in width.

Chemical profile of *B. orellana* L.

To identify the constituents, present in the fresh leaf of *B. orellana* L., we used the gas chromatography technique coupled to Mass Spectrometry (GC-MS) in the Fuel, Catalysis and Environmental Center (NCCA) of the Federal University of Maranhão (UFMA). The identification was also made in the dry leaf and EO constituents that presented the best results regarding antimicrobial and toxicity assays.

The conditions of analysis were as follows: Method: Adams. M; Injected volume: 0.3 μL; Column: Capillary HP-5MS (5% diphenyl, 95% dimethyl polysiloxane) (Equivalent DB-5MS or CP-Sil 8CB LB/MS), in dimensions (30 m x 0.25 mm x 0.25 μm); Drag gas : He (99.9995); 1.0 mL/min; Injector : 280 °C, Split mode (1:10); Oven: 40 °C (5.0 min) up to 240 °C at a rate of 4 °C.min^{-1}, from 240 °C to 300 °C (7.5 min) at a rate of 8 °C.min^{-1}; t = 60.0 min; Detector : EM1; EI (70 eV); Scan mode (0.5 sec/scan); Mass range: 40 - 500 daltons (one); Line transfer: 280 °C; Filament: off 0.0 to 4.0 min; Linear quadrupole mass spectrometer. The AMDIS (Automated Mass spectral Deconvolution Mass & Identification System) program was used to identify the compounds in the sample.

Determination of the initial moisture percentage (%) and drying

The determination of the initial humidity (%) of the leaves of *B. orellana* L. was obtained through a Quimis moisture scale. For each replicate of the assay, approximately 1g of the plant material with a temperature of 105 °C per 10 min was used. As a comparison, the gravimetric method was used, using approximately 2 g of the samples previously weighed on an analytical scale and packed in a drying oven at 105 °C, for 5 h, until it reached constant mass, in three replications according to the ANVISA [17].

The drying of the leaves of *B. orellana* L. was conducted digital greenhouse of convective air FANEM 520, with standard air velocity in 1 m/s, on alternate days using the temperatures of 35, 45 and 55 °C and the relative humidity (RH) of the ambient air was monitored through a digital thermohygrometer (model INS-28 Intrusul).

A mass of 200 g was used for each drying temperature and about 3g of the samples were placed on plates coated with aluminum of dimensions 90 x 15 mm, and the mass was monitored throughout the process by discontinuous weighing at intervals of 5, 10, 20, 30 and 60 min by means of a Shimadzu AUY220 analytical scale, until the end of the process. The weighings were performed until the mass variations were insignificant. Completed when there was no mass variation in 0.0100 g between five successive weighings. Equation (1) was used to determine the moisture ratio (RU) during the drying of annatto leaves for the different drying temperatures:

$$RU_{(adm)} = \frac{Ubs\text{-}Ue}{Ubs_{initial}\text{-}Ue} \quad (1)$$

Note: RU: moisture ratio, non-dimensional; U_{bs}: annatto water content, decimal b.s.; $Ubs_{initial}$: initial water content, decimal b.s; Ue: equilibrium water content, decimal b.s.

Mathematical modeling

The RU values obtained for each drying air temperature were analyzed through six different empirical and semiempirical equations and nonlinear regression, traditionally used in the description of the drying process of agricultural products [18-21], according to table 1.

Table 1. Mathematical models of nonlinear regression to predict the drying phenomenon of *B. orellana* leaves.

Model	RU_{pre}	Eq.
Two terms	$ae^{-kt}+be^{-kt}$	(2)
Logarithm	$ae^{-kt}+c$	(3)
Newton	e^{-kt}	(4)
Henderson and Pabis	ae^{-kt}	(5)
Logistic	$\frac{a_0}{1+ae^{kt}}$	(6)
Verma	$ae^{-kt}+(1-a)e^{-k_1 t}$	(7)

Note: k, k_1 = drying constants (s^{-1}); a, a_0, b, c = coefficients of the models.

For the adjustment of mathematical models, nonlinear regression analysis was performed using the QuasiNewton method and the statistical program Statistica 10.0.

The criteria adopted to determine the best fit of the models to the experimental data were the coefficient of determination (R^2) and the mean quadratic deviation (DQM) by equation (8). Subsequently, the residuals and the standard error for each model was analyzed.

$$DQM=\sqrt{\frac{\sum\left(RU_{exp}\text{-}RU_{pred}\right)^2}{N}} \quad (8)$$

Note: RU_{exp}: value observed experimentally; RU_{pred}: value calculated by the model; N: number of experimental observations.

Extraction of Eos

The leaves of *B. orellana* L. dried in the convective air-drying oven at temperatures of 35 °C, 45 °C and 55 °C were individually crushed in an electric knife mill (Fritsch Pulverisette 14, Oberstein, Germany), and subsequently stored for extraction of their EOs.

For the extractions of the EOs, the hydrodistillation technique was used, with a modified glass Clevenger extractor, coupled to a round bottom balloon of 6000 mL packed in an electric blanket as a heat generating source. The leaves in each extraction routine were packed in the round bottom flask, adding distilled water in a ratio of 1:10.

Hydrodistillation was conducted at 100 °C for 3h, collecting the extracted EOs. After extraction, the EO's were dried with sodium anhydrous sulfate (Na_2SO_4) and stored in amber glass ampoules under 4 °C refrigeration to avoid possible losses of volatile constituents.

The physicochemical parameters of the EO extracted from dry leaves at 35, 45 and 55 °C were analyzed for density, refractive index, alcohol solubility 70% (v/v), color and appearance as described by the Brazilian Pharmacopoeia [22].

Toxicity

This test was performed according to the methodology described by Meyer *et al.* [23]. In a rectangular container, with a partition containing holes of approximately 0.02 cm thickness spaced by 0.5 cm and evenly distributed, artificial saline solution (60 g L^{-1} of distilled water) were added (60 g of sea salt/ 1L of distilled water). The container was placed inside an incubator illuminated by a fluorescent lamp, with aeration. On one side of this container, about 64 mg of *Artemia salina* cysts were added, taking care that they did not cross the partition. The part of the system containing artemia saline cysts was covered with aluminum foil, so that the organisms, at birth, were attracted by light on the other side of the system, forcing them to cross the partition. This procedure aims at homogenizing the physical conditions of the test organisms. Incubation was performed for a period of 48 h. Throughout the test the temperature was monitored.

For the evaluation of the lethality of *Artemia salina* Leach, a saline solution was prepared stock of each EO in the concentration of 10 000 mg L^{-1} and 0.02 mg of Tween 80 (active tense). Rates of 5, 50 and 500 μL of this were transferred to test tubes and supplemented with saline solution previously prepared up to 5 mL, obtaining at the end concentrations of 10, 100 and 1000 mg L^{-1}, respectively. All tests were carried out in triplicates, where ten larvae in the nauplium phase were transferred to each of the test tubes. For white control, 5 mL of the saline solution was used for positive control $K_2Cr_2O_7$ and for negative control 5 mL of a 4 mg L^{-1} solution of Tween 80. After 24 h of exposure, the count of the live larvae was performed, considering dead those that did not move during observation or with the slight agitation of the vial.

The criterion established by Dolabela *et al.* [24] was adopted for classification of EOs toxicity, being considered highly toxic when $LC_{50} \leq 80$ mg L^{-1}, moderately toxic to 80 mg $L^{-1} \leq LC_{50} \geq 250$ mg L^{-1} and slightly toxic or nontoxic when $LC_{50} \geq 250$ mg L^{-1}. Statistical analysis of the data for the toxicity test was performed according to the Reed and Muench [25].

Antimicrobial activity

Four strains of bacteria were used: *Escherichia coli* (ATCC® 25922™) and *Staphylococcus aureus* (ATCC® 25923™). These were previously identified and confirmed by biochemical tests. Pure microbial cultures maintained in TSA Agar were peaked for brain and Heart Infusion Broth (HIB) and incubated at 35 °C until they reached exponential growth phase (4-6 h). After this period, the cultures had their cell density adjusted in 0.85% sterile saline solution, in order to obtain turbidity comparable to that of the standard McFarland solution 0.5, which results in a microbial suspension containing approximately $1.5x10^8$ CFU mL^{-1} according to Clinical and Laboratory Standards Institute [26].

The disc diffusion technique was performed according to the Clinical and Laboratory Standards Institute [26], which standardizes the sensitivity tests of antimicrobials by disc-diffusion. First, the plates were prepared with the Mueller Hinton Agar (MHA) culture medium after its solidification was distributed to the microbial suspension on the surface of the agar and left at room temperature for 30 min. Soon after the discs containing 50 μL of EOs and discs with defined concentrations of antibiotics. Using sterile tweezers, the discs were distributed on the surface of the agar. The plates were incubated in a bacteriological greenhouse at 35 °C for 24 h. The diameters of the inhibition halos were measured, including the diameter of the disc. These trials were done in triplicate. The values of the inhibition halos were the mean measurements of the three results. Tests performed in triplicate.

Results and discussion

Chemical profile of fresh leaves and drying

Figure 1 shows the chromatogram obtained for the fresh leaves of *B. orellana* L. Thirty compounds were identified in the fresh leaf of *B. orellana*, listed in table 2, of which are predominantly sesquiterpenes and hydrocarbons. The major components were isocaryophillene (26.58%), 1R-α-pinene (19.49%) and β-pinene (12.04%).

β-caryophillene present in the composition was described as being responsible for the anti-inflammatory, antibacterial, anti-endemic and antifungal action, analgesic and anti-inflammatory β-bisabolen [27]. And the karyophyllene oxide described as acting directly in the inhibition of fungi [28]. The compounds γ-muurolene and β-bisabolene were described as being responsible for microbial inhibition [29].

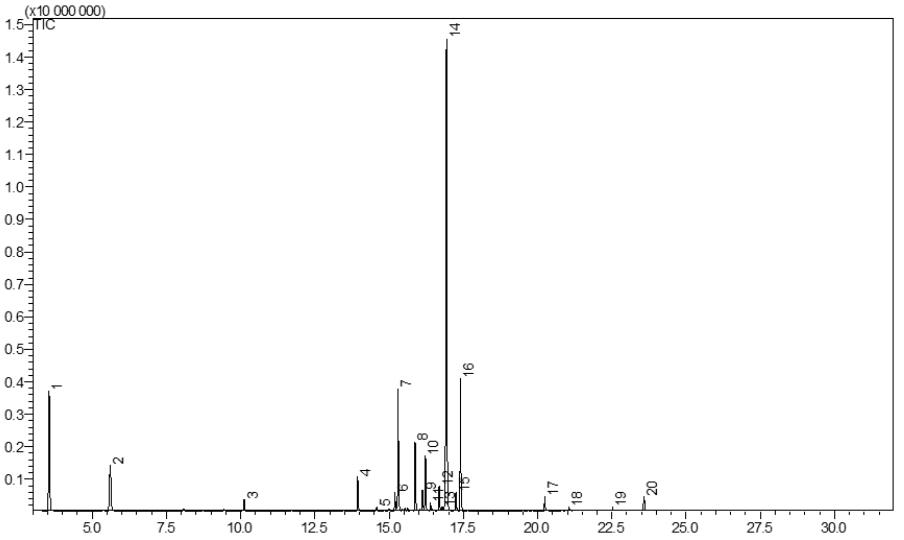

Figure 1. Chromatogram of fresh *B. orellana* leaves (annatto).

Figure 2 shows the drying curves of the annatto leaves *B. orellana* L. at temperatures of 35, 45 and 55 °C, represented by the moisture ratio as a function of time. It is possible to observe the influence of temperature on drying curves, presenting consistent reduction in drying times with temperature increase, providing curves with a typical exponential trend, behavior reported in products [18-21].

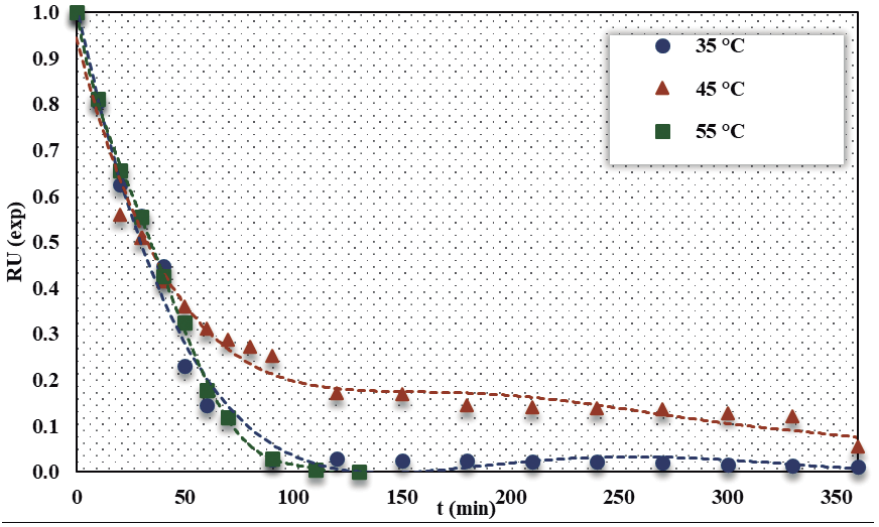

Figure 2. Drying curves of annatto leaves *B. orellana* L. at different temperatures.

Table 2. Chemical constituents identified in the fresh leaf of *B. orellana* (annatto).

Order	RT (min)	%	Compounds NIST08	Ret. Index
1	3.547	19.49	1R-α-pinene	948
2	5.583	12.04	(-)-β-pinene	943
3	8.063	0.80	β-myrcene	958
4	8.153	0.29	cyclobutanemethanol	-
5	8.726	0.14	limonene	-
6	9.452	0.16	n-hex-trans-2-enal	-
7	9.784	3.35	trans-ocimene	-
8	9.831	1.12	γ-terpinene	-
9	10.108	4.13	cis-β-ocimene	-
10	11.361	0.21	cis-3-hexenyl acetate	-
11	12.452	4.44	γ-hexenol	-
12	13.932	1.08	copaene	-
13	15.189	0.35	α-bergamotene	-
14	15.297	5.39	caryophyllene	-
15	15.868	1.11	α-guaiene	-
16	16.121	0.30	α-bergamotene	-
17	16.218	1.40	β-garnesene	-
18	16.682	1.30	isoledene	-
19	16.910	26.58	isocaryophillene	-
20	16.959	3.85	elixene	-
21	17.238	0.71	α-himachalene	-
22	17.397	4.44	isocaryophillene	-
23	20.242	0.18	nerolidol	-
24	20.785	0.23	ethyl tetradecyl ester	2832
25	21.245	0.16	phenoxethol	1212
26	22.524	0.13	di-epi-α-cedrene	1403
27	22.779	0.32	dimethyl phthalate;	1440
28	23.582	4.50	palatinol A	1639
29	26.100	0.98	pentadecanoic acid	1869
30	26.477	0.82	n-hexadecanoic acid	1968

This behavior is due to the higher rate of water removal from the product due to the higher energy transfer in the form of heat, caused by the increase in temperature [30]. This is based on the principle that by increasing the temperature the heat transfer to the leaves is increased, so the rate of migration of water from the interior to the surface-environment will be higher. In addition, there is a high correspondence between the data observed experimentally and the data estimated by the model, evidencing that the statistical indexes employed were effective to select the model.

Maximum drying times were around 11am for the temperature of 30 °C, 7 h for the temperature of 45 °C and 2 h for the temperature of 55 °C. Table 3 shows the statistical indices of the adjustments obtained through nonlinear regression using the Statistica 10 software of the mathematical models of Two Terms, Logarithm, Newton, Henderson and Pabis, Logistic to the experimental data of the kinetics of drying of annatto leaves and their respective coefficients of determination (R^2) and mean quadratic deviations (MDD). Used in the selection of mathematical models.

Table 3 presents the statistical criteria used to choose the models that best describe the drying process of *B. orellana* L leaves [31]. All adjusted models presented an adjusted coefficient of determination higher than 99%, except for the temperature of 45 °C where only the Verma model was higher than 0.9900.

Table 3. Adjustment of the analyzed models to the experimental data of the drying kinetics of the leaves of *B. orellana* L.

Model	35 °C		45 °C		55 °C	
	R^2	DQM	R^2	DQM	R^2	DQM
Two terms	0.9962	0.0335	0.9647	0.0973	0.9943	0.0496
Logarithm	0.9963	0.0334	0.9808	0.0808	0.9977	0.0318
Newton	0.9960	0.0346	0.9440	0.1208	0.9936	0.0526
Henderson and Pabis	0.9962	0.0335	0.9647	0.0973	0.9943	0.0496
Logistic	0.9962	0.0335	0.9647	0.0973	0.9943	0.0496
Verma	0.9965	0.0322	0.9912	0.0472	0.9943	0.0496

Thus, this being a criterion for selecting the models we could infer that the satisfactory models to predict the drying of the species would be the Verma and Logarithm models. As emphasized by Madamba *et al.* [32] and Almeida *et al.* [33], in addition to the coefficient of determination (R^2) to better predict the most satisfactory model, the NDMD (deviation for estimation) applies. Based on this, it can be seen that for the same models this parameter remained acceptable.

Figure 3 presents examples of waste distribution observed in this work, being a random distribution (a) and a biased (b) for the Verma and Logarithm models for drying at 35 °C, respectively, in the adjustment of b drying data.

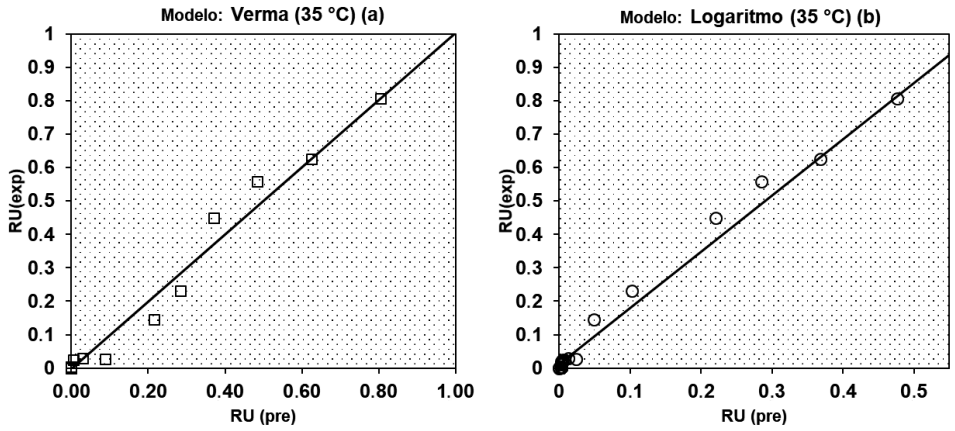

Figure 3. Distribution of residues randomly (a) and a biased (b) for Verma and logarithm models at 35 °C.

In figure 4 and figure 5 show the distribution of residues for the temperatures of 45 and 55 °C, respectively, for both models. The results found are similar to the temperature of 35 °C, with random distribution (a) and a biased (b) for the Verma and logarithm models.

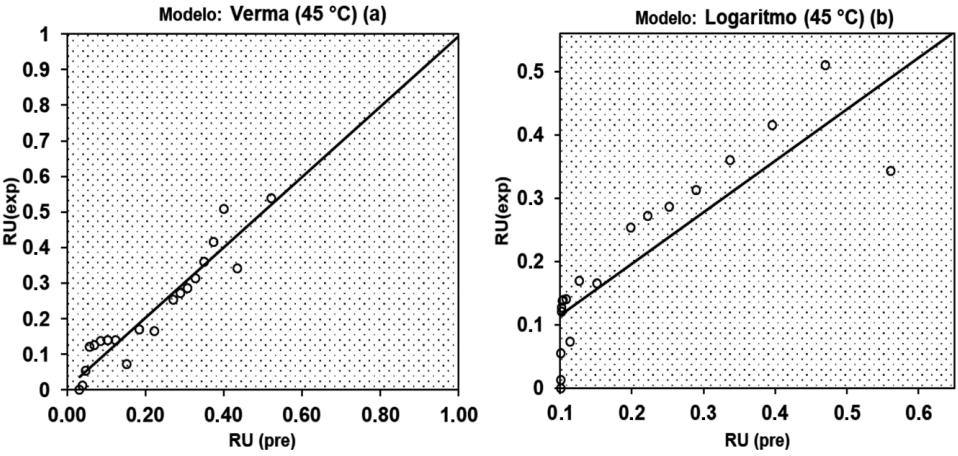

Figure 4. Distribution of residues randomly (a) and a biased (b) for verma and logarithm models at 45 °C.

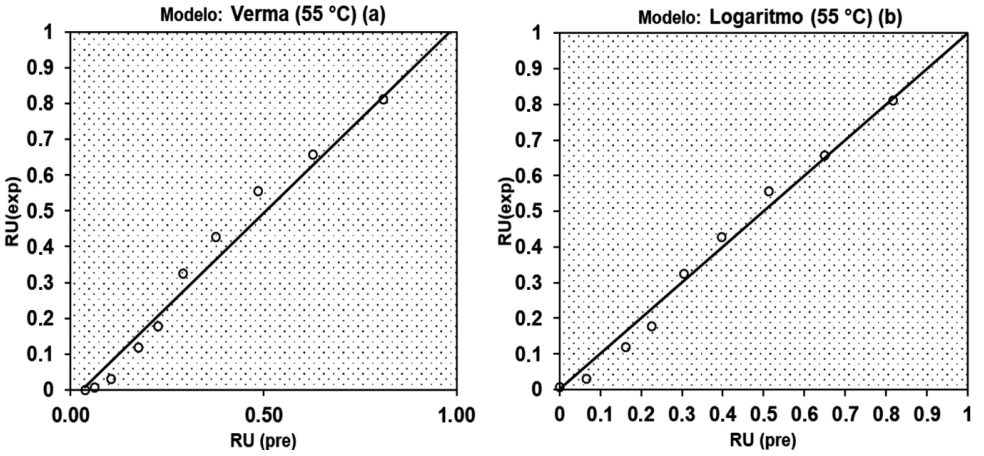

Figure 5. Distribution of residues randomly (a) and a biased (b) for Verma and logarithm models at 55 °C.

The distribution of residuals is a subjective evaluation, but usually a model is considered acceptable if the residual values are in a horizontal zone close to zero, forming random distributions. If the distributions of the residues form geometric figures, present regions in which the model underestimates or overestimates the actual condition or tends to accumulate at a point outside the axis, the distribution of its residues is considered biased and the model is to represent the phenomenon in question [34].

One of the criteria also commonly used for model selection is the standard error of the analysis of the residues and according to Reis *et al.* [35] values lower than 1 indicate a good fit of the models. Both Verma and Logarithm models were also within this criterion since the parameter values observed in table 4 were relatively low.

Table 4. Standard error obtained for adjusting the models.

Model	Standard error		
	35 °C	45 °C	55 °C
Two terms	0.0655	0.0425	0.0745
Logarithm	0.0652	0.0517	0.0626
Newton	0.0659	0.0664	0.0685
Henderson and Pabis	0.0682	0.0425	0.0745
Logistic	0.0682	0.0425	0.0745
Verma	0.0695	0.0465	0.0745

The aim was to recommend a model that had the widest possible scope to describe the drying kinetics. Thus, among the recommended models, Verma was selected, since it was the only model with adequate adjustment to describe drying in all proposed conditions. The Verma model is a traditional model, often recommended to describe the drying of agricultural products in works similar to this [34, 36, 37].

According to Coradi *et al.* [38], the increase in drying air temperature causes the deterioration of the material and consequently alters the integrity of the cell structure. Thus, possibly at a temperature of 45 °C, the cell membrane system remained intact, and was more resistant to water removal, explaining the drying time. Because of this the temperature of 45 °C made it possible to obtain the smallest error for the models tested among this one of Verma, which was the model chosen for the representation. Since the drying process can interfere with the biologically active principle of medicinal plants, greater knowledge about the chemical properties of *B. orellana* L becomes necessary.

Chemical profile of dry leaves at 45 °C

Figure 6 shows the chromatogram obtained for dry leaves at 45 °C of *B. orellana* L.

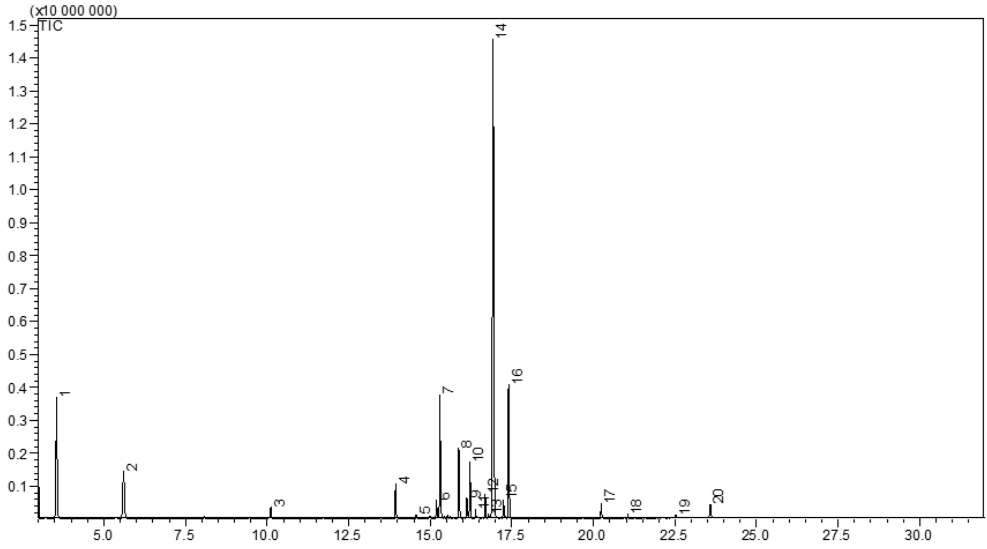

Figure 6. Chromatogram obtained for dry leaves of *B. orellana* L. at 45 °C.

Twenty compounds were identified in the dry leaf at 45 °C of *B. orellana* (table 5). The major components were β-bisabolene (42.45%), 1R-α-pinene (11.82%), β-farnesene (9.54%), caryophyllene (9.01%), β-pinene (5.84%) and α-guaiene (5.15%).

Table 5. Chemical constituents identified in EO of dry leaves at 45 °C of *B. orellana* (annatto).

Order	RT (min)	%	Compounds NIST08	Ret. Index
1	3.547	11.82	1R-α-pinene	948
2	5.601	5.84	(-)-β-pinene	943
3	10.112	0.79	cis-β-ocimene	976
4	13.934	2.30	copaene	1221
5	14.574	0.24	isoledene	1419
6	15.191	1.28	bergamotene	1425
7	15.299	9.01	caryophyllene	1494
8	15.871	5.15	α-guaiene	1490
9	16.121	1.36	β-cedrene	1398
10	16.218	3.85	(Z)-β-Farnesene	1440
11	16.386	0.48	β-farnesene	1440
12	16.682	1.78	isoledene	1419
13	16.782	0.29	valencene	1474
14	16.927	42.45	β-Bisabolene	1500
15	17.241	1.28	α-patchoulene	1403
16	17.399	9.54	β-farnesene	1440
17	20.239	0.88	trans-nerolidol	1564
18	21.056	0.25	spathulenol	1536
19	22.521	0.21	α-bergamotene	1430
20	23.580	1.20	palatinol A	1639

Therefore, when comparing these results to the studies by Amorim *et al.*[39] and Viuda-Martons *et al.* [40] on the composition of the EO of *B. orellana* L. leaves, differences were found in relation to the chemical substances present and their concentrations. Rather *et al.* [41] also studied the chemical characterization of *B. orellana* L. seeds and found twenty-four substances, among them, the ones with the highest concentrations were: ishwarane (18.6), β-farnesene (10.52%) and caryophyllene (8.01%). These variations of substances and their quantities can be attributed mainly to environmental conditions, plant age and harvesting methods. Possibly the habitat of the plant contributed to the different substances and their concentrations, since the climate and soil type [42].

Due to the drying conditions of 45 °C temperature, some substances showed variation in their concentration, such as 1R-α-pinene oxide and β-pinene (5.84%) that showed an increase in the mean concentration with the increase in drying temperature, isocaryophyllene was not found with the drying of the leaf at 45 °C, possibly, with the increase in temperature and speed of the drying air, the volatilization of some substances, causing their concentrations to be reduced, evidencing the thermosensitivity of these substances. It is believed that the stress caused by drying induces an increase in the terpene content in dry plants, compared to the fresh plant [43].

Physicochemical parameters of Eos

After drying at established temperatures, The EO's were extracted and their physicochemical properties were determined. The physicochemical parameters of EOs are important not only for quality determination, but also for the control of their purity. The results are presented in table 6.

Table 6. Physicochemical EO parameters of *B. orellana* L. leaves (annatto).

EO	Density	Refractive index	Color	Yield
EO 35°C	0.9998 (g mL^{-1})	1.4200 (n_D 25 °C)	Yellow	0.21 %
EO 45°C	1.0779 (g mL^{-1})	1.5300 (n_D 25 °C)	Yellow	2.23 %
EO 55°C	1.0500 (g mL^{-1})	1.4900 (n_D 25 °C)	Yellow	0.38 %

A small change in density and refractive index was observed, with the increase in temperature. Unlike the other parameters, the color did not present visual differentiation of the extracted EOs. The drying temperature mainly influenced the yield of the applied process, and a yield of 2.23% was observed for the EO obtained from the dry leaves at 45 °C, being an extremely significant increase. Martins *et al.* [44] reports that temperatures above 45 °C damage plant organs and their contents, as they cause a "cooking" of plants and not a drying. Thus, reflecting that even with the temperature of 55 °C processing the product faster, part of it is quantitatively lost.

EO's are heat-sensitive substances, so increasing the temperature of the drying air can volatilize these compounds, resulting in lower extractive yield [45, 46]. In relation to the yield of the EO obtained from the leaves dried at 45 °C, according to what was also reported by Souza *et al.* [30] the grinding facilitated the extraction, because it exposed the structures that contained the EO to the process and increased the contact surface of the leaves with the water used hydrodistillation. Giwa-Ajeniya *et al.* [47] found similar results when they evaluated the yield of EO through hydrodistillation of *B. orellana* leaves in the Alimosho area, Lagos State, Nigeria.

Schimitbertger *et al.* [48], Ahmed *et al.* [46], Memarrzadeh *et al.* [49] and Sefidkon *et al.* [50] made a visual evaluation of the staining of EOs obtained in their studies. Regarding the color, it was visually verified that the color of the extracted EO presented pale yellowish coloration. This difference in color was justified by differences in chemical composition. Comparing the values for the EO studied with those of the literature, it can be observed that there was a similarity in the temperature range 35-55 °C, with regard to the parameters analyzed. The small differences in the values found can be attributed to factors such as collection time, different soil types, conditions and storage time.

Antimicrobial activity of EO's

The Disc Diffusion Method was evaluated for each of the EOs obtained their bactericidal potentials. The result of this assay is visualized by an inhibition halo formed by the ability of EO to inhibit microbial growth. The diameters of the inhibition halos for the action of The EO's against the bacteria are presented in table 7.

According to Moreira *et al.* [51], bacteria are considered sensitive to the action of EO's when they present inhibition halos greater than 9 mm in view of the action of these natural products. From this classification, it was possible to verify that *E. coli* was sensitive only to the action of EO extracted by drying *B. orellana* L. at 45 °C. For *S. aureus* only the EO of 55 °C showed no bactericidal activity and the temperature of 35 °C was not sensitive.

Table 7. Diameter of inhibition halos (mm) for EO action against the tested microorganisms.

Microorganisms	GEN (30 μg)	EO 35°C	EO 45 °C	EO 55 °C
E. coli (ATCC 25922)	25 mm	NI	12 mm	NI
S. aureus (ATCC 25923)	27 mm	7 mm	21 mm	NI

Note: *NI: there was no inhibition of the microorganism by the action of the EO tested.

The results observed in the disc diffusion test presented in table 7 show that EO obtained by drying *B. orellana* L. at 45 °C was more efficient in inhibiting *S. aureus* bacteria, revealing a 21 mm inhibition halo, comparing to EO obtained using the temperature of 35 °C where it inhibited the same bacterium by only 7 mm, while the EO obtained from the dry plant at 55 °C did not present bactericidal biological potential. Therefore, the bactericidal potential was definitive in the choice of drying temperature.

For the Bacterium *E. coli*, the drying temperature again influenced the biological potential of the EO. The EO obtained from the dry leaves at 45 °C presented the best

bactericidal performance with a halo of 12 mm and again the EO of 55 °C did not present bactericidal potential as well as the EO of 35 °C.

Studies have already reported the inhibitory action of annatto on *S. aureus*. Gonçalves *et al.* [52] performed tests with commercial annatto seed extract on Gram-positive bacteria including *S. aureus* and proved that it presented antimicrobial activity inhibition halos of 15 mm. In another research done by Silva *et al.* [53] confirmed antimicrobial activity of mature seed extract on the bacterium *S. aureus* and *E. coli* with halo of 18 mm and 12 mm in diameter, respectively.

Several authors have analyzed the bactericidal activity of leaf EO for the bacteria *S. aureus* and *E. coli*. Enciso-Díaz *et al.* [54] using the extract of *Eucalyptus globulus* (eucalyptus), observed that the inhibition halos were similar to that of annatto at 45 °C, being 22.5 mm for *S. aureus* and 8 mm for *E. coli*. Moreover, with the aqueous extract of *Eucalyptus globulus* González-Burgosa *et al.* [55] reported that there was no longer inhibition for *E. coli*, having only inhibition in the growth of *S. aureus* with a halo of inhibition of less than 15 mm. The potential for inhibition in annatto is justified by Majolo *et al.* [56], which explains that the potential of the plant is due to the presence of artemisin (sesquiterpene), known for its anti-malarial properties, which have the ability to complex proteins and bacterial cell wall, causing its lysis.

Toxicity of Eos

The results obtained in the toxicity assay of The EO's are presented in table 8, respectively, where it is possible to observe that the increase in lethal concentration increases with increasing temperature. At all temperatures, the EO of *B. orellana* leaves showed nontoxic.

Table 8. LC_{50} for EOs action against *Artemia salina*.

EO	LC_{50}	Classification
EO 35 °C	261.11 mg L^{-1} ± 5.10	Nontoxic
EO 45 °C	280.25 mg L^{-1} ± 2.30	Nontoxic
EO 55 °C	315.44 mg L^{-1} ± 4.44	Nontoxic

The *in vitro* toxicity assay against *Artemia salina* is a fast and low-cost bioassay and has been one of the most used tools for preliminary toxicity assessment and can be used in the screening of new antispasmodic drugs and antimalarials [57, 58]. Toxicity is classified from obtaining LC_{50} (Lethal Concentration 50%) for the action of The EO against larvae of *Artemia salina* Leach. A LC_{50}. Many studies have shown that the tox-

icity of a compound against *Artemia salina* correlates with cytotoxic activity against human tumors, McLaughlin *et al.* [59] reported that this bioassay led to the discovery of a new class of agents active antitumor (*Annonaceous acetogenins*), and is also related to activity against *Trypanosoma cruzi*, a protozoan causing chagas disease [60, 61], with viruscidal, antifungal and antimicrobial activity [62].

In a study conducted by Kumar *et al.* [63] when using extracts from the leaves of *B. orellana* showed a non-toxic effect against *Artemia salina*, demonstrating that extracts from other parts of the same plant may contain different active ingredients, which can toxically effect against the same tested species. Vilar *et al.* [64] found that the roots showed negative results for toxicity for *Artemia salina*.

Chemical EO profile of dry leaves at 45 °C

Figure 7 shows the chromatogram obtained for EO from the leaves of *B. orellana* L at 45 °C.

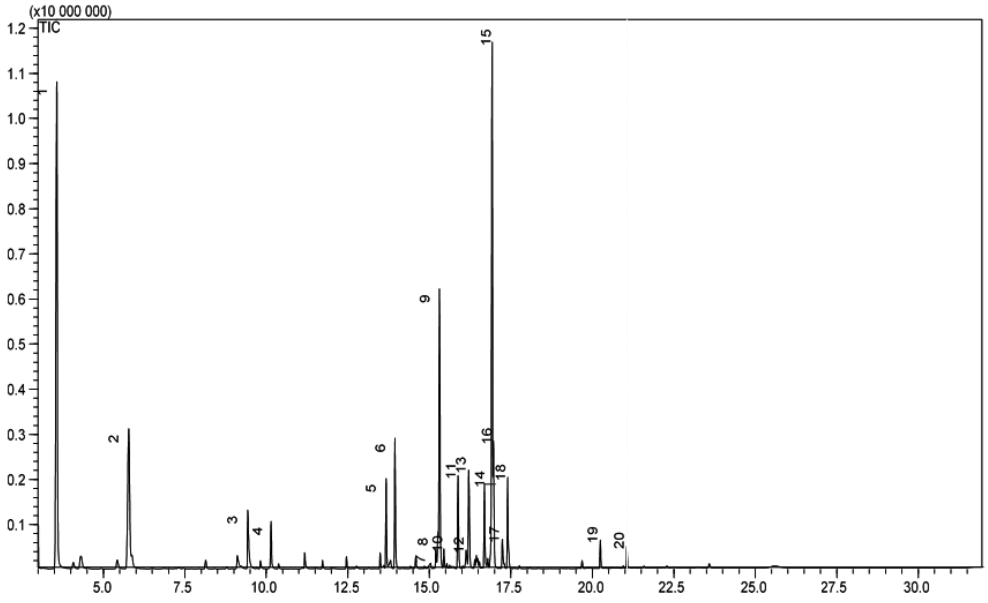

Figure 7. Chromatogram obtained for EO from the leaves of *B. orellana* L at 45 °C.

Twenty compounds were identified in the EO of the dry leaf at 45 °C, listed in table 9, of which are predominantly sesquiterpenes and hydrocarbons. The major components were 1R-α-pinene (26.5%), β-bisabolene (19.71%), caryophyllene (10.42%) and β-pinene (9.23%).

Table 9. Chemical constituents identified in EO of dry leaves at 45 °C.

Order	RT(min)	%	Compounds NIST08	Ret. Index
1	3.569	26.50	1R-α-pinene	948
2	5.777	9.23	(-)-β-pinene	943
3	9.431	2.55	2-trans-hexenal	814
4	10.141	1.55	β-cis-ocimene	976
5	13.670	2.83	α-chamigrene	1512
6	13.944	4.28	copaene	1221
7	15.197	0.60	α-bergamotene	1430
8	15.260	1.20	β-elemene	1398
9	15.309	10.42	caryophyllene	1494
10	15.443	0.61	allo-Aromadendrene	1386
11	15.876	3.28	γ-gurjunene	1461
12	16.127	0.59	β-Cedrene	1398
13	16.207	4.05	α-Caryophyllene	1579
14	16.686	2.92	isoledene	1419
15	16.923	19.71	β-bisabolene	1500
16	16.965	3.95	α-chamigrene	1512
17	17.238	0.93	δ-cadinene	1469
18	17.399	3.26	β-cedrene	1398
19	20.241	0.86	Nerolidol	1564
20	21.058	0.68	Spathulenol	1536

Pino and Correa [65] analyzed the chemical constitution of EO from annatto seeds by GC/MS, 73 compounds were detected, of which 65 compounds (80.1%) were identified, ishwarane was the main component, constituting 18.6% of the composition of The EO, followed by geranylgeraniol (9.1%), bicyclogermacrene (8.4%), germacrene D (6.9%) and δ-selinene (6.2%).

Discordant results were found by Giwa-Ajeniya *et al.* [47], who verified in EO samples of *B. orellana* leaves, from Nigeria, higher α-guaiene contents (49.3%), together with guaiol (8.1%), valenceno (7.7%) and β-elemeno (5.9%). As well as Silva *et al.* [66] under study with the EO of the roots. The major constituents were α-guaieno (25.0%), espathulenol (12.0%) and β-cayophyllene (9.7%). However, several monoterpenes

were found in the annatto extracts of the seeds, with a higher amount of monoterpene hydrocarbons (45.0%). Among the major constituents α-pinene (29.1%), β-pinene (14.5%), germacreno D (10.0%) and espatulenol (9.0%) compounds [67].

It is noteworthy that ishwarane, one of the main compounds of leaf oils and seeds of *B. orellana* was not present in the study sample. This can be explained by environmental factors such as location of the species and climate of the region. In the literature there are still few studies published, with the need for further studies of the EO of the leaves of *B. orellana* L.

Through the results obtained, it is possible to conclude that the increase in drying temperature promoted a reduction in dehydration times. The Verma and logarithm models presented the highest coefficients of determination ($R^2 > 0.98$) and the lowest mean quadratic deviations (DQM < 0.10), however, the Verma model was the only one with random distribution of the residues of the studied temperatures. The drying temperature at 45 °C is the most indicated for the species *Bixa orellana* L., in this study. Since, at this temperature, it presented the best yield, the best bactericidal activity of the essential oil obtained, thus encouraging its application potential.

Acknowledgments

The authors thank Laboratório de Pesquisa e Aplicação de Óleos Essenciais (PCQA-UFMA) and Universidade Federal do Maranhão (UFMA).

Disclosure statement

No potential conflict of interest was reported by the authors.

References

1. J.A. Campos, N.J.F. de Oliveira, J.S.V. Chamba, F. Colen, C.A. da Costa, A. da Silva-Santos Filho, Brotação de ora-pro-nóbis em substrato alternativo de casca de arroz carbonizada, *HOLOS*, **7**, 148-167 (2017).

2. A.G. Atanasov, B. Waltenberger, E.-M. Pferschy-Wenzig, *et al.*, Discovery and resupply of pharmacologically active plant-derived natural products: A review, *Biotechnol. Adv.*, **33**, 1582-1614 (2015).

3. V.B.R. Sousa, *Efeito antimicrobiano e fenólicos totais de extratos aquosos de erva cidreira (Lippia alba), capim limão (Cymbopogon citratus) e eucalipto (Eucaliptus globulus)* (B. Sc. thesis), Universidade Federal do Maranhão, São Luís, Maranhão, Brazil, 2018.

4. R.L. Ferreira, A.D. de L. Coelho-Novembre, Teste de germinação de sementes de urucum (*Bixa Orellana* L.). *Multi-Sci. J.*, **1**, 46-52 (2015).

5. P.P. Gasparin, D. Christ, S.R.M. Coelho, Secagem de folhas *Mentha piperita* em leito fixo utilizando diferentes temperaturas e velocidades de ar. *Rev. Ciênc. Agronôm.*, **48**, 242-250 (2017).

6. A.P. Martinazzo, E.D.C. Melo, A.J. Demuner, P.A. Berbert, Avaliação do óleo essencial folhas de *Cymbopogon citratus* (DC.) Stapf após o processo de secagem, *Bol. Latinoam. Caribe Plant. Med. Aromát.*, **12**, 523-536 (2013).

7. A. Castro, E. Mayorga, F. Moreno, Mathematical modelling of convective drying of fruits: A review, *J. Food Eng.*, **223**, 152-167 (2018).

8. D.R.H. Lemos, E. de Castro-Melo, R.P. Rocha, L.C. de Almeida-Barbosa, A.L. Pinheiro, Influence of drying air temperature on the chemical composition of the essential oil of melaleuca, *Revista Engenharia na Agricultura*, **20**, 5-11 (2012).

9. Y. Ozdemir, H. Yavas, U. Ozyurt, Olive semidrying process: oleuropein degradation in relation to sensory bitterness, *J. Food Sci. Nutr.*, **1**(2), 1-8 (2018).

10. S.M. Mirzahosseini, S.A.S. Noori, Y. Amanzadeh, M.G. Javid, M.S. Howyzeh, Phytochemical assessment of some native ajowan (*Therachyspermum ammi* L.) ecotypes in Iran, *Ind. Crops Prod.*, **105**, 142-147 (2017).

11. M.S. Howyzeh, S.A.A. Noori, V. Shariati, Essential oil profiling of Ajowan (*Trachyspermum ammi*) industrial medicinal plant, *Ind. Crops Prod.*, **119**, 255-259 (2018).

12. M. Modarresi, M.R. Farahpour, B. Baradaran, Topical application of *Mentha piperita* essential oil accelerates wound healing in infected mice model, *Inflammopharmacology*, **27**, 531-537 (2019).

13. F. Bakkali, S. Averbeck, D. Averbeck, M. Idaomar, Biological effects of essential oils, a review, *Food Chem. Toxicol.*, **46**, 446-475 (2008).

14. M.F. Andrés, A. González-Coloma, J. Sanz, J. Burillo, P. Sainz, Nematicidal activity of essential oils: a review, *Phytochem. Rev.*, **11**, 371-390 (2012).

15. J. Gutierrez, C. Barry-Ryan, P. Bourke, The antimicrobial efficacy of plant essential oil combinations and interactions with food ingredients, *Int. J. Food Microbiol.*, **124**, 91-97 (2008).

16. M. Hyldgaard, T. Mygind, R.L. Meyer, Essential oils in food preservation: mode of action, synergies, and interactions with food matrix components, *Front. Microbiol.*, **3**, 12 (2012).

17. ANVISA, *Descrição dos meios de cultura empregados nos exames microbiológicos*, Brazil, 2010.

18. H.V. Alexandre, F.L. da Silva, J.P. Gomes, O.S. da Silva, J.P. Carvalho, E.E. de Lima, Cinética de secagem do resíduo de abacaxi enriquecido, *Rev. Bras. Eng. Agric. Amb.*, **17**, 640-646 (2013).

19. J.J.A. Martins, J.I. Marques, D. da Costa-Santos, A.P.T. Rocha, Modelagem matemática da secagem de cascas de mulungu, *Biosci. J.*, **30**, 1652-1660 (2014).

20. J.C. Melo, E.D. Pereira, K.P. Oliveira, C.H. Costa, R.M. Feitosa, Estudo da cinética de secagem da pimenta de cheiro em diferentes temperaturas, *Revista Verde (Pombal-PB-Brasil)*, **10**, 9-14 (2015).

21. J.Q. Gonçalves, M.A.P. da Silva, G.R. Plácido, M. Caliari, R.M. Silva, L.C. Moura, D.G. Souza, Secagem da casca e polpa da banana verde (*Musa acuminata*): propriedades físicas e funcionais da farinha, *Global Sci. Technol.*, *Rio Verde*, **9**, 62-72 (2016).

22. *Farmacopéia Brasileira*, Agência Nacional de Vigilância Sanitária, Brazil, 2010.

23. S. Meyer, W. House, R. Welch, Some metabolic interrelationships between toxic levels of cadmium and nontoxic levels of selenium fed to rats, *J. Nutrition*, **112**, 954-961 (1982).

24. M. Dolabela, *Triagem in vitro para atividade antitumoral e anti Trypanossoma cruzi de extratos vegetais, produtos naturais e substâncias sintéticas* (M. Sc. thesis), Instituto de Ciências Biológicas, Universidade Federal de Minas Gerais - UFMG, Belo Horizonte, 1997, p.128.

25. L.J. Reed, H. Muench, A simple method of estimating fifty per cent endpoints, *Am. J. Hygiene*, **27**, 493-497 (1938).

26. CLSI, *Performance Standards for Antimicrobial Susceptibility Testing*, 28th ed., CLSI Supplement M100, Clinical and Laboratory Standards Institute, Wayne, PA, 2018.

27. F. Pieri, V. Silva, C. Souza, J. Costa, L. Santos, M. Moreira, Antimicrobial profile screening of two oils of Copaifera genus, *Arq. Bras. Med. Vet. Zootecn.*, **64**, 241-244 (2012).

28. V.F. Veiga-Junior, A.C. Pinto, O gênero *copaifera* L, *Quím. Nova*, **25**, 273-286 (2002).

29. M.J. Marques de Faria, C. Afonso da Silva-Bitencourt-Braga, J.R. de Paula, *et al.*, Antimicrobial activity of *copaifera* spp. against bacteria isolated from milk of cows with mastitis, *Cienc. Anim. Bras.*, **18**, 1-14, e-39068 (2017).

30. K.A. de Sousa, O. Resende, T.H. Chaves, L.M. Costa, Cinética de secagem do nabo forrageiro (*Raphanus sativus* L.), *Rev. Ciênc. Agronôm.*, **42**, 883-892 (2011).

31. C. Ertekin, M.Z. Firat, A comprehensive review of thin-layer drying models used in agricultural products, *Crit. Rev. Food Sci. Nutr.*, **57**, 701-717 (2017).

32. P.S. Madamba, R.H. Driscoll, K.A. Buckle, The thin-layer drying characteristics of garlic slices, *J. Food Eng.*, **29**, 75-97 (1996).

33. F.N.C. Almeida, J.V. Berni, J.F. Medeiros, N.W. Siqueira, N.C. Pereira, *Cinética da secagem da semente de Moringa oleifera LAM*, XXXVII Congresso Brasileiro de Sistemas Particulados, Universidade Federal de São Carlos, SP, 2015.

34. F.M. Botelho, T.R.B. Garcia, J.L. Viana, S.D.C.C. Botelho, A.M.B. de Sousa, Cinética de secagem e determinação do coeficiente de difusão efetivo de grãos de sorgo. *Rev. Bras. Milho Sorgo*, **14**, 260-272 (2015).

35. R.C. de Reis, I.A. Devilla, D.P. Ascheri, A.C. Servulo, A. Souza, Cinética de secagem de folhas de manjericão (*Ocimum basilicum* L.) via infravermelho, *Rev. Bras. Eng. Agríc. Amb.*, **16**, 1346-1352 (2012).

36. S.K. Pandey, S. Diwan, R. Soni, Review of mathematical modelling of thin layer drying process, *Int, J. Curr. Eng. Sci. Res.*, **3**, 96-107 (2015).

37. D.E.C. de Oliveira, O. Resende, J. Bessa, A. Kester, T.A.S. Smaniotto, Mathematical modeling and thermodynamic properties for drying soybean grains, *African J. Agricult. Res.*, **10**, 31-38 (2014).

38. P.C. Coradi, A. Müller, D.A. Schmidt, R.E. Lima, F.H.R. Baio, A.V. Borsato, M. Blanco, Electric conductivity test for quality assessment of aromatic and medicinal plants after drying, *Drying Technol.*, **36**, 545-556 (2018).

39. P.K. Amorim, *Purificação, caracterização e avaliação de atividade antimicrobiana de lectina de folha de Bixa orellana L.*, M. Sc. thesis, Universidade Federal de Pernambuco, Recife, Brazil, 2018.

40. M. Viuda-Martos, G.L. Ciro-Gómez, Y. Ruiz-Navajas, J.E. Zapata-Montoya, E. Sendra, J.A. Pérez-Álvarez, J. Fernández-López, *In vitro* antioxidant and antibacterial activities of extracts from annatto (*Bixa orellana* L.) leaves and seeds, *J. Food Safety*, **32**, 399-406 (2012).

41. S.U. Rather, Trimetallic catalyst synthesized multi-walled carbon nanotubes and their application for hydrogen storage, *Korean J. Chem. Eng.*, **33**, 1551-1556 (2016).

42. T. Misharina, Influence of the duration and conditions of storage on the composition of the essential oil from coriander seeds, *Appl. Biochem. Microbiol.*, **37**, 622-628 (2001).

43. J. Chao, Y. Dai, H.Y. Cheng, *et al.*, Improving the concentrations of the active components in the herbal tea ingredient, *Uraria crinita*: The effect of post-harvest oven-drying processing, *Sci. Reports*, **7**, 38763 (2017).

44. E. Martins, Estudos em *Ocimum selloi* Benth: isoenzimas, morfologia e óleo essencial, *Plant Med. Arom. Condiment.: Avanç. Pesq. Agronôm.*, *São Paulo: UNESP*, **217**, 97-126 (1998).

45. M.T. Ebadi, M. Azizi, F. Sefidkon, N. Ahmad, Influence of different drying methods on drying period, essential oil content and composition of *Lippia citriodora* Kunth, *J. Appl. Res. Med. Arom. Plants*, **2**, 182-187 (2015).

46. A. Ahmed, K. Ayoub, A.J. Chaima, L. Hanaa, C. Abdelaziz, Effect of drying methods on yield, chemical composition and bioactivities of essential oil obtained from Moroccan *Mentha pulegium* L. *Biocatal. Agricult.uBiotechnol.*, **16**, 638-643 (2018).

47. A.O. Giwa-Ajeniya, A. Ademefun, O.A. Lawal, I.A. Ogunwande, Chemical composition of essential oils from the leaves, seeds, seed-pods and stems of *Bixa orellana* L. (Bixaceae), *Arch. Curr. Res. Int.*, **6**(3), 1-6, 2016.

48. V.M.B. Schimitberger, D.L. de Almeida-Pratti, L.C. Cavalcanti, V.F. Ramalho, A.P.F. da Costa, R. Scherer, R.M. Kuster, A.C. Ramos, A.G. da Silva, Volatile compounds profile changes from unripe to ripe fruits of Brazilian pepper (*Schinus terebinthifolia* Raddi), *Ind. Crops Prod.*, **119**, 125-131 (2018).

49. S.M. Memarzadeh, A.G. Pirbalouti, M. AdibNejad, Chemical composition and yield of essential oils from Bakhtiari savory (*Satureja bachtiarica* Bunge.) under different extraction methods, *Ind. Crops Prod.*, **76**, 809-816 (2015).

50. F. Sefidkon, K. Abbasi, Z. Jamzad, S. Ahmadi, The effect of distillation methods and stage of plant growth on the essential oil content and composition of *Satureja rechingeri* Jamzad, *Food Chem.*, **100**, 1054-1058 (2007).

51. M. Moreira, A. Ponce, C. del Valle, S. Roura, Inhibitory parameters of essential oils to reduce a foodborne pathogen, *LWT-Food Sci. Technol.*, **38**, 565-570 (2005).

52. A. Gonçalves, A. Alves Filho, H. Menezes, Estudo comparativo da atividade antimicrobiana de extratos de algumas árvores nativas, *Arq. Inst. Biol.*, **72**, 353-358 (2005).

53. S. Oliveira-Silva, J. Marques de Carvalho, E.C. Pereira, L.M. da Cunha Lima-Melo, R. dos Santos -Araújo, Atividade antimicrobiana e caracterização físico-química de urucum (*Bixa orellana* L.) em diferentes estádios de maturação, *Rev. Bras. Prod. Agroind.*, *Campina Grande*, **20**, 49-57 (2018).

54. O.J. Enciso-Díaz, A. Méndez-Gutiérrez, L.H. de Jesús, A. Sharma, M.L. Villarreal, A.C. Taketa, Antibacterial activity of *Bougainvillea glabra*, *Eucalyptus globulus*, *Gnaphalium attenuatum*, and propolis collected in Mexico, *Pharmacol. Pharm.*, **2012**; 3, 433-438 (2012).

55. E. González-Burgos, M. Liaudanskas, J. Viškelis, V. Žvikas, V. Janulis, M.P. Gómez-Serranillos, Antioxidant activity, neuroprotective properties and bioactive constituents analysis of varying polarity extracts from *Eucalyptus globulus* leaves, *J. Food Drug Anal.*, **26**, 1293-1302 (2018).

56. C. Majolo, H.H. Carvalho, J.M. Wiest, Atividade antibacteriana "*in vitro*" de diferentes acessos de urucum (*Bixa orellana* L.) e sua relação com o teor de bixina presente nas sementes, *Bol. Centr. Pesq. Process. Aliment.*, *Curitiba*, **31**, 115-124 (2013).

57. O. Ameen, L. Usman, I. Oladosu, N. Olawore, I. Ogunwande, Bioactivity of rhizome essential oils from two varieties of *Cyperus articulatus* (L.) grown in Nigeria, using brine shrimp (*Artemia salina*) lethality tests, *J. Med. Plants Res.*, **5**, 1031-1033 (2011).

58. B.G. Kpadonou-Kpoviessi, E.Y. Ladekan, D.S. Kpoviessi, *et al.*, Chemical variation of essential oil constituents of *Ocimum gratissimum* L. from Benin, and impact on antimicrobial properties and toxicity against *Artemia salina* Leach, *Chem. Biodivers.*, **9**, 139-150 (2012).

59. J.L. Mclaughlin, L.L. Rogers, J.E. Anderson, The use of biological assays to evaluate botanicals, *Drug Inf. J.*, **32**, 513-524 (1998).

60. T.M. de Almeida-Alves, A. Fonseca-Silva, M. Brandão, T.S. Mesquita-Grandi, E. de F. A. Smânia, A. Smânia Júnior, C.L. Zani, Biological screening of Brazilian medicinal plants, *Mem. Inst. Oswaldo Cruz*, **95**, 367-373 (2000).

61. C.L. Zani, P.P.G. Chaves, R. Queiroz, A.B. de Oliveira, J.E. Cardoso, A.M.G. Anjos, T.S.M. Grandi, Brine shrimp lethality assay as a prescreening system for anti-*Trypanosoma cruzi* activity, *Phytomedicine*, **2**, 47-50 (1995).

62. W. McRae, J. Hudson, F. Towers, Studies on the pharmacological activity of Amazonian Euphorbiaceas, *J. Ethnopharmacol.*, **22**, 143-172 (1988).

63. S.B. Aseervatham, J. Sasikumar, D. Kumar, Studies on in vitro free radical scavenging activity of *Bixa orellana* L. bark extract, *Int. J. Pharm. Pharm. Sci.*, **4**, 719-726 (2012).

64. D. de A. Vilar, *Estudo fitoquímico da bixina e fração oleosa extraídos da Bixa orellana biomonitorado pela atividade leishmanicida*, Ph. D. thesis, Universidade Federal da Paraíba, João Pessoa, Paraíba, Brazil, 2015.

65. J.A. Pino, M.T. Correa, Chemical composition of the essential oil from annatto (*Bixa orellana* L.) seeds, *J. Essent. Oil Res.*, **15**, 66-67 (2003).

66. R.B. Silva, C.R. Almeida, J.M. Chavasco, J.K. Chavasco, Antimycobacterial activity evaluation and MIC determination of liophilizated hydroalcoholic extracts of *Bixa orellana* L., Bixaceae, *Rev. Bras. Farmacogn.*, **20**, 171-174 (2010).

67. V. Galindo-Cuspinera, M.B. Lubran, S.A. Rankin, Comparison of volatile compounds in water-and oil-soluble annatto (*Bixa orellana* L.) extracts, *J. Agric. Food Chem.*, **50**, 2010-2015 (2002).

How to cite this article

G. Oliveira-Everton, E. Holanda-Sales, N. Silva Costa-Mafra, R.J. Araújo, P.S. Santos-Júnior, P.V. Serra-Rosa, A.P. Matos-Pereira, F. Silva-Souza, C. de J. Silva-Mendonca, F. Carvalho-Silva, P.R. Barros-Gomes, V.E. Mouchrek-Filho, Drying kinetics of *Bixa orellana* Labil (annatto) leaves and the influence of temperature on the physicochemical and biological properties of its essential oil, *Rev. Colomb. Cienc. Quím. Farm.*, **49**(3), 614-640 (2020).

Artigo de pesquisa científica / *http://dx.doi.org/10.15446/rcciquifa.v49n3.91253*

Caracterização química, atividade antimicrobiana e toxicidade dos óleos essenciais da *Pimenta dioica* L. (pimenta da Jamaica) e *Citrus sinensis* L. Osbeck (laranja doce)

Gustavo Oliveira Everton[1]*, Rebecca Jemima Pereira Araújo[1], Ana Beatriz da Silva dos Santos[1], Paulo Victor Serra Rosa[1], Rafael Gustavo de Oliveira Carvalho Junior[1], Amanda Mara Teles[2], Paulo Roberto Barros Gomes[3], Victor Elias Mouchrek Filho[1]

[1]Laboratório de Pesquisa e Aplicação de Óleo Essenciais (PCQA-UFMA), Universidade Federal do Maranhão, São Luís, Maranhão, Brasil.

[2]Laboratório de Microbiologia de Alimentos e Água (PCQA-UFMA), Universidade Federal do Maranhão, São Luís, Maranhão, Brasil.

[3]Instituto Federal de Educação, Ciência e Tecnologia do Pará, Paragominas, Pará, Brasil.

*Autor para correspondência: gustavooliveiraeverton@gmail.com

Recebido: 25 de novembro de 2019

Revisado: 16 de junho de 2020

Aceto: 18 de junho de 2020

Resumo

Este estudo avaliou a toxicidade e a atividade antimicrobiana frente a *Escherichia coli* e *Staphylococcus aureus* dos óleos essenciais de *Pimenta dioica* Lindl. e *Citrus sinensis* L. Os óleos essenciais (OE) foram extraídos por hidrodestilação, com caracterização química através de cromatografia gasosa acoplada a espectrometria de massas (CG-EM). Os parâmetros físico-químicos foram determinados de acordo com a Farmacopeia Brasileira. O ensaio de toxicidade seguiu o bioensaio com *Artemia salina Leach*, os OE aprovados neste ensaio seguiram para avaliação das suas propriedades biológicas. A atividade antimicrobiana seguiu a metodologia descrita pelo *Clinical and Laboratory Standards Institute* utilizando o método de difusão de disco, diluição em caldo para concentração inibitória mínima (CIM) e posterior concentração bactericida mínima para avaliar a ação dos OE frente a *Escherichia coli* e *Staphylococcus aureus*. Ambos os OE apresentaram toxicidade baixa, e assim foram avaliados quanto as propriedades biológicas antimicrobianas. Ambos os OE apresentaram potenciais bactericidas frente aos microrganismos testados, exibindo resultados satisfatórios para a ação deles. Os resultados indicam que os OE avaliados são compostos por substâncias que propiciam e incentivam sua aplicação em virtude de seus potenciais para atividade biológicas moluscicida e antimicrobiana.

Palavras-chave: Óleos essenciais, atividade antimicrobiana, *Pimenta dioica* Lindl., *Citrus sinensis* L., toxicidade.

Summary

Chemical characterization, antimicrobial activity, and toxicity of the essential oils of *Pimenta dioica* L. and *Citrus sinensis* L. Osbeck (laranja doce)

This study evaluated the toxicity and antimicrobial activity in the face of *Escherichia coli* and *Staphylococcus aureus* of essential oils of *Pimenta dioica* Lindl. and *Citrus sinensis* L. The essential oils (EO) were extracted by hydrodistillation, with chemical characterization by gas chromatography coupled and mass spectrometry (GC-MS). Physicochemical parameters were determined according to the Brazilian Pharmacopeia. The toxicity test followed the bioassay with *Artemia salina* Leach, the EO approved in this assay followed to evaluate its biological properties. The antimicrobial activity followed the methodology described by the Clinical and Laboratory Standards Institute using the disc diffusion method, broth dilution for minimum inhibitory concentration (MIC) and subsequent minimum bactericide concentration for to evaluate the action of EO against *Escherichia coli* and *Staphylococcus aureus*. Both OE showed low toxicity, and thus were evaluated for the biological antimicrobial properties. Both OE presented bactericidal potential against the microorganisms tested, showing satisfactory results for their action. The results indicate that the evaluated OE are composed of substances that provide and encourage their application due to their potentials for biological molluscicide and antimicrobial activity.

Key words: Essential oils, antimicrobial activity, *Pimenta dioica* Lindl., *Citrus sinensis* L., toxicity.

Introdução

Os óleos essenciais (OE) são misturas complexas de compostos voláteis de baixo peso molecular e insolúveis em água [1] extraídos a partir de diferentes técnicas de extração, tais como a destilação que inclui a destilação por arraste à vapor, prensagem a frio e maceração [2]. Estes OE constituem um dos mais importantes grupos de matérias primas para as indústrias de alimentos, farmacêutica, perfumaria e afins.

Nos últimos anos, plantas aromáticas e seus produtos têm sido avaliados quanto à sua eficácia em relação à segurança alimentar. Grande parte das suas propriedades são atribuídas aos óleos essenciais e outros componentes do metabolismo secundário das plantas [3], que tem despertado interesse na indústria de alimentos devido à sua atividade antioxidante e antimicrobiana [4].

Dentre várias espécies de plantas compostas por OE em que se podem encontrar estas propriedades encontram-se a *Pimenta dioica* Lindl. e *Citrus sinensis* (L.) Osbeck (laranja doce). A *P. dioica* recebe maior destaque como especiaria, mas também é muito utilizada para o tratamento de certas doenças por possuir propriedades anti-hipertensivas, anti-inflamatórias, analgésicas, antimicrobianas e antioxidantes [5].

O OE de *C. sinensis* pode ser classificado como uma mistura de terpenos, hidrocarbonetos e compostos oxigenados, considerados quimicamente instáveis. O OE de laranja doce é constituído por aproximadamente 98% de R-limoneno sendo os 2% restantes referentes a uma mistura de outros terpenos e aldeídos alifáticos [6].

Ao longo dos últimos anos vem sendo procuradas alternativas naturais aos produtos sintéticos, os produtos naturais são uma opção com menor toxicidade em comparação a outros produtos de natureza sintética. Assim, o presente estudo caracterizou quimicamente, avaliou a toxicidade e a atividade antimicrobiana dos OE de *P. dioica* e *C. sinensis*, com a perspectiva de oferecer uma alternativa natural ao uso de antimicrobianos sintéticos.

Metodologia

Obtenção dos óleos essenciais

As folhas de *P. dioica* L. utilizadas neste estudo estão registradas nos arquivos botânicos do Instituto Biodinâmico (IBD) de Botucatu de acordo com certificado nº CA021205. As cascas de *C. sinensis* L foram registradas no Instituto Federal do Maranhão pelo setor de fruticultura, como D-25 (laranja doce, variação: pera).

Obtenção dos óleos essenciais

As folhas de *P. dioica* L. e cascas de *C. sinensis* L. foram coletadas e transportadas para o Laboratório de Pesquisa e Aplicação de Óleos Essenciais da Universidade Federal do Maranhão (UFMA), onde foram secas em temperatura ambiente, trituradas e armazenadas para extração do OE.

Para extração dos OE, utilizou-se a técnica de hidrodestilação com um extrator de Clevenger de vidro acoplado a um balão de fundo redondo acondicionado em manta elétrica como fonte geradora de calor. Foram utilizadas 30 g das folhas secas de *P. dioica* e 120 g das cascas *C. sinensis*, adicionando-se água destilada (1:10). A hidrodestilação foi conduzida a 100 °C por 5 h recolhendo-se o OE extraído. Cada OE foi seco por percolação com sulfato de sódio anidro (Na_2SO_4) e centrifugado. Essas operações foram realizadas em triplicatas e as amostras armazenadas em ampolas de vidro âmbar sob

refrigeração de 4 °C. Posteriormente submetido as análises. O procedimento experimental é apresentado na figura 1.

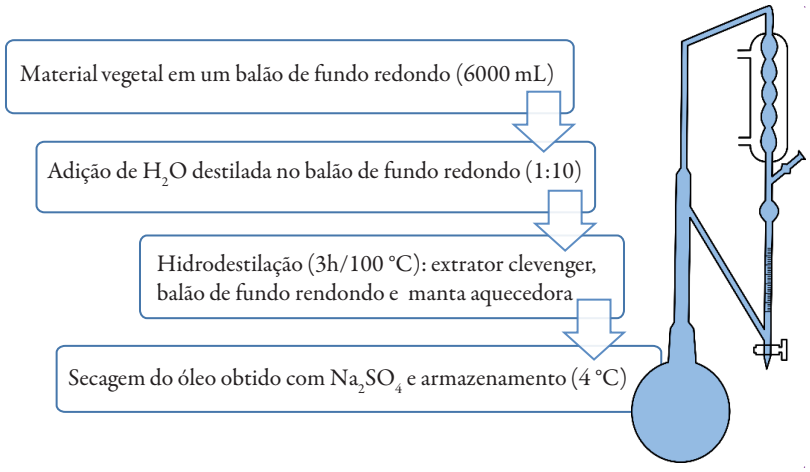

Figura 1. Esquema experimental da extração dos OE.

Os parâmetros físico-químicos dos OE foram determinados: densidade, solubilidade, cor e aparência de acordo com a Farmacopeia Brasileira [7]. O rendimento do OE foi expresso em porcentagem na relação massa/volume pela medida de densidade.

Análises químicas

Os constituintes dos OE foram identificados por cromatografia gasosa acoplada à espectrometria de massas (CG-EM) na Central Analítica do Instituto de Química da Universidade Estadual de Campinas. Foi dissolvido 1,0 mg da amostra em 1000 μL de diclorometano (pureza 99,9%). As condições de análise foram as seguintes: método: Adams. M; volume injetado: 0,3 μL; coluna : capilar HP-5MS (5% difenil, 95% dimetil polisiloxano) (equivalente DB-5MS ou CP-Sil 8CB LB/MS), nas dimensões (30 m x 0,25 mm x 0,25 μm); gás de arraste: He (99,9995); 1,0 mL.min^{-1}; injetor: 280 °C, modo split (1:10); forno : 40 °C (5,0 min.) até 240 °C numa taxa de 4 °C min^{-1}, de 240 °C até 300 °C (7,5 min) numa taxa de 8 °C min^{-1}); t_T = 60,0 min; detector: EM; EI (70 eV); modo varredura (0,5 seg scan^{-1}); faixa de massas: 40-500 daltons (uma); linha transferência: 280 °C; filamento: desligado 0,0 a 4,0 min; espectrômetro de massas tipo quadrupolo linear.

Para a identificação dos compostos na amostra utilizou-se o programa AMDIS (Automated Mass spectral Deconvolution Mass & Identification System).

Toxicidade

Para a avaliação da letalidade de *Artemia salina* Leach, foi preparada uma solução salina estoque de cada OE na concentração de 10 000 mg L^{-1} e 0,02 mg de Tween 80 (tenso ativo). Alíquotas de 5, 50 e 500 μL desta foram transferidas para tubos de ensaio e completados com solução salina já preparadas anteriormente até 5 mL, obtendo-se no final concentrações de 10, 100 e 1000 mg L^{-1}, respectivamente. Todos os ensaios foram realizados em triplicatas, onde dez larvas na fase náuplio foram transferidas para cada um dos tubos de ensaio.

Para o controle do branco utilizou-se 5 mL da solução salina, para o controle positivo $K_2Cr_2O_7$ e para o controle negativo 5 mL de uma solução 4 mg L^{-1} de Tween 80. Após 24 h de exposição, realizou-se a contagem das larvas vivas, considerando-se mortas aquelas que não se movimentaram durante a observação e nem com a leve agitação do frasco.

Adotou-se o critério estabelecido por Dolabela [8] para classificação da toxicidade dos OE, sendo considerado altamente tóxico quando $CL_{50} \leq 80$ mg L^{-1}, moderadamente tóxico para 80 mg $L^{-1} \leq CL_{50} \geq 250$ mg L^{-1} e levemente tóxico ou atóxico quando $CL_{50} \geq 250$ mg L^{-1}.

Padronização do inóculo microbiano para ensaios de sensibilidade

Foram utilizadas duas cepas de bactérias: *Escherichia coli* (ATCC 25922) e *Staphylococcus aureus* (ATCC 25923). Foram identificadas e confirmadas pelas provas bioquímicas: citrato de Simmons (CIT), vermelho de metila (VM), Voges-Proskauer (VP), malonato (MAL), fermentação de carboidratos, descarboxilação de aminoácidos, indol (IND), motilidade (MOT) e produção de H_2S, teste de catalase, teste de coagulase e coloração de Gram e teste da urease (UR).

Culturas microbianas puras mantidas em ágar TSA foram repicadas para caldo de infusão de cérebro e coração (BHI) e incubadas a 35 °C até atingirem fase exponencial de crescimento (4-6 h). Após esse período, as culturas tiveram sua densidade celular ajustada em solução salina 0,85% estéril, de modo a se obter uma turbidez comparável à da solução padrão de McFarland 0,5, o que resulta em uma suspensão microbiana contendo aproximadamente 1,5 x 10^8 UFC mL^{-1} de acordo com as normas do *Clinical and Laboratory Standards Institute* [9].

Método de difusão de disco (MDD)

A técnica de difusão de disco foi realizada segundo *Clinical and Laboratory Standards Institute* [9] que padroniza os testes de sensibilidade de antimicrobianos por disco-difusão. Primeiro foram preparadas as placas com o meio de cultura Ágar Mueller Hinton (AMH) após sua solidificação foi distribuído à suspensão microbiana na superfície

do ágar e deixado em repouso à temperatura ambiente por 30 min. Logo após são preparados os discos contendo 50 µL dos OE e os discos com concentrações definidas dos antibióticos. Utilizando-se pinça esterilizada, os discos foram distribuídos sobre a superfície do ágar. As placas foram incubadas em estufa bacteriológica a 35 °C por 24 h. Os diâmetros dos halos de inibição foram mensurados, incluindo o diâmetro do disco. Esses ensaios foram feitos em triplicata. Os valores dos halos de inibição foram as médias das medidas dos três resultados. Ensaios realizados em triplicata.

Concentração inibitória mínima (CIM) e concentração bactericida mínima (CBM)

O ensaio de concentração inibitória mínima (CIM) foi realizado empregando-se a técnica de diluição em caldo, proposta pela Clinical and Laboratory Standards Institute [9].

Primeiramente foram preparadas soluções dos OE utilizando-se dimetilsufoxido (DMSO) a 2%, sendo preparadas diluições seriadas em Caldo MH, resultando nas concentrações de 10 a 1000 $\mu g\, mL^{-1}$. A cada concentração foram adicionadas suspensão microbiana contendo 1,5 x 10^8 UFC mL^{-1} das cepas *E. coli* e *S. aureus*. Os tubos foram incubados a 35 °C por 24 h. Foram realizados os controles de esterilidade e crescimento para o ensaio realizado.

Após o período de incubação, foi verificada CIM dos OE, sendo definida como a menor concentração que visivelmente inibiu o crescimento bacteriano (ausência de turvação visível). Ensaios realizados em triplicata.

Para o ensaio de concentração bactericida mínima (CBM) empregou-se uma alíquota de 100 µL das diluições provenientes do caldo MH que visivelmente inibiram o crescimento microbiano. As alíquotas foram inoculadas em Ágar Mueller Hinton (AMH) com posterior incubação a 35 °C por 24 h. A CBM foi determinada como a menor dose que visualmente no ensaio de CIM apresentou inibição de crescimento e que na cultura em AMH também não apresentou crescimento bacteriano.

Resultados e discussão

Propriedades físico-químicas

Os parâmetros físico-químicos dos OE são importantes não apenas para determinação da qualidade, como também para o controle da sua pureza e estes são apresentados na tabela 1. Observa-se que o OE de *C. sinensis* obteve um rendimento de 2,47% superior ao OE de *P. dioica* de 1,80%.

Tabela 1. Parâmetros físico-químicos dos OE.

Parâmetro físico-químicos	*P. dioica*	*C. sinensis*
Densidade (g mL^{-1})	0,9820 ± 0,0012	0,8500 ± 0,0053
Índice de refração (n_D 25 °C)	1,5185 ± 0,020	1,4760 ± 0,0063
Solubilidade em álcool a 70% (v/v)	1:3	1:3
Cor	Amarelo	Incolor
Aparência	Límpido	Límpido
Rendimento (%)	1,80 ± 0,35	2,47 ± 0,15

Ao compararmos individualmente o rendimento do OE de *C. sinensis* aos resultados obtidos por Silva *et al.* [10] que extraiu os OE da casca de frutos secos e frescos, os autores perceberam seu rendimento variando entre 1,80-2,00%, sendo que este estudo obteve um rendimento de +0,47% acima do rendimento máximo obtido pelos autores, visto que a densidade dos mesmos autores variou entre 0,8480 a 0,8490 g mL^{-1}, densidade essa que está semelhante este trabalho em uma variação de +0,0010 g mL^{-1}.

Mesmo o rendimento do OE da *P. dioica* sendo menor que o rendimento do *C. sinensis* é importante enfatizar que para os OE rendimentos acima de 1,5% são de extrema significância. Em estudo realizado Voris *et al.* [11] ao extrair esse mesmo OE do fruto adquirido em um mercado varejista do Rio de Janeiro (RJ), os autores empregaram um período de 4 h em sua hidrodestilação, mas seu rendimento máximo foi de 1,60%, comparando-se ao estudo atual que empregou um tempo menor de hidrodestilação (3h-100 °C) e obtivemos um rendimento de 1,80% utilizando uma parte regenerativa da planta, torna-se de extrema importância e significância para a visualização do seu potencial de aplicação.

Comparando os valores para o OE estudado com os da literatura, pode-se observar que houve uma similaridade entre eles, no que diz respeito aos parâmetros analisados. As pequenas diferenças nos valores encontrados podem ser atribuídas a fatores tais como época de coleta, diferentes tipos de solo, condições e tempo de armazenamento [12]. Sendo importante enfatizar o rendimento de 2,47% para o OE de *C. sinensis* que foi observado em resultados superiores a literatura, incentivando sua produção em virtude do aproveitamento de cascas que são comumente descarte em feiras públicas ou bairros locais de São Luís-MA.

Caracterização química dos óleos essenciais

Os picos cromatográficos foram identificados através da comparação dos respectivos espectros de massa com os dados das espectrotecas (1) WILEY 139; (2) NIST107 e (3)

NIST21. De acordo com os resultados obtidos são apresentados na tabela 2 os compostos identificados no OE extraído das cascas de *C. sinensis* e na tabela 3 os compostos identificados no OE extraído das folhas da *P. dioica*.

Como pode ser observado na tabela 2 foram identificados 15 componentes na amostra do OE de *C. sinensis*, sendo o constituinte majoritário do OE d-limoneno com 81,50% da composição, seguido do linalol (6,36%) e do β-Mirceno (2,95%).

Tabela 2. Constituintes químicos na amostra do OE de *C. sinensis*, sendo tr*: Tempo de retenção dos compostos na coluna em minutos.

Pico	tr* (min)	Componentes	Teor (%)
1	5,155	α-Pineno	0,33
2	6,350	β-Mirceno	2,95
3	6,861	Octanal	1,93
4	7,610	d-limoneno	81,50
5	8,287	1, Octanol	0,46
6	8,919	Linalol	6,36
7	8,959	Nonanal	1,08
8	9,866	Citronelal	0,06
9	10,523	Terpineol	0,12
10	10,873	α-Terpineol	1,39
11	10,926	Decanal	0,25
12	11,352	β-Citronelol	0,08
13	11,643	Neral	1,13
14	12,210	Citral	1,17
15	12,496	1, Ciclohexano	1,20

O composto químico d-limoneno é confirmado como constituinte majoritário do OE por Araújo *et al.* [13] que ao extraí-lo das cascas de frutos de *C. sinensis* do mercado local de Aracaju, Sergipe realizou a caracterização química do mesmo através de CG/EM e notou a presença do constituinte em 91,88% de sua amostra.

Resultados semelhantes a este estudo também é notificado por Martins *et al.* [14] que ao realizarem a caracterização química de OE comerciais do gênero Citrus, observaram a presença do d-limoneno em 83,33% da composição do OE de *C. sinensis*.

O d-limoneno é um terpeno relativamente estável que possui aplicações na literatura para o desenvolvimento de bioprodutos vegetais [15]. Os OE do gênero *Citrus* possuem esse componente como majoritário em sua composição e propriedades como a atividade antimicrobiana pode ser comprovada por Rodrigues [16], porém ao retratarmos o *C. sinensis* seu potencial bactericida foi pouco estudado, sendo relatados muitos trabalhos com relação a sua ação antimicrobiana antifúngica [17] e larvicida [13]. Assim, observa-se que o OE de *C. sinensis* possui potencial para explorarmos sua atividade bactericida neste estudo, sendo de vital importância para o estado e para o país um produto natural obtido através da parte de um vegetal que é comumente descartado ou de aplicações superficiais.

Como pode ser observado na tabela 3 foram identificados 7 componentes na amostra, sendo o constituinte majoritário do OE o eugenol com 85,673%, seguido do chavicol (6,79%) e do mirceno (2,76%).

Tabela 3. Constituintes químicos identificados em amostras do OE de *P. dioica*, sendo tr*: tempo de retenção dos compostos na coluna em minutos.

Pico	tr* (min)	Componentes	Teor (%)
1	8,772	Octenol	1,19
2	9,164	Mirceno	2,76
3	10,488	Limoneno	1,73
4	13,251	Linalol	0,88
5	16,122	Terpineol	0,97
6	19,026	Chavicol	6,79
7	22,755	Eugenol	85,67

O teor de eugenol (85,67%) relatado neste estudo torna-se significante ao compararmos com Oliveira [18] que extraiu o OE das folhas de *P. dioica* coletadas em Minas Gerais também observou que o eugenol como o constituinte majoritário, porém o teor observado foi de 44,9%. Outro fato relatado foi a presença do limoneno em 10,1% da composição e o chavicol sendo exibindo em um teor de 7,5%. Essa composição também poderá estar ligada ao rendimento inferior de 0,49% obtido por Oliveira [18], ainda sendo ressaltado que os autores utilizaram um tempo de extração de 4 h.

Resultados semelhantes foram relatados por Oliveira *et al.* [19] utilizando plantas do sul do estado da Bahia coletadas em 2006, onde obtiveram o eugenol (75,07%) como constituinte majoritário da sua amostra do OE das folhas de *P. dioica*, porém diferente

deste estudo componente secundário dos autores foi o mirceno com 8,19% e o chavicol esteve em seguida com 6,35%.

O eugenol é uma molécula extraordinariamente versátil e foi incluída como um aroma picante em sorvete, produtos de panificação e doces em concentrações restritas [20], enxaguatórios bucais, preparações farmacêuticas e dentárias [21,22]. Além de possuir propriedades biológicas comprovadas por Kamatou *et al.* [23], assim é de vital importância o estudo do OE extraído da *P. dioica* como uma fonte natural significativa de eugenol tanto para aplicações biológicas quanto para as indústrias em geral.

Toxicidade

Na tabela 4 são apresentadas as concentrações letais 50% referentes a ação dos OE frente a *Artemia salina* L. e sua posterior classificação segundo o critério de Dolabela [8].

Tabela 4. Concentração Letal 50% para ação dos OE frente a *Artemia salina* L. e classificação dos óleos quanto a sua toxicidade pelo critério de Dolabela.

OE	CL_{50}	Classificação
P. dioica	141,3 mg L^{-1}	Moderadamente tóxico
C. sinensis	511,6 mg L^{-1}	Atóxico

A concentração letal 50% (CL_{50}) refere-se ao ponto em que o número de animais sobreviventes é igual ao número de animais mortos, e seguindo o critério de Dolabela [8] é possível determinar a toxicidade de produtos naturais visando uma aplicação específica do agente no organismo alvo, visto que óleos com toxicidade elevada não são recomendados para aplicações biológicas.

Na tabela 4 foi possível observar que nenhum dos óleos foi classificado como tóxico, logo, suas aplicações podem ser relativamente aceitáveis e sendo encorajadas. Desta forma, os ensaios de atividade antimicrobiana foram iniciados. É importante ressaltar que o OE de *C. sinensis* extraído das cascas do fruto apresenta até agora um rendimento significativo e componentes químicos de importância biológica e neste ensaio de toxicidade apresenta a CL_{50} de 511,6 mg L^{-1}, muito acima do critério que era de apenas 250 mg L^{-1} para ser classificado como atóxico. Logo, este OE tem seu potencial de aplicação novamente incentivado.

É importante enfatizar que estudos relativos à toxicidade de produtos naturais são de vital importância para aplicações biológicas e estudos da literatura ainda não divulgam

toxicidade das plantas em estudo em um teste específico como o bioensaio frente a *Artemia salina*.

Os resultados referentes aos ensaios para determinação da atividade antimicrobiana são apresentados na tabela 5. Todos os óleos apresentaram atividade antimicrobiana frente a *Escherichia coli* e *Staphylococcus aureus*.

Tabela 5. Halos de inibição (HI), concentração inibitória mínima (μg/mL) dos OE frente a *Staphylococcus aureus* e *Escherichia coli*.

	OE *P. dioica*				**OE *C. sinensis***		
	GEN 30 μg (mm)	**HI (mm)**	**CIM (μg mL^{-1})**	**CBM (μg mL^{-1})**	**HI (mm)**	**CIM (μg mL^{-1})**	**CBM (μg mL^{-1})**
E. coli (ATCC 25922) Gram-negativa	25 ±1,11	15 ±0,50	25 (15-40)	50 (40-70)	15 ±0,70	75 (40-70)	100 (90-120)
S. aureus (ATCC 25923) Gram-positiva	27 ±1,31	25 ±1,20	10 (5-25)	25 (15-35)	30 ±0,90	10 (40-70)	25 (20-40)

Ao observarmos a tabela 5 notamos que o OE de *P. dioica* foi mais eficiente ao inibir a bactéria *Staphylococcus aureus* pelo método de difusão de disco se compararmos o seu halo de 25 mm com o 15 mm resultado da ação do óleo frente a *Escherichia coli*. Ambos os halos de inibição permitem classificar as bactérias como sensíveis pelo critério estabelecido por Moreira *et al.* [23]. O ensaio de concentração inibitória mínima revelou que o OE de *P. dioica* inibe o crescimento microbiano de *Escherichia coli* a partir de 25 μg mL^{-1} e de *Staphylococcus aureus* a partir de 10 μg mL^{-1}.

O estudo de Oliveira [18], onde a autora relata a atividade do mesmo óleo com uma CIM de 5 μg mL^{-1} para *E. coli* e 20 μg mL^{-1} para *S. aureus* retrata a diferença deste estudo onde o mesmo óleo obtido em dois locais diferente possuem propriedades diferentes, visto que o óleo da autora foi mais eficiente frente a *E. coli* do que a *S. aureus*, enquanto que, neste estudo ocorreu o inverso do observado pela autora.

Em um estudo recente Lorenzo-Leal *et al.* [24] em Puebla, México, utilizou a técnica de micropoços para determinar a CIM do OE da *P. dioica* extraída de frutos comercializados e diferentemente deste estudo não observou atividade do óleo frente a *E. coli* e obteve uma CIM extremamente alta de 2000 μg mL^{-1} para *S. aureus*, o que revigora os resultados satisfatórios obtidos neste estudo, onde para *S. aureus* obtivemos uma CIM de 10 μg mL^{-1}.

Ao notarmos a tabela 5 podemos visualizar que o OE de *C. sinensis* também foi mais eficiente ao inibir a bactéria *Staphylococcus aureus* pelo Método de Difusão de Disco se compararmos o seu halo de 30 mm com o halo de 15 mm resultado da ação do óleo frente a *Escherichia coli*. Ambos os halos de inibição permitem classificar as bactérias como sensíveis pelo critério estabelecido por Moreira *et al.* [23]. O ensaio de concentração inibitória mínima revelou que o OE de *P. dioica* inibe o crescimento microbiano de *Escherichia coli* a partir de 50 $\mu g\ mL^{-1}$ e de *Staphylococcus aureus* a partir de 10 $\mu g\ mL^{-1}$.

É importante ressaltarmos que os estudos antimicrobianos no Brasil com a espécie *C. sinensis* são relativamente novos, destacando a importância do estudo para obtenção de um produto natural com potencial biológico obtido de uma parte comumente descartada de um fruto de alto consumo local tanto para o estado quanto para o país.

Desta forma, os resultados obtidos foram comparados aos dos autores Eldahshan e Halim [25] que extraíram o OE das folhas de *C. sinensis* coletadas no Egito realizando uma hidrodestilação por 5 h. Os autores obtiveram um halo de 20,1 mm para a ação do OE frente a *S. aureus* e um resultado semelhante de 16,2 mm frente a *E. coli*, visto que neste estudo obtivemos um halo de 15 mm empregando o OE obtido da casca.

Eldahshan e Halim [25] ainda enfatizam que esse óleo teve essa atividade pela presença dos compostos oxigenados em sua composição. Os autores realçam o potencial do OE para ser utilizado como aditivos antibacterianos em alimentos e em produtos cosméticos em a fim de reduzir a dependência de produtos químicos sintéticos preservação de alimentos [25]. Por fim, destaca-se novamente o potencial biológico de ambas as espécies estudadas neste trabalho como extremamente eficientes no controle de microrganismos patogênicos, representados pela *Escherichia coli* como Gram-negativa e *Staphylococcus aureus* como Gram-positiva.

Através dos resultados obtidos nos estudos químicos, na avaliação da toxicidade e antimicrobiana dos OE de *P. dioica* e *C. sinensis*, conclui-se que os OE avaliados são compostos por substâncias que propiciam e incentivam sua aplicação em virtude de seus potenciais para atividade biológica antimicrobiana.

Agradecimentos

Os autores agradecem ao Laboratório de Pesquisa e Aplicação de Óleos Essenciais (PCQA-UFMA) e a Universidade Federal do Maranhão (UFMA).

Conflito de interesses

Os autores declaram que não tem conflito de interesses.

Referências

1. C. Dima, S. Dima, Essential oils in foods: extraction, stabilization, and toxicity, *Current Opinion in Food Science*, **5**, 29-35 (2015).

2. F. Solórzano-Santos, M.G. Miranda-Novales, Essential oils from aromatic herbs as antimicrobial agents, *Current Opinion in Biotechnology*, **23**, 136-141 (2012).

3. J. R. Calo, P.G. Crandall, C.A. O'Bryan, S.C. Ricke, Essential oils as antimicrobials in food systems- A review, *Food Control*, **54**, 111-119 (2015).

4. M. Kfoury, L. Auezova, H. Greige-Gerges, S. Fourmentin, Promising applications of cyclodextrins in food: Improvement of essential oils retention, controlled release and antiradical activity, *Carbohydrate Polymers*, **131**, 264-272 (2015).

5. J.A.M.D. Paula, J.B. Reis, L.H.M. Ferreira, A.C.S. Menezes, J.R. Paula, Gênero *Pimenta*: aspectos botânicos, composição química e potencial farmacológico, *Revista Brasileira de Plantas Medicinais*, **12**, 363-379 (2010).

6. J.G. Galvão, V.F. Silva, S.G. Ferreira, F.R.M. França, D.A. Santos, L.S. Freitas, P.B. Alves, A.A.S. Araújo, S.C.H. Cavalcanti, R.S. Nunes, β-cyclodextrin inclusion complexes containing *Citrus sinensis* (L.) Osbeck essential oil: An alternative to control *Aedes aegypti* larvae, *Thermochimica Acta*, **608**, 14-19 (2015).

7. *Farmacopeia Brasileira*, 5 ed., Editora Atheneu, São Paulo, 2010.

8. M.F. Dolabella, *Triagem in vitro para a atividade antitumoral e anti-T. cruzi de extratos vegetais, produtos naturais e sintéticos*, tese de mestrado, Universidade Federal de Minas Gerais, Belo Horizonte, 1997.

9. Clinical and Laboratory Standards Institute (CLSI), *Performance standards for antimicrobial disk susceptibility tests*, Approved Standard, 11th ed., 32, 2015.

10. F.K.B.D. Silva, V.C. Hermes, L.E.M. Machado, M. Leão, R.D.C.D.S. Schneider, C.D.M.D. Silva, *Obtenção do óleo essencial da laranja doce Citrus sinensis (L.) Osbeck a partir das cascas secas e frescas para desenvolvimento de aromatizante de ambiente*, Seminário de Iniciação Científica, 82 2016.

11. D.G.D.R. Voris, C.H. Afonso, C.A. Almeida Filho, C.O. Fernandes, D.Q. Brito, C.S. Moraes, K.E. Avelar, Estudos etnofarmacológicos de óleos essenciais com atividade larvicida contra o mosquito *Aedes aegypt*, *Semioses*, **11**, 86-94 (2017).

12. D.A. Costa, G.A.L.D. Oliveira, J.P. Costa, G.F.D. Souza, D.P.D. Sousa, R.M. Freitas, Avaliação da toxicidade aguda e do efeito ansiolítico de um derivado sintético da carvona, *Revista Brasileira de Ciências da Saúde*, **16**, 303-310 (2012).

13. A.F.D.O. Araujo, J.T. Ribeiro-Paes, J.T.D. Deus, S.C.D.H. Cavalcanti, R.D.S. Nunes, P.B. Alves, M. D.L.D.G. Macoris, Larvicidal activity of *Syzygium aromaticum* (L.) Merr and *Citrus sinensis* (L.) Osbeck essential oils and their antagonistic effects with temephos in resistant populations of *Aedes aegypti*, *Memorias do Instituto Oswaldo Cruz*, **111**, 443-449 (2016).

14. G.D.S.O. Martins, H.B. Zago, A.V. Costa, L.M.D. Araujo Junior, J.R.D. Carvalho, Chemical composition and toxicity of Citrus essential oils on *Dysmicoccus brevipes* (Hemiptera: Pseudococcidae), *Revista Caatinga*, **30**, 3, 811-817 (2017).

15. D.R. Granja, F.K.B.D. Silva, J. Eizemann, L.E.M. Machado, C.D.M.D. Silva, L.T. Kist, *Obtenção do óleo essencial das cascas de Citrus sinensis L. para desenvolvimento de bioprodutos vegetais*, *Seminário de Iniciação Científica*, 73, 2015.

16. V. Mello Avelar-Costa, P. Sena da Mata, K.C. Ugolini-Mugnol, Atividade antimicrobiana de óleo essencial de *Citrus aurantium* L. ssp. Bergamia associado a antibióticos, *Revista Científica UMC*, **4**(3), 1-5 (2018).

17. L.D. Rodríguez-Rodríguez, Á.A. Jiménez-Rodríguez, W. Murillo-Arango, E.A. Rueda-Lorza, J. Méndez-Arteaga, Actividad antimicrobiana de cáscaras y semillas de *Citrus limonia* y *Citrus sinensis*, *Actualidades Biológicas*, **39**, 53-59 (2017).

18. F.S. Oliveira, *Atividade antioxidante e antimicrobiana de óleos essenciais aplicados na preservação de lingüiça frescal de frango*, tese de mestrado, Montes Claros, Universidade Federal de Minas Gerais, 2017.

19. R.A. Oliveira, T.V. Reis, C.K. Sacramento, L.P. Duarte, F.F. Oliveira, Constituintes químicos voláteis de especiarias ricas em eugenol, *Revista Brasileira de Farmacognosia*, **19**, 771-775 (2009).

20. K.P. Padmakumari, I. Sasidharan, M.M. Sreekumar, Composition and antioxidant activity of essential oil of pimento (*Pimenta dioica* (L) Merr.) from Jamaica, *Natural Product Research*, **25**, 152-160 (2011).

21. M. Martinez-Velazquez, G.A. Castillo-Herrera, R. Rosario-Cruz, J.M. Flores-Fernandez, J. Lopez-Ramirez, R. Hernandez-Gutierrez, E. de C. Lugo-Cervantes, Acaricidal effect and chemical composition of essential oils extracted from *Cuminum cyminum*,

Pimenta dioica and *Ocimum basilicum* against the cattle tick *Rhipicephalus (Boophilus) microplus* (Acari: Ixodidae), *Parasitology Research*, **108**, 481-487 (2011).

22. G.P. Kamatou, I. Vermaak, A.M. Viljoen, Eugenol—from the remote Maluku Islands to the international market place: a review of a remarkable and versatile molecule, *Molecules*, **17**, 6953-6981 (2012).

23. M.R. Moreira, A.G. Ponce, C.E. del Valle, S.I. Roura, Inhibitory parameters of essential oils to reduce a foodborne pathogen, *LWT-Food Science and Technology*, **38**, 565-570 (2005).

24. A.C. Lorenzo-Leal, E. Palou, A. López-Malo, H. Bach, Antimicrobial, cytotoxic, and anti-inflammatory activities of *Pimenta dioica* and *Rosmarinus officinalis* essential oils, *BioMed Research International*, **2019**, ID 1639726 (2019).

25. O.A. Eldahshan, A.F. Halim, Comparison of the composition and antimicrobial activities of the essential oils of green branches and leaves of Egyptian navel orange (*Citrus sinensis* (L.) Osbeck var. *malesy*), *Chemistry & Biodiversity*, **13**, 681-685 (2016).

Como citar este artigo

G. Oliveira-Everton, R.J. Pereira-Araújo, A.B. da Silva dos Santos, P.V. Serra-Rosa, R.G. de Oliveira-Carvalho Junior, A.M. Teles, P.R. Barros-Gomes, V.E. Mouchrek Filho, Caracterização química, atividade antimicrobiana e toxicidade dos óleos essenciais da *Pimenta dioica L.* (pimenta da Jamaica) e *Citrus sinensis* L. Osbeck (laranja doce), *Rev. Colomb. Cienc. Quím. Farm.*, **49**(3), 641-655 (2020).

Artigo de pesquisa científica / *http://dx.doi.org/10.15446/rcciquifa.v49n3.91336*

Composição química e atividade antibacteriana do óleo essencial dos frutos da *Pimenta dioica*

Paulo Roberto Barros Gomes[1*], Joelkson Diniz Ribeiro[3], Myrcéia Carolyne Guimarães da Costa[2], Marcelo Werneck da Silva Castro[2], Nagib Buzar Neto[2], Andréa Vasconcelos Melo[3], Gustavo Oliveira Everton[3], Hilton Costa Louzeiro[4], Maria Alves Fontenele[5], Helson Souza de Lima[3], Eduardo Fonseca Silva[3], Maria do Livramento de Paula[6], Victor Elias Mouchrek Filho[3], Adenilde Nascimento Mouchrek[3]

[1]Instituto Federal de Educação, Ciência e Tecnologia do Pará, Paragominas, PA, Brasil.

[2]Instituto Federal de Educação, Ciência e Tecnologia do Pará, 68440-000 Abaetetuba,PA, Brasil.

[3]Universidade Federal do Maranhão, 65080-805, São Luís, MA, Brasil.

[4]Universidade Federal do Maranhão, Campus Pinheiro, MA, Brasil.

[5]Coordenação de Engenharia de Alimentos, Universidade Federal do Maranhão, 65915-240, Imperatriz, MA, Brasil.

[6]Universidade Federal do Maranhão, Departamento de Farmácia, 65080-805, São Luís, MA, Brasil.

*Autor para correspondência: prbgomes@yahoo.com.br

Recebido: 11 de maio de 2020

Revisado: 16 de junho de 2020

Aceto: 18 de junho de 2020

Resumo

Neste estudo descrevemos a extração, composição química e a atividade antibacteriana do óleo essencial extraído dos frutos da *Pimenta dioica*. Para isso, extraímos o óleo por hidrodestilação; identificamos os compostos por cromatografia gasosa acoplada ao espectrômetro de massa (CG/EM); quantificamos o componente majoritário por espectrometria UV-vis e voltametria; e determinamos a atividade antibacteriana contra *Escherichia coli*, *Staphylococcus aureus*, *Proteus mirabilis*, *Pseudomonas aeruginosa* e *Serratia odorifera* pelo método de difusão em disco. Os resultados mostraram que o óleo é composto em sua maioria por eugenol e sua quantidade está em, aproximadamente, 78,15%, cuja classe predominante foi a dos monoterpenos. Além disso, as bactérias testadas com o óleo essencial apresentaram halos de inibição, variando de 11 a 21 mm. Portanto, o óleo é um potencial agente antibacteriano.

Palavras-chave: Eugenol, hidrodestilação, compostos voláteis, *Pimenta dioica*, bactérias.

Summary

Chemical composition and antibacterial activity of essential oil from fruits of *Pimenta dioica*

In this study we describe the extraction, chemical composition, and antibacterial activity of the essential oil extracted from fruits of *Pimenta dioica*. For this, we extracted the oil by hydrodistillation; we identified the compounds by Gas Chromatography coupled to the Mass Spectrometer (CG/MS); we quantified the major component by vis-UV Spectrometry and Voltammetry; and we determined the antibacterial activity against *Escherichia coli*, *Staphylococcus aureus*, *Proteus mirabilis*, *Pseudomonas aeruginosa*, and *Serratia odorifera*, using the disk diffusion method. The results showed that the oil is composed mostly of eugenol and its quantity is approximately 78.15%, whose predominant class was that of monoterpenes. In addition, the bacteria tested with the essential oil showed inhibition halos, ranging from 11 to 21 mm. Therefore, the oil is a potential antibacterial agent.

Keywords: Eugenol, hydrodistillation, volatile compounds, *Pimenta dioica*, bacteria.

Introdução

As bactérias patogênicas de origem alimentar despertam o interesse na busca de agentes antibacterianos. Os dados da Organização Mundial da Saúde (OMS) mostram que uma em cada dez pessoas adoecem quando ingerem alimentos contaminados e 420 000 vêm ao óbito a cada ano. Entre os principais fatores responsáveis por esses resultados estão as doenças transmitidas por bactérias e o processo de deterioração alimentar [1-3].

Para conter este processo, a indústria de alimento utiliza os agentes antibacterianos sintéticos. No entanto, apesar destes possuírem eficácia no controle de surtos destas doenças, suas aplicações provocaram acúmulo de resíduos no meio ambiente, resistência bacteriana aos produtos químicos aplicados e efeitos colaterais na saúde humana [4, 5]. Além disso, outra desvantagem está na preocupação dos consumidores com os efeitos colaterais a médio e longo prazo e com a segurança destes produtos. Dentro desta perspectiva, os pesquisadores precisam buscar novos agentes antibacteriano [6]. Logo, uma alternativa viável está nos estudos de produtos de origem natural, especialmente os óleos essenciais, devido a sua alta biodegrabilidade e baixa toxicidade para os mamíferos [7].

Os produtos extraídos de plantas, sejam extratos ou óleos essenciais, sobretudo da *Pimenta dioica*, possuem aplicações em alimentos, na medicina tradicional e em

algumas atividades biológicas. Originária da América Central, principalmente da Jamaica e Cuba, esta planta é utilizada como condimento justamente pelo seu aroma e sabor picante. Por conta disto, a indústria de alimentos o utiliza não só para realçar sabor, mas também como conservante de carnes, devido a sua capacidade antioxidante [8].

Na medicina tradicional os extratos obtidos da folha são utilizados no tratamento da flatulência e diarreia, já os frutos pulverizados são empregados no trato de calos, neuralgia e reumatismo [8]. No que diz respeito às atividades biológicas, observamos relatos da utilização do óleo como antioxidante e citotóxico contra algumas linhagens de câncer [9], moluscicida contra *Biomphalaria glabrata* [10], acaricida [11], antibacteriano em alimentos [12,13], larvicida e adulticida contra *Aedes aegypti* [14], antirradical [15] e antifúngico contra *Fusarium oxysporum* e *F. verticillioides* [16]. Apesar das inúmeras aplicações, no que diz respeito à atividade biológica, observamos que a maioria dos estudos se concentram mais em extrair o óleo a partir das folhas do que frutos. Devido a esta condição, neste estudo descreveremos a extração, composição química e atividade antibacteriana do óleo essencial dos frutos da *P. dioica* (L). Merr e do padrão do constituinte majoritário desse óleo.

Material e métodos

Obtenção e extração do óleo essencial

A coleta dos frutos foi realizada na Cooperativa Agrícola Mista do Projeto Onça LTDA, município de Taperoá-BA, Brasil, em agosto de 2005, recebendo o certificado orgânico pelo Instituto Biodinâmico (IBD) de número CA0212/05. Após a coleta, a secagem foi feita através de ventilação natural, posteriormente os frutos foram triturados no moinho elétrico (Tecnal, modelo TE–340) e armazenados em recipientes de polietileno. Extraímos o óleo por hidrodestilação e calculamos o rendimento médio a partir das medidas de densidade e do peso do material bruto. Para isso, pesamos 30 gramas das amostras e misturamos em 300 mL de água destilada. Em seguida colocamos esta mistura em um frasco de fundo redondo de 1000 mL e o acoplamos ao extrator de Clevenger sob aquecimento de 100 °C em uma manta elétrica por 3,5 h. Após esse tempo, o óleo destilado foi coletado e seco por percolação em sulfato de sódio anidro. Realizamos essas operações em triplicatas e armazenamos as amostras em ampolas de vidro âmbar sob refrigeração para evitar possíveis perdas de constituintes voláteis. Medimos a densidade a partir de um picnômetro a 25 °C.

Análise cromatográfica CG/EM

Identificamos os componentes do óleo essencial por cromatografia gasosa acoplada à espectrometria de massas (CG-EM) em um cromatógrafo a gás da marca Varian 2100,

acoplado a um espectrômetro de massa por impacto de elétrons e analisador de *ions trap*, utilizando hélio como gás de arraste com fluxo na coluna de 1 $mL.min^{-1}$; temperatura do injetor: 270 °C, split 1:50; coluna capilar (15 m x 0,25 mm) com fase estacionária VF-1ms (100% metilsiloxano 0,25 μm) e programação de temperatura do forno de 60 a 200 °C com taxa de aquecimento de 8 $°C.min^{-1}$, e de 200 e 290 °C, com taxa de aquecimento de 15 $°C.min^{-1}$. Noespectrômetro de massas, as temperaturas do main fold íon trap e da linha de transferência foram de 50, 190 e 200 °C. Injetamos alíquotas de 1 μL (injetor automático CP-8410) das amostras diluídas na proporção de 20 μL em 1,5 mL de hexano. Identificamos os componentes do óleo a partir da comparação destes com os dados obtidos de substâncias autênticas existentes em bibliotecas de referência a partir do tempo de retenção.

Solução tampão e padrão

Utilizamos o tampão Britton-Robson (BR) em todos os experimentos eletroquímicos, onde foi ajustado ao pH desejado uma solução NaOH 1,0 mol L^{-1}. Preparamos o tampão a partir de ácido bórico 0,04 mol L^{-1}, ácido fosfórico 0,04 mol L^{-1} e perclorato de sódio 0,10 mol L^{-1}, o que resultou numa solução de pH 1,8. O perclorato de sódio tinha a função de manter a força iônica na casa de 10^{-1}.

As soluções padrões de eugenol (98% de pureza e procedência Chem Service) foram preparadas em diferentes concentrações para cada técnica analítica aplicada. Para a voltametria, utilizamos uma solução estoque de concentração 5,79 x 10^{-3} mol L^{-1}, a qual foi preparada misturando-se 10 μL do padrão em balão de 10 mL e aferindo-se com uma solução etanol/tampão BR pH 3.3 a 55% (v/v). Já para a espectroscopia no UV, a solução estoque apresentava concentração de 5,79 x 10^{-2} mol L^{-1} e foi preparada acrescentando-se 100 μL do padrão de eugenol em um balão de 10 mL, aferido com solução etanol/água destilada a 60% (v/v). As soluções estoque do óleo essencial foram preparadas semelhantemente às do padrão de eugenol para cada método analítico, ou seja, 10 μL e 100 μL, respectivamente.

Determinações voltamétricas e espectroscópicas UV vis para quantificação de eugenol

As medidas eletroquímicas foram realizadas em um potenciostato, modelo CV50W, da Bioanalytical Systems, acoplado aos eletrodos e a um computador para captura dos dados, além de uma célula eletroquímica de vidro de 10 mL contendo tampa com entradas para os eletrodos e um agitador magnético. O eletrodo de trabalho utilizado (área = 0,06 cm^2), o de referência e o eletrodo auxiliar foram, respectivamente, de carbono vítreo, prata em solução de cloreto de prata (Ag/AgCl) e platina. O eletrólito suporte usado foi uma solução etanol/tampão BR pH 3,3 a 55%.

A quantificação do eugenol, no óleo, foi determinada por voltametria de pulso diferencial com o método da adição padrão, para o qual 10 mL de uma solução contendo o óleo —preparada com 100 μL da respectiva solução estoque e com eletrólito suporte em um balão volumétrico— foi adicionado à célula eletrolítica e o valor da corrente da referida solução foi lido. Em seguida, adicionaram-se volumes crescentes da solução estoque do padrão de eugenol, devidamente calculados, para resultar em concentrações de 2×10^{-5} a $1{,}4 \times 10^{-4}$ mol L^{-1}, e as respectivas correntes eram lidas.

Para a quantificação por espectroscopia UV-vis, realizamos os testes em comprimento de onda de 280 nm e com as amostras diluídas em solução de etanol/água destilada a 60% (v/v). A quantificação do eugenol foi determinada pelo método da adição padrão. Para tanto, foram utilizados cinco balões volumétricos de 10 mL (contendo cada um 20 μL da solução estoque do óleo essencial), nos quais foram adicionados individualmente volumes crescentes da solução estoque do padrão de eugenol (0, 20, 40, 60 e 80 μL); sendo, em seguida, aferidos com a solução etanol/água destilada a 60%. A absorbância das novas soluções assim obtidas foi lida, tendo como branco a solução de etanol/água. Os espectros de absorção observados, assim com a curva de adição padrão, foram obtidos por várias concentrações de eugenol no intervalo de $1{,}28 \times 10^{-4}$ a $5{,}12 \times 10^{-4}$ mol L^{-1} em solução de etanol/água a 60%.

Testes da atividade antibacteriana

As cepas de *Escherichia coli*, *Staphylococcus aureus*, *Proteus mirabilis, Pseudomonas aeruginosa e Serratia odorifera* utilizadas neste trabalho foram provenientes de alimentos e isoladas no Laboratório de Microbiologia da Universidade Federal do Maranhão.

Avaliamos a atividade antibacteriana do óleo essencial e do padrão de eugenol a partir do método de difusão em disco recomendado pela *Clinical Laboratory Standards Institute* (CLSI) [17]. Inoculamos as culturas bacterianas em caldo BHI (Brain and Heart Infusion) e após 24 h de incubação a 37 °C, procedemos a diluição até a obtenção de uma suspensão padronizada pelo grau 0,5 da escala de McFarland (108 microrganismos mL^{-1}). Posteriormente, semeamos o inóculo de cada cultura bacteriana (0,10 mL) com swab estéril na superfície das placas contendo ágar Mueller Hinton solidificado, e sobre a mesma foram aderidos, com auxílio de uma pinça previamente flambada, pequenos discos de papel de filtro com 6 mm de diâmetro impregnados, individualmente, com 75 μL do óleo essencial e com o padrão (eugenol), sendo pressionados levemente sobre a superfície do meio. Por fim, as placas foram incubadas a 37 °C por 24 h e os halos de inibição foram medidos em uma régua milimetrada, certificada pelo Instituto Nacional de Metrologia, Qualidade e Tecnologia (INMETRO).

Testamos o comportamento das cepas de *Escherichia coli*, *Staphylococcus aureus*, *Proteus mirabilis*, *Pseudomonas aeruginosa e Serratia odorifera* frente à ação de antimicrobianos comerciais seguindo o método de difusão de disco [17]. Os discos impregnados com os antimicrobianos foram distribuídos nas placas com o auxílio de uma pinça previamente flambada, sendo em seguida levemente pressionados contra a superfície do meio. Na sequência, as placas foram incubadas a 37 °C por 24 h. Os antimicrobianos utilizados foram escolhidos pela sua eficácia ao respectivo microrganismo conforme recomendação da CLSI [18], sendo estes: tetraciclina (TET 30 μg), vancomicina (VAN 30 μg), cefoxitina (CFO 30 μg), ampicilina (AMP 10 μg), cloranfenicol (CLO 30 μg), eritromicina (ERI 15 μg), gentamicina (GEN 10 μg), sulfazotrim (SUT 25 μg) e penicilina (PEN 10 μg).

Resultados

Extração do óleo, análise cromatográfica GC/EM, UV-vis e voltametria de pulso diferencial

Extraindo o óleo pela técnica de hidrodestilação, obtivemos um rendimento médio e densidade média, respectivamente, 2.16 % (m/m) e 0.968 gmL^{-1}. Da análise cromatográfica, identificamos a presença de 17 compostos, o que observamos no cromatograma (figura 1), onde o majoritário foi o eugenol e o minoritário o α-cariofileno, enquanto a classe predominante foi a dos monoterpenos, com 90,77% (tabela 1).

Tabela 1. Identificação dos componentes presentes no óleo essencial.

Compostos	Tempo de retenção (min)	Desvio padrão	Área normalizada (%)
1-Octen-3-ol	2,15	0,04	1,40
β-pineno	2,33	0,08	6,52
α-pineno	2,49	0,00	0,28
o-cimeno	2,66	0,04	1,94
Limoneno	2,77	0,05	4,09
Linalol	3,56	0,02	0,64
Cis-Hidrato de sabineno	4,64	0,01	0,22
α-terpineol	4,80	0,01	0,13
5-indanol	5,76	0,20	5,88

(*Continue*)

Tabela 1. Identificação dos componentes presentes no óleo essencial.

Compostos	Tempo de retenção (min)	Desvio padrão	Área normalizada (%)
Eugenol	7,23	0,32	76,98
α-Cubebeno	7,80	0,01	0,35
Cariofileno	8,41	0,00	0,09
α-Cariofileno	8,90	0,00	0,08
γ-muroleno	9,22	0,01	0,25
α-cadineno	9,58	0,00	0,19
α-muroleno	9,74	0,01	0,22
δ-cadineno	9,88	0,01	0,76
Álcool			1,40
Fenol			5,88
Monoterpenos			90,77
Sesquiterpenos			1,94

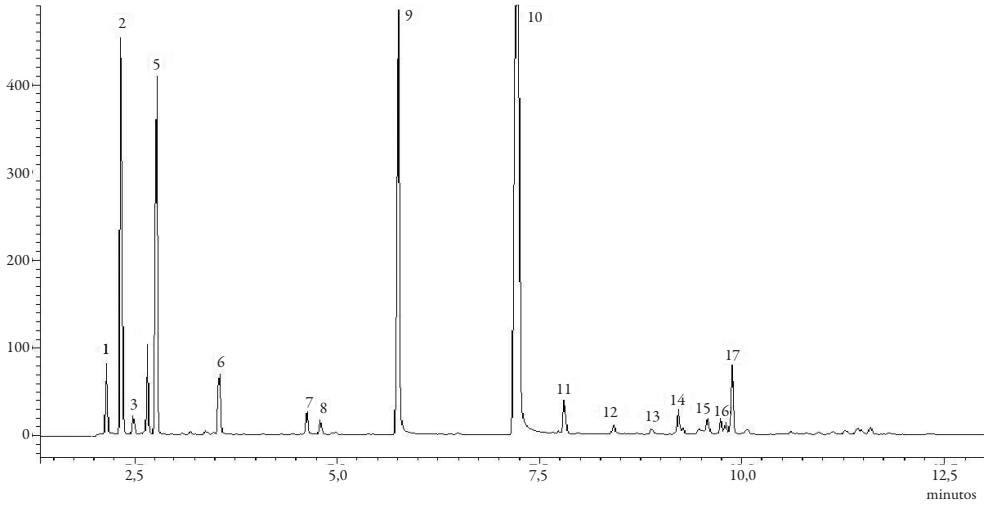

Figura 1. Cromatograma do óleo essencial dos frutos da *Pimenta dioica* Lindl.

No entanto, ao quantificarmos o eugenol pela técnica de adição por padrão por espectroscopia de ultravioleta (UV-vis) e por voltametria de pulso diferencial, observamos pouca diferença nos valores. Da análise espectroscópica, constatamos que o eugenol estava presente em uma quantidade de 78,15% (figura 2) enquanto este valor foi de

74,63% na voltametria (figura 3). Por fim, na figura 4, mostramos o comportamento eletroquímico do padrão eugenol e do óleo essencial enquanto na figura 5 observamos os voltamogramas de pulso diferencial da amostra e do padrão de eugenol.

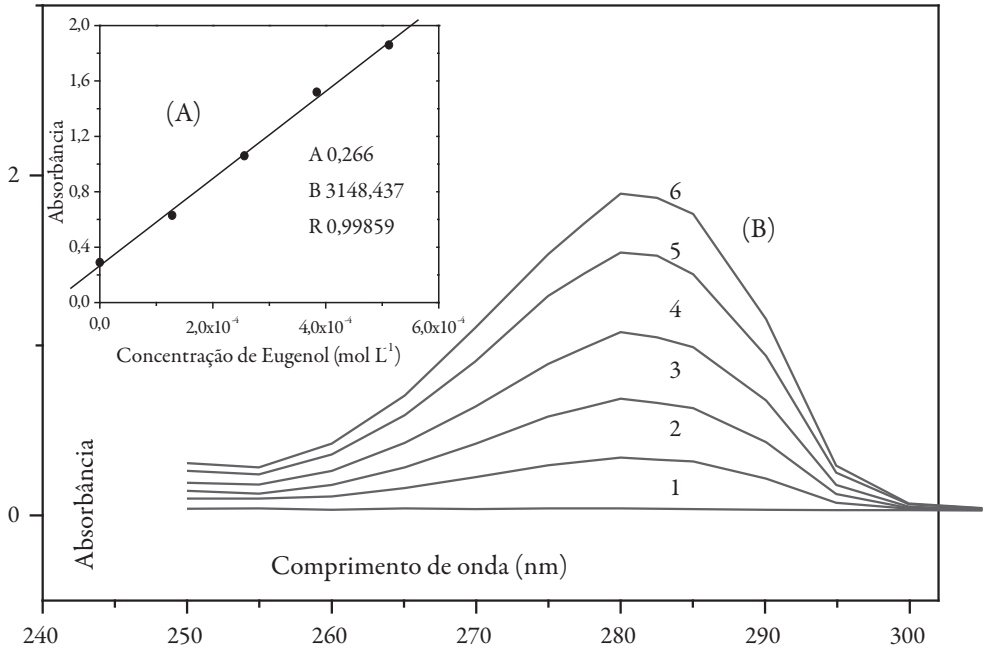

Figura 2. Determinação quantitativa do eugenol por espectroscopia de UV foi acompanhada pelo aumento da absorção da banda do anel aromático ($\lambda_{máx}$=280nm), em função do aumento da concentração do eugenol no óleo. A curva analítica de adição padrão foi caracterizada pelo coeficiente de correlação linear igual a 0,9986 e desvio padrão de 0,039. Nessa figura, mostramos a curva de adição padrão da solução estoque do padrão sobre 20 μL de solução estoque da amostra do óleo essencial em solução etanol/água a 60% (A); Em (B) Espectros de absorção da mistura etanol/água a 60%, respectivamente, (1), da amostra (2) e das concentrações do padrão de eugenol: (3) 1,28 x 10^{-4} mol L^{-1}, (4) 2,56 x 10^{-4} mol L^{-1}, (5) 3,85 x 10^{-4} mol L^{-1} e (6) 5,12 x 10^{-4} mol L^{-1}.

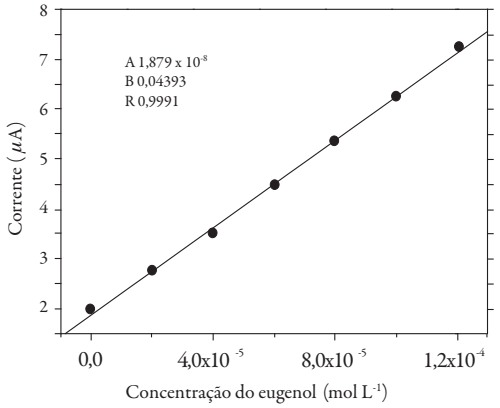

Figura 3. Curva da adição padrão obtida a partir do voltamograma de pulso diferencial da amostra e do padrão de eugenol em solução 55% etanol/tampão BR pH 3,3. Calculamos a concentração de eugenol no óleo essencial dos frutos da *Pimenta dioica* Lindl a partir da curva de adição padrão para o pico anódico. O valor da corrente lida para o óleo foi de 1,978 x 10^{-6} mol L^{-1}, o que resultou numa concentração inicial de eugenol na célula de 4,273 x 10^{-5} mol L^{-1} que ao ser levado em consideração a pureza do padrão utilizado (98%) e as devidas correlações de diluição, chegamos a um teor de 74,63% de eugenol presente no óleo essencial.

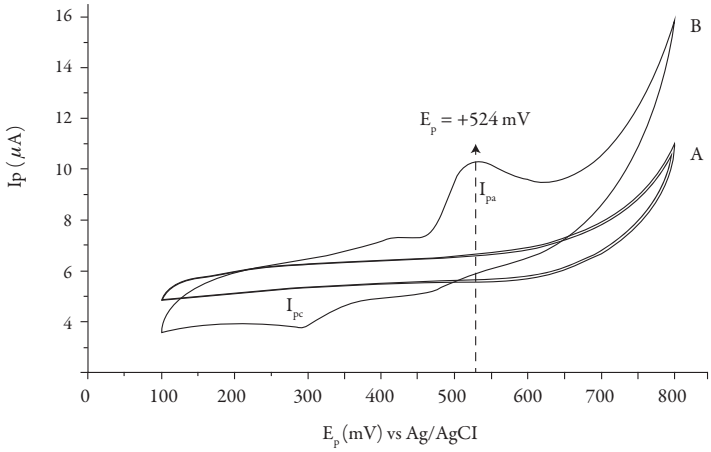

Figura 4. O comportamento eletroquímico do eugenol e o seu intervalo de potencial, nos quais foram obtidos por voltametria cíclica, utilizando eletrodo de carbono vítreo versus eletrodo de Ag/AgCl em solução de etanol/tampão BR pH 3,3 a 55%. Quando o eletrodo era apenas polido e uma varredura de potencial era executada (A), nenhuma resposta eletroquímica era obtida na faixa trabalhada, enquanto que na presença do óleo da *Pimenta dioica* Lindl (B) apareceram dois picos referentes à oxidação (524 mV) e redução (285 mV), indicando que o eugenol sofre processo redox quase reversível.

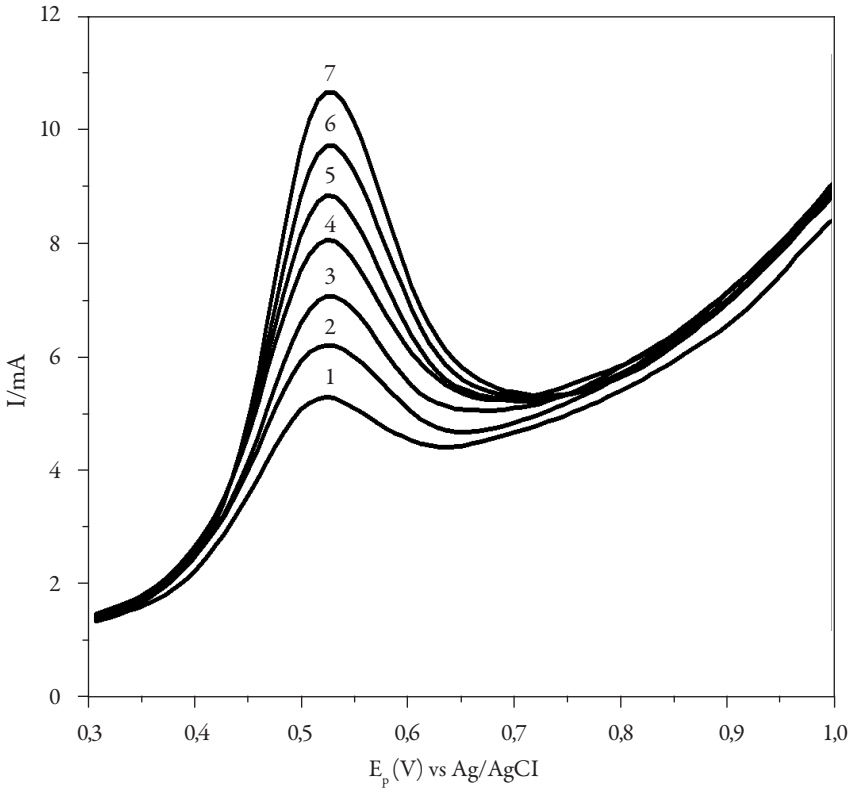

Figura 5. Inicialmente, leu-se a corrente de 100 µL da solução estoque da amostra (1) no eletrólito e no potencial de oxidação de 524 mV. Em seguida, adicionamos volumes pré-determinados de solução padrão de eugenol que resultou nas concentrações: 2 x 10^{-5} mol L^{-1} (2), 4 x 10^{-5} mol L^{-1} (3), 6 x 10^{-5} mol L^{-1} (4), 8 x 10^{-5} mol L^{-1} (5), 10 x 10^{-5} mol L^{-1} (6) e 12 x 10^{-5} mol L^{-1} (7), obtidos em solução 55% etanol/tampão BR pH 3,3. O tempo de deposição foi de 100 s, amplitude de pulso de 100 mV e velocidade de varredura de 50 mV s^{-1}.

Atividade antibacteriana

Na tabela 2 apresentamos o resultado da suscetibilidade microbiana do óleo essencial dos frutos da *Pimenta dioica* (L). Merr e padrão eugenol pelo método da difusão em disco em relação às bactérias *Escherichia coli, Staphylococcus aureus, Proteus mirabilis, Pseudomonas aeruginosa* e *Serratia odorifera*. Na figura 6, mostramos as imagens dos halos de inibição para óleo essencial. Deste resultado, observamos uma variação nos halos de 11 a 21 mm para o óleo essencial e 13 a 19 mm para o padrão eugenol.

Tabela 2. Sensibilidade das bactérias *Escherichia coli, Staphylococcus aureus, Proteus mirabilis, Pseudomonas aeruginosa e Serratia odorifera* ao óleo essencial dos frutos da *Pimenta dioica* (L.) Merr e ao padrão eugenol, utilizando-se o método de difusão em disco.

	Bactérias (média das medidas dos halos em milímetro)				
Compostos	*Escherichia coli*	*Staphylococcus aureus*	*Proteus mirabilis*	*Pseudomonas aeruginosa*	*Serratia odorifera*
Óleo essencial	21	21	20	16	13
Padrão eugenol	19	15	15	16	11

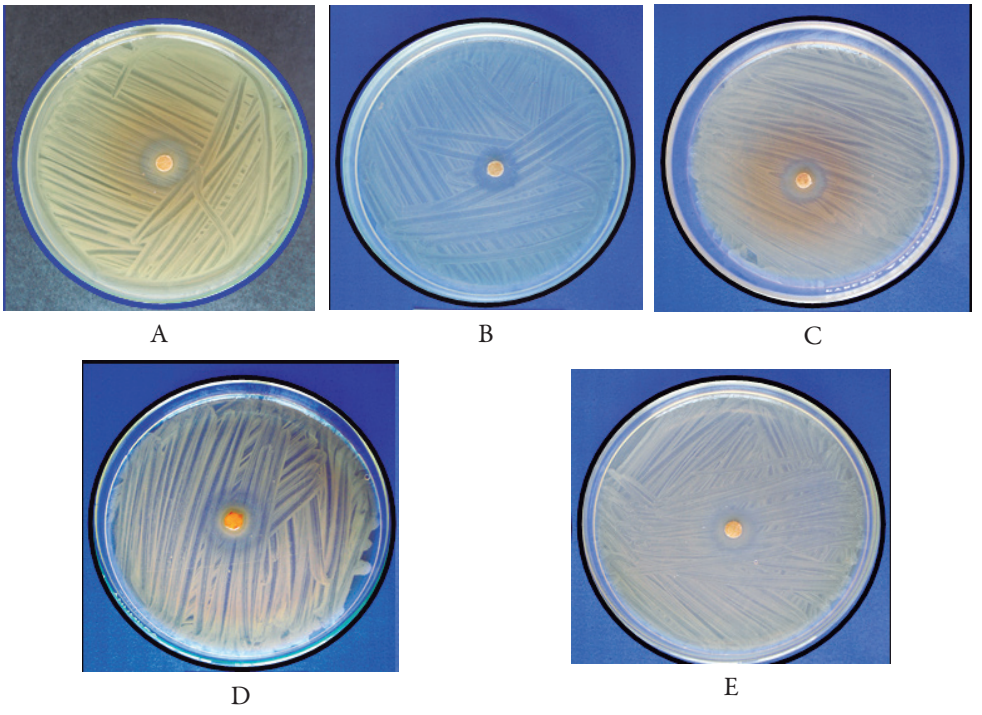

Figura 6. Atividade antibacteriana do óleo essencial da *Pimenta dioica* contra as bactérias (A) *Pseudomonas aeruginosa*, (B) *Staphylococcus aureus*, (C) *Escherichia coli*, (D) *Proteus mirabilis* e (E) *Serratia odorífera*.

Na tabela 3, observamos que os halos de inibição variaram de 8 a 40 mm para algumas bactérias frente aos antibióticos, sendo a penicilina mais efetiva contra a *S. aureus*. Na tabela 4, mostramos os parâmetros utilizados para considerar quando há sensibilidade alta, moderada ou resistência da bactéria ao antibiótico. A partir disso, observamos que

a bactéria *P. mirabilis* resistiu ao antibiótico ampicilina e cefoxitina. Enquanto a bactéria *Pseudomonas aeruginosa* apresentou sensibilidade alta à gentamicina, moderada ao clorafenicol e sulfazotrim e resistente à tetraciclina. Por fim, a *Serratia odorifera* resistiu à tetraciclina, pouco sensível ao cloranfenicol e moderadamente sensível à ampicilina e cefoxitina.

Tabela 3. Sensibilidade das bactérias *Escherichia coli*, *Staphylococcus aureus*, *Proteus mirabilis*, *Pseudomonas aeruginosa* e *Serratia odorífera* frente a alguns antibióticos.

Antibiótico	Bactéria*				
	Escherichia coli	***Staphylococcus aureus***	***Proteus mirabilis***	***Pseudomonas aeruginosa***	***Serratia odorifera***
Ampicilina	16	nt	0	nt	15
Cefoxitina	23	nt	0	nt	16
Cloranfenicol	22	nt	21	13	21
Eritromicina	nt	20	nt	nt	nt
Gentamicina	nt	19	nt	15	nt
Penicilina	nt	40	nt	nt	nt
Sulfazotrim	nt	nt	nt	12	nt
Tetraciclina	16	nt	14	12	8
Vancomicina	nt	16	nt	nt	nt

* halo medido em milímetro; nt: não foi testado.

Embora a ação inibitória do óleo seja semelhante aos antibióticos, observamos que houve diferenças para algumas bactérias. Para *Pseudomonas aeruginosa* (halo igual a 16 mm) estes valores para o tratamento com óleo essencial estão acima dos obtidos pelos antibióticos correspondentes. No caso da *Serratia odorifera*, este valor foi menor para o óleo e maior do que o teste com a tetraciclina, porém próximo ao resultado do teste com a ampicilina e cefoxitina.

Discussão

Em decorrência dos problemas provocados pelo uso dos antibacterianos químicos, a busca por produtos de origem natural incitou o interesse no desenvolvimento de novos agentes antibacterianos. Portanto, neste estudo mostramos que o óleo essencial extraído dos frutos da *Pimenta dioica*, que possui em sua maior quantidade o eugenol, e o

Tabela 4. Adaptação dos parâmetros da *Clinical and Laboratory Standards Institute* (CLSI) para os antibióticos testados.

Antibiótico	Código	Concentração (µg/L)	Zona de inibição (mm)		
			R	MS	S
Ampicilina	AMP	10	≤13	14-16	≥17
Cefoxitina	CFO	30	≤14	15-17	≥18
Cloranfenicol	CLO	30	≤12	13-17	≥ 18
Eritromicina	ERI	15	≤13	14-22	≥ 23
Gentamicina	GEN	10	≤12	13-14	≥15
Penicilina	PEN	10	≤28	–	≥ 29
Sulfazotrim	SUT	25	≤10	11-15	≥ 16
Tetraciclina	TET	30	≤14	15-18	≥19
Vancomicina	VAN	30	≤9	10-11	≥12

S = sensível; MS = moderadamente sensível; R = resistente (CLSI, 2008 [17]).

padrão eugenol possuem atividade contra as bactérias *Escherichia coli*, *Staphylococcus aureus*, *Proteus mirabilis*, *Pseudomonas aeruginosa* e *Serratia odorifera*.

Diversos fatores explicam as diferenças no rendimento e na composição química dos óleos essenciais. Em nosso estudo, o principal componente da *P. dioica* foi o eugenol. Geralmente as quantidades deste composto nos frutos estão em torno de 85% para um rendimento de 2 a 5% de óleo [19, 20]. Para explicar estas diferenças na composição, recorremos ao estudo realizado por Jiang *et al.* [21] que obtiveram diferentes rendimentos ao extrair o óleo essencial dos frutos da *P. dioica* por hidrodestilação e hidrodestilação assistida por micro-ondas. De acordo com os autores, esta diferença ocorre devido às facilidades de infiltração, difusão e troca entre as células do tecido vegetal durante a radiação com micro-ondas. Como este processo é mais lento na hidrodestilação convencional, as perdas de alguns constituintes também são afetadas quando a extração acontece de forma rápida ou lenta [22, 23]. Além do método de extração, outros fatores influenciam na diminuição do rendimento e, consequentemente, na alteração da composição dos constituintes do óleo são elas: as diferenças de temperatura, a geologia e a altitude [21].

Apesar do eugenol está em grande quantidade no óleo essencial da *P. dioica*, sabemos que a atividade antibacteriana está mais relacionada com o sinergismo do que com a classe funcional, a potência de grupos funcionais ou ao componente em si. Os

achados do nosso estudo estão concordantes com o estudo realizado por Wang *et al.* [24] quando estes avaliaram que os óleos essenciais *N. chinens*is e *V. officinalis* da China, cujos componentes pertenciam em sua maior parte à classe dos monoterpenos e sesquiterpenos, apresentaram atividade antimicrobiana em três tipos de bactérias Gram-positivas (*Bacillus subtilis*, *Staphylococcus aureus* e *Staphylococcus haemolyticus*), e cinco Gram-negativas (*Agrobacterium tumefaciens*, *Escherichia coli*, *Pseudomonas lachrymans*, *Salmonella typhimurium* e *Xanthomonas vesicatória*).

Bactérias Gram-negativas diferenciam-se das Gram-positivas a partir da camada dual que estas possuem e as protege da ação de agentes antimicrobianos. Para penetrar na célula, a parte hidrofóbica do óleo essencial deverá atingir a membrana celular de modo a partir a camada lipídica. Quando isto é provocado, a permeabilidade aumenta e, consequentemente, a célula bacteriana é desestabilizada. Embora isso aconteça com a maioria dos compostos, esta ação é menor nos sesquiterpenos devido à baixa solubilidade deste em água [25-27].

No que diz respeito à potência do grupo funcional, sabemos que constituintes fenólicos tais como eugenol e timol são efetivos contra bactérias de origem alimentar [28]. A razão para isto está relacionada com a parte hidrofóbica do composto; as interações da ligação de hidrogênio dos fenóis com a água e, por conseguinte, sua constante de acidez; e a inativação de enzimas e materiais genéticos [29]. Como os componentes do óleo neste estudo pertencem a diferentes funções, a atividade antibacteriana não é exclusiva de um ou outro composto, mas sim da ação conjunta de todos, em um processo chamado de sinergismo [30].

É fato que a atividade antibacteriana de um óleo essencial é comprovada pelo tamanho dos halos de inibição. Em nosso estudo mostramos que o tamanho dos halos de inibição das bactérias tratadas com óleo essencial foi um pouco menor (variação de 11 a 21 mm) em relação aos antibióticos (variação de 8 a 40 mm). Apesar de baixos valores nos halos, é consenso entre os autores considerarem um composto com atividade antibacteriana aquele que possui um valor mínimo no diâmetro dos halos de inibição entre 8 e 10 mm em testes feitos pelo método de difusão em disco [31-33].

Geralmente, os valores baixos obtidos neste método estão relacionados com a velocidade de difusão. Como o óleo essencial é viscoso e possui baixa polaridade, este encontra dificuldade em se difundir no ágar, cuja natureza é hidrófila. Assim, por menor que sejam os valores dos halos, um óleo essencial sempre será considerado um bom agente antibacteriano [34].

Enquanto o agente antibacteriano a base de óleo essencial pode ter qualquer valor no tamanho dos halos, os antibióticos possuem um padrão. Como mostramos na tabela 3, a resistência das bactérias dependerá do tipo de antibiótico.

Em nosso estudo, observamos que algumas bactérias apresentaram resistência, concordando assim com os dados da literatura. O estudo realizado por Fernández-Delgado *et al.* [35] mostrou que a bactéria *Proteus mirabilis* isolada de ostras da costa Venezuelana resistiu à maioria dos antibióticos testados, entre eles a ampicilina, cefoxitina e tetraciclina. Já o estudo realizado por Stock *et al.* [36] mostrou a baixa sensibilidade da *Serratia odorífera* à tetraciclina, estreptomicina e espectinomicina. Enquanto os estudos de Gonçalves *et al.* [37] mostraram que a *Escherichia coli* foi sensível à vancomicina e resistente à tetraciclina, e o *Staphylococcus aureus* à vancomicina, cefoxitina e cloranfenicol.

Esta resistência acontece devido às sucessivas mutações que alteram a permeabilidade celular, à degradação celular dos antimicrobianos e às alterações de alvos celulares [38]. Apesar da resistência de algumas bactérias aos antibióticos, neste estudo mostramos que o uso do óleo essencial apresentou resultados de inibição semelhantes aos antibióticos. Portanto, devido a estas pequenas diferenças, concluímos que o óleo essencial da *P. dioica* tem potencial atividade antibacteriana e que pode ser utilizado tanto na indústria de alimentos quanto na farmacêutica.

Conclusões

Destilamos o óleo essencial das folhas da *Pimenta dioica* por hidrodestilação e concluímos que este é constituído em sua maior parte por monoterpenos e pelo composto eugenol, no qual apresentou atividade antibacterianas contra a *Escherichia coli*, *Staphylococcus aureus*, *Proteus mirabilis*, *Pseudomonas aeruginosa* e *Serratia odorífera*.

Declaração de conflito de interesses

Os autores declaram que não tem conflito de interesses.

Referências

1. P. Sockett, Social and economic aspects of food-borne disease, *Food Policy*, **18**, 110-119 (1993).

2. D.W. Acheson, Foodborne infections, *Current Opinion in Gastroenterology*, **15**, 538-545 (1999).

3. Q. Shu, Y. Niu, W. Zhao, Q. Chen, Antibacterial activity and mannosylerythritol lipids against vegetative cells and spores of *Bacillus cereus*, *Food Control*, **106,** 106711 (2019).

4. K. Akinyemi, O. Oluwa, E. Omomigbehin, Antimicrobial activity of crude extracts of three medicinal plants used in south-west Nigerian folk medicine on some food borne bacterial pathogens, *African Journal of Traditional, Complementary and Alternative Medicines* **3**, 13-22 (2006).

5. D. Bialonska, P. Ramnani, S.G. Kasimsetty, K.R. Muntha, G.R. Gibson, D. Ferreira, The influence of pomegranate by-product and punicalagins on selected groups of human intestinal microbiota, *International Journal of Food Microbiology*, **140**, 175-182 (2010).

6. F. He, K. Li, X. Zhang, Y. Yang, Y. Fang, F. Xiang, Components, and antibacterial activity of a novel essential oil from the nutrient broth of *Eremothecium ashbyii* H4565, *LWT – Food Science and Technology*, **101,** 389-394 (2019).

7. S. Bedini, G. Flamini, R. Ascrizzi, F. Venturi, G. Ferroni, A. Bader, J. Girardi, B. Conti, Essential oils sensory quality and their bioactivity against the mosquito *Aedes albopictus*, *Scientific Reports*, **8**, 1-10 (2018).

8. P.S. Rao, S. Navinchandra, K. Jayaveera, An important spice, *Pimenta dioica* (Linn.) Merill: A review, *International Current Pharmaceutical Journal*, **1,** 221-225 (2012).

9. N.F. Morsy, K.S. Hammad, Volatile constituents, radical scavenging, and cytotoxic activities of Mexican allspice (*Pimenta dioica* L. Merrill) berries essential oil, *Journal of Essential Oil-Bearing Plants*, **21**, 859-868 (2018).

10. G.O. Everton, A.M. Teles, A.N. Mouchrek, E. Victor Filho, Aplicação do óleo essencial de *Pimenta dioica* Lindl. como moluscicida frente ao caramujo transmissor da esquistossomose, *Revista Processos Químicos*, **12**, 85-93 (2018).

11. M. Martinez-Velazquez, G.A. Castillo-Herrera, R. Rosario-Cruz, J.M. Flores-Fernandez, J. Lopez-Ramirez, R. Hernandez-Gutierrez, E. del C. Lugo-Cervantes, Acaricidal effect and chemical composition of essential oils extracted from *Cuminum cyminum*, *Pimenta dioica* and *Ocimum basilicum* against the cattle tick *Rhipicephalus (Boophilus) microplus* (Acari: Ixodidae), *Parasitology Research*, **108,** 481-487 (2011).

12. A.C. Lorenzo-Leal, E. Palou, A. López-Malo, Evaluation of the efficiency of allspice, thyme and rosemary essential oils on two foodborne pathogens in *in-vitro* and on alfalfa seeds, and their effect on sensory characteristics of the sprouts, *International Journal of Food Microbiology*, **295,** 19-24 (2019).

13. C.S. Marques, S.G. Carvalho, L.D. Bertoli, J.C.O. Villanova, P.F. Pinheiro, D.C.M. dos Santos, M.I. Yoshida, J.C.C. de Freitas, D.F. Cipriano, P.C. Bernardes, β-Cyclodextrin inclusion complexes with essential oils: Obtention, characterization, antimicrobial activity and potential application for food preservative sachets, *Food Research International*, **119**, 499-509 (2019).

14. D.G. da Rocha-Voris, L. dos Santos-Dias, J.A. Lima, K. dos Santos Cople-Lima, J.B. Pereira-Lima, A.L. dos Santos-Lima, Evaluation of larvicidal, adulticidal, and anticholinesterase activities of essential oils of *Illicium verum* Hook. f., *Pimenta dioica* (L.) Merr., and *Myristica fragrans* Houtt. against Zika virus vectors, *Environmental Science and Pollution Research*, **25**, 22541-22551 (2018).

15. T. Misharina, E. Alinkina, I. Medvedeva, Antiradical properties of essential oils and extracts from clove bud and pimento, *Applied Biochemistry and Microbiology*, **51**, 119-124 (2015).

16. M. Zabka, R. Pavela, L. Slezakova, Antifungal effect of *Pimenta dioica* essential oil against dangerous pathogenic and toxinogenic fungi, *Industrial Crops and Products*, **30**, 250-253 (2009).

17. J.L. Watts, T. Shryock, M. Apley, *et al.*, *Performance standards for antimicrobial disk and dilution susceptibility tests for bacteria isolated from animals; approved standard—third edition*, M31-A3 Vol. 28, No. 8, Clinical and Laboratory Standards Institute, Wayne, PA, 2008.

18. J.B. Patel, F.R. Cockerill, P.A. Bradford, *et al.*, *Performance standards for antimicrobial susceptibility testing: fifteenth informational supplement*, *M100-S25*, Vol. **35**, No. 3 Clinical and Laboratory Standards Institute, Wayne, PA, 2005.

19. M. González de Cosío, *Especies vegetales de importancia económica en México: contribución a su conocimiento*, Porrúa, México, 1984.

20. D.A. Minott, H.A. Brown, Differentiation of fruiting and non-fruiting *Pimenta dioica* (L.) Merr. trees based on composition of leaf volatiles, *Journal of Essential Oil Research*, **19**, 354-357 (2007).

21. Z.-T. Jiang, X. Feng, R. Li, Y. Wang, Composition comparison of essential oils extracted by classical hydro distillation and microwave-assisted hydrodistillation from *Pimenta dioica*, *Journal of Essential Oil Bearing Plants*, **16,** 45-50 (2013).

22. J. da S. Chaar, *Estudos analíticos e modificação química por acetilação do linalol contido no óleo essencial da espécie Aniba duckei Kostermans*, tese de doutorado, Instituto de Química de São Carlos, Universidade de São Paulo, São Carlos, 2000.

23. V.E. Mouchrek Filho, *Estudos Analíticos e modificações químicas por metilação e acetilação do eugenol contido no óleo essencial extraído das folhas da espécie Pimenta dioica Lindl.*, tese de doutorado, Universidade Federal de São Carlos, São Carlos, 2000.

24. J. Wang, J. Zhao, H. Liu, L. Zhou, Z. Liu, J. Wang, J. Han, Z. Yu, F. Yang, Chemical analysis and biological activity of the essential oils of two Valerianaceous species from China: *Nardostachys chinensis* and *Valeriana officinalis*, *Molecules* **15**, 6411-6422 (2010).

25. M.M. Cowan, Plant products as antimicrobial agents, *Clinical Microbiology Reviews*, **12**, 564-582 (1999).

26. S.G. Griffin, S.G. Wyllie, J.L. Markham, D.N. Leach, The role of structure and molecular properties of terpenoids in determining their antimicrobial activity, *Flavour and Fragrance Journal*, **14**, 322-332 (1999).

27. B.F. Brehm-Stecher, E.A. Johnson, Sensitization of *Staphylococcus aureus* and *Escherichia coli* to antibiotics by the sesquiterpenoids nerolidol, farnesol, bisabolol, and apritone, *Antimicrobial Agents and Chemotherapy*, **47**, 3357-3360 (2003).

28. R.A. Holley, D. Patel, Improvement in shelf-life and safety of perishable foods by plant essential oils and smoke antimicrobials, *Food Microbiology*, **22,** 273-292 (2005).

29. C.N. Wendakoon, M. Sakaguchi, Combined effect of sodium chloride and clove on growth and biogenic amine formation of *Enterobacter aerogenes* in mackerel muscle extract, *Journal of Food Protection***, 56**, 410-413 (1993).

30. S. Burt, Essential oils: their antibacterial properties and potential applications in foods--a review, *International Journal of Food Microbiology*, **94**, 223-253 (2004).

31. K. Cimanga, K. Kambu, L. Tona, S. Apers, T. de Bruyne, N. Hermans, J. Totté, L. Pieters, A.J. Vlietinck, Correlation between chemical composition and antibacterial activity of essential oils of some aromatic medicinal plants growing in the Democratic Republic of Congo, *Journal of Ethnopharmacology*, **79**, 213-220 (2002).

32. P.V. Farago, J.P. de Paula, J.I.M. Bittencourt, V. Zarpellon, L.E.M. Checchia, Atividade antibacteriana de óleos essenciais de *Ocimum selloi* Benth. (Lamiaceae), *Publicatio UEPG: Ciências Biológicas e da Saúde*, **10**, 59-63 (2004).

33. M.R. Moreira, A.G. Ponce, C.E. del Valle, S.I. Roura, Inhibitory parameters of essential oils to reduce a foodborne pathogen. *LWT – Food Science and Technology*, **38**, 565-570 (2005).

34. S. Glisic, S. Milojevic, S. Dimitrijevic, A. Orlovic, D. Skala, Antimicrobial activity of the essential oil and different fractions of *Juniperus communis* L. and a comparison with some commercial antibiotics, *Journal of the Serbian Chemical Society*, **72**, 311-320 (2007).

35. M. Fernández-Delgado, M. Contreras, M.A. García-Amado, P. Gueneau, P. Suárez, Occurrence of *Proteus mirabilis* associated with two species of Venezuelan oysters, *Revista do Instituto de Medicina Tropical de São Paulo*, **49**, 355-359 (2007).

36. I. Stock, Natural antimicrobial susceptibilities of strains of "unusual" Serratia species: *S. ficaria*, *S. fonticola*, *S. odorifera*, *S. plymuthica* and *S. rubidaea*, *Journal of Antimicrobial Chemotherapy*, **51**, 865-885 (2003).

37. F.A. Gonçalves, M. Andrade Neto, J.N.S. Bezerra, A. Macrae, O.V. de Sousa, A.A. Fonteles-Filho, R.H.S.F. Vieira, Antibacterial activity of GUAVA, *Psidium guajava* Linnaeus, leaf extracts on diarrhea-causing enteric bacteria isolated from Seabob shrimp, *Xiphopenaeus kroyeri* (Heller), *Revista do Instituto de Medicina Tropical de São Paulo*, **50**, 11-15 (2008).

38. H. Nikaido, Prevention of drug access to bacterial targets: permeability barriers and active efflux, *Science*, **264**, 382-388 (1994).

Como citar este artigo

P.R. Barros-Gomes, J.D. Ribeiro, M.C. Guimarães da Costa, M.W. da Silva Castro, N.B. Neto, A. Vasconcelos-Melo, G. Oliveira-Everton, H. Costa-Louzeiro, M. Alves-Fontenele, H. Souza de Lima, E. Fonseca-Silva, M. do L. de Paula, V.E. Mouchrek Filho, A.N. Mouchrek, Composição química e atividade antibacteriana do óleo essencial dos frutos da *Pimenta dioica*, *Rev. Colomb. Cienc. Quím. Farm.*, **49**(3), 656-674 (2020).

Scientific research article / *http://dx.doi.org/10.15446/rcciquifa.v49n3.91337*

Thermodynamic analysis and preferential solvation of gatifloxacin in DMF + methanol cosolvent mixtures

Mónica Rojas-Motta[1], Jhon Edinson Rojas-Motta[1], Jorge Luis Diaz-Jimenez[1], Fabio Andrés Bahos-Narváez[2], Joaquín H. Blanco-Márquez[3], Claudia Patricia Ortiz[4], Daniel Ricardo Delgado[5]*

[1]Universidad Cooperativa de Colombia, Department of Engineering, Industrial Engineering Program, Research Seedbed Industrial Engineering and Research, Calle 11 N.° 1 - 51, Neiva, Huila, Colombia.

[2]Servicio Nacional de Aprendizaje, Centro de Industria la Empresa y los Servicios, Tecnoparque Nodo Neiva, Departamento de Electrónica, Diagonal 20 N.° 38-16, Neiva, Huila, Colombia.

[3]Grupo de investigación Ciencia, Ingeniería e Innovación, Sifati Group Ingeniería S.A.S, Palermo, Colombia.

[4]Corporación Universitaria Minuto de Dios-UNIMINUTO, Programa de Administración en Salud Ocupacional, Grupo de Investigación en Seguridad y Salud en el Trabajo, Neiva, Colombia.

[5]Universidad Cooperativa de Colombia, Department of Engineering, Industrial Engineering Program, GRIAUCC Research Group, Calle 11 N.° 1 - 51, Neiva, Huila, Colombia.

*Corresponding author: danielr.delgado@ucc.edu.co;
ORCID: http://orcid.org/0000-0002-4835-9739

Received: 25 May 2020

Revised: 1 July 2020

Accepted: 3 July 2020

Summary

This paper presents the thermodynamic analysis of solubility of gatifloxacin in the N,N-Dimethylformamide (DMF) + methanol (MeOH) cosolvent system at 10 temperatures. From the solubility data, the thermodynamic functions of solution, mixing, and transfers are calculated and analyzed using the Perlovich graphical method. On the other hand, an enthalpy-entropy compensation analysis is performed and the preferential solvation parameters are calculated using the inverse Kirkwood-Buff integral (IKBI) method. The result of the performed calculations indicates that the gatifloxacin solution process is endothermic with entropic favor, where the addition of DMF has a positive cosolvent effect in all cases. Regarding preferential solvation, the results are not entirely conclusive, since in all cases the values of the preferential solvation parameter are less than 0.01, so that, negligible preferential solvation takes place.

Key words: gatifloxacin, solubility, *N,N*-dimethylformamide, IKBI, preferential solvation.

Resumen

Análisis termodinámico y solvatación preferencial de gatifloxacina en mezclas cosolventes DMF + metanol

Este artículo presenta el análisis termodinámico de la solubilidad de gatifloxacina en el sistema cosolvente de *N*,*N*-Dimetilformamida (DMF) + metanol (MeOH) a 10 temperaturas. A partir de los datos de solubilidad se calculan las funciones termodinámicas de solución, mezcla y transferencia. Para el análisis además se utiliza el método gráfico Perlovich. Por otro lado, se realiza un análisis de compensación entalpía-entropía y se calculan los parámetros de solvatación preferencial utilizando el método de las integrales inversas de Kirkwood-Buff (IIKB). Los resultados del análisis termodinámico indican que el proceso de solución de gatifloxacina es endotérmica con favorecimiento entrópico, donde la adición de DMF tiene un efecto cosolvente positivo en todos los casos. En cuanto a la solvatación preferencial, los resultados no son del todo concluyentes, debido a que en todos los casos los valores del parámetro de solvatación preferencial son menores a 0,01 indicando una solvatación insignificante.

Palabras clave: gatifloxacina, solubilidad, *N*,*N*-dimetilformamida, IIKBI, solvatación preferencial.

Introduction

Gatifloxacin (1-cyclopropyl-6-fluoro-8-methoxy-7-(3-methylpiperazin-1-yl)-4-oxoquinoline-3-carboxylic acid; CAS: 112811-59-3) (figure 1) is an antibiotic agent and a member of the fourth-generation fluoroquinolone family. It works by inhibiting the bacterial enzymes DNA gyrase and topoisomerase IV [1, 2]. Gatifloxacin is effective against a broad spectrum of bacteria that may cause ocular infections in humans including endopthalmitis and conjunctivitis. Melo *et al.* found that gatifloxacin was effective against a range of both Gram positive and Gram negative microorganisms including anaerobes when tested in vitro, which transforms this drug into a dangerous agent for the aquatic systems, if used indiscriminately [3].

In addition, the pharmaceutical industry is a potential source of contamination, since most processes, such as synthesis, purification of raw materials, chemical analysis for quality assessment, and pre-formulation and formulation studies, tend to produce large masses of waste containing these chemical agents [4, 5].

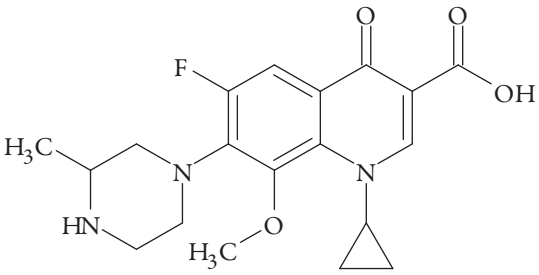

Figure 1. Molecular structure of gatifloxacin.

In this sense, the development of strategies that lead to the design of more environmental-friendly methodologies, focused on environmental management systems supported by ISO 14001, and leading to promoting the development of cleaner production practices have been consolidated as an important tool for the prevention and correction of contaminating processes [6, 7]. Thus, the generation of experimental data and the development of mathematical models that allow predicting properties such as solubility contribute greatly to reducing experimental tests, which in turn decreases the mass of pollutants (e.g., drugs, solvents, disposable material, and energy) produced in processes of the pharmaceutical industry [8, 9].

In this context, mathematical models tending to predict the solubility of drugs in different solvents and/or cosolvents mixtures at different temperatures have become an important tool for the pharmaceutical industry [10], not only for drugs but also for other large organic molecules, such as polycyclic aromatic hydrocarbons, which, like drugs, are also a source of contamination by the oil industry [11, 12]. Thus, based on thermodynamic properties, models such as the "nearly ideal binary solvent" approach by Acree *et al.* allow to successfully determine solubility in some types of cosolvent mixtures [13, 14]. Another model, which is an improvement of the previous one, is that proposed by Jouyban *et al.*, which involves polar and non-polar solvents [15, 16]. Other models based on area surfaces, contribution of UNIFAC groups, Hildebrand solubility parameters, and Kirkwood-Buff integrals have been proposed and refined to improve their predictability [17-20].

Thus, based on the solubility data of gatifloxacin in *N*,*N*-Dimethylformamide + methanol cosolvent mixtures, published by Wu *et al.* [21], and some data on the physicochemical properties of the drug (table 1) [22], the objective of the present work is perform a thermodynamic analysis and of preferential solvation.

Table 1. Physicochemical information of the gatifloxacin.

Chemicals	CAS reg. no.	molar mass / g mol^{-1}	Melting point / K	Melting enthalpy / kJ mol^{-1}
Gatifloxacin	112811-59-3	375.39	435.15[a]	34.95[a]

[a] *Ref* [22].

Results and discussion

Solubility of Gatifloxacin in DMF + methanol cosolvent mixtures

Figure 2 show the solubility of gatifloxacin (3) in DMF (1) + methanol (2) cosolvent mixtures, in this plot, can look an increase in solubility, as a consequence of an increase in temperature, which implies that the solution process in DMF (1) + methanol (2) cosolvent mixtures is favored by supplying energy to the system. This demonstrates that the process is endothermic [23, 24], where we can obtain the lowest solubility in pure methanol at 273.15 K (1.9 x 10^{-4}) and the maximum solubility in pure DMF (9.891 x 10^{-3}) at 318.15 K.

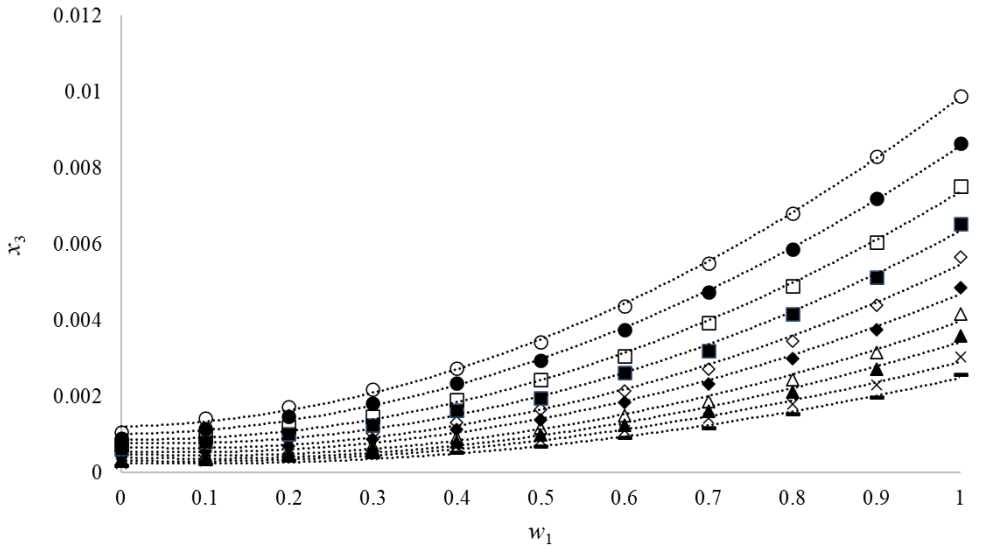

Figure 2. Solubility of gatifloxacin (3) expressed in molar fraction (x_3) in DMF (1) + methanol (2) cosolvent mixtures as a function of mass fraction at different temperatures. **-**: 273.15, **x**: 278.15 K; ▲: 283.15 K; Δ: 288.15 K; ♦: 293.15 K; ◊: 298.15 K; ▪: 303.15 K; □: 308.15 K; ●: 313.15 K; and ○: 318.15 K.

According to Hildebrand's theory, it would be expected that the maximum solubility would be reached in a cosolvent mixture and not in a pure solvent, as it happens in this case, because the polarity of la gatifloxacin (28.08 $MPa^{1/2}$ [25, 26]) (table 2) is between the polarity of DMF (24.1 $MPa^{1/2}$ [25]) and the polarity of methanol (29.7 $MPa^{1/2}$) [25].

Table 2. Application of the Fedors' method to estimate internal energy, molar volume, and Hildebrand solubility parameter of gatifloxacin (3) [25, 26].

Group	Group number	$V°$ / cm^3 mol^{-1}	$U°$ / kJ mol^{-1}
–NH–	1	4.5 x 1 = 4.5	8.4 x 1 = 8.4
>N–	2	-9 x 2 = -18	4.2 x 2 = 8.4
$–CH_3$	2	33.5 x 2 = 67	4.71 x 2 = 9.42
$–CH_2$	5	16.1 x 5 = 80.5	4.94 x 5 = 24.7
>CH–	3	-1 x 3 = -3	3.43 x 3 = 10.29
>C=	1	-5.5 x 1= -5.5	4.3 x 1 = 4.3
–C=O	1	10.8 x 1 = 10.8	17.4 x 1 = 17.4
–COOH	1	28.5 x 1 = 28.5	27.6 x 1 = 27.6
–O–	1	3.8 x 1 = 3.8	3.4 x 1 = 3.4
–F	1	18 x 1 = 18	4.19 x 1 = 4.19
Phenyl (pentasubstituted)	1	-4.6 x 1 = -4.6	31.9 x 1 = 31.9
Halogen attached to C atom with double bond	1	-	-0.2 x 4.19 = -0.84
Ring closure 5 or more atoms	2	16 x 2 = 32	1.05 x 2 = 2.10
Ring closure 3 or 4 atoms	1	18 x 1 = 18	3.14 x 1 = 3.14
Total		232.0	156.04
Solubility parameter			25.93 $MPa^{1/2}$

Activity coefficients

From the activity coefficients, the possible molecular interactions that govern the process of gatifloxacin solubility in the DMF + methanol cosolvent mixture can be inferior.

Table 3 presents the values of the activity coefficients in the DMF + methanol cosolvent system at nine temperatures calculated according to equation 1 [27], from the solubility data [21] and the ideal solubility calculated according to equation 2, which can be analyzed based on the solute-solute (e_{33}), solvent-solvent (e_{11}), and solute-solvent (e_{13}) molecular interactions using equation 3 [28]:

$$\gamma_3 = x_3^{id} / x_3 \tag{1}$$

$$\ln x_3^{id} = -\left\{\left[\Delta_{fus}H\left(T_{fus} - T\right)\right]\left[RT_{fus}T\right]^{-1}\right\} + \left\{\Delta C_P R^{-1}\left[\left(T_{fus} - T\right)T^{-1} + \left(\ln T - \ln T_{fus}\right)\right]\right\} \tag{2}$$

here x_3^{id} is the ideal solubility of the solute as mole fraction, $\Delta_{fus}H$ is the molar enthalpy of fusion of the pure solute (at the melting point), T_{fus} is the absolute melting point, T is the absolute solution temperature, R is the gas constant (8.314 J mol^{-1} K^{-1}), and ΔC_p is the difference between the molar heat capacity of the crystalline form and the molar heat capacity of the hypothetical super-cooled liquid form, both at the solution temperature. Since ΔC_p cannot be easy experimentally determined it is usual assuming that it may be approximated to the entropy of fusion, $\Delta_{fus}S$ [29,30].

$$\ln \gamma_3 = \left(e_{11} + e_{33} - 2e_{13}\right)V_3\varphi_1^2\left(RT\right)^{-1} \tag{3}$$

where V_3 is the molar volume of the supercooled liquid solute, and finally, ϕ_1 is the volumetric fraction of the solvent. A good approximation, for relatively low solubilities, is that the term $V_3\varphi^2{}_1/RT$ can be considered a constant, and therefore, ln γ_3 depends solely on $e_{11} + e_{33} - 2e_{13}$ [31]. The e_{11} and e_{33} terms are unfavorable for drug solubility and the term e_{13} favors the solubility thereof [32].

In all cases (table 3), the activity coefficients are greater than unity, which according to equation 3 [33], indicates that the solute-solute (e_{33}) and solvent-solvent (e_{11}) molecular interactions, which demerit the process of the solution, surpass the solute-solvent interactions, which favor the process.

In general, with an increase in temperature, the activity coefficients decrease and the cosolvent system's polarity decreases; thus, from pure methanol to the pure DMF, the activity coefficients decrease, showing a possible increase in the solute-solvent interactions, due to increased solubility of gatifloxacin (e_{13}).

Thermodynamic functions of solution

The standard thermodynamic functions of the solution (table 4) are calculated from the experimental solubility data and study temperatures. Thus, the mathematical expressions of Gibbs and van't Hoff, under Krug's approach, are presented as follows [4, 34, 35]:

$$T_{hm} = n / \sum_{i=1}^{n} 1/T_i \tag{4}$$

Table 3. Coefficient activity of gatifloxacin (3) in DMF (1) + methanol (2) cosolvent mixtures at different temperatures and pressure p = 0.1 MPa.

w_1 [a]	T / K									
	273.15	278.15	283.15	288.15	293.15	298.15	303.15	308.15	313.15	318.15
0.00	58.6	57.1	53.6	51.8	50.3	48.8	47.8	47.4	46.2	45.3
0.10	45.6	42.6	42.4	39.7	40.1	39.7	37.7	38.0	36.2	34.1
0.20	34.4	33.3	32.5	31.8	31.2	30.2	30.3	29.8	28.4	28.2
0.30	26.8	25.7	25.5	25.8	24.8	25.1	24.4	24.1	22.7	22.3
0.40	20.5	19.2	19.7	20.3	19.3	19.5	18.7	18.6	17.8	17.7
0.50	15.8	15.5	15.9	15.8	15.8	15.6	15.4	14.6	14.2	14.1
0.60	11.9	12.0	12.5	12.4	12.0	12.1	11.6	11.6	11.1	11.1
0.70	9.4	9.3	9.7	9.9	9.4	9.6	9.5	9.1	8.8	8.8
0.80	7.2	7.4	7.4	7.6	7.4	7.5	7.3	7.3	7.1	7.1
0.90	5.6	5.8	5.8	5.9	5.9	5.9	5.9	5.9	5.8	5.8
1.00	4.3	4.3	4.4	4.5	4.5	4.6	4.7	4.7	4.8	4.9

[a] w_1, mass fraction of DMF (1) in the gatifloxacin -free DMF (1) + methanol (2) mixture.

$$\Delta_{\text{soln}}H^{\circ} = -R\partial \ \text{In}\, x_3 / \partial\left(T^{-1} - T_{hm}^{-1}\right) \tag{5}$$

$$\Delta_{\text{soln}}G^{\circ} = -RT \times \text{intercept} \tag{6}$$

$$\Delta_{\text{soln}}S^{\circ} = T_{hm}^{-1}\left(\Delta_{\text{soln}}H^{\circ} - \Delta_{\text{soln}}G^{\circ}\right) \tag{7}$$

$$\xi_H = \left(\left|\Delta_{\text{soln}}H^{\circ}\right|\right)\left(\left|\Delta_{\text{soln}}H^{\circ}\right| + \left|T_{hm}\Delta_{\text{soln}}S^{\circ}\right|\right)^{-1} \tag{8}$$

$$\xi_{TS} = 1 - \xi_H \tag{9}$$

where T_{hm} is the harmonic temperature, $\Delta_{\text{soln}}G^{\circ}$ is the standard Gibbs energy of solution, $\Delta_{\text{soln}}H^{\circ}$ is the standard enthalpy of solution, and $\Delta_{\text{soln}}S^{\circ}$ is the standard entropy of solution. ξ_H y ξ_{TS} are the enthalpy and entropy contributions to the solution process and the intercept corresponds to the linear equation of the plot $\ln x_3$ vs. $(1/T - 1/T_{\text{hm}})$ [36, 37].

Table 4. Thermodynamic functions of solution of gatifloxacin (3) in DMF (1) + methanol (2) cosolvent mixtures at 294.95 K and pressure p = 0.1 MPa.

w_1 [a]	$\Delta_{soln}G°$ / kJ mol^{-1}	$\Delta_{soln}H°$ / kJ mol^{-1}	$\Delta_{soln}S°$ / J mol^{-1} K^{-1}	$T\Delta_{soln}S°$ / kJ mol^{-1}	ξ_H	ξ_{TS}
0.00	18.8	27.8	30.45	8.98	0.76	0.24
0.10	18.2	27.6	31.75	9.36	0.75	0.25
0.20	17.6	26.7	30.99	9.14	0.75	0.25
0.30	17.0	26.2	31.17	9.19	0.74	0.26
0.40	16.4	25.7	31.59	9.32	0.73	0.27
0.50	15.9	25.5	32.61	9.62	0.73	0.27
0.60	15.2	25.1	33.56	9.90	0.72	0.28
0.70	14.7	24.8	34.51	10.18	0.71	0.29
0.80	14.1	24.2	34.26	10.11	0.71	0.29
0.90	13.5	23.2	32.85	9.69	0.71	0.29
1.00	12.9	21.5	29.19	8.61	0.71	0.29
Ideal	9.2	23.7	49.07	14.47	0.62	0.38

[a] w_1 is mass fraction of DMF (1) in the gatifloxacin-free DMF (1) + methanol (2) mixture.

Gibbs energy is positive in all cases and decreases from pure methanol to pure DMF. As for the standard solution, it is positive in all cases, indicating an endothermic process, and decrease from pure methanol to pure DMF, possibly due to an increase in solute-solvent interactions, which is consistent with the gatifloxacin solubility increase in DMF-rich mixtures and pure DMF.

Regarding the standard solution entropy, it is positive in all cases, presenting an entropic favor to the gatifloxacin solution process in DMF + MeOH cosolvent mixtures.

From the results of equations 8 and 9, it can be concluded that the solution process is favored in all cases by enthalpy. A graphical method that allows corroborating the previously exposed is that developed by Perlovich (figure 3) (all values are within sector I: $\Delta_{soln}H° > T\Delta_{soln}S° > 0$ [38, 39]). Thus, the contribution of the solution's standard enthalpy to Gibbs energy values in all cases is greater than 71%, being greater in methanol-rich mixtures and less in DMF-rich mixtures.

Although there is an enthalpy predominance, the solution entropy promotes a decrease in Gibbs energy values, which generally favors the solution process.

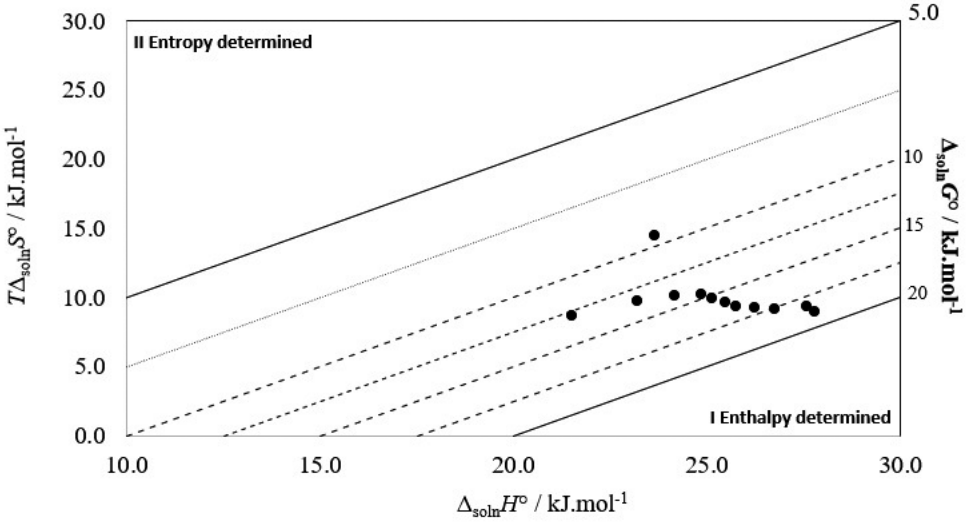

Figure 3. Relation between enthalpy ($\Delta_{soln}H°$) and entropy ($T\Delta_{soln}S°$) terms of the process of gatifloxacin solution in DMF (1) + methanol (2) cosolvent mixtures at 294.95 K. The isoenergetic curves for $\Delta_{soln}G°$ are represented by dotted lines.

Thermodynamic transfer functions

One way to identify the cosolvent effect on the thermodynamic behavior of the solution process is to analyze the transfer functions. Starting from a hypothetical transfer process from a medium of greater polarity to a medium of lower polarity, the thermodynamic transfer functions are calculated as [40]:

$$\Delta_{tr} f^0 = \Delta_{soln} f^0_{less\ polar} - \Delta_{soln} f^0_{more\ polar} \tag{10}$$

where, f represents thermodynamic functions, Gibbs energy, enthalpy, or entropy.

Table 5 shows the most representative values of the gatifloxacin transfer process from pure methanol to pure DMF. From the results of equation 10, a Perlovich plot [39] (figure 4) is drawn, which provides a good analysis of the results.

Thus, according to the Perlovich plot [4, 37, 39, 41, 42], from pure methanol to $w_{0.10}$ (Sector III $\Delta_{tr}H° < 0$, $T\Delta_{tr}S° > 0$, and $|T\Delta_{tr}S°| > |\Delta_{tr}H°|$) the process is driven by entropy; from $w_{0.10}$ to $w_{0.20}$ (Sector V $\Delta_{tr}H° < 0$, $T\Delta_{tr}S° < 0$, and $|T\Delta_{tr}S°| < |\Delta_{tr}H°|$) the process is driven by enthalpy; from $w_{0.20}$ to $w_{0.40}$ (Sector IV $\Delta_{tr}H° < 0$, $T\Delta_{tr}S° > 0$, and $|T\Delta_{tr}S°| < |\Delta_{tr}H°|$), the process is again driven by enthalpy; from $w_{0.40}$ to $w_{0.50}$ (Sector

Table 5. Thermodynamic functions of transfer of gatifloxacin (3) in DMF (1) + methanol (2) co-solvent mixtures at 294.95 K and pressure p = 0.1 MPa.

More polar→less polar	$\Delta_{tr}G°$ / kJ mol^{-1}	$\Delta_{tr}H°$ / kJ mol^{-1}	$\Delta_{tr}S°$ / J mol^{-1} K^{-1}	$T\Delta_{tr}S°$ / kJ mol^{-1}
[a]$w_{0.00}$→ $w_{0.10}$	-0.60	-0.22	1.3	0.38
$w_{0.10}$→ $w_{0.20}$	-0.60	-0.82	-0.8	-0.22
$w_{0.20}$→ $w_{0.30}$	-0.56	-0.50	0.2	0.05
$w_{0.30}$→ $w_{0.40}$	-0.63	-0.50	0.4	0.12
$w_{0.40}$→ $w_{0.50}$	-0.55	-0.25	1.0	0.30
$w_{0.50}$→ $w_{0.60}$	-0.62	-0.35	0.9	0.28
$w_{0.60}$→ $w_{0.70}$	-0.58	-0.30	0.9	0.28
$w_{0.70}$→ $w_{0.80}$	-0.60	-0.67	-0.2	-0.07
$w_{0.80}$→ $w_{0.90}$	-0.56	-0.98	-1.4	-0.42
$w_{0.90}$→ $w_{1.00}$	-0.60	-1.67	-3.7	-1.07

[a] w_1, mass fraction of DMF (1) in the gatifloxacin-free DMF (1) + methanol (2) mixture.

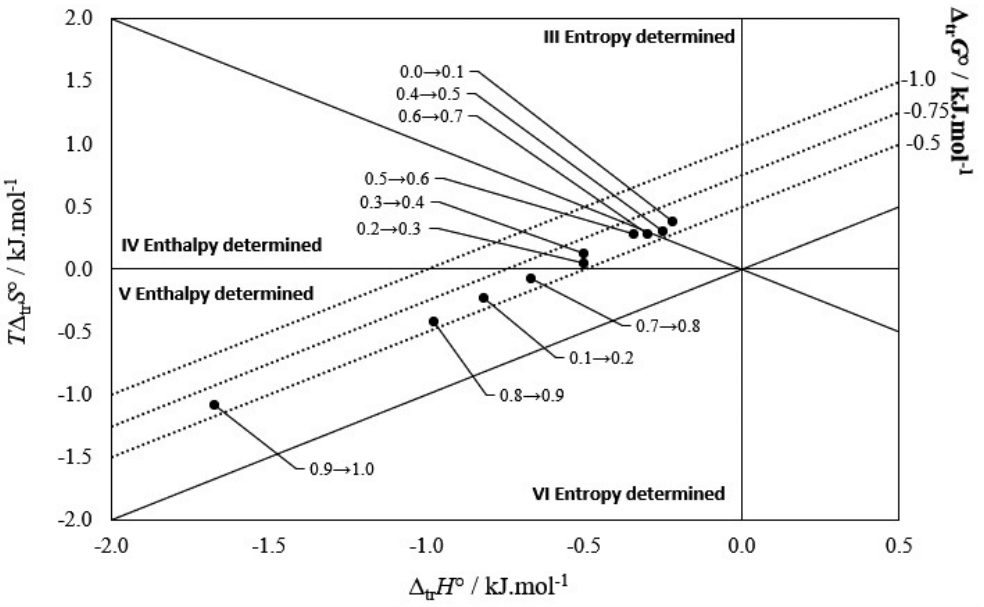

Figure 4. Relationship between the enthalpy ($\Delta_{tr}H°$) and entropy ($T\Delta_{tr}S°$) terms of the transfer process of gatifloxacin from more polar mixtures to less polar mixtures at 294.95 K. The isoenergetic curves of $\Delta_{tr}G°$ are represented by dotted lines.

III $\Delta_{tr}H° < 0$, $T\Delta_{tr}S° > 0$, and $|T\Delta_{tr}S°| > |\Delta_{tr}H°|$) the process is driven by entropy; from $w_{0.50}$ to $w_{0.70}$ (Sector IV $\Delta_{tr}H° < 0$, $T\Delta_{tr}S° > 0$, and $|T\Delta_{tr}S°| < |\Delta_{tr}H°|$), the process is driven by enthalpy and from $w_{0.70}$ to pure DMF (Sector V $\Delta_{tr}H° < 0$, $T\Delta_{tr}S° < 0$, and $|T\Delta_{tr}S°| < |\Delta_{tr}H°|$) the process continues to be driven by enthalpy.

So, in all cases there is an enthalpy favor (negative enthalpy), therefore there is an enthalpy conduction in the whole process, however, from $w_{0.10}$ to $w_{0.20}$ and from $w_{0.90}$ to DMF the entropy is negative, therefore, entropy disadvantages the transfer process. In other cases, entropy is positive, indicating that the solution process is favored by enthalpy and entropy.

Thermodynamic functions of the mixing

The solute behavior in the dissolution process can generally be divided into two stages, the solute fusion and its subsequent mixing with the solvent, so this hypothetical process can be represented according to the following scheme [43, 44]:

$$\text{Solute}_{(\text{Solid})} \text{ at } T \rightarrow \text{Solute}_{(\text{Solid})} \text{ at } T_{\text{fus}} \rightarrow \text{Solute}_{(\text{Liquid})} \text{ at } T_{\text{fus}} \rightarrow \text{Solute}_{(\text{Liquid})} \text{ at } T \rightarrow \text{Solute}_{(\text{Solution})} \text{ at } T$$

In this way, thermodynamic solution functions can be represented by the following equation:

$$\Delta_{\text{soln}} f^0 = \Delta_{\text{f}} f^0 + \Delta_{\text{mix}} f^0 \tag{11}$$

where, f represents the thermodynamic functions (G, H or S) and the subscripts ***f*** and **mix** represent fusion and mixing, respectively.

Thus, the mixing functions are determined as [45]:

$$\Delta_{\text{mix}} f^0 = \Delta_{\text{soln}} f^{0-T_{fm}} - \Delta_{\text{f}} f^0 \tag{12}$$

where $\Delta_{\text{f}} f°$ is replaced by the ideal thermodynamic functions, which are thus calculated as[46]

$$\Delta_{\text{mix}} G^{\text{o}} = \Delta_{\text{soln}} G^{\text{o}} + \Delta_{\text{soln}} G^{\text{o-id}} \tag{13}$$

$$\Delta_{\text{mix}} H^{\text{o}} = \Delta_{\text{soln}} H^{\text{o}} + \Delta_{\text{soln}} H^{\text{o-id}} \tag{14}$$

$$\Delta_{\text{mix}} S^{\text{o}} = \Delta_{\text{soln}} S^{\text{o}} + \Delta_{\text{soln}} S^{\text{o-id}} \tag{15}$$

Table 6 shows the thermodynamic mixing functions; from pure methanol to pure DMF, the mixing Gibbs energy decreases in value as the DMF concentration increases, whereby the DMF addition has a positive cosolvent effect, favoring the solvent-solvent interactions (e_{13}). As for the mixing enthalpy, it is positive from pure methanol to $w_1 = 0.8$, this factor it does not favor the dissolution process, it is observed that the enthalpy is greater in methanol-rich and intermediate mixtures possibly due to the fact that the formation of the cavity (required for solute accommodation) in these mixtures requires more energy. The foregoing may indicate that MeOH-MeOH interactions are stronger than those of DMF-DMF, In DMF-rich mixtures ($0.90 \leq w_1 \leq 1.00$), the enthalpy is negative, which favors the mixing process.

Regarding the entropy of the mixture, it is negative in all cases, which unfavors the mixing process.

Table 6. Thermodynamic functions of mixing gatifloxacin (3) in DMF (1) + methanol (2) cosolvent mixtures at 294.95 K and pressure $p = 0.1$ MPa.

w_1 [a]	$\Delta_{mix}G°$ / kJ mol^{-1}	$\Delta_{mix}H°$ / kJ mol^{-1}	$\Delta_{mix}S°$ / J mol^{-1} K^{-1}	$T\Delta_{mix}S°$ / kJ mol^{-1}
0.00	9.6	4.1	-18.6	-5.5
0.10	9.0	3.9	-17.3	-5.1
0.20	8.4	3.1	-18.1	-5.3
0.30	7.9	2.6	-17.9	-5.3
0.40	7.2	2.1	-17.5	-5.2
0.50	6.7	1.8	-16.5	-4.9
0.60	6.1	1.5	-15.5	-4.6
0.70	5.5	1.2	-14.6	-4.3
0.80	4.9	0.5	-14.8	-4.4
0.90	4.3	-0.5	-16.2	-4.8
1.00	3.7	-2.1	-19.9	-5.9

[a] w_1, mass fraction of DMF (1) in the gatifloxacin -free DMF (1) + methanol (2) mixture.

From Perlovich's analysis (figure 5), it is concluded that in all cases the process is driven by entropy, both in the sector VII, from pure methanol to $w_1 = 0.80$ (sector VII: $\Delta_{mix}H° < T\Delta_{mix}S°$ and $|T\Delta_{mix}S°| > |\Delta_{mix}H°|$), and in the sector VI, from $w_1 = 0.90$ to pure DMF (sector VI: $\Delta_{mix}H° < 0$, $T\Delta_{mix}S° < 0$, and $|T\Delta_{mix}S°| > |\Delta_{mix}H°|$).

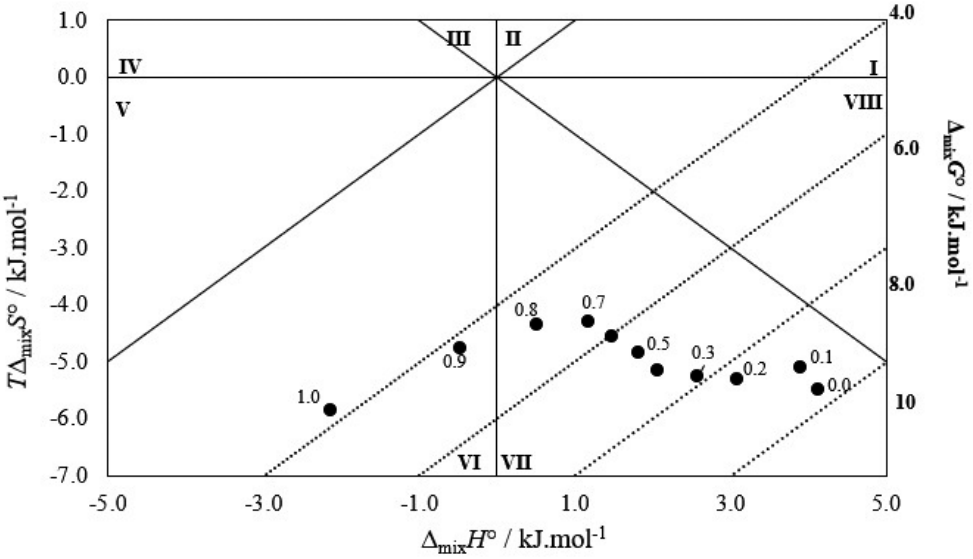

Figure 5. Relationship between the enthalpy ($\Delta_{mix}H°$) and entropy ($T\Delta_{mix}S°$) terms of the mixing process of gatifloxacin in DMF (1) + methanol (2) cosolvent mixtures at 294.95 K. The isoenergetic curves of $\Delta_{mix}G°$ are represented by dotted lines.

Enthalpy-entropy compensation

An analysis that identifies changes in the mechanism that controls the cosolvent action is that of enthalpy–entropy compensation, which is performed by plotting $\Delta_{soln}H°$ vs. $\Delta_{soln}G°$, where in most cases, a nonlinear behavior is observed. Thus, this graphic analysis allows to identify the thermodynamic consequences of bond formation and rupture, where the hydrogen bond is the most relevant interaction [42, 47].

The plot interpretation ($\Delta_{soln}H°$ vs. $\Delta_{soln}G°$) is based on the sign of the slopes; thus, negative slopes indicate that the process is entropy-driven, which may be a consequence of the system's molecular rearrangement, while positive slopes indicate that the process is enthalpy-driven, which could be a consequence of changes in intermolecular interactions between the drug and solvents through hydrogen bonds and van der Waals forces such as the induced or permanent dipole–dipole interactions, and therefore, can be considered as quantitative indicator of changes in the intermolecular bond energies that occur during the interaction [48-50].

Figure 6 shows the behavior of gatifloxacin enthalpy-entropy compensation in the DMF + MeOH system. Thus, in all cases the solution process is driven by enthalpy.

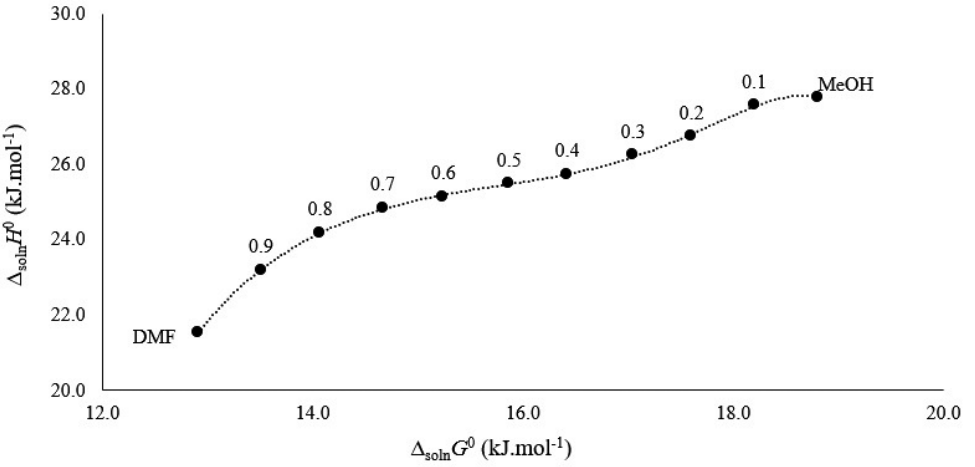

Figure 6. Enthalpy-entropy compensation graph $\Delta_{soln}H°$ vs. $\Delta_{soln}G°$ for the solution process of gatifloxacin (3) in DMF (1) + methanol (2) cosolvent mixtures at 294.95 K.

Preferential solvation

An analysis that allows a more precise evaluation of molecular interactions and solvent composition in the immediate environment of solute molecules, is the mathematical model proposed by Ben-Naim denominating the inverse Kirkwood-Buff integral (IKBI) [51-53], which expresses its results according to the preferential solvation parameters $\delta x_{1,3}$ and $\delta x_{2,3}$, indicates the solute preference (3) for solvent (1) or (2) according to [10, 54, 55]:

$$\delta x_{1,3} = x_{1,3}^{L} - x_1 = -\delta x_{2,3} \tag{16}$$

where x_1 is the mole fraction of 1 in the cosolvent mixture and $x^{L}_{1,3}$, is the local mole fraction of 1 in the vicinity of the solute (3). If $\delta x_{1,3} > 0$, the solute is preferentially solvated by 1, and if $\delta x_{1,3} < 0$, the solute is preferentially solvated by 2. However, if $|\delta x_{1,3}| \leq 0.01$, the values are probably within the error of determination, indicating an insignificant preferential solvation. On the other hand, if $\delta x_{1,3} \approx x_2$, it means that $x^{L}_{1,3} = 1$ or a complete preferential solvation of 3 by 1 [10, 54].

The application expressions of the IKBI approach given by Ben-Naim are [56, 57]:

$$\delta x_{1,3} = \left[x_1(1-x_1)(G_{1,3} - G_{2,3})\right]\left[x_1 G_{1,3} + (1-x_1)G_{2,3} + V_{cor}\right]^{-1} \tag{17}$$

where $G_{1,3}$ and $G_{2,3}$ are the Kirkwood-Buff integrals (in cm^3 mol^{-1}) and V_{cor} is the volume of correlation around 3 (gatifloxacin), within which preferential solvation occurs. Thus, $G_{1,3}$ and $G_{2,3}$ are calculated as [58, 59]:

$$G_{1,3} = RT\kappa_T - V_3 + (1-x_1)V_2 DQ^{-1} \tag{18}$$

$$G_{2,3} = RT\kappa_T - V_3 + x_1 V_1 DQ^{-1} \tag{19}$$

and the correlation volume is calculated as [54, 60 ,61]:

$$V_{cor} = 2522.5\left[r_3 - 0.1363\sqrt[3]{\left(x_{1,3}^L V_1\right) + \left(x_{2,3}^L V_2\right)} - 0.085\right]^3 \tag{20}$$

where $\varkappa_T$ is the isothermal compressibility of DMF + MeOH mixtures (DMF: 0.698 GPa^{-1} [62], Methanol: 1.248 GPa^{-1} [63]), V_1 and V_2 are DMF and methanol Gadžurić *et al.* [64] and Kijevčanin *et al.* [65], V_3 is the molar volume of gatifloxacin (232 cm^3 mol^{-1}), r is the radius of the gatifloxacin molecule (0.4476 nm), and D and Q (in kJ mol^{-1}, as RT) are calculated using equations 21 and 22 [66, 67]:

$$D = d\Delta_t G_{3,2\to 1+2}^0 / dx_1 \tag{21}$$

$$Q = RT + x_1(1-x_1)\left(d^2 G_{1,2}^E / dx_2^2\right) \tag{22}$$

$\Delta_t G_{3,2\to 1+2}^0$ is the transfer Gibbs energy of gatifloxacin from the methanol to each DMF + MeOH cosolvent mixture (equation 23), and $G_{1,2}^E$ is the excess Gibbs energy of the cosolvent mixture of DMF + MeOH free of gatifloxacin (equation 24) [54, 68]:

$$\Delta_t G_{3,2\to 1+2}^0 = 0.6098x_1^2 - 6.5647x_1 + 0.0228 \tag{23}$$

$$G^E = x_2 x_1\left[-1264 + 67(1-2x_2)\right] \tag{24}$$

The values of D, $G_{1,3}$, $G_{2,3}$, V_{cor} and $\delta x_{1,3}$ are presented in table 7, and the behavior of $\delta x_{1,3}$ is presented in Figure 7. The $\delta x_{1,3}$ values show that the preferential solvation of gatifloxacin by both methanol (from pure methanol to $w_1 = 0.25$, $\delta x_{1,3}$ has negative values) and DMF (From $w_1 = 0.25$ to pure DMF, $\delta x_{1,3}$ has positive values) is insignificant, because all the $\delta x_{1,3}$ values are less than 0.01.

It could be expected (however, because the values of $\delta x_{1,3}$ are less than 0.01, the analyzes are not conclusive) that the gatifloxacin, it behaves as a Lewis base against the

methanol-rich medium because the methanol (β = 0.62 [69]) has a less basic character than DMF (β = 0.71 [70]) according to the β-scale of Taft and Kamlet, and like a Lewis acid against the DMF. Table 7. Some properties associated to preferential solvation gatifloxacin (3) in DMF (1) + MeOH (2) cosolvent mixtures at 313.15 K and pressure p = 0.096 MPa.

Table 7. Solubility and preferential solvation of gatifloxacin in DMF+ methanol mixtures at 313.15 K.

x_1[a]	D / kJ mol^{-1}	$G_{1,3}$ / cm^3 mol^{-1}	$G_{2,3}$ / cm^3 mol^{-1}	V_{cor} / cm^3 mol^{-1}	100 $\delta x_{1,3}$
0.00	-6.56	-274.5	-228.8	1485.1	0.000
0.05	-6.50	-270.2	-235.4	1521.3	-0.129
0.10	-6.44	-266.3	-241.7	1557.8	-0.169
0.15	-6.38	-262.7	-247.6	1594.3	-0.143
0.20	-6.32	-259.5	-253.2	1630.7	-0.073
0.25	-6.26	-256.5	-258.6	1667.0	0.028
0.30	-6.20	-253.8	-263.8	1702.9	0.146
0.35	-6.14	-251.3	-268.8	1738.6	0.270
0.40	-6.08	-249.0	-273.8	1773.9	0.394
0.45	-6.02	-246.9	-278.7	1808.9	0.510
0.50	-5.95	-244.9	-283.7	1843.4	0.613
0.55	-5.89	-243.1	-288.7	1877.5	0.699
0.60	-5.83	-241.4	-293.8	1911.3	0.762
0.65	-5.77	-239.9	-299.2	1944.5	0.801
0.70	-5.71	-238.4	-304.8	1977.4	0.811
0.75	-5.65	-237.0	-310.8	2009.8	0.789
0.80	-5.59	-235.6	-317.4	2041.7	0.731
0.85	-5.53	-234.3	-324.6	2073.2	0.631
0.90	-5.47	-233.0	-332.7	2104.1	0.482
0.95	-5.41	-231.6	-341.9	2134.5	0.276
1.00	-5.35	-230.2	-352.7	2164.3	0.000

[a] x_1, mole fraction of acetonitrile (1) in the gatifloxacin-free DMF (1) + methanol (2) mixture.

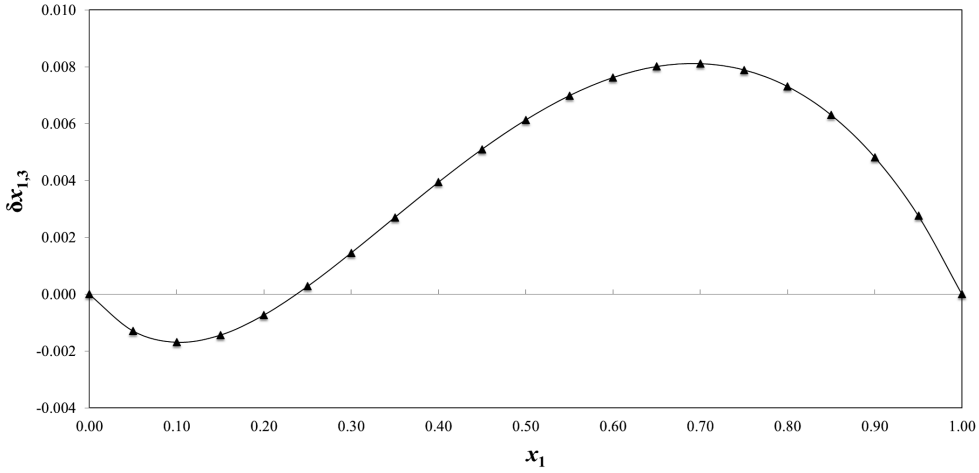

Figure 7. $\delta x_{1,3}$ values of gatifloxacin (3) in DMF (1) + methanol (2) mixtures at 313.15 K.

Conclusions

From thermodynamic analysis and preferential solvation of gatifloxacin in DMF + MeOH cosolvent mixtures, it is concluded that the solution process is endothermic with a marked enthalpy favor, which increases as the polarity of the cosolvent system decreases due to the addition of DMF, presenting a positive cosolvent effect that leads to increased gatifloxacin solubility. Finally, regarding gatifloxacin's preferential solvation, the results are not conclusive, because in all cases the values of the preferential solvation parameter are less than 0.01, so that, negligible preferential solvation takes place.

Acknowledgments

We would like to express our gratitude to the National Directorate of Research and National Committee for Research Development of the Universidad Cooperativa de Colombia for providing financial support for this study with code INV2352.

Disclosure statement

No potential conflict of interest was reported by the authors.

References

1. C. Schultz, gatifloxacin ophthalmic solution for treatment of bacterial conjunctivitis: Safety, efficacy and patient perspective, *Ophthalmol. Eye Dis.*, **4**, 65-70 (2012).

2. D. Deshpande, J.G. Pasipanodya, S. Srivastava, P. Bendet, T. Koeuth, S.M. Bhavnani, P.G. Ambrose, W. Smythe, H. Mcilleron, G. Thwaites, M. Gumusboga, A. Van Deun, T. Gumbo, gatifloxacin pharmacokinetics/pharmacodynamics-based optimal dosing for pulmonary and meningeal multidrug-resistant tuberculosis, *Clin. Infect. Dis.*, **67**, 274-283 (2018).

3. P.S. Coburn, F.C. Miller, A.L. LaGrow, C. Land, H. Mursalin, E. Livingston, O. Amayem, Y. Chen, W. Gao, L. Zhang, M.C. Callegan, Disarming pore-forming toxins with biomimetic nanosponges in intraocular infections, *mSphere*, **4**, e00262-19 (2019).

4. A.M. Romero-Nieto, N.E. Cerquera, F. Martínez, D.R. Delgado, Thermodynamic study of the solubility of ethylparaben in acetonitrile + water cosolvent mixtures at different temperatures, *J. Mol. Liq.*, **287**, 110894 (2019).

5. D.R. Delgado, D.I. Caviedes-Rubio, C.P. Ortiz, Y.L. Parra-Pava, M.Á. Peña, A. Jouyban, S.N. Mirheydari, F. Martínez, W.E. Acree, Jr., Solubility of sulphadiazine in (acetonitrile + water) mixtures: Measurement, correlation, thermodynamics and preferential solvation, *Phys. Chem. Liq.*, **58**, 381-396 (2020).

6. J.A. Oliveira, O.J. Oliveira, A.R. Ometto, A.S. Ferraudo, M.H. Salgado, Environmental management system ISO 14001 factors for promoting the adoption of cleaner production practices, *J. Clean Prod.*, **133**, 1384-1394 (2016).

7. D.I. Caviedes-Rubio, D.R. Delgado, A. Olaya-Amaya, Normatividad ambiental dirigida a regular la presencia de los productos farmacéuticos residuales en ambientes acuáticos, *Rev. Jurídica Piélagus*, **16**, 121-130 (2017).

8. D. Yue, W.E. Acree, M.H. Abraham, Applications of Abraham solvation parameter model: estimation of the lethal median molar concentration of the antiepileptic drug levetiracetam towards aquatic organisms from measured solubility data, *Phys. Chem. Liq.*, **58**, 302-308 (2020).

9. D.R. Delgado, M.A. Peña, F. Martínez, A. Jouyban, W.E. Acree, Further numerical analyses on the solubility of sulfapyridine in ethanol + water mixtures, *Pharm. Sci.*, **22**, 143-152 (2016).

10. Y. Marcus, On the preferential solvation of drugs and PAHs in binary solvent mixtures, *J. Mol. Liq.*, **140**, 61-67 (2008).

11. S.K. Samanta, O.V. Singh, R.K. Jain, Polycyclic aromatic hydrocarbons: Environmental pollution and bioremediation, *Trends Biotechnol.*, **20**, 243-248 (2002).

12. N.T. Edwards, Polycyclic aromatic hydrocarbons (PAH's) in the terrestrial environment-A Review, *J. Environ. Quality*, **12**, 427-441 (1983).

13. W.E. Acree, Jr., J.H. Rytting, Solubility in binary solvent systems I: Specific versus nonspecific interactions, *J. Pharm. Sci.*, **71**, 201-205 (1982).

14. A. Jouyban-Gharamaleki, L. Valaee, M. Barzegar-Jalali, B.J. Clark, W.E. Acree, Jr., Comparison of various cosolvency models for calculating solute solubility in water-cosolvent mixtures, *Int. J. Pharm.*, **177**, 93-101 (1999).

15. A. Jouyban, Solubility prediction of drugs in water-polyethylene glycol 400 mixtures using Jouyban-Acree model, *Chem. Pharm. Bull.*, **54**, 1561-1566 (2006).

16. Z.J. Cárdenas, D.M. Jiménez, G.A. Rodríguez, D.R. Delgado, F. Martínez, M. Khoubnasabjafari, A. Jouyban, Solubility of methocarbamol in some cosolvent + water mixtures at 298.15 K and correlation with the Jouyban-Acree model, *J. Mol. Liq.*, **188**, 162-166 (2013).

17. W.E. Acree, Jr., J.H. Rytting, Solubility in binary solvent systems. IV. Prediction of naphthalene solubilities using the UNIFAC group contribution model, *Int. J. Pharm.*, **13**, 197-204 (1983).

18. A. Martin, J. Newburger, A. Adjei, Extended Hildebrand solubility approach: Solubility of theophylline in polar binary solvents, *J. Pharm. Sci.*, **69**, 487-491 (1980).

19. W.E. Acree, Jr., S.A. Tucker, Thermochemical investigations of hydrogen-bonded solutions Part 6. Comparison of mobile order theory versus Kretschmer-Wiebe association model for describing anthracene solubilities in binary hydrocarbon + alcohol solvent mixtures, *Fluid Phase Equilib.*, **102**, 17-29 (1994).

20. E. Ruckenstein, I. Shulgin, Solubility of drugs in aqueous solutions: Part 1. Ideal mixed solvent approximation, *Int. J. Pharm.*, **258**, 193-201 (2003).

21. J. Wu, R. Xu, J. Wang, H. Zhao, Thermodynamic solubility of gatifloxacin in non-aqueous solvent mixtures of *N,N*-dimethylformamide plus isopropanol/methanol/ n-propanol/ethanol, *J. Chem. Eng. Data*, **64**, 6071-6077 (2019).

22. K. Shi, L. Feng, L. He, H. Li, Solubility determination and correlation of gatifloxacin, enrofloxacin, and ciprofloxacin in supercritical CO_2, *J. Chem. Eng. Data*, **62**, 4235-4243 (2017).

23. J.H. Blanco-Márquez, Y.A. Quigua-Medina, J.D. García-Murillo, J.K. Castro-Camacho, C.P. Ortiz, N.E. Cerquera, D.R. Delgado, Thermodynamic analysis and applications of the Abraham solvation parameter model in the study of the solubility of some sulfonamides, *Rev. Colomb. Cienc. Quím. Farm.*, **49**, 234-255 (2020).

24. I.P. Osorio, F. Martínez, D.R. Delgado, A. Jouyban, W.E. Acree, Jr., Solubility of sulfacetamide in aqueous propylene glycol mixtures: Measurement, correlation, dissolution thermodynamics, preferential solvation and solute volumetric contribution at saturation, *J. Mol. Liq.*, **297**, 111889 (2020).

25. A.F.M. Barton, *Handbook of solubility parameters and other cohesion parameters*, 2nd ed., CRC Press, Boca Raton (FL), 1991.

26. R.F. Fedors, A method for estimating both the solubility parameters and molar volumes of liquids, *Polym. Eng. Sci.*, **14**,147-154 (1974).

27. J.H. Blanco-Márquez, C.P. Ortiz, N.E. Cerquera, F. Martínez, A. Jouyban, D.R. Delgado, Thermodynamic analysis of the solubility and preferential solvation of sulfamerazine in (acetonitrile + water) cosolvent mixtures at different temperatures, *J. Mol. Liq.*, **293**, 111507 (2019).

28. J.H. Blanco-Márquez, D.I. Caviedes Rubio, C.P. Ortiz, N.E. Cerquera, F. Martínez, D.R. Delgado, Thermodynamic analysis and preferential solvation of sulfamethazine in acetonitrile + water cosolvent mixtures, *Fluid Phase Equilib.*, **505**, 112361 (2020).

29. S.H. Yalkowsky, M. Wu, Estimation of the ideal solubility (crystal-liquid fugacity ratio) of organic compounds, *J. Pharm. Sci.*, **99**, 1100-1106 (2010).

30. A.M. Romero-Nieto, D.I. Caviedes-Rubio, J. Polania-Orozco, N.E. Cerquera, D.R. Delgado, Temperature and cosolvent composition effects in the solubility of methylparaben in acetonitrile + water mixtures, *Phys. Chem. Liq.* Forthcomming 2020, doi: 10.1080/00319104.2019.1636379.

31. M. Mirmehrabi, S. Rohani, L. Perry, Thermodynamic modeling of activity coefficient and prediction of solubility: Part 1 predictive models, *J. Pharm. Sci.*, **95**, 790-797 (2006).

32. D.R. Delgado, A. Jouyban, F. Martínez, Solubility and preferential solvation of meloxicam in methanol+ water mixtures at 298.15 K, *J. Mol. Liq.*, **197**, 368-376 (2014).

33. D.R. Delgado, F. Martínez, Solution thermodynamics of sulfadiazine in ethanol + water mixtures, *J. Mol. Liq.*, **187**, 99-105 (2013).

34. R.R. Krug, W.G. Hunter, R.A. Grieger, Enthalpy-entropy compensation. 1. Some fundamental statistical problems associated with the analysis of van't Hoff and arrhenius data, *J. Phys. Chem.*, **80**, 2335-2341 (1976).

35. R.R. Krug, W.G. Hunter, R.A. Grieger, Enthalpy-entropy compensation. 2. Separation of the chemical from the statistical effect, *J. Phys. Chem.*, **80**, 2341-2351 (1976).

36. D.R. Delgado, A. Romdhani, F. Martínez, Solubility of sulfamethizole in some propylene glycol+water mixtures at several temperatures, *Fluid Phase Equilib.*, **322**,-113-119 (2012).

37. D.R. Delgado, G.A. Rodríguez, F. Martínez, Thermodynamic study of the solubility of sulfapyridine in some ethanol + water mixtures, *J. Mol. Liq.*, **177**, 156-161 (2013).

38. G.L. Perlovich, A.M. Ryzhakov, N.N. Strakhova, V.P. Kazachenko, K.-J. Schaper, O.A. Raevsky, Thermodynamic aspects of solubility and partitioning processes of some sulfonamides in the solvents modeling biological media, *J. Chem. Thermodyn.*, **69**, 56-65 (2014).

39. G.L. Perlovich, N.N. Strakhova, V.P. Kazachenko, T.V. Volkova, V.V. Tkachev, K.-J. Schaper, O.A. Raevsky, Sulfonamides as a subject to study molecular interactions in crystals and solutions: Sublimation, solubility, solvation, distribution and crystal structure, *Int. J. Pharm.*, **349**, 300-313 (2008).

40. A.R. Holguín, D.R. Delgado, F. Martínez, Thermodynamic study of the solubility of triclocarban in ethanol + propylene glycol mixtures, *Quim. Nova*, **35**, 280-285 (2012).

41. G.L. Perlovich, V.V. Tkachev, N.N. Strakhova, V.P. Kazachenko, T.V. Volkova, O.V. Surov, K.J. Schaper, O.A. Raevsky, Thermodynamic and structural aspects of sulfonamide crystals and solutions, *J. Pharm. Sci.*, **98**, 4738-4755 (2009).

42. D.R. Delgado, E.M. Mogollon-Waltero, C.P. Ortiz, M.Á. Peña, O.A. Almanza, F. Martínez, A. Jouyban, Enthalpy-entropy compensation analysis of the triclocarban dissolution process in some {1,4-dioxane (1) + water (2)} mixtures, *J. Mol. Liq.*, **271**, 522-529 (2018).

43. M.A. Ruidiaz, D.R. Delgado, F. Martínez, Y. Marcus, Solubility and preferential solvation of indomethacin in 1,4-dioxane+water solvent mixtures, *Fluid Phase Equilib.*, **299**, 259-265 (2010).

44. R.A. Gutiérrez, D.R. Delgado, F. Martínez, Solution thermodynamics of lysine clonixinate in some ethanol + water mixtures, *Lat. Am. J. Pharm.*, **31**, 226-234 (2012).

45. D.R. Delgado, E.F. Vargas, F. Martínez, Thermodynamics of the mixing process of several sodium sulfonamides in ethanol + water cosolvent mixtures, *Vitae, Rev. Fac. Quim. Farm.*, **18**, 192-200 (2011).

46. D.M. Cristancho, R.G. Sotomayor, D.R. Delgado, A. Romdhani, F. Martínez, Thermodynamics of mixing of the β-adrenergic blocker propranolol-HCl in ethanol + water mixtures, *Rev. Colomb. Cienc. Quim. Farm.*, **40**, 261-271 (2011).

47. P. Bustamante, B. Escalera, Enthalpy and entropy contributions to the solubility of sulphamethoxypyridazine in solvent mixtures showing two solubility maxima, *J. Pharm. Pharmacol.*, **47**, 550-555 (1995).

48. D.R. Delgado, A.R. Holguín, O.A. Almanza, F. Martínez, Y. Marcus, Solubility and preferential solvation of meloxicam in ethanol+water mixtures, *Fluid Phase Equilib.*, **305**, 88-95 (2011).

49. J.W. Mauger, A.N. Paruta, R.J. Gerraughty, Solubilities of sulfadiazine, sulfisomidine, and sulfadimethoxine in several normal alcohols, *J. Pharm. Sci.*, **61**, 94-97 (1972).

50. R. Lumry, S. Rajender, Enthalpy-entropy compensation phenomena in water solutions of proteins and small molecules: A ubiquitous properly of water, *Biopolymers*, **9**, 1125-1227 (1970).

51. A. Ben-Naim, Theory of preferential solvation of nonelectrolytes, *Cell Biophys.*, **12**, 255-269 (1988).

52. A. Ben-Naim, A.M. Navarro, J.M. Leal, A Kirkwood-Buff analysis of local properties of solutions, *Phys. Chem. Chem. Phys.*, **10**, 2451-2460 (2008).

53. A. Ben-Naim, Inversion of the Kirkwood-Buff theory of solutions: Application to the water-ethanol system, *J. Chem. Phys.*, **67**, 4884-4890 (1977).

54. Y. Marcus, *Solvent mixtures: Properties and selective solvation*, Marcel Dekker, Inc, New York , 2002.

55. D.R. Delgado, O.A. Almanza, F. Martínez, M.A. Peña, A. Jouyban, W.E. Acree, Jr., Solution thermodynamics and preferential solvation of sulfamethazine in (methanol + water) mixtures, *J. Chem. Thermodyn.*, **97**, 264-276 (2016).

56. A. Ben-Naim, Preferential solvation in two- and in three-component systems, *Pure Appl. Chem.*, **62**, 25-34 (1990).

57. J.J. Sandoval-Castro, C.P. Ortiz, J.D Rodríguez-Rubiano, G.A. Rodríguez-Rodríguez, D.R. Delgado, Preferential solvation of tricin in {ethanol (1) + water (2)} mixtures at several temperatures, *Rev. Colomb. Cienc. Quím. Farm.*, **47**, 135-148 (2018).

58. A.C. Gaviria-Castillo, J.D. Artunduaga-Tole, J.D. Rodríguez-Rubiano, J.A. Zuñiga-Andrade, D.R. Delgado, A. Jouyban, F. Martínez, Solution thermodynamics and preferential solvation of triclocarban in {1,4-dioxane (1) + water (2)} mixtures at 298.15 K, *Phys. Chem. Liq.*, **57**, 55-66 (2019).

59. D.R. Delgado, F. Martínez, Preferential solvation of sulfadiazine, sulfamerazine and sulfamethazine in ethanol + water solvent mixtures according to the IKBI method, *J. Mol. Liq.*, **193**, 152-159 (2014).

60. Z.J. Cárdenas, D.M. Jiménez, D.R. Delgado, O.A. Almanza, A. Jouyban, F. Martínez, W.E. Acree, Jr., Solubility and preferential solvation of some n-alkyl-parabens in methanol + water mixtures at 298.15 K, *J. Chem. Thermodyn.*, **108**, 26-37 (2017).

61. D.R. Delgado, F. Martínez, Preferential solvation of some structurally related sulfonamides in 1-propanol + water co-solvent mixtures, *Phys. Chem. Liq.*, **53**, 293-306 (2015).

62. P. García-Giménez, J.F. Martínez-López, S.T. Blanco, I. Velasco, S. Otín, Densities and isothermal compressibilities at pressures up to 20 MPa of the systems *N*,*N*-dimethylformamide or *N*,*N*-dimethylacetamide + α,ω- dichloroalkane, *J. Chem. Eng. Data*, **52**, 2368-2374 (2007).

63. Y. Marcus, *The Properties of Solvents*, John Wiley & Sons, Ltd., New York, 1999.

64. S. Gadžurić, A. Tot, N. Zec, S. Papović, M. Vraneš, Volumetric properties of binary mixtures of 1-butyl-1-methylpyrrolidinium tris(pentafluoroethyl)trifluorophosphate with *N*-methylformamide, *N*-ethylformamide, *N*,*N*-dimethylformamide, *N*,*N*-dibutylformamide, and *N*,*N*-dimethylacetamide from (293.15 to 323, *J. Chem. Eng. Data*, **59**, 1225-1231 (2014).

65. M.L. Kijevčanin, M.M. Djuriš, I.R. Radović, B.D. Djordjević, S.P. Šerbanović, Volumetric properties of the binary methanol + chloroform and ternary methanol + chloroform + benzene mixtures at (288.15, 293.15, 298.15, 303.15, 308.15, and 313.15) K, *J. Chem. Eng. Data*, **52**, 1136-1140 (2007).

66. M.Á. Peña, D.R. Delgado, F. Martínez, Preferential solvation of indomethacin in 1,4-dioxane + water mixtures according to the inverse Kirkwood-Buff integrals method, *Phys. Chem. Liq.*, **54**, 462-474 (2016).

67. D.M. Jiménez, Z.J. Cárdenas, D.R. Delgado, M.A. Peña, F. Martínez, Solubility temperature dependence and preferential solvation of sulfadiazine in 1,4-dioxane+water co-solvent mixtures, *Fluid Phase Equilib.*, **397**, 26-36 (2015).

68. M.Á. Peña, D.R. Delgado, F. Martínez, Preferential solvation of some n-alkyl p-substituted benzoates in propylene glycol + water cosolvent mixtures, *Phys. Chem. Liq.*, **53**, 455-466 (2015).

69. M.J. Kamlet, R.W. Taft, The solvatochromic comparison method. I. The β-scale of solvent hydrogen-bond acceptor (HBA) basicities, *J. Am. Chem. Soc.*, **98**, 377-383 (1976).

70. C. Laurence, J. Legros, P. Nicolet, D. Vuluga, A. Chantzis, D. Jacquemin, Solvatomagnetic comparison method: A proper quantification of solvent hydrogen-bond basicity, *J. Phys. Chem. B*, **118**, 7594-7608 (2014).

How to cite this article

M. Rojas-Motta, J.E. Rojas-Motta, J.L. Diaz-Jimenez, F.A. Bahos-Narváez, J.H. Blanco-Márquez, C.P. Ortiz, D.R. Delgado, Thermodynamic analysis and preferential solvation of gatifloxacin in DMF + methanol cosolvent mixtures, *Rev. Colomb. Cienc. Quím. Farm.*, **49**(3), 675-698 (2020).

Artigo de pesquisa científica / *http://dx.doi.org/10.15446/rcciquifa.v49n3.91338*

O estudo teórico do desempenho dos polímeros condutores dos corantes azoicos na detecção eletroquímica de indigo-carmim

Volodymyr V. Tkach[1,2*], Marta V. Kushnir[1], Yana G. Ivanushko[3], Lyudmyla V. Romaniv[1], Sílvio C. de Oliveira[2], Oleksandra V. Ahafonova[3], Nataliia S. Serhata[4], Petro I. Yagodynets´[1]

[1]Universidade Nacional de Chernivtsi, 58012, Rua de Kotsyubyns'ky, 2, Chernivtsi, Ucrânia.

[2]Universidade Federal de Mato Grosso do Sul, Av. Sen. Felinto. Müller, 1555, C/P. 549, 79074-460, Campo Grande, MS, Brazil.

[3]Universidade Estatal de Medicina de Bucovina, 58000, Praça Teatral, 9, Chernivtsi, Ucrânia.

[4]Academia Nacional de Reabilitação e Recuperação De Khortytsya, 69600, Ilha de Khortytsya, Rua da Vila Científica, 55, Zaporizhzhya, Ucrânia.

*Autor para correspondência: nightwatcher2401@gmail.com

Recebido: 6 de junho de 2018

Revisado: 2 de julho de 2020

Aceto: 3 de julho de 2020

Resumo

O desempenho dos polímeros condutores dos corantes azoicos durante a detecção eletroquímica de indigo-carmim foi investigado do ponto de vista teórico, sendo o modelo, correspondente ao caso, descrito e analisado mediante a teoria de estabilidade lineal e da análise de bifurcações. Foi mostrado que o sistema eletroanalítico depende fortemente do pH, pois as concentrações excessivas dos prótons levam à ineficiência eletroanalítica, haja vista o bloqueio dos centros ativos da reação. No entretanto, malgrado o supracitado, os polímeros dos corantes azoicos são modificadores eficientes para determinação do indigo-carmim. A possibilidade das instabilidades oscilatória e monotônica também foi verificada.

Palavras-chave: Polímeros condutores, sensores eletroquímicos, indigo-carmim, corantes alimentares, corantes azoicos, estado estacionário estável.

Summary

The theoretical study of the function of conducting polymers of the azo-dyes in the electrochemical detection of indigo-carmine

The function of the conducting polymers of azo-dyes during the indigo-carmine electrochemical detection has been investigated from the theoretical point of view. The correspondent model has been described and analyzed by means of linear stability theory and bifurcation analysis. It has been shown that the electroanalytical system depends strongly on pH, as the excessive protons concentrations drive the system to the electroanalytical inefficiency, as they block the reaction active sites. Nevertheless, despite of the mentioned, the azo-dyes conducting polymers are efficient modifiers for indigo-carmine electrochemical determination. The possibility of oscillatory and monotonic instabilities has also been verified.

Keywords: Conducting polymers, electrochemical sensors, indigo-carmine, food dyes, azo-dyes, stable steady-state.

Introdução

Os polímeros condutores pertencem a uma classe de compostos, amplamente estudada ao longo das cinco últimas décadas [1-5]. Combinando as propriedades dos plásticos com a condutividade dos metais, eles têm um espectro amplo, vasto e rico de uso, com aplicações desde os revestimentos protetores de corrosão até os sensores e biossensores.

Por outro lado, indigo-carmim (índigo-5-5'-dissulfonato de sódio, CAS: 860-22-0) (figura1) [6] é um corante natural, derivado do índigo. Ele existe em formas cetônica e enólica, sendo a primeira a mais capaz de eletrooxidar-se. Ele é capaz de ser indicador de pH, tornando-se azul, se o pH é inferior a 11,4 e amarelo, se o pH é superior a 13,0.

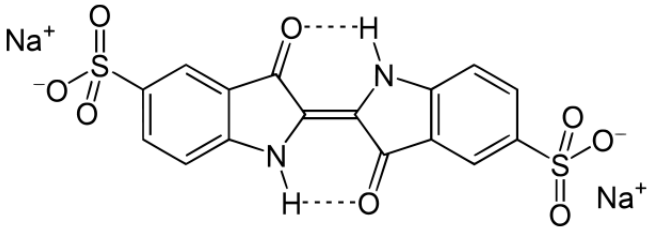

Figura 1. Índigo-carmim.

Tendo o sistema conjugado de ligações, ele é usado como corante [7-10]. É aprovado como corante alimentar na União Europeia e nos Estados Unidos de América. O seu código na codificação de suplementos alimentares é E132. Ele é usado, também para a produção de tintas, como contraste em análises médicas e farmacêuticas, como agente redox para a detecção de nitratos e, também, como formador de complexos na detecção de metais pesados como cobre e outros [11, 12] para colorir as formulações farmacêuticas e até tecidos. É possível o uso dele como dopante na síntese de polímeros condutores [13, 14].

No entanto, este corante pertence ao grupo de substâncias perigosas [7-9]. Ele também pode provocar reações alérgicas, e, na sua presença, podem ocorrer reações ideossincráticas. Outrossim, no organismo ele é capaz de transformar-se em indigotindisulfonato de sódio, um dos poucos sais insolúveis neste metal [7, 15], o que pode levar ao decrescimento da concentração de sódio no organismo. Destarte, o desenvolvimento de métodos eficientes da detecção eletroquímica do índigo-carmim é realmente muito atual [16-18].

Já foram conhecidos vários métodos da detecção eletroquímica de indigo-carmim na presença dos polímeros condutores [13, 19]. No entanto, o desenvolvimento de novos métodos de análise e, mesmo, a aplicação dos existentes podem enfrentar os problemas como:

- Indecisão quanto ao mecanismo do desempenho do analito e(ou) modificador no sistema eletroanalítico (por exemplo, indecisão acerca do papel de certas substâncias, presentes na solução, na geração do sinal analítico).

- Aparição de instabilidades eletroquímicas, capazes de piorar a sensibilidade do processo e a interpretação da resposta eletroanalítica e características para os processos afins [20-24].

- A possível concorrência dos mecanismos paralelos do processo eletroquímico do analito, ou a presença de duas ou mais reações eletroquímicas ou químicas sucessivas.

Diante do exposto, faz-se necessário desenvolver e analisar um modelo matemático, capaz de descrever adequadamente o comportamento deste sistema. A modelagem também providenciará a comparação do comportamento deste sistema com o dos semelhantes sem ensaios experimentais. Assim, o objetivo geral deste trabalho é uma análise mecanística teórica da possibilidade da eletrooxidação da indigocarmina em meio ácido, assistida por um polímero de um corante azoico. Para alcançá-lo, resolvemos objetivos específicos como:

- A proposta de um mecanismo da sequência de reações eletroanalíticas, que levam à formação da nova camada polimérica e à aparição do sinal analítico.
- O desenvolvimento do modelo de equações de balanço, correspondente ao sistema eletroanalítico.
- Análise e interpretação do modelo.
- Investigação de estabilidade do estado estacionário e das instabilidades eletroquímicas neste sistema.
- Comparação do comportamento deste sistema com o dos semelhantes [25-27].

O sistema e o seu modelo

É possível prever que, durante a oxidação, o indigo-carmim perde os dois prótons, transferindo-os para o grupo diazo do Sudão I, tranformando-o no grupo hidrazo, conforme a equação:

$$H_2Ind + R–N=N–R \rightarrow Ind + R–NH–NH–R \quad (1)$$

A forma reduzida vem, depois, sendo oxidada conforme (2):

$$R–NH–NH–R - 2e^- \rightarrow R–N=N–R + 2H^+ \quad (2)$$

Os prótons atacam o polímero, conforme o mecanismo diferente, o que pode acarretar a eletrooxidação do polímero conforme um mecanismo híbrido. Destarte, para descrever o comportamento do sistema, é preciso introduzir as três variáveis:

c: a concentração de indigo-carmim na camada pré-superficial;

h: a concentração dos prótons na camada pré-superficial;

ϑ: o grau de recobrimento da forma reduzida do polímero.

Para simplificar a modelagem, supomos que o reator esteja agitando-se intensamente (para menosprezar o fluxo de convecção), que o eletrólito de suporte esteja em excesso (para menosprezar o fluxo de migração). Também é suposto que a distribuição concentracional na camada pré-superficial seja lineal, e a sua espessura, constante, igual a δ.

É possível mostrar que o comportamento do sistema pode ser descrito pelo conjunto clássico de três equações diferenciais de balanço:

$$\begin{cases} \dfrac{dc}{dt} = \dfrac{2}{\delta}\left(\dfrac{\Delta}{\delta}(c_0 - c) - r_1\right) \\ \dfrac{dh}{dt} = \dfrac{2}{\delta}\left(\dfrac{\Delta}{\delta}(h_0 - h) + r_3 - r_2\right) \\ \dfrac{d\theta}{dt} = \dfrac{1}{G}(r_1 + r_2 - r_3 - r_4) \end{cases} \quad (3)$$

em que Δ é o coeficiente da difusão, c_0 é a concentração do corante no interior da solução, h_0 é a concentração dos prótons no interior da solução, G é a concentração superficial máxima do polímero na forma reduzida e protonizada, r_1, r_2, r_3, r_4 são velocidades correspondentes, que se podem calcular como:

$$r_1 = k_1(1-\theta)c\exp(-\alpha c) \quad (4)$$

$$r_2 = k_2(1-\theta)h^2\exp(-\beta h) \quad (5)$$

$$r_3 = k_3\theta\exp\frac{2F\varphi_0}{RT} \quad (6)$$

$$r_4 = k_4\theta\exp\frac{\nu F\varphi_0}{RT} \quad (7)$$

Sendo os parâmetros k as constantes de velocidades de reações correspondentes, α e β as variáveis, que descrevem as influências da aparição-desaparição de compostos iônicos durante a etapa química na dupla camada elétrica (DCE), ν é o número de elétrons, transferidos durante a realização do mecanismo da oxidação paralela do polímero, F é o número de Faraday, φ_0 é o salto de potencial na DCE, relativo ao potencial da carga zero, R é a constante universal de gases e T a temperatura absoluta do vaso.

Neste caso, contrariamente aos semelhantes [25-27], a hibridez do mecanismo da eletrooxidação aumenta a probabilidade da realização de instabilidades eletroquímicas, explicadas pela mudança constante e cíclica da estrutura e da composição (e, por conseguinte, a capacitância) da DCE. Malgrado o supracitado, o poli(sudão I) pode ser considerado eficiente para a determinação eletroanalítica de indigo-carmim, conforme exposto abaixo.

Resultados e discussão

Para investigar a determinação eletroanalítica do corante alimentar indigo-carmim sobre o polímero do corante Sudão I, analisamos o conjunto de equações diferenciais (3), haja vista as relações algébricas (4-7) mediante a teoria de estabilidade linear. Os elementos estacionários da matriz funcional de Jacobi expor-se-ão conforme:

$$\begin{pmatrix} a_{11} & a_{12} & a_{13} \\ a_{21} & a_{22} & a_{23} \\ a_{31} & a_{32} & a_{33} \end{pmatrix} \tag{8}$$

em que:

$$a_{11} = \frac{2}{\delta}\left(-\frac{\Delta}{\delta} - k_1(1-\theta)\exp(-\alpha c) + \alpha k_1(1-\theta)c\exp(-\alpha c)\right) \tag{9}$$

$$a_{12} = 0 \tag{10}$$

$$a_{13} = \frac{2}{\delta}\left(k_1 c\exp(-\alpha c)_1\right) \tag{11}$$

$$a_{21} = 0 \tag{12}$$

$$a_{22} = \frac{2}{\delta}\left(-\frac{D}{\delta} - 2k_2(1-\theta)h\ \exp(-\beta h) + \beta k_2(1-\theta)h^2\exp(-\beta h)\right) \tag{13}$$

$$a_{23} = \frac{2}{\delta}\left(k_3\exp\frac{2F\varphi_0}{RT} - jk_3\theta\exp\frac{2F\varphi_0}{RT} + k_2h^2\exp(-\beta h)\right) \tag{14}$$

$$a_{31} = \frac{1}{G}\left(k_1(1-\theta)\exp(-\alpha c) - \alpha k_1(1-\theta)c\exp(-\alpha c)\right) \tag{15}$$

$$a_{32} = \frac{1}{G}\left(2k_2(1-\theta)h\ \exp(-\beta h) - \beta k_2(1-\theta)h^2\exp(-\beta h)\right) \tag{16}$$

$$a_{33} = \frac{1}{G}\left(-k_1 c\exp(-\alpha c)_1 - k_3\exp\frac{2F\varphi_0}{RT} + jk_3\theta\exp\frac{2F\varphi_0}{RT} - k_2h^2\exp(-\beta h)\right) \tag{17}$$

Avaliando as expressões (9), (13) e (17), podemos ver que, dentro dos elementos da diagonal principal da matriz, existem elementos positivos, relacionados à positiva conexão

de retorno. Destarte, confirma-se a possibilidade da realização da Bifurcação de Hopf, o que significa que *o comportamento oscilatório* neste sistema é passível de realizar.

Além do elemento $+jk_3\theta\exp\frac{2F\varphi_0}{RT}>0$, se j>0, que define o comportamento oscilatório, causado pelas influências da etapa eletroquímica nas capacitâncias da DCE, característico, também, para os sistemas semelhantes, na diagonal principal da matriz confirma-se também, a presença dos elementos $\beta k_2(1-\theta)h^2\exp(-\beta h)>0$, se β>0 e $\alpha k_1(1-\theta)c\exp(-\alpha c)>0$, se α>0, o que define o comportamento oscilatório, causado pela mudança da composição dos compostos iônicos na DCE aquando das etapas químicas e a sua influência nas capacitâncias da DCE. As oscilações se esperam frequentes e de pequena amplitude.

Aplicando o critério Routh-Hurwitz, obtemos o requisito de *estabilidade do estado estacionário*.Para simplificar a análise da matriz, introduzimos as novas variáveis, para dar ao seu determinante a forma:

$$\frac{4}{\delta^2 G}\begin{vmatrix} -\kappa-\Lambda & 0 & \Omega \\ 0 & -\lambda-\mathrm{X} & \Phi \\ \Lambda & \mathrm{X} & -\Omega-\Phi \end{vmatrix} \qquad (18)$$

Abertas os parênteses e aplicada a condição Det J<0, saliente do critério, o requisito de estabilidade descrever-se-á conforme:

$$-\kappa(\lambda\Omega+\mathrm{X}\Omega+\lambda\Phi)-\Lambda\lambda\Phi<0 \qquad (19)$$

O que, como em sistemas semelhantes [25-27], descreve um sistema, em que o estado estacionário se torna estável facilmente. O comportamento do sistema é controlado pela difusão.

Do ponto de vista eletroanalítico, porém, adiciona-se o critério de eficiência eletroanalítica, dependente do pH, já que, à medida que o pH decresce, diminui o número de centros reacionais disponíveis na superfície, por causa dos ataques constantes dos prótons na camada polimérica. Assim, o sistema tornar-se-á insuficientemente ativo do ponto de vista eletroanalítico, malgrado que o estado estacionário siga sendo estável. Destarte, o melhor desempenho eletroanalítico neste sistema deve ser observado com o pH levemente ácido a neutro.

Satisfeitas estas condições, a estabilidade do estado estacionário corresponder-se-á à linearidade da dependência entre o parâmetro eletroquímico e a concentração do corante.

A instabilidade monotônica, correspondente ao limite de detecção, é possível neste sistema. A condição principal para a sua realização é Det J=0, ou seja:

$$-\kappa(\lambda\Omega + X\Omega + \lambda\Phi) - \Lambda\lambda\Phi = 0 \qquad (20)$$

Além dos corantes azoicos, existe, também, a possibilidade de usar, também os compostos fosfazoicos [25], bases de Schiff [26] como modificadores individuais e monômeros. Nestes casos, o comportamento do sistema reger-se-á por este mesmo modelo.

Quanto ao indigo-carmim, este também pode, em princípio, ser utilizado como modificador de elétrodo para eletroanálise e como monômero de polímero condutor. Este tipo de seu uso, que envolve a sua sensibilidade ao pH, bem como as transformações das suas formas iônicas em vários meios, será descrito num dos nossos próximos trabalhos.

Conclusões

A análise do sistema com a detecção eletroanalítica do indigo-carmim, assistida pelo polímero condutor de um corante azoico deixou concluir que:

- Se trata de um sistema eletroanalítico, cuja eficiência é dependente do pH do sistema. O melhor desempenho consegue-se nos valores, correspondentes aos meios ligeiramente ácido e neutro.
- O processo eletroanalítico é controlado pela difusão – tanto dos prótons, como do corante.
- O comportamento oscilatório, neste caso, é mais provável que nos casos afins, haja vista a influência da transformação de íons aquando da etapa química nas capacitâncias da DCE.
- O mesmo modelo também pode ser referente ao processo eletroanalítico, assistido por outros corantes conjugados semelhantes.

Conflito de interesse

Os autores não têm conflito de interesse.

Referências

1. C.C. Vishvanatha, B. Kumara Swamy, K. Vasantakumar Pai, Electrochemical studies of dopamine, ascorbic acid and uric acid at lignin modified carbon paste electrode by cyclic voltammetry, *J. Anal. Bioanal. Techn.*, **6**, ID: 1000237 (2015).

2. M.A. Sheikh-Mohseni, S. Pirsa, Simultaneous determination of dopamine and acetaminophen by a carbon paste electrode doubly modified with poly (pyrrole) and CuO nanoparticles, *Anal. Bioanal. Electrochem.*, **8**, 777-789 (2016).

3. T. McQuade, A. Pullen, T.M. Swager, Conjugated polymer-based chemical sensor, *Chem. Rev.*, **100**, 2537-2574 (2000).

4. R. Singh., Prospects of organic conducting polymer modified electrodes: Enzymosensors, *Int. J. Electrochem.*, **2012**, ID: 502707 (2012).

5. A. Ramanavicius, A. Ramanaviciene, A. Malinauskas, Electrochemical sensors based on conducting polymer—polypyrrole, *Electrochim. Acta*, **51**, 6025-6037 (2006).

6. National Library of Medicine, *Indigo carmine*, URL: https://pubchem.ncbi.nlm.nih.gov/compound/Indigo_carmine#section=Top, acesso aos 6 de julho de 2017.

7. Таблица пищевых Е-добавок, URL: http://dobavkam.net/additives/e132, acesso aos 6 de julho de 2017.

8. RxList, *Indigo carmine*, URL: http://www.rxlist.com/indigo-carmine-drug.htm, acesso aos 6 de julho de 2017.

9. Merck, *Indigo carmine*, URL: http://www.sigmaaldrich.com/MSDS/MSDS/DisplayMSDSPage.do?country=TH&language=en&productNumber=131164&brand=SIAL&PageToGoToURL=http%3A%2F%2Fwww.sigmaaldrich.com%2Fcatalog%2Fproduct%2Fsial%2F131164%3Flang%3Den, acesso aos 6 de julho de 2017.

10. FDA, *Summary of color additives for use in the United States in Foods, Drugs, Cosmetics, and Medical Devices*, URL: https://www.fda.gov/ForIndustry/ColorAdditives/ColorAdditiveInventories/ucm115641.htm, acesso aos 6 de julho de 2017.

11. Th. B. Zanoni, A.A. Cardoso, M.V. Baldrin *et al.*, Exploratory study on sequestration of some essential metals by indigo carmine food dye, *Braz. J. Pharm. Sci.*, **46**, 723-730 (2010).

12. P.A. Pushpanjali, J.G. Manjunatha, C. Raril, D.K. Ravishankar, Determination of indigo carmine at poly(adenine) modified carbone nanotube paste electrode, *Res. J. Life Sci. Bioinf. Pharm. Chem. Sci.*, **5**, 820-832 (2019).

13. J.G.G. Manjunatha, A novel poly (glycine) biosensor towards the detection of indigo carmine: A voltammetric study, *J. Food & Drug Anal.*, **26**, 292-299 (2018).

14. L.F. Loguercio, P. Domingos, L. Manica *et al.*, Simple one-step method to synthesize polypyrrole-indigo carmine-silver nanocomposite, *J. Chemistry*, **2016**, ID: 5284259 (2016).

15. Drugs.com, *Indigo carmine*,https://www.drugs.com/pro/indigo-carmine.html, acesso aos 6 de julho de 2017.

16. Th. Bechtold, R. Mussak, *Handbook of Natural Colorants*, John Wiley and Sons, London (UK), 2009.

17. M.A. El Hamd, S.M. Deraya, O.S. Abdelmajeed, H.F. Askal, Spectrophotometric method for determination of five 1,4-dihydropyridine drugs using N-bromosuccinimide and indigo carmine dye, *Int. J. Spectroscopy*, **2013**, ID: 243059 (2013).

18. K.G. Gilbert, H.G. Maule, B. Rudolph, Quantitative analysis of indigo and indigo precursors in leaves of Isatis Spp. and *Polygonum tinctorium*, *Biotechnol. Prog.*, **20**, 1289-1292 (2004).

19. M. Arvand, M. Saberi, M. Ardaki, A. Mohammadi, Mediated electrochemical method for the determination of indigo carmine levels in food products, *Talanta*, **173**, 60-68 (2017).

20. S.U. Rahman, M.S. Ba-Shammakh, Thermal effects on the process of electropolymerization of pyrrole on mild steel, *Synth. Met.*, **140**, 207-210 (2004).

21. A.J. Pearlstein, J.A. Johnson, Global and conditional stability of the steady and periodic solutions of the Franck-FitzHugh model of electrodissolution of Fe in H_2SO_4, *J. Electrochem. Soc.*, **136**, 1290-1298 (1991).

22. I. Das, N.R. Agrawal, S.A. Ansari, S.K. Gupta, Pattern formation and oscillatory electropolymerization of thiophene, *Indian J. Chem. A*, **47**, 1798-1803 (2008).

23. K. Aoki, I. Mukoyama, J. Chen, Polymerization and dissolution of polythiophene films, *Russ. J. Electrochem.*, **40**, 319-323 (2004).

24. M. Bazzaoui, E.A. Bazzaoui, L. Martins, J.I. Martins, Electropolymerization of pyrrole on zinc-lead-silver alloys electrodes in acidic and neutral organic media, *Synth. Met.*, **130**, 73-83 (2002).

25. V.V. Tkach, Ya. G. Ivanusko, S. M. Lukanova *et al.*, 9-triphenylphosphazoacridine. Synthesis and modeling of electroanalytical action, *Appl. J. Env. Eng. Sci.*, **3**, 365-370 (2017).

26. V.V. Tkach, M.V. Kushnir, N.M. Storoshchuk *et al.*, The theoretical description of cathodic deposition of new conducting polymer composite, assisted by a perrhenate of a novel triazolic derivative, *Orbital Electr. J. Chem.*, **12**, 34-38 (2020).

27. V.V. Tkach, M.V. Kushnir, Ya. G. Ivanushko *et al.*, A descrição matemática do desempenho do novo derivado acridínico na detecção eletroanalítica do conteúdo total do ácido gálico em alfarroba, *Rev. Colomb. Cienc. Quím. Farm.*, **47**, 441-451 (2018).

Como citar este artigo

V.V. Tkach, M.V. Kushnir, Y.G. Ivanushko, L.V. Romaniv, S.C. de Oliveira, O.V. Ahafonova, N.S. Serhata, P.I. Yagodynets´, O estudo teórico do desempenho dos polímeros condutores dos corantes azoicos na detecção eletroquímica de indigo-carmim, *Rev. Colomb. Cienc. Quím. Farm.*, **49**(3), 699-709 (2020).

Artigo de pesquisa científica / *http://dx.doi.org/10.15446/rcciquifa.v49n3.91339*

A descrição matemática da detecção eletroanalítica dos íons de zinco em formas farmacêuticas de uso oftálmico, baseada na complexação de zinco com algumas bases de Schiff

Volodymyr V. Tkach[1,2*], Marta V. Kushnir[1], Sílvio C. de Oliveira[2], Volodymyr V. Parchenko[3], Vira M. Odyntsova[3], Ilona I. Aksyonova[3], Olga V. Luganska[4], Yana G. Ivanushko[1], Svitlana M. Lukanova[1], Olga V. Pishak[1], Petro I. Yagodynets´[1]

[1]Universidade Nacional de Chernivtsi, 58012, Rua de Kotsyubyns'ky, 2, Chernivtsi, Ucrânia.

[2]Universidade Federal de Mato Grosso do Sul, Av. Sen. Felinto. Müller, 1555, C/P. 549, 79074-460, Campo Grande, MS, Brasil.

[3]Universidade Estatal de Medicina de Zaporizhzhya, 69000, Av. de Maiakovs´ky, 26, Zaporizhzhya, Ucrânia.

[4]Universidade Nacional de Zaporizhzhya, Faculdade de Biologia, 69095, Rua de Zhukovs'ky, 66, Zaporizhzhya, Ucrânia.

*Autor para correspondência: nightwatcher2401@gmail.com

Recebido: 17 de junho de 2019

Revisado: 3 de julho de 2020

Aceto: 6 de julho de 2020

Resumo

Um processo eletroanalítico da detecção quantitativa dos íons de zinco bivalente sobre as novas bases de Schiff no modo galvanostático tem sido simulado teoricamente. O respectivo modelo matemático tem sido desenvolvido e analisado mediante a teoria de estabilidade linear e da análise de bifurcações. Foi estabelecido que o sistema é eficiente tanto do ponto de vista eletroanalítico, como do ponto de vista eletrossintético, por ser facilmente estabilizado o estado estacionário. Todavia, o comportamento oscilatório, neste sistema é mais provável que no caso clássico do desempenho de sensores, baseados em polímeros condutores e outros materiais orgânicos, por haver influências na dupla camada elétrica, causadas pela reação química da formação de complexo.

Palavras-chave: Zinco, elétrodos quimicamente modificados, bases de Schiff,complexos, eletropolimerização estado estacionário estável.

Summary

The mathematical description for the electroanalytical detection of zinc ions in ophthalmic pharmaceutical forms, based on zinc complexation with some Schiff bases

An electroanalytical process of the quantitative determination of bivalent zinc ions over the novel Schiff bases in galvanostatic mode has been theoretically simulated. The correspondent mathematical model has been developed and analyzed by means of linear stability theory and bifurcation analysis. It was shown that the system is efficient from both electroanalytical and electrosynthetical points of view, as the steady-state is easily stabilized. Nevertheless, the oscillatory behavior in this system is more probable than in the classic case of the sensors, based on conducting polymers and other organic materials, as there are double electric layer influences, caused by complex formation.

Key words: Zinc, chemically modified electrodes, Schiff bases, complexes, electropolymerization, stable steady-state.

Introdução

Zinco é um dos microelementos, que, em concentrações mínimas, é necessário para a manutenção da homeostase [1, 2]. Os compostos de zinco são usados durante a ativação do sistema protetor do organismo contra várias doenças. A falta de zinco no organismo pode provocar deficiência no crescimento, diarreia em crianças e lentidão no fechamento de cicatrizes [3, 4].

Na medicina oftálmica, o zinco é utilizado no tratamento de degeneração macular, da cegueira noturna, durante a "síndrome de olho digital" e para a prevenção de cataratas [5, 6]. Outros usos farmacológicos incluem a prevenção da doença de Alzheimer, aliviação da síndrome de hiperatividade e falta de atenção [7, 8]. Nada obstante, o zinco, como qualquer outro metal pesado e, ainda por cima, pertencente ao mesmo grupo do cádmio e do mercúrio, forma compostos, que soem ser altamente tóxicos no organismo humano [9, 10]. A toxicidade de zinco pode levar, predominantemente, à insuficiência renal. Outrossim, a mudança da composição de lipoproteínas e a redução da concentração de compostos cúpricos também podem ser observadas. Destarte, o desenvolvimento de um método, capaz de determinar as concentrações de zinco em diferentes meios, é, deveras, uma tarefa atual, e os métodos eletroanalíticos, envolvento a determinação direta e indireta, providenciar-lhe-iam uma boa solução [11-15].

Vários métodos da determinação de zinco, baseados na formação de complexos, têm sido desenvolvidos [16-20]. Além disso, os complexos de zinco podem ser usados como monômeros em polímeros condutores, o que faz possível reunir, num só process, os fins eletroanalíticos com os eletrossintéticos.

Não obstante, para o desenvolvimento prático de um processo eletroanalítico, é preciso realizar, a priori, uma investigação teórica comportamental do sistema, com a análise do modelo matemático correspondente. Esta análise dar-nos-á resposta a perguntas, que surgem da indecisão acerca do mecanismo mais provável do desempenho eletroanalítico do sistema, da possibilidade das instabilidades eletroquímicas, que não necessariamente estão aquém do atual desiderato da eficiência eletroanalítica [21-24] e, outrossim, da mera comparação entre este processo eletroanalítico e os já descritos [25, 26].

Destarte, o objetivo geral do nosso trabalho é avaliar, do ponto de vista teórico o processo da detecção eletroanalítica de zinco por um ânodo, modificado por uma base de Schiff com a subsequente eletropolimerização do complexo resultante. A sua realização far-se-á mediante o desenvolvimento e a análise comportamental de estabilidade do modelo matemático, correspondente ao sistema. Ademais, comparar-se-ão este sistema e os análogos, com ênfase às diferenças mecanísticas e do desempenho [25, 26]. Neste trabalho avalia-se o comportamento durante as medidas potenciométricas no modo galvanostático.

O sistema e seu modelo

Reagindo com as bases de Schiff, descritas em [27, 28], o zinco forma o complexo, conforme a figura 1:

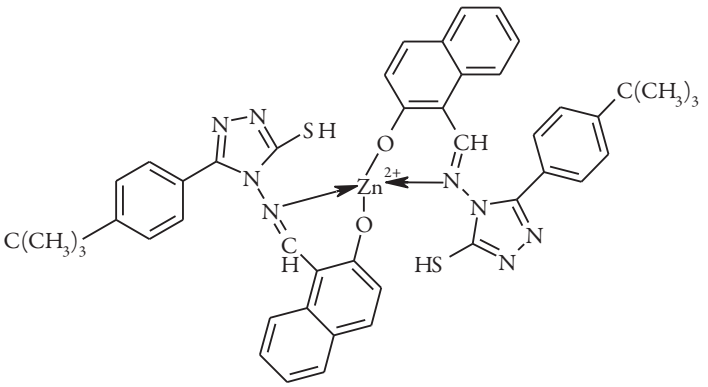

Figura 1. Exemplo de um complexo de zinco com uma base de Schiff.

Noutras condições, a formação do complexo realizar-se-á, também, pelos grupos -SH. Haja vista o efeito doador de elétrons dos íons Zn^{2+}, o complexo sói polimerizar-se a potenciais inferiores aos característicos para os triazóis e outros compostos análogos. Isso é especialmente relevante, em se tratando do modo galvanostático, em que o potencial do ânodo depende da intensidade da reação eletroquímica e do valor escolhido da densidade da corrente.

Assim, sendo, para descrever o desempenho do sistema eletroanalítico, nós introduzimos as três variáveis:

z: a concentração dos íons de zinco na camada pré-superficial.

ϑ: o grau de recobrimento do complexo de zinco com a base de Schiff na sua forma monomérica.

q :a carga do elétrodo.

Para simplificar a modelagem, supomos que o reator esteja agitando-se intensamente, o que nos deixa menosprezar o fluxo de convecção e as suas influências. Outrossim, supomos que o eletrólito de suporte esteja em excesso, o que nos permite menosprezar o fluxo de migração e as suas influências. Além disso, supomos que o perfil da distribuição de concentrações das substâncias na camada pré-superficial seja lineal, e a espessura da camada, estável, igual a δ.

É possível mostrar que o comportamento do sistema pode ser descrito pelo conjunto de equações diferenciais a seguir:

$$\begin{cases} \dfrac{dz}{dt} = \dfrac{2}{\delta}\left(\dfrac{\Delta}{\delta}(z_0 - z) - r_c\right) \\ \dfrac{d\theta}{dt} = \dfrac{1}{G}(r_c - r_p) \\ \dfrac{dq}{dt} = i - i_F \end{cases} \quad (1)$$

em que z_0 é a concentração dos íons de zinco na camada pré-superficial, r_c e r_p são as velocidades da complexação e da polimerização, G é a concentração superficial máxima do complexo no ânodo, i é a corrente de entrada e i_F, a corrente de Faraday.

As velocidades dos respectivos processos e a corrente de Faraday podem ser calculadas conforme:

$$r_c = k_c z(1-\theta)^2 \exp(\gamma\theta) \quad (2)$$

$$r_p = k_p \theta^n \exp \frac{2nF\gamma\theta}{RT} \tag{3}$$

$$i_F = 2nFk_p \theta^n \exp \frac{2nF\gamma\theta}{RT} \tag{4}$$

em que os parâmetros k são as constantes de velocidade das respectivas reações, n é o número de unidades monoméricas no polímero complexo, γ é uma variável, que descreve as influências entre a capacitância da dupla camada elétrica (DCE) e o grau de recobrimento da superfície pelo monômero complexo, F é o número de Faraday, R é a constante universal de gases e T, a temperatura absoluta.

O comportamento do sistema no modo potenciostático é mais dinâmico que no modo galvanostático, o que será descrito abaixo.

Resultados e discussão

Para investigar o comportamento do sistema com a determinação eletroquímica de zinco no modo galvanostático no ânodo, modificado por uma base de Schiff, com a eletropolimerização subsequente do complexo resultante, investigamos o conjunto de equações diferenciais (1), mediante a teoria de estabilidade linear. Os elementos estacionários do Jacobiano expor-se-ão conforme:

$$\begin{pmatrix} a_{11} & a_{12} & a_{13} \\ a_{21} & a_{22} & a_{23} \\ a_{31} & a_{23} & a_{33} \end{pmatrix} \tag{5}$$

em que:

$$a_{11} = \frac{2}{\delta}\left(-\frac{\Delta}{\delta} - k_c (1-\theta)^2 \exp(\gamma\theta)\right) \tag{6}$$

$$a_{12} = \frac{2}{\delta}\left(2k_c z(1-\theta)\ \exp(\gamma\theta) - \gamma k_c (1-\theta)^2 \exp(\gamma\theta)\right) \tag{7}$$

$$a_{13} = 0 \tag{8}$$

$$a_{21} = \frac{1}{G}\left(k_c (1-\theta)^2 \exp(\gamma\theta)\right) \tag{9}$$

$$a_{22} = \frac{1}{G}\begin{pmatrix} -2k_c z(1-\theta)\ \exp(\gamma\theta) + \gamma k_c (1-\theta)^2 \exp(\gamma\theta) - nk_p\theta^{n-1}\exp\dfrac{2nF\gamma\theta}{RT} \\ -\gamma nk_p\theta^n \exp\dfrac{2nF\gamma\theta}{RT} \end{pmatrix} \quad (10)$$

$$a_{23} = \frac{1}{G}\left(-\lambda nk_p\theta^n \exp\frac{2nF\gamma\theta}{RT}\right) \quad (11)$$

$$a_{31} = 0 \quad (12)$$

$$a_{32} = 2nF\left(-nk_p\theta^{n-1}\exp\frac{2nF\gamma\theta}{RT} - \gamma nk_p\theta^n \exp\frac{2nF\gamma\theta}{RT}\right) \quad (13)$$

$$a_{33} = 2nF\left(-\lambda nk_p\theta^n \exp\frac{2nF\gamma\theta}{RT}\right) \quad (14)$$

Observando as equações (6), (10) e (14), observamos que os elementos da diagonal principal da matriz contêm os elementos positivos, que descrevem apositiva conexão de retorno. Destarte, o *comportamento oscilatório*, neste caso, é possível. Otrossim, graças à presença da influência da reação de ligação na DCE, ela é mais provável que em casos mais simples da determinação eletroquímica assistida. Além disso, no modo galvanostático, essas influências podem também influenciar a carga do elétrodo.

Além do elemento $\gamma nk_p\theta^n \exp\dfrac{2nF\gamma\theta}{RT} > 0$, que descreve as influências desestabilizadoras do rearranjo da composição da camada pré-superficial, outro elemento positivo é o $\alpha k_l cl(1-\theta)\exp(-\alpha\theta) > 0$, que descreve as influências na mesma camada da formação das novas formulações iônicas. Outro elemento, que pode ser positivo, é $-\lambda nk_p\theta^n \exp\dfrac{2nF\gamma\theta}{RT} > 0$. As oscilações, neste caso, se esperam frequentes e de pequena amplitude.

Para investigar a estabilidade do estado estacionário, aplicamos ao conjunto de equações diferenciais (1) o critério de Routh-Hurwitz. Evitando as expressões grandes, introduzimos as novas variáveis, de modo que o determinante se descreve como:

$$\frac{4nF}{G\delta}\begin{vmatrix} -\kappa_1 - \mathrm{X}_1 & -\Pi_2 & 0 \\ \mathrm{X}_1 & \Pi_2 - \Pi_3 & -\mathrm{M} \\ 0 & -\Pi_3 & -\mathrm{M} \end{vmatrix} \quad (16)$$

Que, aplicada a condição Det J<0, saliente do critério, será reescrita, conforme:

$$-(\kappa_1 + X_1)2\Pi_2 M < 0 \qquad (17)$$

E esta condição é correspondente a um processo eficiente do ponto de vista eletroanalítico, capaz de ser controlado, de igual maneira, pela difusão ou pela reação. Mas, visto que a formação de complexo é um processo relativamente rápido nas condições da análise, ser-nos-á possível concluir que o processo eletroanalítico será controlado pela difusão dos cátions de zinco.

A sua satisfação é correspondente à dependência linear entre a concentração dos íons de zinco e o potencial do ânodo e realiza-se com certeza, desde que os parâmetros Π_2 e *M*, que incluem as influências das etapas química e eletroquímica do processo na DCE e na carga de elétrodo, tenham valores positivos, isto é, as influências se enfraqueçam.

A instabilidade monotônica, correspondente ao limite de detecção do ponto de vista eletroanalítico, também é possível para este sistema, e as suas condições descrevem-se como:

$$-(\kappa_1 + X_1)2\Pi_2 M = 0 \qquad (16)$$

No caso da *formação de dois tipos de complexo*, de fato, ocorre a copolimerização deles dois, o que faz o comportamento do sistema ainda mais dinâmico. Este fenômeno, em que o comportamento oscilatório é ainda mais frequente, será descrito num dos nossos próximos trabalhos.

Conclusões

Da simulação teórica da determinação de zinco em fármacos oftálmicos no elétrodo, modificado por uma base de Schiff, junto com a eletropolimerização do composto resultante, é possível concluir que:

- A base de Schiff é um modificador eficiente de elétrodo durante a quantificação de zinco em fármacos oftálmicos. O estado estacionário no Sistema é fácil de obter e manter.
- O processo eletroanalítico no modo galvanostático é controlado pela difusão.
- O comportamento oscilatório, no modo galvanostático, é mais provável que no potenciostático, podendo, além das influências das reações químicas e eletroquímicas na DCE, ser causado, também, pela eletropolimerização do complexo na carga do elétrodo.

Conflito de interesse

Os autores não têm conflito de interesse.

Referências

1. S. Frassinetti, G. Bronzetti, L. Caltavuturo *et al.*, The role of zinc in life: A review, *J. Environm. Pathol. Toxicol. Oncol.*, **25**, 597-610 (2006).
2. J. Osredkar, N. Sustar, Copper and zinc, biological role and significance of copper/zinc imbalance, *J. Clin. Toxicol.*, **S3**, 001-1-18 (2011).
3. A. Krezel, W. Maret, The biological inorganic chemistry of zinc ions, *Arch. Biochem. Biophys.*, **611**, 3-19 (20106).
4. K. Kaur, R. Gupta, S.A. Saraf, S. K. Saraf, Zinc: The metal of life, *Comprehensive Rev. Food Sci. Food Safety*, **11**, 358-376 (2014).
5. *The Pharmaceutical Journal, Physiological and medicinal zinc,* https://www.pharmaceutical-journal.com/cpd-and-learning/learning-article/physiological-and-medicinal-zinc/10997386.article?firstPass=false, acesso aos 3 de julho de 2020.
6. R. Vishvanatan, M. Chung, E. Johnson, A systematic review on zinc for the prevention and treatment of age-related macular degeneration, *Invest. Ophthalmol. Vis. Sci.*, **54**, 3985-3998 (2013).
7. N. Watt, I. Whitehouse, N. Hooper, Metals and Alzheimer's disease, *Int. J. Alzheimer Dis.*, **2011**, ID: 971021 (2011).
8. K. Dodig-Curkovic, J. Dovhani, M. Curkovic *et al.*, The role of zinc in the treatment of hyperactivity disorder in children, *Acta Med. Croat.*, **63**, 307-313 (2009).
9. K.Y. Djoko, Ch. Y. Ong, M.J. Walker, A.G. McEven, The role of copper and zinc toxicity in innate immune defense against bacterial pathogens, *J. Biol. Chem.*, **290**, 18954-18961 (2015).
10. J. Sheqwara, Y. Alkhatib, Sideroblastic anemia secondary to zinc toxicity, *Blood*, **122**, 311 (2013).
11. Z. Koudelkova, T. Syrovy, P. Ambrozova *et al.*, Determination of zinc, cadmium, lead, copper and silver using a carbon paste electrode and a screen printed electrode modified with chromium(III) oxide, *Sensors*, **17**, 1832-1850 (2017).

12. A. Lutka, Z. Kokot, H. Powidzka, Validation of electrochemical determination of zinc in selected pharmaceutical preparations, *Acta Pol. Pharm.*, **61**, 243-247 (2004).

13. J. Kudr, L. Richtera, L. Nejdl *et al.*, Improved electrochemical detection of zinc ions using electrode modified with electrochemically reduced graphene oxide, *Materials*, **9**, 31-1-12 (2016).

14. A. Lutka, H. Bukowska, Voltammetric Determination of zinc in compound pharmaceutical preparations--Validation of method, *Acta Pol. Pharm.*, **66**, 471-475 (2009).

15. K. Kiran, Spectrophotometric determination of zinc in water samples using 3-hydroxybenzylaminobenzoic acid, *Chem. Sci. Trans.*, **1**, 669-673 (2012).

16. C. L. Donnici, C.C. Souza, M.A. Beinner, J. B. da Silva, Fast determination of iron and zinc in hair and human serum samples after alkaline solubilization by GF AAS, *J. Braz. Chem. Soc.*, **27**, 119-126 (2016).

17. D. Bakircioglu, N. Topraksever, Y.Kurtulus, Determination of zinc in edible oils by flow injection FAAS after extraction induced by emulsion breaking procedure, *Food Chem.*, **151**, 219-224 (2013).

18. H. Barfeie, G. Grivani, V. Eigner *et al.*, Copper(II), nickel(II), zinc(II) and vanadium(IV) Schiff base complexes: Synthesis, characterization, crystal structure determination, and thermal studies, *Polyhedron*, **146**, 19-25 (2018).

19. V. Milosavljevic, Y. Haddad, M.A. Merlos-Rodrigo *et al.*, The zinc-Schiff base-novicidin complex as a potential prostate cancer therapy, *PloS One*, **11**(10), e0163983 (2016).

20. M. Sahin, N. Kocak, D. Erdenay, U. Arslan, Zn(II), Ni(II), Cu(II) and Pb(II) complexes of tridentate asymmetrical Schiff base ligands: Synthesis, characterization, properties and biological activity, *Spectrochim. Acta*, **15**, 400-408 (2013).

21. P.S. Ganesh, B.E.K. Swamy, A.B. Teradale, Simultaneous electroanalysis of norepinephrine, ascorbic acid and uric acid at poly(niacinamide) modified carbon paste electrode, *Anal. Bioanal. Electrochem.*, **10**, 612-620 (2018).

22. D. Sazou, The dynamic behavior of the electrochemical polymerization of indole in acetonitrile - water mixtures, *Synth. Met.*, **130**, 45-55 (2002).

23. I. Das, N. Goel, N.R. Agrawal, S.K. Gupta, Growth patterns of dendrimers and electric potential oscillations during electropolymerization of pyrrole using mono- and mixed surfactants, *J. Phys. Chem.*, **114**, 12888-12893 (2010).

24. M. Bazzaoui, E.A. Bazzaoui, L. Martins, J.I. Martins, Electropolymerization of pyrrole on zinc-lead-silver alloys' electrodes in neutral and acid organic media, *Synth. Met.*, **130**, 73-80 (2002).

25. V. Tkach, B. Kumara Swamy, R. Ojani *et al.*, El mecanismo de la oxidación de omeprazol sobre el electrodo de carbono vitroso, modificado por polializarina, y su descripción matemática, *Orbital Electr. J. Chem.*, **7**, 1-5 (2017).

26. V. Tkach, B. Kumara Swamy, R. Ojani *et al.*, Comportamento de paracetamol durante a sua oxidação eletrocatalítica sobre poli(azul da anilina) e a sua descrição matemática, *Rev. Colomb. Cienc. Quím. Farm.*, **44**, 148-158 (2015).

27. I.I. Aksyonova, O.I. Panasenko, Ye. G. Knysh, Synthesis and physical-chemical properties of 3-(4-(tert-butyl)phenyl)-5-(R-ylthio)-4H-1,2,4-triazol-4-amines, *Act. Probl. Med. Pharm. Sci.*, **20**, 31-34 (2016).

28. V.M. Odyntsova, Ye. S. Pruglo, A.S. Gotsulya *et al.*, Antihypoxic activity of salts of (2-(5-(adamantane-1-yl)-4H-1,2,4-triazole-3-ylthio) acetate acids, *Zapor. J. Med.*, **2**, 94-96 (2014).

Como citar este artigo

V.V. Tkach, M.V. Kushnir, S.C. de Oliveira, V.V. Parchenko, V.M. Odyntsova, I.I. Aksyonova, O.V. Luganska, Y.G. Ivanushko, S.M. Lukanova, O.V. Pishak, P.I. Yagodynets´, A descrição matemática da detecção eletroanalítica dos íons de zinco em formas farmacêuticas de uso oftálmico, baseada na complexação de zinco com algumas bases de Schiff, *Rev. Colomb. Cienc. Quím. Farm.*, **49**(3), 710-719 (2020).

Scientific research article / *http://dx.doi.org/10.15446/rcciquifa.v49n3.91340*

Ultrasonic investigation of lacosamide in various alcohols at 298.15 K

Shipra Baluja*, Swati Oza, Divyata Lava, Rami Pampaniya

Physical Chemistry Laboratory, Department of Chemistry, Saurashtra University, Rajkot-360005 (Gujarat), India.

*Corresponding author: shipra_baluja@rediffmail.com

Received: 12 July 2019

Revised: 16 July 2020

Accepted: 20 July 2020

Summary

Ultrasonic velocity, density and viscosity of Lacosamide were measured in various alcohols at 298.15 K. From these measured experimental data, various acoustical parameters such as Specific acoustical impedance (Z), Adiabatic compressibility (κ_s), Intermolecular free path length (L_f), Rao's molar sound function (R_m), Molar compressibility (W), van der Waals constant (b), Solvation number (S_n), Thermal conductivity (K_{bm}), Relaxation strength (r) have been calculated for understanding the molecular interactions occurring in the solution.

Key words: Lacosamide, ultrasonic velocity, alcohols, acoustical parameters.

Resumen

Investigación ultrasónica de lacosamida en varios alcoholes a 298,15 K

Se midieron la velocidad ultrasónica, la densidad y la viscosidad de soluciones de lacosamida en varios alcoholes a 298,15 K. A partir de estos datos experimentales, se calcularon varios parámetros acústicos para comprender las interacciones moleculares que ocurren en la solución, tales como la impedancia acústica específica (Z), la compresibilidad adiabática (κ_s), la longitud del camino libre intermolecular (L_f), la función molar de sonido de Rao (R_m), la compresibilidad molar (W), la constante de van der Waals (b), el número de solvatación (Sn), la conductividad térmica (K_{bm}), y la fuerza de relajación (r).

Palabras clave: Lacosamida, velocidad ultrasónica, alcoholes, parámetros acústicos.

Introduction

Ultrasonic technology has a wide range of applications in the fields of biology [1-3], pharmacy [4], polymer [5, 6], civil engineering [7], nuclear power generation [8], sonochemistry [9], medical [10], material science [11], agriculture [12], navigation system [13] etc. Due to its non- destructive nature [14], it is also used in various industries such as plastic [15], cement [16], soap [17], paper [18], petrochemicals [19], glass [20], food [21], dairy [22] etc. Further, ultrasonic and related thermodynamic parameters of solid substances provide useful information related to structure of molecules, molecular packing and inter and intra molecular interactions [23]. In liquid mixtures [24, 25] and solutions [26], these parameters help to interpret type of molecular interactions [27].

Lacosamide is an amino acid derivative; N-methyl-D-aspartic acid and is non-hygroscopic white to yellow crystalline compound of molecular weight 250.294 $g.mol^{-1}$ and of molecular formula $C_{13}H_{18}N_2O_3$. It is R-enantiomer of IUPAC name (*R*)-2-acetamido-*N*-benzyl-3-methoxy propionamide [28].

The preclinical and clinical result of the drug has demonstrated an excellent anticonvulsant activity [29-32] and is used for the treatment of both epilepsy and diabetic neuropathic pain [33]. Further, drug was found to be more potent than sodium channel blocking drug phonation and barbiturate phenobarbital [34] and is used in combination with other agents as therapy of partial onset seizures.

Ultrasonic study of drugs in various solvents are provide valuable information related to interactions of drug with the solvent which is useful to prepare appropriate concentrated dose for tablets, injection and oral dose in appropriate solvents [35-37]. The ultrasonic data and related thermoacoustic parameters are also useful to study the pharmacodynamic and pharmacokinetics of drugs [38].

In the present study, various acoustical properties of lacosamide in various alcohols have been studied at 298.15 K over a wide range of concentrations by measuring ultrasound velocity, density and viscosity. The results are interpreted to understand the interactions of lacosamide in alcohols. The evaluated data may be useful for further research and development of drug lacosamide.

Experimental

The solvents selected for the study were alcohols such as methanol, ethanol, 1-propanol, 1-butanol and1-pentanol.The drug lacosamide was recrystallized before use. Figure 1 shows the structure of lacosamide.

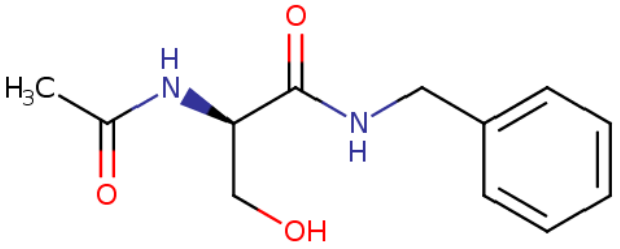

Figure 1. Molecular structure of lacosamide.

The solutions of lacosamide of various concentrations were prepared in all selected alcohols by using weight balance (Mettler Toledo AB204-S, Switzerland).

Measurements of ultrasonic velocity and density

The Ultrasonic velocity and density of all the pure alcohols and solutions were measured at 298.15 K using Anton Paar density and sound velocity meter (Model DSA 5000M). The accuracy of ultrasound velocity and density are ±0.5 $m.sec^{-1}$ and ±0.005 $kg.m^{-3}$ respectively.

Measurements of viscosity

The Ubbelohde viscometer with 25 ml capacity was used for the viscosity measurement. In the viscometer, milli Q-water/pure solvent/solution were filled, and flow time of liquid was measured at 298.15 K. The digital stopwatch (Model: RACER HS–10W), with an accuracy of +0.01 second was used to determine flow time of solutions. The temperature stability was maintained by circulating water from a thermostat (NOVA NV-8550 E, accuracy of ± 0.1 K around the viscometer. The accuracy of viscosity is ± 0.05 %. Using the flow time of water and solution/ pure solvent and viscosity of standard water sample, viscosity of solvent/ solution was determined according to equation:

$$\frac{\eta_1}{\eta_2} = \frac{t_1}{t_2}\frac{\rho_1}{\rho_2} \tag{1}$$

where η_1 and η_2 are viscosities of water and solution/pure solvent, respectively. t_1 and t_2 are the flow time for water and sample solution/pure solvent whereas ρ_1 and ρ_2 are density of water and solution/pure solvent, respectively.

Results and discussion

The experimental data of density, viscosity and sound velocity of pure solvents are given in table 1 along with theoretical values taken from literature.

Table 1. Experimental values of density, sound velocity and viscosity of pure solvents at 298.15 K*.

Liquid	Density ($kg \cdot m^{-3}$)	Viscosity (mPa·s)	Ultrasonic velocity ($m \cdot s^{-1}$)
Methanol	787.37 (787.20)[a]	0.549 (0.545)[a]	1104.90 (1104.00)[a]
Ethanol	805.94 (790.00)[b]	1.124 (1.105)[c]	1204.92 (1207.00)[b]
1-Propanol	800.22 (800.80)[d]	1.946 (1.943)[d]	1206.13 (1205.80)[e]
1-Butanol	807.88 (806.60)[f]	2.581 (2.585)[g]	1243.92 (1240.60)[f]
1-Pentanol	811.67 (811.00)[h]	3.348 (3.412)[i]	1275.32 (1275.33)[h]

*The values in parenthesis are from literature (a: [39], b: [40], c: [41], d: [42], e: [43], f: [44], g: [45], h: [46], i: [47]).

Table 2 shows the experimental data of density, viscosity and sound velocity of all the solutions in different solvents. It is clear from table 2 that ultrasonic velocity increases with increase in concentration in all selected alcohols. Further, it is minimum for methanol and maximum for 1-pentanol.

Table 2. Experimental values of density, viscosity, and ultrasound velocity of lacosamide in different alcohols at 298.15 K.

Conc. (M)	Density ($kg \cdot m^{-3}$)	Viscosity (mPa·s)	Ultrasonic velocity ($m \cdot s^{-1}$)
Methanol			
0.00	787.37	0.5499	1104.90
0.01	788.59	0.5697	1105.91
0.02	789.45	0.5761	1107.06
0.04	791.28	0.5854	1109.10
0.06	792.77	0.5957	1110.96
0.08	794.75	0.6073	1112.85
0.10	796.88	0.6141	1115.16

(*Continued*)

Table 2. Experimental values of density, viscosity, and ultrasound velocity of lacosamide in different alcohols at 298.15 K.

Conc. (M)	Density (kg·m^{-3})	Viscosity (mPa·s)	Ultrasonic velocity (m·s^{-1})
Ethanol			
0.00	805.94	1.1240	1204.92
0.01	807.38	1.1370	1205.85
0.02	808.17	1.1602	1206.64
0.04	810.36	1.1855	1208.05
0.06	812.05	1.2213	1209.29
0.08	813.65	1.2682	1210.60
0.10	815.21	1.3041	1211.73
1-Propanol			
0.00	800.22	1.9466	1206.13
0.01	800.95	1.9922	1207.09
0.02	802.08	2.0498	1208.18
0.04	803.80	2.1091	1209.72
0.06	805.36	2.1572	1211.04
0.08	806.91	2.1945	1212.64
0.10	808.29	2.2424	1213.89
1-Butanol			
0.00	807.29	2.5816	1243.92
0.01	807.88	2.6056	1244.15
0.02	808.55	2.6409	1244.75
0.04	810.12	2.6903	1245.62
0.06	811.56	2.7506	1246.56
0.08	812.91	2.8218	1247.62
0.10	814.00	2.8812	1248.57
1-Pentanol			
0.00	811.67	3.3484	1275.32
0.01	812.10	3.3921	1275.99
0.02	813.25	3.4493	1276.43
0.04	814.40	3.5172	1277.37
0.06	816.09	3.5771	1278.23
0.08	817.31	3.6457	1279.30
0.10	818.78	3.6944	1280.17

The graphical presentation of concentration dependence of ultrasonic velocity in different alcohols is shown in figure 2. It is clear from figure 2 that there is linear increase of ultrasonic velocity with concentration in all the alcohols. The order of ultrasound velocity in alcohols is: methanol > ethanol > 1-propanol > 1-butanol > 1-pentanol. However, there is overlapping in velocity values for ethanol and 1-Propanol. This may be due to the fact that the ethanol in the present study used was only 99% pure. So, the presence of impurity affects the velocity. Overall, ultrasound velocity increases with increase in CH_2 group of alcohols.

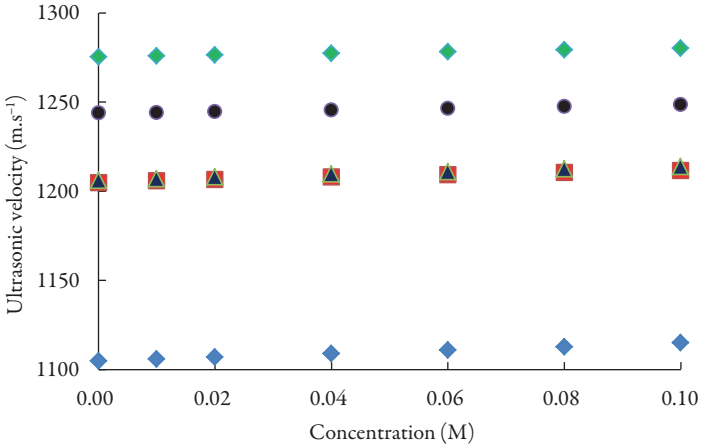

Figure 2. The variations of sound velocity of lacosamide with concentrations in alcohols at 298.15 K. ♦: Methanol; ■: Ethanol; ▲:1-Propanol; ●:1-Butanol; ♦:1-Pentanol.

From the experimental data of density (ρ), viscosity (η) and sound velocity (U), following acoustical parameters were calculated.

Specific acoustical impedance (Z) [48]:

$$Z = U \cdot \rho \tag{2}$$

Adiabatic compressibility (κ_s) [49]:

$$\kappa_s = \frac{1}{U^2 \rho} \tag{3}$$

Intermolecular free path length (L_f):

$$L_f = K_J \cdot K_S^{1/2} \tag{4}$$

where K_J is the Jacobson constant (= 2.0965 × 10^{-6}) at 298.15 K.

Rao's molar sound function (R_m) [50]:

$$R_m = \left(\frac{M}{\rho}\right) U^{\frac{1}{3}} \tag{5}$$

where M is the molar mass of solution and can be calculated by following equation: $M = M_1 W_1 + M_2 W_2$.

Molar compressibility (W):

$$W = \left(\frac{M}{\rho}\right) \kappa_s^{-1/7} \tag{6}$$

Van der Waals constant (b):

$$b = \frac{M}{\rho}\left\{1 - \left(\frac{RT}{MU^2}\right)\left[\sqrt{1 + \frac{MU^2}{3RT}} - 1\right]\right\} \tag{7}$$

where R is the gas constant (8.3143 $J.K^{-1}.mol^{-1}$) and T is absolute temperature.

Solvation number (S_n):

$$S_n = \frac{M_2}{M_1\left[1 - \frac{\kappa_a}{\kappa_{a1}}\right]\left[\left(\frac{100 - X}{X}\right)\right]} \tag{8}$$

where X is the number of grams of solute in 100 g of the solution. M_1 and $_{M2}$ are the molar masses and κ_{a1} and κ_a are adiabatic compressibility of solvent and solution respectively.

Thermal conductivity (K_{bm}) [51]:

$$K_{bm} = 3\left(\frac{\rho \cdot N_A}{M}\right)^{\frac{2}{3}} k_B U \tag{9}$$

where N_A is the Avogadro's number (6.0221×10^{23}), k_B is the Boltzmann constant ($k_B = 1.38064852 \times 10^{-23}\ m^2.kg^{-2}.K^{-1}$) and M is the molar mass of solution.

Relaxation strength (r):

$$r = 1 - \left(\frac{U}{U_\infty}\right)^2 \tag{10}$$

where $U_\infty = 1.6 \times 10^3$ m.s^{-1}

Some of these evaluated acoustical parameters are reported in table 3. The variation of specific acoustical impedance with concentration is shown in figure 3. The specific acoustical impedance is the measurement of opposition in acoustical flow by acoustic pressure in the solution [52]. It is observed from figure 2 that specific acoustical impedance (Z) increases with increase of concentration. Further, as CH_2 group increases in alcohols, Z increases i.e., it is maximum in 1-pentanol and minimum in methanol. The increase in specific acoustical impedance indicates the existence of solvent-solute interactions in solutions.

Table 3. Some evaluated acoustical parameters of lacosamide in different alcohols at 298.15 K.

Conc. (M)	r	R_m ($m^{10/3} \cdot s^{-1/3} \cdot mol^{-1}$)	S_n	K_{bm} ($W \cdot K^{-1} \cdot m^{-1}$)	W	b ($m^3 \cdot mol^{-1}$)
Methanol						
0.00	0.5231	4.207 x 10^{-4}	-	0.2759	7.812 x 10^{-4}	5.725 x 10^{-5}
0.01	0.5222	4.292 x 10^{-4}	7.4	0.2725	7.973 x 10^{-4}	5.944 x 10^{-5}
0.02	0.5212	4.380 x 10^{-4}	7.7	0.2692	8.136 x 10^{-4}	6.170 x 10^{-5}
0.04	0.5194	4.553 x 10^{-4}	8.0	0.2629	8.459 x 10^{-4}	6.627 x 10^{-5}
0.06	0.5179	4.726 x 10^{-4}	8.5	0.2570	8.783 x 10^{-4}	7.096 x 10^{-5}
0.08	0.5162	4.895 x 10^{-4}	8.6	0.2516	9.099 x 10^{-4}	7.570 x 10^{-5}
0.10	0.5142	5.062 x 10^{-4}	8.7	0.2466	9.411 x 10^{-4}	8.055 x 10^{-5}
Ethanol						
0.00	0.4329	6.083 x 10^{-4}	-	0.2398	1.129 x 10^{-3}	1.190 x 10^{-4}
0.01	0.4320	6.157 x 10^{-4}	5.1	0.2381	1.143 x 10^{-3}	1.217 x 10^{-4}
0.02	0.4313	6.236 x 10^{-4}	6.1	0.2363	1.157 x 10^{-3}	1.245 x 10^{-4}
0.04	0.4299	6.386 x 10^{-4}	6.4	0.2329	1.186 x 10^{-3}	1.300 x 10^{-4}
0.06	0.4288	6.540 x 10^{-4}	6.9	0.2295	1.215 x 10^{-3}	1.356 x 10^{-4}
0.08	0.4275	6.693 x 10^{-4}	7.3	0.2263	1.243 x 10^{-3}	1.413 x 10^{-4}
0.10	0.4264	6.845 x 10^{-4}	7.7	0.2232	1.272 x 10^{-3}	1.470 x 10^{-4}

(*Continued*)

Table 3. Some evaluated acoustical parameters of lacosamide in different alcohols at 298.15 K.

Conc. (M)	r	R_m ($m^{10/3} \cdot s^{-1/3} \cdot mol^{-1}$)	S_n	K_{bm} ($W \cdot K^{-1} \cdot m^{-1}$)	W	b ($m^3 \cdot mol^{-1}$)
1-propanol						
0.00	0.4317	7.993×10^{-4}	-	0.2002	1.482×10^{-3}	1.876×10^{-4}
0.01	0.4308	8.067×10^{-4}	4.2	0.1991	1.495×10^{-3}	1.908×10^{-4}
0.02	0.4298	8.137×10^{-4}	4.6	0.1982	1.509×10^{-3}	1.938×10^{-4}
0.04	0.4284	8.280×10^{-4}	5.1	0.1962	1.535×10^{-3}	2.000×10^{-4}
0.06	0.4271	8.422×10^{-4}	5.5	0.1943	1.562×10^{-3}	2.062×10^{-4}
0.08	0.4256	8.565×10^{-4}	5.6	0.1924	1.589×10^{-3}	2.125×10^{-4}
0.10	0.4244	8.708×10^{-4}	5.8	0.1905	1.616×10^{-3}	2.189×10^{-4}
1-butanol						
0.00	0.3956	9.874×10^{-4}	-	0.1805	1.830×10^{-3}	2.742×10^{-4}
0.01	0.3953	9.940×10^{-4}	5.5	0.1798	1.842×10^{-3}	2.774×10^{-4}
0.02	0.3948	1.001×10^{-3}	6.3	0.1791	1.855×10^{-3}	2.807×10^{-4}
0.04	0.3939	1.013×10^{-3}	6.8	0.1777	1.879×10^{-3}	2.871×10^{-4}
0.06	0.3930	1.026×10^{-3}	6.7	0.1764	1.903×10^{-3}	2.936×10^{-4}
0.08	0.3920	1.039×10^{-3}	6.7	0.1751	1.927×10^{-3}	3.001×10^{-4}
0.10	0.3910	1.052×10^{-3}	6.8	0.1738	1.952×10^{-3}	3.068×10^{-4}
1-pentanol						
0.00	0.3647	1.178×10^{-3}	-	0.1655	2.182×10^{-3}	3.739×10^{-4}
0.01	0.3640	1.184 x 10–3	4.5	0.1650	2.193×10^{-3}	3.774×10^{-4}
0.02	0.3636	1.189×10^{-3}	4.7	0.1646	2.203×10^{-3}	3.805×10^{-4}
0.04	0.3626	1.201×10^{-3}	5.4	0.1637	2.226×10^{-3}	3.872×10^{-4}
0.06	0.3618	1.212×10^{-3}	5.4	0.1628	2.246×10^{-3}	3.937×10^{-4}
0.08	0.3607	1.224×10^{-3}	5.5	0.1619	2.269×10^{-3}	4.005×10^{-4}
0.10	0.3598	1.235×10^{-3}	5.5	0.1611	2.290×10^{-3}	4.071×10^{-4}

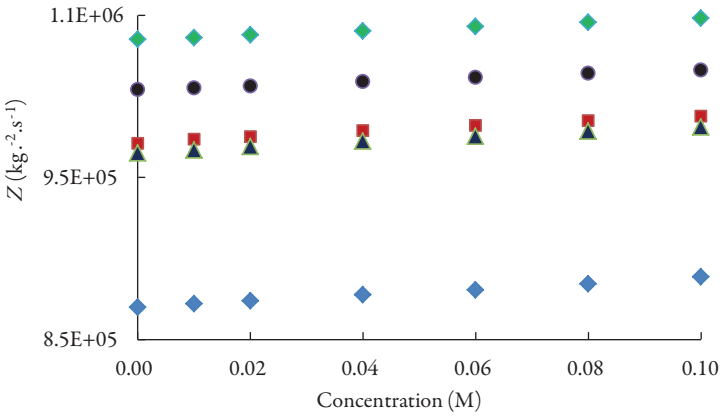

Figure 3. The variations of specific acoustical impedance of lacosamide with concentrations in alcohols at 298.15 K. ♦: Methanol; ■: Ethanol; ▲:1-Propanol; ●:1-Butanol; ♦:1-Pentanol.

The variation of adiabatic compressibility (κ_s) and intermolecular free path length (L_f) with concentration are given in figures 4 and 5 respectively. Both these parameters are observed to decrease with concentration. Further, as number of CH_2 group increases, these parameters decrease. The decrease of intermolecular free path length suggests that distance between solute i.e., lacosamide and solvent molecules decreases with concentration. So, when distance decreases, velocity increases (figure 2).

The compressibility of the solution is mainly due to free solvent molecules around solute i.e., drug molecules. So, when there is strong interaction between solvent and lacosamide molecules, compressibility decreases which is the case in present study. By increase in concentration of lacosamide, molecular associations are enhanced and newly formed aggregates cause adiabatic compressibility to decrease.

Table 3 shows the decrease in relaxation strength (r) also with concentration which also suggests the predominance of solvent-solute interactions in studied solutions.

It is also observed from table 3 that Rao's molar sound function (R_m), molar compressibility (W) and van der Waals constant (b) increase with increases in concentration. The variation of Rao's molar function (R_m) with concentrations is also shown in figure 6 for all the studied alcohols and is found to increase linearly. The least square equation and correlation coefficient (γ) values for some of the evaluated parameters are given in table 4. It is observed that for Rao's molar sound function, van der Waals constant and molar compressibility, correlation coefficient is almost unity. This indicates that although there are interactions between drug molecules with alcohol molecules, there is no complex formation.

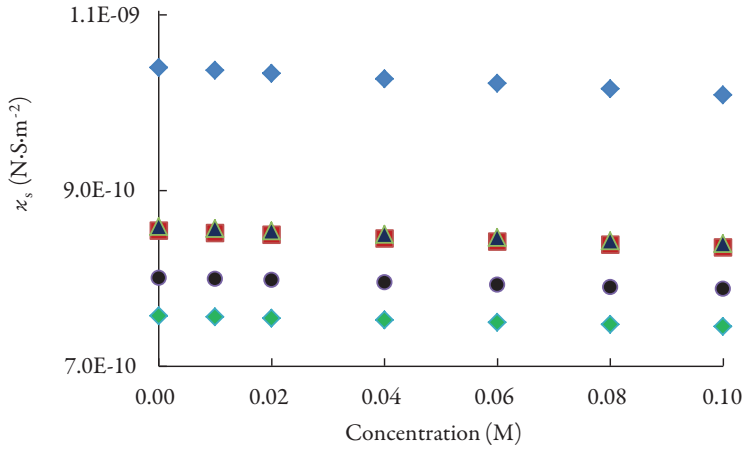

Figure 4. The variations of adiabatic compressibility of lacosamide with concentrations in alcohols at 298.15 K. ♦: Methanol; ■: Ethanol; ▲:1-Propanol; ●:1-Butanol; ♦:1-Pentanol.

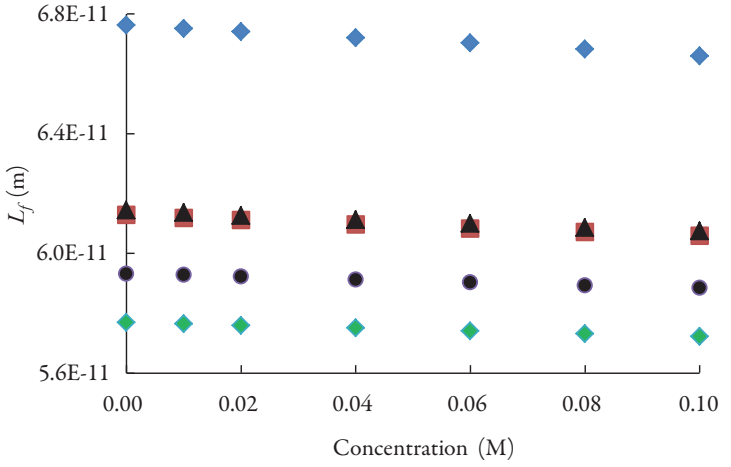

Figure 5. The variations of intermolecular free path length of lacosamide with concentrations in alcohols at 298.15 K. ♦: Methanol; ■: Ethanol; ▲:1-Propanol; ●:1-Butanol; ♦:1-Pentanol.

The type of interactions of lacosamide drug with alcohols is further confirmed by another parameter known as solvation number (S_n). This gives information regarding structure forming or structure breaking capacity of a solute in different solvents. The solvation number can be positive or negative. For the studied alcohols, solvation number of lacosamide is plotted against concentrations as shown in figure 7. It is observed from figure 7 and table 3 that the solvation number is positive for all the alcohols.

For all the alcohols, it increases with increase in concentration. However, in some cases, it becomes almost constant at higher concentrations. The positive solvation number indicates structure forming tendency of lacosamide in alcohols. This again proves strong molecular interactions between lacosamide and alcohol molecules.

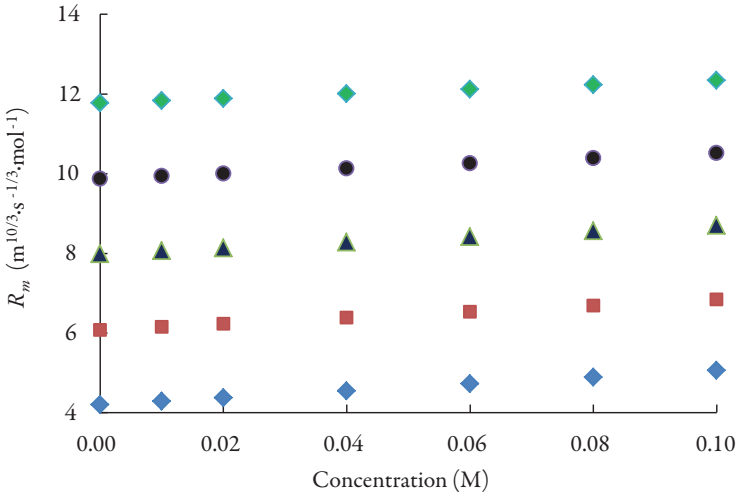

Figure 6. The variation of Rao's molar sound function of lacosamide with concentrations in alcohols at 298.15 K. ♦: Methanol; ■: Ethanol; ▲:1-Propanol; ●:1-Butanol; ♦:1-Pentanol.

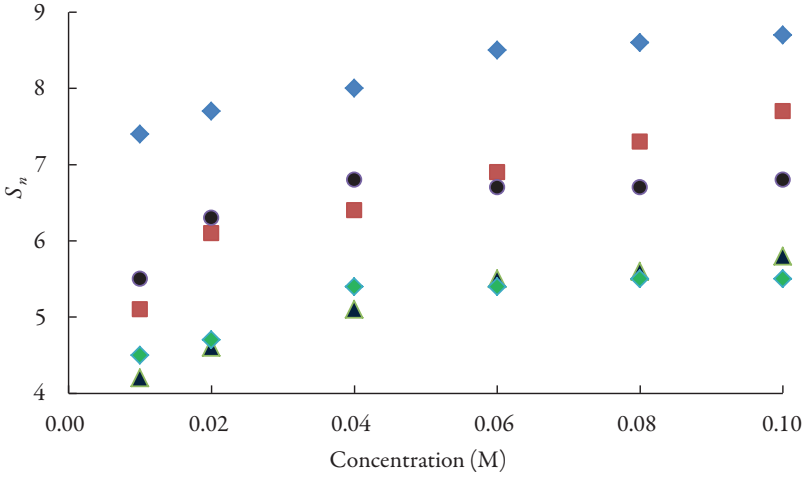

Figure 7. The variations of solvation number of lacosamide with concentrations in alcohols at 298.15 K. ♦: Methanol; ■: Ethanol; ▲:1-Propanol; ●:1-Butanol; ♦:1-Pentanol.

The thermal conductivity of solution is also found to decrease linearly with concentration as given in table 3. The variation in thermal conductivity with concentration is attributed to various factors such as Brownian motion, clustering etc. [51]. The decrease of thermal conductivity with concentration is similar to decrease of intermolecular free path length. As solute-solvent interaction increases with concentration, thermal conductivity is found to decrease which may be due to decrease in Brownian motion. In different alcohols, order of thermal conductivity is: methanol > ethanol > 1-propanol > 1-butanol > 1-pentanol i.e., it decreases with increase of CH_2 groups of alcohol.

The predominance of solute- solvent interactions in studied alcohols is further proved by the increases in viscosity with concentration which is shown in table 2. The experimental viscosity data have also been analyzed using the Jones-Dole equation [53]:

$$\frac{\eta}{\eta_0} = 1 + AC^{\frac{1}{2}} + BC \tag{11}$$

Where η and η_0 are the viscosity of solutions and pure solvents, respectively. C is the molar concentration of lacosamide. The parameters A and B are characteristic of solvents and lacosamide. The coefficient A represents the contribution from interionic electrostatic forces and is a measure of solute-solute interactions whereas B is an empirical parameter which gives information related to ion solvent interactions and structure factors [54]. The values of A and B parameters have been evaluated from the intercept and slope of plots of $(\eta/\eta_0 - 1)$. $C^{1/2}$ vs. $C^{1/2}$ and are reported in table 5. It is observed that A values are small and are negative for two alcohols whereas B values are positive and for some alcohols, it is larger as compared to other alcohols. However, no regular trend is observed for both A and B coefficients in selected alcohols. The smaller or negative A values proves that ion-ion interactions i.e. solute-solute interactions are weak in studied solutions whereas positive B coefficient indicates the presence of strong solute-solvent interactions [55] i.e., structure forming tendency of lacosamide [56]. Thus, evaluated acoustical parameters and Jones-Dole coefficients both confirm the structure forming tendency of lacosamide in studied alcohols.

Table 4. The least square equation and correlation coefficient γ (in parenthesis) for some evaluated parameters of lacosamide in different alcohols at 298.15 K.

Solvents	U (m·s^{-1})	Z (kg·m^{-2}·s^{-1})	$\varkappa_s$ (N·S·m^{-2})	L_f (m)
Methanol	101.0222C + 1,104.9462 (0.9992)	1.8197×10^5C + 8.7015×10^5 (0.9986)	-3.0543×10^{-10}C + 1.0400×10^{-9} (0.9989)	-1.0001×10^{-11}C + 6.7610×10^{-11} (0.9989)
Ethanol	67.3567C + 1,205.1713 (0.9960)	1.6515×10^5C + 9.7178×10^5 (0.9950)	-1.8953×10^{-10}C + 8.5382×10^{-10} (0.9947)	-6.8351×10^{-12}C + 6.1261×10^{-11} (0.9949)
1-Propanol	76.9181C + 1,206.4065 (0.9951)	1.6075×10^5C + 9.6551×10^5 (0.9967)	-1.9426×10^{-10}C + 8.5848×10^{-10} (0.9958)	-6.9876×10^{-12}C + 6.1428×10^{-11} (0.9960)
1-Butanol	47.4676C + 1,243.7822 (0.9977)	1.2461×10^5C + 1.0041×10^6 (0.9989)	-1.2827×10^{-10}C + 8.0073×10^{-10} (0.9990)	-4.7703×10^{-12}C + 0.9325×10^{-11} (0.9990)
1-Pentanol	47.7065C + 1,275.4316 (0.9984)	1.3079×10^5C +1.0352×10^6 (0.9988)	-1.2242×10^{-10}C + 7.5740×10^{-10} (0.9992)	-4.6814×10^{-12}C + 5.7698×10^{-11} (0.9992)

Solvents	R_m (m$^{10/3}$·s$^{-1/3}$·mol^{-1})	b (m^3·mol^{-1})	W	K_{bm} (W·K·m^{-1})	r
Methanol	8.5681×10^{-4}C + 4.2082×10^{-4} (0.9999)	2.3302×10^{-4}C + 5.7089×10^{-5} (0.9998)	1.6027×10^{-3}C + 7.8148×10^{-4} (1.0000)	-0.2938C + 0.2752 (0.9975)	-0.0876C + 0.5231 (0.9992)
Ethanol	7.6304×10^{-4}C + 6.0820×10^{-4} (1.0000)	2.8069×10^{-4}C + 1.1886×10^{-4} (0.9999)	1.4330×10^{-3}C + 1.1286×10^{-3} (1.0000)	-0.1668C + 0.2397 (0.9995)	-0.0636C + 0.4326 (0.9961)
1-Propanol	7.1335×10^{-4}C + 7.9944×10^{-4} (1.0000)	3.1209×10^{-4}C + 1.8759×10^{-4} (1.0000)	1.3408×10^{-3}C + 1.4818×10^{-3} (1.0000)	-0.0962C + 0.2001 (0.9998)	-0.0727C + 0.4315 (0.9952)
1-Butanol	6.4517×10^{-4}C + 9.8754×10^{-4} (1.0000)	3.2554×10^{-4}C + 2.7413×10^{-4} (1.0000)	1.2158×10^{-3}C + 1.8301×10^{-3} (1.0000)	-0.0665C + 0.1805 (0.9996)	-0.0462C + 0.395 (0.9977)
1-Pentanol	5.6854×10^{-4}C + 1.1780×10^{-4} (0.9999)	3.3106×10^{-4}C + 3.7394×10^{-4} (0.9999)	1.0779×10^{-3}C + 2.1821×10^{-3} (0.9999)	-0.0439C + 0.1655 (0.9998)	-0.0476C + 0.3646 (0.9985)

Table 5. Jones-Dole equation parameters *A* and *B* for lacosamide in alcohols.

Solvents	***A***	***B***
Methanol	0.175	5.556
Ethanol	-0.075	1.600
1-Propanol	0.285	0.471
1-Butanol	-0.009	1.073
1-Pentanol	0.100	0.629

Conclusions

In the solutions of drug lacosamide in studied alcohols, solute-solvent interactions dominate. These interactions increases from methanol to 1-pentanol i.e., interactions increase with increase in CH_2 group of alcohols. Thus, lacosamide exhibited structure forming tendency in studied alcohols due to predominance of solute- solvent interactions.

Disclosure statement

No potential conflict of interest was reported by the authors.

References

1. J. Lynn, R. Zwemer, A. Chick, A. Miller, A new method for the generation and use of focused ultrasound in experimental biology, *J. Gen. Physiol.*, **26**, 179-193 (1942).

2. P. Wells, Ultrasonics in medicine and biology, *J. Phys. Med. Biol.*, **22**, 629-669 (1977).

3. F. Fry, *Ultrasound: its applications in medicine and biology*, Elsevier, Amsterdam, 2013.

4. S. Nicholls, I. Sipahi, P. Schoenhagen, T. Crowe, T. Murat, S. Nissen, Biomarkers: Application of intravascular ultrasound in anti-atherosclerotic drug development, *Nature Rev. Drug Discov.*, **5**, 485-492 (2006).

5. J. Paulusse, R. Sijbesma, Ultrasound in polymer chemistry: revival of an established technique, *J. Polym. Sci. A: Poly. Chem.*, **44**, 5445-5453 (2006).

6. J. Kost, K. Leong, R. Langer, Ultrasound-enhanced polymer degradation and release of incorporated substances, *Proc. Nat. Acad. Sci.*, **86**, 7663-7666 (1989).

7. B. Han, X. Guan, J. Ou, Application of ultrasound for preparation of carbon fiber cement-based composites, *Mater. Sci. Tech.*, **17**, 368-372 (2009).

8. S. Riffat, M. Xiaoli, Thermoelectrics: a review of present and potential applications, *Appl. Thermal Eng.*, **23**, 913-935 (2003).

9. T.J. Mason, *Sonochemistry: The uses of ultrasound in chemistry*, Royal Society of Chemistry, London, 1990.

10. W. Lee, Y. Roh, Ultrasonic transducers for medical diagnostic imaging, *Biomed. Eng. Lett.*, **7**, 91-97 (2017).

11. K. Suslick, G. Price, Applications of ultrasound to materials chemistry, *Annu. Rev. Mater. Sci.*, **29**, 295-326 (1999).

12. H. Yang, W. Ding, K. Chen, Y. Ding, Application of ultrasonic technique in agricultureactuality and prospect, *J. Agric. Mech. Res.*, **1**, 365-370 (2004).

13. D. Aguerrevere, M. Choudhury, A. Barreto, *Portable 3D sound/sonar navigation system for blind individuals*, Second LACCEI International Latin American and Caribbean Conference for Engineering and Technology (LACCETí2004), Challenges and Opportunities for Engineering Education, Research and Development, Miami, Florida, USA, 2-4 June 2004.

14. S. Najafi, G. Ebrahimi, S. Behjati, Nondestructive evaluation of wood plastic composites using ultrasonic technique, *Dalam Proceeding Ceska Spolecnost Pro Nendestruktivni Zkouseni Material*, **38**, 87-94 (2008).

15. C. Leonelli, T. Mason, Microwave and ultrasonic processing: Now a realistic option for industry, *Chem. Eng. Process., Process Intensif.*, **49**, 885-900 (2010).

16. X. Zhang, Y. Guimond, Y. Bellec, Production of complex chalcogenide glass optics by molding for thermal imaging, *J. Non-Cryst. Sol.*, **326**, 519-523 (2003).

17. M. Yuehong, L. Jiangyun, L. Yingjie, Technology and application of water treatment by ultrasonic wave, *Ind. Water. Treat. -Tianjin*, **26**, 10-17 (2006).

18. T. Mahmood, A. Elliott, A review of secondary sludge reduction technologies for the pulp and paper industry, *Water Res.*, **40**, 2093-2112 (2006).

19. L. Ying, Z. Dezhi, Y. Qiuju, Research, development and application of ultrasound wave in petrochemical industry, *Petrochem. Tech.*, **2**, 17-23 (2005).

20. F.J. Gilbert, R.S. Campbell, A.P. Bayliss, The role of ultrasound in the detection of non-radiopaque foreign bodies, *Clin. Radiol.*, **41**, 109-112 (1990).

21. T. Mason, L. Paniwnyk, J. Lorimer, The uses of ultrasound in food technology, *Ultrason. Sonochem.*, **3**, S253-S260 (1996).

22. S. Muthukumaran, S. Kentish, G. Stevens, A. Muthupandian, R. Mawson, The application of ultrasound to dairy ultrafiltration: the influence of operating conditions, *J. Food Eng.*, **81**, 364-373 (2007).

23. A. Baltazar, L. Wang, B. Xie, S. Rokhlin, Inverse ultrasonic determination of imperfect interfaces and bulk properties of a layer between two solids, *J. Acoust. Soc. Amer.*, **114**, 1424-1434 (2003).

24. A.K. Dash, R. Paikaray, Molecular interaction studies in ternary liquid mixture of dimethylacetamide using ultrasonic technique at 308 K, *Phys. Chem. Liq.*, **53**, 230-241 (2014).

25. A. Ali, S. Hyder, A.K. Nain, Studies on molecular interactions in binary liquid mixtures by viscosity and ultrasonic velocity measurements at 303.15 K, *J. Mol. Liq.*, 79, 89-99 (1999).

26. V. Gupta, A.K. Sharma, M. Sharma, Ultrasonic investigation of molecular interaction in aqueous glycerol and aqueous ethylene glycol solution, *J. Chem. Pharm. Res.*, **6**, 714-720 (2014).

27. V. Kannappan, S.C. Vinayagam, Ultrasonic investigation of ion-solvent interactions in aqueous and non-aqueous solutions of transition and inner transition metal ions, *Indian J. Pure Appl. Phys.*, **44**, 670-676 (2006).

28. R. Bodmeier, J. McGinity, Solvent selection in the preparation of poly (DL-lactide) microspheres prepared by the solvent evaporation method, *Int. J. Pharm.*, **43**, 179-186 (1988).

29. J. Chung, M. Yokoyama, M. Yamato, T. Aoyagi, Y. Sakurai, T. Okano, Thermoresponsive drug delivery from polymeric micelles constructed using block copolymers of poly (*N*-isopropylacrylamide) and poly (butylmethacrylate), *J. Control. Rel.*, **62**, 115-127 (1999).

30. Y. Wang, K. Park, C. Salomé, S. Wilson, J. Stables, R. Liu, R. Khanna, H. Kohn, Development and characterization of novel derivatives of the antiepileptic drug lacosamide that exhibit far greater enhancement in slow inactivation of voltage-gated sodium channels, *ACS Chem. Neurosci.*, **2**, 90-106 (2010).

31. A. Rapacz, J. Obniska, P. Koczurkiewicz, K. Wójcik-Pszczoła, A. Siwek, A. Gryboś, S. Rybka, A. Karcz, E. Pękala, B. Filipek, Antiallodynic and antihyperalgesic activity of new 3,3-diphenyl-propionamides with anticonvulsant activity in models of pain in mice, *Eur. J. Pharmacol.*, **821**, 39-48 (2018).

32. D. Holtkamp, T. Opitz, I. Niespodziany, C. Wolff, H. Beck, Activity of the anticonvulsant lacosamide in experimental and human epilepsy via selective effects on slow Na^+ channel inactivation, *Epilepsia*, **58**, 27-41 (2017).

33. B. Beyreuther, J. Freitag, C. Heers, N. Krebsfänger, U. Scharfenecker, T. Stöhr, Lacosamide: a review of preclinical properties, *CNS Drug Rev.*, **13**, 21-42 (2007).

34. A. LeTiran, J.P. Stables, H. Kohn, Functionalized amino acid anticonvulsants: synthesis and pharmacological evaluation of conformationally restricted analogues, *Biorg. Med. Chem.*, **9**, 2693-2708 (2001).

35. R. Naik, S. Bawankar, S. Kukade, Acoustical studies of molecular interaction in the solution of propranolol hydrochloride drug at different temperatures and concentrations, *Russ. J. Phys. Chem.*, **89**, 2149-2154 (2015).

36. R. Naik, S. Bawankar, V. Ghodki, Acoustical studies of molecular interactions in the solution of anti-malarial drug, *J. Polym. Biopolym. Phys. Chem.*, **3**, 1-5 (2015).

37. S. Baluja, A. Solanki, N. Kachhadia, An ultrasonic study of some drugs in solutions, *Russ. J. Phys. Chem.*, **81**, 742-746 (2007).

38. H.C. Swaisland, M. Ranson, R.P. Smith, J. Leadbetter, A. Laight, D. McKillop, M.J. Wild, Pharmacokinetic drug interactions of gefitinib with rifampicin, itraconazole and metoprolol, *Clin. Pharmacokinet.*, **44**, 1067-1081 (2005).

39. B. González, A. Domínguez, J. Tojo, Dynamic viscosities, densities, and speed of sound and derived properties of the binary systems acetic acid with water, methanol, ethanol, ethyl acetate and methyl acetate at T=(293.15, 298.15, and 303.15) K at atmospheric pressure, *J. Chem. Eng. Data*, **49**, 1590-1596 (2004).

40. G.W. Willard, Temperature coefficient of ultrasonic velocity in solutions, *J. Acoust. Soc. Amer.*, **19**, 235-241 (1947).

41. J. Canosa, A. Rodriguez, J. Tojo, Dynamic viscosities of (methyl acetate or methanol) with (ethanol, 1-propanol, 2-propanol, 1-butanol, and 2-butanol) at 298.15 K, *J. Chem. Eng. Data*, **43**, 417-421 (1998).

42. U.B. Kadam, A.P. Hiray, A.B. Sawant, M. Hasan, Densities, viscosities, and ultrasonic velocity studies of binary mixtures of trichloromethane with methanol, ethanol, propan-1-ol, and butan-1-ol at T=(298.15 and 308.15) K, *J. Chem. Thermodyn.*, **38**, 1675-1683 (2006).

43. S.S. Bittencourt, H.E. Hoga, R.B. Torres, J.V.H. d'Angelo, Thermodynamic and spectroscopic properties of binary mixtures of n-butylammonium butanoate ionic liquid with alcohols at T=(293.15–313.15) K, *J. Chem. Thermodyn.*, **105**, 238-252 (2017).

44. K. Anil-Kumar, C.H. Srinivasu, K.T.S.S. Raju, Theoretical evaluation of ultrasonic velocity in 1,4-dioxane with 1-butanol at temperatures range 298.15-318.15 K, *Int. J. Pharm. Chem. Sci.*, **2**, 1993-1996 (2013).

45. M. Hasan, A.P. Hiray, U.B. Kadam, D.F. Shirude, K.J. Kurhe, A.B. Sawant, Densities, viscosities, speeds of sound, FT-IR and 1 H-NMR studies of binary mixtures of n-butyl acetate with ethanol, propan-1-ol, butan-1-ol and pentan-1-ol at 298.15, 303.15, 308.15 and 313.15 K, *J. Solution Chem.*, **40**, 415-429 (2011).

46. H. Kumar, S. Sharma, Acoustical studies of binary liquid mixtures of cyclopentane with 1-alkanol at different temperatures and different approaches for ideal mixing laws, *J. Solution Chem.*, **39**, 967-986 (2010).

47. X. Wang, X. Wang, B. Song, Densities and viscosities of binary mixtures of 2, 2, 4-trimethylpentane + 1-propanol, + 1-pentanol, + 1-hexanol, and + 1-heptanol from (298.15 to 323.15) K, *J. Chem. Eng. Data*, **60**, 1664-1673 (2015).

48. V. Gibbs, D. Cole, A. Sassano, *Ultrasound Physics and Technology: How, Why and When, Elsevier*, Amsterdam, 2009, p. 21-23.

49. M. Roy, V. Dakua, B. Sinha, Partial molar volumes, viscosity B-coefficients, and adiabatic compressibilities of sodium molybdate in aqueous 1, 3-dioxolane mixtures from 303.15 to 323.15 K, *Int. J. Thermophys.*, **28**, 1275-1284 (2007).

50. S. Oswal, P. Oswal, R. Phalak, Speed of sound, isentropic compressibilities, and excess molar volumes of binary mixtures containing p-dioxane, *J. Solution Chem.*, **27**, 507-520 (1998).

51. M. Rashin, J. Hemalatha, A novel ultrasonic approach to determine thermal conductivity in CuO–ethylene glycol nanofluids, *J. Mol. Liq.*, **197**, 257-262 (2014).

52. S. Kant, D. Singh, S. Kumar, Molar volume and ultrasonic studies of some alkaline earth metal chlorides in water + NaCl + fructose system, *Arch. Appl. Sci. Res.*, **3**, 70-84 (2011).

53. G. Jones, M. Dole, The viscosity of aqueous solutions of strong electrolytes with special reference to barium chloride, *J. Am. Chem. Soc.*, **51**, 2950-2964 (1929).

54. H. Shekaari, M. Taghi, N. Seyyedeh, Density, viscosity, speed of sound, and refractive index of a ternary solution of aspirin, 1-butyl-3-methylimidazolium bromide, and acetonitrile at different temperatures *T*=(288.15 to 318.15 K), *J. Chem. Eng. Data*, **60**, 1572-1583 (2015).

55. Y. Litaiem, M. Dhahbi, Physicochemical properties of hydrophobic ionic liquid (Aliquat 336) in polar protic solvent (Formamide) at different temperatures, *J. Dispers. Sci. Tech.*, **36**, 641-651 (2013).

56. Z. Hai-Lang, H. Shi-Jun, Viscosity and density of water + sodium chloride + potassium chloride solutions at 298.15 K, *J. Chem. Eng. Data*, **41**, 516-520 (1996).

How to cite this article

Sh. Baluja, S. Oza, D. Lava, R. Pampaniya, Ultrasonic investigation of lacosamide in various alcohols at 298.15 K, *Rev. Colomb. Cienc. Quím. Farm.*, **49**(3), 720-739 (2020).

Artículo de investigación clínica / *http://dx.doi.org/10.15446/rcciquifa.v49n3.XXXXX*

Principales enfermedades según el grupo sanguíneo en población mayor de 60 años en provincia de Cuenca (España)

Ma. Carmen Batanero-Hernán[1]*, Begoña Escalera Izquierdo[2], María José Fresno Contreras[3], Miguel Angel Rodríguez-Chamorro[4]

[1]Doctora en Farmacia, Farmacéutica Comunitaria en Guadalajara, España.

[2]Profesoras titulares, Departamento de Ciencias Biomédicas, Universidad de Alcalá, carretera Madrid-Barcelona km 33,6, Alcalá de Henares, España.

[3]Doctor en Farmacia, Farmacéutico Comunitario en Talavera de la Reina, Toledo, España.

*Autora para correspondencia: cabaher@live.com

Recibido: 20 de junio de 2020

Revisado: 17 de julio de 2020

Aceptado: 20 de julio 2020

Resumen

Objetivo: conocer la prevalencia de enfermedades según el grupo sanguíneo de la población estudiada en la provincia de Cuenca (España). *Métodos*: estudio observacional, descriptivo, corte transversal y base poblacional. La muestra de 73 personas (39 varones, 34 mujeres), mayores de 60 años. Se identificaron todos los grupos sanguíneos, estudiándolos por edad y género. *Resultados*: los porcentajes de grupos sanguíneos de la población estudiada por género son 42,6% (grupo A); 42,4% (O); 13% (B) y 1,4% (AB). Predomina el A+ (35,6%), seguido del O+ (27,4%). Se estudia la prevalencia de una determinada enfermedad en función del grupo sanguíneo. En este sentido, se detectan diferencias dentro de un mismo grupo, según el fator Rh. Los grupos Rh positivos padecen más de HTA, insomnio y depresión que los Rh negativos. Los grupos A y O padecen mayor aumento de colesterol que los del grupo B. Los del grupo O tienen más HTA que el resto y el O+ padece mayor porcentaje de anemia (Fe), mientras que los A+ anemia (B12). La osteoporosis es mayor en los grupos negativos que en los positivos, salvo en el grupo AB+. *Conclusiones*: el grupo sanguíneo con el que nacemos puede condicionar las enfermedades que padeceremos a lo largo de nuestra vida. El ser 0 podría predisponerlos a tener HTA, anemia (Fe), colesterol, enfermedades pulmonares e insomnio, mientras que el A depresión, anemia (B12) y problemas de próstata en varones.

Palabras clave: Grupo sanguíneo, enfermedades, población mayor de 60 años.

Summary

Main diseases according to blood group in population over 60 years of age in the province of Cuenca (Spain)

Objective: To know the prevalence of diseases according to the blood group of the population studied in the province of Cuenca (Spain). *Methods*: An observational, descriptive, cross-sectional, and population-based study. The sample is 73 people (39 men and 34 women), over 60 years. All blood groups were identified, studying them by age and gender. *Results*: The percentages of blood groups of the population studied by gender are 42.6% (group A), 42.4% (O), 13% (B) and 1.4% (AB). A+ predominates (35.6%), followed by O+ (27.4%).The prevalence of a certain disease based on blood group is studied. In this sense, differences are detected within the same group, according to the Rh factor. Rh positive groups suffer more from hypertension, insomnia and depression than Rh negative groups. Groups A and 0 O suffer a greater increase in cholesterol than those of group B. Those in group 0 O have more hypertension than the rest and the 0O + suffer a higher percentage of anemia (Fe), while those A + anemia (B12). Osteoporosis is greater in the negative groups than in the positive ones, except in the AB + group. *Conclusions*: The blood group with which we are born can condition the diseases that we will suffer throughout our lives. Being 0 could predispose them to have hypertension, anemia (Fe), cholesterol, lung diseases and insomnia, while A could predispose them to have depression, anemia (B12) and prostate problems in men.

Keywords: Blood group, diseases, population over 60.

Introducción

Karl Landsteiner investigó la genética de la sangre humana, respecto la de los simios [1, 2]. Observó que, al mezclar la sangre de dos personas, a veces, los glóbulos rojos se aglutinaban formando grumos visibles. Analizó la sangre de 22 personas, incluyendo la suya. Separó el suero de la sangre total, lavó los glóbulos rojos y los sumergió en una solución de suero salino fisiológico. Después, ensayó cada suero con los diferentes glóbulos rojos obtenidos y observó los resultados. Descubrió tres tipos distintos de hematíes, denominados A, B y O, que generaban reacciones de aglutinación. Dos años después, dos discípulos suyos analizaron 155 muestras y descubrieron un cuarto grupo, al que llamaron AB.

La sangre humana posee anticuerpos que reaccionan con los antígenos de los glóbulos rojos, produciendo, como resultado de la interacción antígeno-anticuerpo, su aglutinación. Estos anticuerpos (que no existen en el tipo AB) son responsables de la incompatibilidad de las transfusiones sanguíneas. En 1911, Ottenberg acuñó el término *donante universal* para el grupo O, por carecer de antígenos en los eritrocitos [3]. En 1908, Epstein y Ottenberg sugieren que los grupos sanguíneos son hereditarios. En 1910, E. von Dungern y L. Hirszfeld descubrieron que la herencia de estos grupos sanguíneos sigue las leyes de Mendel, con un patrón dominante para los tipos A y B [4].

En 1940, Landsteiner y Alexander Wiener, descubrieron otro antígeno en los hematíes al que llamaron factor Rh, por haberse hallado en el suero de conejos inmunizados con sangre procedente de un mono de la India, el macaco Rhesus (*Macaca mulatta*). Un niño que tiene el factor Rh es Rh+ y puede inmunizar a su madre Rh- durante la gestación [5-7]; esta desarrolla anticuerpos específicos anti-Rh que podrían, en su segundo embarazo, atravesar la placenta y producir el aborto o una enfermedad hemolítica en el recién nacido.

Por tanto, el grupo sanguíneo es una clasificación de la sangre según los antígenos que están en la superficie de los glóbulos rojos y en la sangre, se definen por el sistema ABO y por el Rh. Existen cuatro tipos de grupos sanguíneos: A (con antígenos A), B (con antígenos B), O (sin ningún antígeno y todas las aglutininas o anticuerpos) y AB (con los antígenos A y B y sin ninguna aglutinina).

Los Rh positivos son aquellas personas que presentan dicha proteína en sus glóbulos rojos, y negativos quienes no presenten la proteína. Un 85% de la población tiene en esa proteína una estructura dominante. Tener Rh- significa que se tiene la misma proteína, pero con modificaciones en ciertos aminoácidos que determinan diferencias significativas en la superficie de los glóbulos rojos, y disponer de anticuerpos en el plasma que reaccionan contra los glóbulos rojos Rh+ [7].

El principal antígeno Rh es el D y el anticuerpo presente en quienes carecen de antígeno D es el anti-D. Si el antígeno D está presente el fenotipo es Rh positivo y si D está ausente (situación representada como "d") es Rh negativo. Se han identificado más de 45 antígenos del sistema Rh, pero de todos ellos apenas cinco son frecuentes, son: D, C, E, c, e. Los anticuerpos a los distintos antígenos Rh aparecen después de exponerse un individuo Rh negativo a eritrocitos de sangre Rh positivo. La herencia de los antígenos Rh está determinada por un complejo de dos genes, de los cuales uno codifica la proteína transportadora de antígeno D y otro codifica la proteína transportadora de antígeno «C» o «c», o de «E» y «e». Las personas Rh positivo poseen genes RHD, que codifica la proteína transportadora de antígeno D y RHCE, que codifica la

especificidad de la proteína transportadora de C y E. Mientras las personas Rh negativo tienen únicamente el gen RHCE.

La transfusión de sangre de un Rh+ a un Rh- que no tiene dicho aglutinógeno induce la formación de anticuerpos, que en sucesivas donaciones puede aglutinar la sangre (formar coágulos) [7]. De ahí su importancia en las donaciones. Al ser dominante el gen +, se considera positivo + +, + – y – + mientras que será negativo si tiene los dos alelos – – (es recesivo).

La distribución mundial de los grupos sanguíneos varía en función de la raza [8] (tabla 1). Por lo anteriormente expuesto, en este trabajo, se pretende observar si existe relación entre tener un grupo sanguíneo determinado y padecer ciertas enfermedades o no, dado que no se ha encontrado ningún artículo que relacione dichos grupos con las principales patologías padecidas.

Tabla 1. Distribución mundial de los grupos sanguíneos en función de la raza.

Grupo sanguíneo	Raza o etnia			
	Caucásica	Afroamericana	Hispana	Asiática
O +	37%	47%	53%	39%
O-	8%	4%	4%	1%
A +	33%	24%	29%	27%
A-	7%	2%	2%	0.5%
B +	9%	18%	9%	25%
B-	2%	1%	1%	0.4%
AB+	3%	4%	2%	7%
AB-	1%	0,3%	0,2%	0.1%

Metodología

Es un estudio observacional, descriptivo, de corte transversal. Se elaboró una encuesta farmacoterapéutica especificando todos los medicamentos consumidos, así se han conocido los tratamientos y enfermedades que padecía cada paciente, dado que no se tiene acceso a la historia médica. Este estudio se ha realizado en Buendía (Cuenca), recogiendo datos de pacientes durante 2017 y 2018, previa firma del consentimiento informado (anexo 1).

La población diana fueron todas las personas de 60 años o mayores, varones o mujeres, que residían en sus casas y acudían a la farmacia o en la residencia de ancianos ubicada en la localidad y que voluntariamente decidieron participar en este trabajo. Para ello se les citó individualmente y se rellenó la encuesta farmacoterapéutica realizada a*d hoc*. La medicación fue obtenida a partir de la historia farmacoterapéutica. También se les hizo el análisis del grupo sanguíneo y Rh mediante los reactivos Cromatest®. El cálculo del tamaño muestral se estimó en 73 pacientes.

Las variables dependientes utilizadas fueron el porcentaje de consumo de medicamentos (respecto al total de los consumidos por esta población estudiada) usando la clasificación ATC *(Anatomical Therapeutic Chemical Classification)* para la codificación de estos medicamentos. Las variables independientes fueron, entre las referidas al paciente, el género (variable nominal dicotómica varón/mujer) y la edad (variable cuantitativa continúa estratificada en cuatro tramos de edad: 60-70 años, 71-80 años, 8-90 y pacientes mayores de 91 años. Se ha querido estratificar así para visualizar qué tramo consume más medicamentos de un grupo ATC u otro.

Tamaño de la muestra

La población mayor de 65 años estimada en el pueblo de Buendia (Cuenca) en 2017 era de 417 habitantes, de ellos el 90% son mayores de 60 años (INE, 2017), para este tamaño de población el cálculo del tamaño muestral se estima de acuerdo a la fórmula:

$$n = \frac{z^2}{e^2}.p.q$$

Donde:

n = tamaño de la muestra, z = valor de z correspondiente al nivel de confianza (95%, que también se expresa así: α = 0,05, y que corresponde a z = 1,96 sigmas o errores típicos), p y q = varianza de la población, que indican la proporción esperada de pacientes que consume o que no consume preparados de plantas medicinales; consideramos la máxima diversidad posible, es decir el 50%, p.q = 0,25, p = la proporción esperada en la población (en este caso, al ser dicotómico, o sea dos respuestas que se excluyen mutuamente, es el 50% de síes), e= el error, que suponemos un 5%, o sea es 0,05. El resultado fue de 73 pacientes.

Definición de las variables

Variables dependientes

- Porcentaje de grupos sanguíneos: consiste en calcular cuántos pacientes de cada cien pertenece a cada uno de los grupos sanguíneos y RH existentes.

- Porcentaje de consumo de medicamentos: se usa la clasificación ATC. Se calculan cuántos pacientes de cada cien consume algún medicamento de cada grupo terapéutico siguiendo la clasificación ATC.

Variables independientes

Hay dos variantes relacionadas con el paciente: género y edad. El género es una variable nominal dicotómica (varón / mujer). La edades una variable cuantitativa continúa estratificada en cuatro tramos de edad: 60-70 años, 71-80, 81-90 y pacientes mayores de 91 años.

Análisis de los datos

En este trabajo se utilizó la estadística con los parámetros más representativos: porcentajes, intervalos de confianza 95%, riesgo relativo, Odds Ratio y p-valor. La información obtenida se ingresó en una base de datos utilizando el programa Microsoft Excel. El análisis estadístico de tipo descriptivo se llevó a cabo utilizando este mismo programa, expresando los resultados en forma porcentual y promedio. Las variables recogidas se analizaron tomando como referencia el número de pacientes incluidos en el estudio. Las variables cualitativas se describieron mediante el cálculo de frecuencias y porcentajes. Se calculó el porcentaje de enfermedades según el grupo sanguíneo por género y por tramos de edad. Igualmente se calculó el consumo de medicamentos de cada grupo ATC. También se estimó la frecuencia relativa del consumo de los fármacos de cada grupo y subgrupo ATC, así como la relación existente entre grupo sanguíneo y medicamentos. Para identificar posibles relaciones grupo sanguíneo-enfermedades se ha hecho un estudio con las variables independientes, un análisis bivariante. En todos los análisis se consideró significativo todo valor de $p \leq 0,05$, Odds Ratio (OR) superior a la unidad, IC 95% que no contenga la unidad y un riesgo relativo (RR) también superior a uno.

Resultados

La caracterización de la muestra se incluye en la tabla 2, en esta se detalla población por tramos de edad, género y residencia. Hay 39 varones y 34 mujeres divididos en cuatro tramos de edad. Se consumieron 629 medicamentos, que equivale a 8,6 medicamentos/ paciente y día.

Tabla 2. Caracterización de la población por género y tramos de edad.

Género y edad	Grupo sanguíneo						
	A+	O+	O-	B-	A--	B+	AB+
Varones	17	14	2	4	1	1	0
Mujeres	9	6	9	4	4	1	1
Total	26	20	11	8	5	2	1
55-60	0	0	0	3	0	0	0
61-65	2	0	0	0	0	0	0
66-70	0	1	0	0	0	0	0
71-75	2	1	0	0	0	0	0
76-80	6	3	4	0	0	1	0
81-85	7	2	4	2	3	1	0
86-90	8	6	2	2	1	0	1
91-95	1	6	0	1	0	0	0
96-100	0	1	1	0	1	0	0

Los grupos sanguíneos de la población estudiada según tabla 3 establecen porcentajes del 42,6% del grupo A; 42,4% del O; 13% del B y 1,4% del AB. El grupo predominante es el A+ con un 35,6%, seguido del O+ con 27,4%. En la tabla 2 se muestra la distribución por edades en la población estudiada.

Tabla 3. Porcentaje de los distintos grupos sanguíneos en la población estudiada.

Grupo sanguíneo	%
A	42,6
O	42,4
B	13
AB	1,4

Los porcentajes de las enfermedades más prevalentes según el grupo sanguíneo se observan en la tabla 4. Los pacientes A+ respecto a A-- tienen mayor prevalencia de enfermedad tiroidea, próstata, HTA, falta de B12 y Alzhéimer, mientras que los A-- tienen anemia (Fe), enfermedades pulmonares y osteoporosis. Los O+ respecto O- tienen más anemia (Fe) y depresión, mientras que los negativos tienen más problemas circulatorios. Los B+ padecen mayor HTA, anemia (Fe), depresión y enfermedades

pulmonares que los B-, estos últimos también tienden a enfermarse más de diabetes y osteoporosis.

Tabla 4. Relación grupos sanguíneos y enfermedades más frecuentes (en %).

Enfermedad o condición	Grupo sanguíneo						
	A+	O+	O-	B-	A--	B+	AB+
Tiroides	4	15	0	0	0	0	0
Insomnio	50	65	63	25	20	100	0
Hipertensión	77	70	72	12	100	50	100
Déficit de hierro	15	35	27	0	60	50	0
Estreñimiento	30	35	36	100	80	0	100
Déficit de B12	50	20	10	100	20	0	0
Alzheimer	4	20	27	100	20	0	0
Circulación	15	15	54	100	20	50	100
Depresión	40	30	0	0	0	100	100
Glaucoma	4	0	0	0	0	0	0
Próstata	30	15	0	0	0	0	0
Epilepsia	4	0	0	0	0	0	0
Parkinson	4	5	27	0	0	0	0
Gota	0	15	0	0	20	0	0
Diabetes	15	0	27	38	0	0	100
Pulmón	27	35	36	50	80	100	0
Colesterol	40	35	72	100	80	0	0
Alergia	4	5	27	0	0	0	100
Osteoporosis	4	5	9	38	60	0	100
Cálculos	4	5	0	0	0	0	0

En la tabla 4 se observa que los grupos A y O padecen mayor aumento de colesterol que los del grupo B.

Los del grupo O presentó mayor porcentaje de enfermedad tiroidea (0,15), insomnio (0,65) anemia (Fe) (0,35), Alzhéimer (0,2), gota (0,15) y enfermedad pulmonar (0,35), mientras que los A+ presentaron anemia (B12) (0,6 casi el triple que el 0), depresión (0,4), colesterol (0,4), glaucoma (0,04), próstata (0,3) y diabetes (0,15); los grupos O y

A tienen porcentajes similares de HTA, Parkinson, alergia, osteoporosis, cálculos renales y problemas circulatorios. Los grupos B y AB no se tienen en cuenta, dado que el porcentaje existente en la población estudiada es bajo.

En general los grupos Rh positivo padecen mayor HTA, insomnio y depresión que los Rh- (tabla 5). Se observa que los grupos A y O padecen mayor aumento de colesterol que los del grupo B. Los del grupo O tienen más HTA que el resto y el O+ padece mayor porcentaje de anemia (Fe), mientras que los A+, anemia (B12). Respecto a osteoporosis es mayor en los grupos negativos que en los positivos (tablas 6 y 7).

Tabla 5. Relación Rh y enfermedades más frecuentes.

Enfermedad o condición	Rh	
	+	–
Tiroides	19	0
Insomnio	100	95
Hipertensión	100	100
Déficit de hierro	50	87
Estreñimiento	65	100
Déficit de B12	70	41
Alzheimer	24	59
Circulación	30	86
Depresión	70	20
Glaucoma	4	0
Próstata	45	0
Epilepsia	4	0
Parkinson	9	27
Gota	15	20
Diabetes	1	6

En cuanto al estudio estadístico de todas estas asociaciones (tabla 7) se observa:

- **Grupo A/colesterol:** el valor de Odds Ratio es 0,283, inferior a 1, el riesgo relativo es superior a 1, por tanto los pacientes del grupo A son más propensos a padecer colesterol, el IC 95% no comprende en su intervalo la unidad lo que nos sugiere que no existe una independencia de las hipótesis y p-valor no es significativo ($p<0,05$), por tanto podemos concluir a la vista de estos resultados (que no son hechos independientes) existe una relación directa no debida al azar.

Tabla 6. Grupos sanguíneos y porcentaje de osteoporosis en mujeres.

Grupo sanguíneo	Osteoporosis en mujeres
A+	0,36
O+	0,3
O-	0,81
B-	1,52
A--	2,4
B+	0
AB+	1

Tabla 7. Tablas estadísticas.

Grupo/factor	Odds Ratio	Riesgo relativo	IC 95%	p-valor
Grupo A/colesterol	0,283	3,536	1,1328-11,0374	p<0,05
Grupo O/colesterol	0,91	1,0958	0,3973-3,0225	p=0,8
Grupo B/colesterol	7,676	0,1303	0,0156-1,0903	p<0,05
Grupo O/HTA	0,912	1,0958	0,3973-3,0225	p=0,8
Grupo A/HTA	0,283	3,536	1,1328-11,0374	p<0,05
Grupo O/hierro	0,494	2,0238	0,6892-5,9426	p=0,2
Grupo A/hierro	1,265	0,822	0,2771-2,4380	p=0,7
Grupo A/B12	0,202	4,9412	1,6173-15,0964	p<001
Grupo O/B12	2,889	0,3462	0,1100-1,0894	p<0,05
Rh+/HTA	0,602	1,6615	0,5863-4,7089	p=0,3
Rh--/HTA	1,661	0,6019	0,2124-1,7057	p=0,3
Rh+/osteoporosis	6,314	0,1584	0,0367-0,6837	p<001
Rh--/osteoporosis	1,433	0,6977	0,1769-2,7508	p= 0,6

- **Grupo 0/colesterol:**la razón de momios es muy próxima a la unidad indica que no hay asociación entre ambas variables. Respecto al riesgo relativo es mayor que 1, hay una relación entre grupo O y tener elevado el colesterol, el IC 95% contiene la unidad nos sugiere independencia de las hipótesis y p-valor no es significativo (p = 0,8), no se confirma, se deja para posteriores estudios.

- **Grupo B/colesterol:** el valor de Odds Ratio es 7,676, superior a 1, el riesgo relativo no lo es, por tanto sugiere que no existe asociación positiva, el IC 95% contiene la unidad nos sugiere independencia de las hipótesis y p-valor sí es significativo ($p < 0,05$), por tanto, podemos concluir a la vista de estos resultados que esto no se confirma.

- **Grupo 0/HTA:** respecto a Odds Ratio está próximo a la unidad indicando que no hay asociación entre ambas variables, riesgo relativo es mayor que 1, hay una relación entre grupo O y tener hipertensión. El intervalo de confianza 95% contiene la unidad, nos sugiere hipótesis no relacionadas y el p-valor no es significativo.

- **Grupo A/HTA:** OR es inferior a 1, lo que indica acción protectora, riesgo relativo es mayor que 1, hay una relación entre grupo A y tener elevado el hipertensión, el IC 95% no contiene la unidad, esto nos sugiere que la relación entre las hipótesis y p-valor sí es significativa $p < 0,05$, por tanto, existe una relación directa no debida al azar.

- **Grupo 0/hierro:** OR es inferior a 1, riesgo relativo es mayor que 1, hay una relación entre grupo O y tener déficit de hierro, el IC 95% contiene la unidad, esto nos sugiere independencia entre las hipótesis y p-valor no es significativo, por tanto, con estos resultados, no se confirma.

- **Grupo A/hierro:** OR es superior a 1, lo que nos indica que existe asociación entre las hipótesis. El RR es inferior a 1 indicando que no hay relación entre ser del grupo A y padecer déficit de hierro, el IC 95% contiene la unidad, esto nos sugiere independencia entre las hipótesis y p-valor no es significativo, por tanto, con estos resultados, no se confirma.

- **Grupo A/B12:** OR es inferior a 1, riesgo relativo es mayor que 1, hay una relación entre grupo A y tener déficit de cianocobalamina, el IC 95% no contiene la unidad, esto nos sugiere que larelación entre las hipótesis y p-valor es significativa, por tanto, con estos resultados, concluimos diciendo que no son hechos independientes, sino que existe una relación directa no debida al azar.

- **Grupo 0/B12:** OR es superior a la unidad lo que nos indica que hay una relación 2,289 a 1 de personas que, siendo del grupo O tienen déficit de vitamina B12. El IC 95% contiene la unidad, esto nos sugiere independencia entre las hipótesis y p-valor no es significativo, por tanto, con estos resultados, no se confirma.

- **Rh +/HTA:** OR es inferior a 1, IC 95% comprende la unidad y p-valor no es significativo, el RR es 1,665 lo cual indica que hay una relación entre tener Rh+ y padecer hipertensión, pero con estos resultados que no se confirma.

- **Rh -/HTA:** OR es superior a 1, esto sugiere que hay una relación de 1,661 a 1 de personas que, siendo Rh negativo padecen hipertensión. El resto de parámetros RR, IC 95% y p-valor no confirman esta hipótesis.
- **Rh +/osteoporosis:** tiene un OR de 6,314, un IC 95% que no comprende la unidad y p-valor significativo ($p<0,01$), por tanto, se concluye diciendo que no son hechos independientes, porque no existe una relación directa.
- **Rh -/osteoporosis:** OR superior a 1 y un RR también superior a 1, hay una relación entre tener Rh negativo y padecer osteoporosis, pero no se ve confirmado por IC 95% ni por p-valor.

Discusión

Uno de los principales factores relacionado con la obesidad es la alimentación, que influye de un 30% a un 60% en el desarrollo de este padecimiento, y a pesar de que se han hecho intervenciones en la cuestión de los hábitos de alimentación, se ha observado que no tienen un impacto importante porque no se sigue con una alimentación saludable con el paso del tiempo [9-11]. Estudios realizados en EEUU mencionan una relación potencial entre el tipo de alimentación y grupo sanguíneo. Varios estudios indican que las personas con tipo de sangre O prefieren comidas ricas en carnes rojas. En personas con el tipo de sangre A, la dieta óptima y recomendada son verduras y carnes blancas. En el grupo sanguíneo B tienden a preferir alimentos como frutas, verduras y alimentos marinos (pescados y marisco). Por último, en el grupo sanguíneo A" es una combinación entre los alimentos recomendado en los dos grupos sanguíneos anteriores [12-14]. Debido a los antecedentes evolutivos de cada grupo sanguíneo, las proteínas de su sangre los hacen compatibles con determinados alimentos o incompatibles con otros.

El grupo O al carecer del antígenos A, B y H es "especial". Poseer este grupo sanguíneo predispone a padecer úlcera estomacal, sin embargo, tienen un 23% menos de probabilidad de enfermedad cardiaca [15] respecto a los AB y B (al inflamarse más fácilmente).

Respecto al cáncer de páncreas el grupo O tiene un 50-70% menos riesgo de padecerlo [16]. Las personas con sangre tipo O también tienen mayor riesgo de ataque cardiaco o dolor torácico y de hematomas, pero menos de trombosis. El grupo O– tiene mayor predisposición a enfermedades autoinmunes degenerativas, siendo más vulnerables a las enfermedades en general, por tener Rh-.

El grupo AB presenta mayores dificultades de memoria, lenguaje y atención (82% respecto al resto de grupos), y un 26% tiende a padecer cáncer de estómago, es decir, un

20% más que los grupos B o O [15, 16] debido a que 2/3 de la población mundial poseen *Helicobacter pylori*, pero que se activa en los grupos A y AB.

Una investigación presentada en el *IV Congreso Mundial sobre Insuficiencia Cardiaca Aguda* [17] concluyó, tras analizar **más de un millón de personas**, que aquellas con sangre tipo A, B o AB eran más propensas a sufrir **dolencia cardiovascular**, como un infarto, que aquellas con grupo sanguíneo tipo O. Aunque el estudio no determinó claramente qué factores hacían a esas personas más propensas a una dolencia del corazón, los científicos apuntan a que podría deberse a una mayor concentración de la proteína **factor de von Willebrand**. Esta proteína favorece el **desarrollo de coágulos**, lo que eleva el riesgo de ataques cardíacos.

También explican que las personas con sangre distinta a O son más propensas a **niveles de colesterol altos.** El de menor riesgo en estudios genéticos es el O. Otro estudio [17] identificó múltiples factores de riesgo, como la recurrencia de trombosis venosa profunda (TVP), el aumento de los niveles de factor VIII (FVIII) y de biomarcadores plasmáticos de inflamación, como la molécula de adhesión molecular 1 (MAC-1) y la persistencia de la obstrucción venosa que están asociados con los grupos sanguíneos distintos de O que, además, aumentan el riesgo de aparición del SPT (síndrome postrombótico).

Hasta el momento, no se conoce ningún estudio que haya tenido en cuenta la posible asociación entre los grupos sanguíneos distintos al O y la aparición del síndrome postrombótico (SPT). Los antígenos ABO influyen sobre la hemostasia, principalmente a través del aumento de los niveles del factor de Von Willebrand (VWF) y FVIII, esta sería una explicación adicional para comprender de qué manera se conjugan estos 3 factores para producir un mayor riesgo en el desarrollo del episodio tromboembólico venoso. Además, los estudios previos mostraron que los pacientes con grupo sanguíneo noO tienen mayor riesgo de recurrencia de TVP (trombosis venosa profunda).

Un estudio reciente [18], realizado en China, con más de 2000 participantes, encontró que las personas con grupo A pueden ser más vulnerables al coronavirus, con mayor tasa de infección y síntomas más graves, por ende necesita mayor protección personal, según los investigadores dirigidos por Wang Xinghuan del Centro de Medicina Basada en la Evidencia y el Hospital Zhongnan de la Universidad de Wuhan, mientras que aquellos que tienen el grupo O son hasta un 20% más resistentes, según un artículo que publicaron en Medrxiv.org el 11 de marzo [18], de los 206 pacientes fallecidos en Wuhan por Covid-19, 85 pertenecían al grupo A, es un el 63% más que los que tenían tipo O, que eran 52 pacientes. Este patrón se repetía en distintos grupos de edad y género.

De otro lado, se sabe que el factor Rh determina la resistencia a la enfermedad [19], "Las personas con factor Rh- son mucho más vulnerables a las enfermedades". En cuanto a los individuos Rh+ se puso en evidencia que los heterocigotos, es decir, los que heredaron de sus progenitores un factor positivo y otro negativo, son mucho más resistentes y caen enfermos con una frecuencia mucho menor", esto corrobora nuestros resultados, dado que los pacientes Rh- poseen mayor porcentaje de padecer HTA, déficit de hierro, estreñimiento, Alzheimer, problemas circulatorios, Parkinson, gota, diabetes, enfermedades pulmonares, colesterol, alergias y osteoporosis. Tarde o temprano estos datos podrían aprovecharse en la medicina personalizada. Es decir, que el tipo de tratamiento y medicamento diferiría según el genotipo del paciente.

Conclusiones

- Los resultados muestran que se consumieron 629 medicamentos, lo que equivale a 8,6 medicamentos por paciente/día.
- Los grupos sanguíneos de la población estudiada según tabla 2 establecen un porcentaje del 42,6% del grupo A; 42,4% del O; 13% del B y 1,4% del AB. El grupo predominante es A+ con un 35,6%, seguido del O+ con 27,4%. Respecto a la distribución por edades en la población estudiada se refleja en la tabla 2.
- El detalle de las enfermedades más prevalentes según el grupo sanguíneo se observa en las tablas 4 y 5:

  a) Los pacientes A+ respecto a A- tienen mayor prevalencia de tiroides, cáncer de próstata, HTA, falta de B12 y Alzheimer, mientras que los A- tienen anemia (Fe), enfermedades pulmonares y osteoporosis.

  b) Los O+ a respecto O- tienen más anemia (Fe) y depresión, mientras que los O-tienen más problemas circulatorios.

  c) Los B+ presentan más HTA, anemia (Fe), depresión y enfermedades pulmonares que los B-, estos presentaron más diabetes y osteoporosis.

  d) Se observa que los grupos A y O padecen mayor aumento de colesterol que los del grupo B (solo demostrado estadísticamente la relación grupo A y colesterol elevado).

  e) Los del grupo O tienen más HTA que el resto, y el O+ presenta mayor porcentaje de anemia (Fe), seguidos por el grupo A que estadísticamente padece más de anemia (B12).

- En general los grupos Rh positivo padecen más de HTA, insomnio y depresión que los Rh-.
- Respecto a la osteoporosis es mayor en los grupos negativos que en los positivos (tabla 6), aunque en este trabajo la relación avalada estadísticamente es Rh+ y padecer osteoporosis. La relación con Rh- se deja para posteriores estudios.
- Las asociaciones estadísticas encontradas en este trabajo son cuatro (tabla 7): relación grupo A y colesterol elevado, grupo A e hipertensión, grupo A y déficit de cianocobalamina y tener Rh+ y padecer osteoporosis.

Limitaciones del proyecto y conflicto de intereses

- El trabajo se ha realizado en un área geográfica determinada, la provincia de Cuenca, por ello, no es extrapolable a otras zonas. La limitación más importante será la reproducibilidad de los datos, por tratarse de un trabajo realizado en una zona y en un tiempo determinado.
- La muestra no se puede extrapolar ya que los pacientes se incluyeron a criterio del investigador principal, sin un muestreo aleatorio al ser un trabajo observacional no experimental. El diseño al no ser experimental, limitará establecer relación causa-efecto y solo establece relación.
- Al no tener acceso a la historia clínica, no pudimos establecer criterios stop/start.
- No hay conflicto de intereses, dado que es un estudio realizado para la obtención del título de doctor, sin beca alguna, ni patrocinadores. Todo abonado únicamente por la doctoranda.

Referencias

1. K. Landsteiner, E. Popper, Übertragung der Poliomyelitis acuta auf Affen, *Zeitschrift für Immunitätsforschung und experimentelle Therapie*, **2**, 377-390 (1909).
2. A. Buzzi, Karl Landsteiner y los grupos sanguíneos, *ALMA Cultura y Medicina*, **1**, 50-60 (2015).
3. E. Manethová, *Dr. Jan Janský, descubridor de los grupos sanguíneos*, Radio Prague International, URL: https://espanol.radio.cz/dr-jan-jansky-descubridor-de-los-grupos-sanguineos-8073177, consultado en mayo de 2020.

4. I.H. Erb, Blood groups classifications (A): Plea for uniformity, *Canadian Medical Association Journal*, **42**, 418-421 (1940).

5. G. Murillo-Godínez, Breve historia de la transfusión sanguínea, *Revista de Hematología (México)*, **20**, 1 (2019).

6. K. Landsteiner, A.S. Wiener, An agglutinable factor in human blood recognized by immune sera for rhesus blood, *Proceedings of the Society for Experimental Biology and Medicine*, **43**, 223 (1940).

7. K. Landsteiner, A.S. Wiener, Studies on an agglutinogen (Rh) in human blood reacting with anti-rhesus sera and with human isoantibodis isoantibodis, *The Journal of Experimental Medicine*, **74**, 309-320 (1941).

8. Erythroblastosis Fetalis, *The Free Dictionary by Farlax*, URL: https://medical-dictionary.thefreedictionary.com/erythroblastosis+fetalis, consultado en mayo de 2020.

9. R. Hernández, Y. Flores, R.E. Ortiz, Grupo sanguíneo, alimentación y sobrepeso/obesidad: Una miscelánea, *Enfermería Global*, **36**, 289-297 (2014).

10. P. Durán, N. Piazza, L. Trifone, Consenso sobre factores de riesgo de enfermedad cardiovascular en pediatría, *Archivos Argentinos de Pediatría*, **103**, 348-366 (2005).

11. S. Olivares, N. Bustos, X. Moreno, L. Lera, S. Cortez, Actitudes y prácticas sobre alimentación y actividad física en niños obesos y sus madres en Santiago, *Revista Chilena de Nutrición*, **33**, 170-179 (2006).

12. M. Gargallo-Fernández, M. Ballesteros-Pomar, Dietas heterodoxas, *Revista Española de Obesidad*, **6**, 75-87 (2006).

13. P. D'Adamo, C. Whitney, *Eat Right 4 Your Type*, G.P. Putnam's Sons, New York, 1996.

14. D. Rocco, Diet analysis: The ABO blood type diet, *Journal of Complementary Medicine*, **2**, 78-79 (2006).

15. C. Bermúdez, J. Insuasty, G. Gamarra, Grupo sanguíneo A y riesgo de cáncer gástrico en el hospital universitario de Santander (Bucaramanga, Colombia), *Acta Médica Colombiana*, **4**, 400-410 (2006).

16. S. Vento, F. Cainelli, *Controversias acerca de infeccion por helicobacter pylori y epidemiologia del cáncer gástrico*, University of Botswana School of Medicine, Gaborone, 2012.

17. La opinión, El Correo de Zamora, *¿Qué tipo de sangre tiene más riesgo de sufrir un infarto?*, URL: https://www.laopiniondezamora.es/vida-y-estilo/salud/2018/03/28/tipo-sangre-riesgo-sufrir-infarto/1073628.html, consultado en mayo de 2020.

18. Z. Jiao, Y. Yan, H. Hanping, L. Dong, G. Dongfeng, L. Xiangfeng *et al*., *Relationship between the ABO blood group and the COVID-19 susceptibility*, URL: https://www.medrxiv.org/content/10.1101/2020.03.11.20031096v2.full.pdf, consultado en mayo de 2020.

19. R. Casado, *Nuevo descubrimiento: el factor Rh determina la resistencia a la enfermedad. Dr. Jan Janský, descubridor de los grupos sanguíneos*, Radio Prague International, URL: https://www.radio.cz/es/rubrica/notas/nuevo-descubrimiento-el-factor-rh-determina-la-resistencia-a-la-enfermedad, consultado en mayo de 2020.

Como citar este artículo

M.C. Batanero-Hernán, B. Escalera-Izquierdo, M.J. Fresno-Contreras, M.A. Rodríguez-Chamorro, Principales enfermedades según el grupo sanguíneo en población mayor de 60 años en provincia de Cuenca (España), *Rev. Colomb. Cienc. Quím. Farm.*, **49**(3), 740-758 (2020).

Anexo 1

Hoja de información al paciente

Estudio: *Principales enfermedades según el grupo sanguíneo en población mayor de 60 años en provincia de Cuenca* (*España*)

Investigador: Carmen Batanero Hernán.

La farmacéutica M. Carmen Batanero Hernán le ha propuesto participar en el presente estudio de investigación. Lea con calma la información que a continuación le proporcionamos y que le permitirá decidir si quiere o no participar. No es necesario que dé una respuesta en este momento, puede llevarse esta información que le proporcionamos y valorarla con calma. Puede consultarlo con sus familiares, amigos o su médico de cabecera, si así lo quiere. Puede hacer cuantas preguntas quiera. La farmacéutica le contestará y resolverá todas las dudas que respecto al estudio puedan surgirle. Debe saber que su participación es completamente voluntaria y que, si decidiera no participar, su decisión no modificará en absoluto su relación con el equipo de salud ni los tratamientos que se le tengan que aplicar ahora o en el futuro.

¿Por qué se realiza este estudio?

Para conocer el grupo sanguíneo que posee relacionarlo con las enfermedades que padece la población mayor de 60 años en la provincia de Cuenca.

¿Cuál es el objetivo del estudio?

Los investigadores del presente estudio tienen como objetivo principal conocer la relación existente entre los diversos grupos sanguíneos y las principales enfermedades que padece la población.

¿Cómo se va a realizar el estudio?

A todos los pacientes que participen en el estudio se les realizará una amplia encuesta farmacoterapéutica.

¿Qué beneficios puedo obtener por participar en este estudio?

Con este estudio se pretende obtener una información que hoy en día no tenemos. Pero es importante que sepa que con su participación en el mismo puede contribuir a un avance científico que sirva para mejorar la calidad de vida de las personas en su misma situación.

¿Qué riesgos o molestias puedo sufrir por participar en el estudio?

Ninguno.

¿Qué datos se van a recoger?

Se recogerán datos personales (edad, sexo, talla, peso), así como todos los medicamentos que está consumiendo y si padece alguna molestia. También se le pedirán datos de su estado físico, actividad, hábitos saludables, hábitos alimenticios.

¿Cómo se tratarán mis datos y cómo se preservará la confidencialidad?

Todos sus datos se tratarán confidencialmente por personas relacionadas con el investigador y obligadas por el deber de secreto profesional. También podrían tener acceso las autoridades sanitarias y algún miembro designado del Comité de Ética de Investigación Clínica que supervisa el estudio, si así lo solicitaran. Estos controles se realizan para garantizar que se han respetado los derechos de los pacientes. No se utilizará su nombre y apellidos para guardar junto con la información registrada. En su lugar se utilizará un código (formado por números y letras) y solamente el investigador principal podrá relacionar su nombre con el código. De acuerdo con la Ley orgánica de protección de datos, debe saber que tiene derecho acceder a los datos que de usted se guarden, a rectificarlos, a cancelarlos y a oponerse a su uso, sin tener que dar ninguna explicación.

¿Me puedo retirar del estudio?

La participación en el estudio es totalmente voluntaria. Usted podrá retirarse en cualquier momento si lo desea, sin tener que dar explicaciones y sin que por ello se produzca perjuicio alguno en la relación con su médico ni en los cuidados que se le deban administrar.

¿Quién supervisa el estudio?

El Comité de Ética de Investigación y Experimentación Animal de la Universidad de Alcalá, que es el organismo encargado de evaluar la seguridad de los pacientes y los aspectos éticos y metodológicos de este estudio, ha aprobado el estudio, así como la presente hoja de información y el formulario de consentimiento informado.

¿Con quién puedo contactar en caso de duda?

Los siguientes investigadores serán los responsables del estudio y de informar y contestar a sus dudas y preguntas:

Dra. Begoña Escalera Izquierdo, Profesora Titular de Ciencias Biomédicas de la Universidad de Alcalá. Teléfono: 91 885 4675, Fax: 91 885 4680.

Dra. Mª José Fresno Contreras, Profesora Titular de Ciencias Biomédicas de la Universidad de Alcalá. Teléfono: 91 885 4675, Fax: 91 885 4680.

Dra. Mª Carmen Batanero Hernán, farmacéutica y nueva doctoranda de la Universidad de Alcalá de Henares. Teléfono 600211736.

Artículo de investigación científica / *http://dx.doi.org/10.15446/rcciquifa.v49n3.91342*

El modelo de ovario artificial como prueba celular para evaluar la seguridad de los extractos de *Spirulina maxima* y *Kéfir*: un estudio preliminar

Diana Carolina Saavedra Plazas[1]*, Ricardo Petterle[2], Cláudio Adriano Piechnik[3]

[1]Departamento de Bioprocesos y Biotecnología, Universidad Federal de Paraná -UFPR, Zip Code 81531-980, Curitiba, Paraná, Brasil.

[2]Departamento de medicina integrativa, Universidad Federal de Paraná - UFPR, Curitiba, Paraná, Brasil.

[3]Faculdades Pequeno Príncipe - FPP, Zip Code 80230-020, Curitiba, Paraná, Brasil.

*Autor de correspondencia: saavedra@ufpr.br, saavedraplazasc@gmail.com

Recibido: 10 de febrero de 2020

Revisado: 23 de julio de 2020

Aceptado: 27 de julio 2020

Resumen

S. maxima y *Kefir* son conocidos y utilizados por sus propiedades antioxidantes e inmunoestimulantes. El objetivo en este estudio fue evaluar los extractos naturales de estos dos agentes con la técnica de manipulación de ovocitos incluidos en folículos preantrales (MFP), porque la técnica puede reemplazar el uso de animales de laboratorio y también podría armonizar las leyes que intentan reducir y mejorar el uso de animales para el estudio de nuevos fármacos y para integrar a las buenas prácticas de laboratorio. Los extractos naturales estudiados fueron obtenidos a partir de *S. maxima* y *Kéfir*, las dos sustancias son conocidas en el mercado por su actividad antioxidante e inmunoestimulante. Los dos extractos fueron evaluados en suspensiones de 10, 50, 100 and 200 $\mu g.mL^{-1}$. Los resultados muestran que *Spirulina* produjo disminución en la sobrevivencia, el desarrollo y el diámetro folicular. Mientras que *Kéfir* no mostró influencias positivas o negativas sobre el crecimiento y desarrollo de los folículos preantrales, sólo la concentración de 200 $\mu g.mL^{-1}$ disminuyó la sobrevivencia folicular. La técnica MFP demostró encajar en la política de las 3R (reemplazo, reducción y refinamiento) y permitió evaluar la citotoxicidad mostrando que la técnica puede ser usada como una prueba de seguridad en extractos naturales.

Palabras clave: pruebas sin animales, efectos adversos, suplemento dietético, probiótico, bienestar, folículo preantral.

Summary

The model of artificial ovary as a cellular test to evaluate the safety of *Spirulina máxima* and *Kefir* extracts: a preliminary study

S. maxima and *Kéfir* are known and used for their antioxidant and immunostimulant properties. This study aimed to evaluate the natural extracts of these two agents with the technique of manipulation of oocytes included in preantral follicles (MFP), because the technique can replace the use of laboratory animals and could also harmonize the laws that try to reduce and improve the use of animals for the study of new drugs and to integrate good laboratory practices. The natural extracts studied were obtained from *S. maxima* and *Kefir*, both substances are known in the market for their antioxidant and immunostimulating activity. Both were evaluated in suspensions of 10, 50, 100 and 200 $\mu g.mL^{-1}$. The results show that *Spirulina* produced a decrease in survival, development, and follicular diameter. While *Kefir* did not show positive or negative influences on the growth and development of preantral follicles, only the concentration of 200 $\mu g.mL^{-1}$ decreased follicular survival. The MFP technique proved to fit into the 3R policy (replacement, reduction, and refinement) and allowed to evaluate cytotoxicity, showing that the technique can be used as a safety test in natural extracts.

Key words: Non animal testing, adverse effect, dietary supplement, pre-biotic, wellness, preantral follicle.

Introducción

El desarrollo de nuevos productos es importante para la continua promoción de la salud humana y animal, sin embargo, es indispensable el estudio de metodologías alternativas que puedan evaluar la eficacia y la seguridad de estos productos. En este contexto, identificar y promover la implementación de métodos alternativos que puedan reducir, refinar y reemplazar (3R) el uso de animales de laboratorio en la investigación es urgente y desafiante [1]. Esta necesidad se hace más notoria con el continuo crecimiento de los productos naturales en el mercado, por ejemplo el uso de *S. maxima* y *Kéfir* como suplemento dietético [2-4]. Por otro lado en la biotecnología la manipulación de ovocitos, incluyendo los folículos preantrales, es usada para estudiar el fenómeno de la foliculogénesis y sus requerimientos metabólicos en cultivo *in vitro* [5-8] y con el propósito de tratar la infertilidad [9].

La técnica de estudio de manipulación de ovocitos incluidos en folículos preantrales (MFP) tiene diferentes ventajas además de los estudios fisiológicos [8, 10, 11], esta metodología puede usarse como un método alternativo que implementa la política de las 3R, que se refieren al uso de animales de laboratorio en investigaciones preliminares de varios fármacos y la evaluación de sustancias como los antioxidantes, las hormonas (FSH, LH, estradiol), los péptidos (péptido intestinal vasoactivo), y los factores de crecimiento (activin, GDF-9, KGF) [8, 12, 13]. Entre las sustancias que se pueden estudiar se encuentran los agentes tóxicos como el tabaco y las drogas utilizadas en la quimioterapia [10].

Un ejemplo de sensibilidad en los ovocitos a los compuestos naturales ha sido descrita en el *Ginkgo biloba,* porque durante su administración oral en ratones albinos suizos (*Mus musculus*) se encontró disminución de la fertilidad a la dosis de 14,8 mg/kg/ día [14].

El Centro Interagencial para la Evaluación de Métodos Toxicológicos Alternativos del Programa Nacional de Toxicología de los Estados Unidos (NICEATM, por sus siglas en inglés) afirma en su sitio web que las pruebas de toxicidad sistémica aguda se realizan tradicionalmente con ratas y que los enfoques como los ensayos de cultivos celulares reducen en gran medida el número de animales necesarios para estas pruebas.

En este artículo se estudiaron dos microorganismos: *S. maxima* y *Kéfir.* En el caso de *Spirulina sp*., esta microalga es una cyanobacteria usada como suplemento nutricional [15], también es conocida porque tiene ácidos fenólicos, tocoferol, betacaroteno y flavonoides con propiedades antioxidantes y antiapoptóticas [2, 16]. Estos antioxidantes han demostrado propiedades antiinflamatorias en ratas [15], así como genotoxicidad [17]. Estos eventos son reportados y monitoreados continuamente por el Comité Experto en Información de Suplementos Dietéticos de los Estados Unidos [18].

Kéfir es un consorcio de microorganismos que incluye bacterias acido lácticas y levaduras, que son usadas para fermentar productos lácteos [4, 19]. Se sabe que *Kéfir* estimula la respuesta inmune, es antiinflamatorio, antioxidante, hipoalergénico y con propiedades anti mutagénicas [20-24]. *Kéfir* contiene un exopolisacárido llamado *Kéfir*an que estimula el sistema inmune y evita la proliferación de células de cáncer [25]. Las funciones biológicas son explicadas porque los productos fermentados contienen fenoles y bioflavonoides clasificados como probióticos y bactericidas [26, 27]. Sin embargo, muchos de estos estudios resaltan la necesidad de estudiar la seguridad biológica antes de poder llamarse producto probiótico [23].

S. maxima and *Kéfir* son estudiados para diversas aplicaciones en salud, pero, se necesita de estudios complementarios para evaluar su toxicidad y su eficacia. Una de las directrices internacionales disponibles es la directriz ICH S6 [28], que facilita la

realización oportuna de los ensayos clínicos y reduce el uso de animales de acuerdo con las 3R. Este apéndice justifica que varios métodos alternativos *in vitro* como: las células derivadas de mamíferos pueden predecir los efectos *in vivo* de un determinado biofármaco. Por otro lado, la FDA y la Unión Europea también alientan el uso de metodologías sin animales [29] y la guía de la Agencia Europea del Medicamento (EMA) en 2008 recomienda el uso de líneas celulares derivadas de mamíferos para predecir la actividad biofarmacéutica *in vivo*.

El presente estudio utilizó la técnica de MFP para evaluar la citotoxicidad de los extractos obtenidos a partir de *S. maxima* y *Kéfir*, con el fin de presentar la técnica de MFP como un posible método que puede contribuir con la política de las 3R por ser un método alternativo al uso de animales de laboratorio.

Materiales y métodos

Extracto de *Spirulina máxima*

La cepa *S. maxima* fue proporcionada por la empresa Ouro-Fino de Ribeirão Preto en São Paulo, Brasil. Estas microalgas fueron cultivadas en tanques *Raceway* de 10 000 cm^3 con medio de cultivo *Zarrouk* al 50 %, bajo agitación constante y con temperatura de 30 °C. Una vez que las microalgas fueron procesadas y secadas al sol, se utilizaron 10 g de estas y se mezclaron con 100 mL de agua estéril. Luego, la solución recibió 10 min de sonicación para causar lisis celular y la suspensión resultante se centrifugó a 12 000 g. El sobrenadante fue separado, liofilizado y esterilizado con óxido de etileno. Después de esto el extracto se mantuvo a temperatura ambiente en un recipiente al vacío. Un día antes de su uso, se prepararon suspensiones con cuatro concentraciones diferentes del extracto de *S. maxima* (10, 50, 100 y 200 $\mu g.mL^{-1}$) y se almacenaron a -20 °C.

Extracto de *Kéfir*

Los granos de *kéfir* se fermentaron en 300 mL de suero de leche durante 48 h a 30 °C, el medio fue suplementado con 30% (p/v) de glucosa, 2% (p/v) de peptona, 4% (p/v) de fosfato y 4% (p/v) de citrato. Luego de la fermentación los granos de *Kéfir* fueron separados del medio líquido por centrifugación a 80 000 g para recuperar el sobrenadante. Posteriormente, se precipitó el sobrenadante con etanol absoluto durante 24 h a 4 °C y se recuperó el precipitado por centrifugación a 80 000 g, el cual fue lavado con agua destilada [27]. A continuación, se realizó una diálisis de 48 h, seguida de liofilización. El extracto obtenido se esterilizó con óxido de etileno y se almacenó al vacío. Un día antes de su uso, se prepararon suspensiones con cuatro concentraciones diferentes de extracto de *Kéfir:* 1,01 $mg.mL^{-1}$; 5,05 $mg.mL^{-1}$; 10,1 $mg.mL^{-1}$ y

20,2 mg.mL^{-1} para obtener una concentración final dentro del ensayo experimental de: 10, 50, 100 y 200 µg.mL^{-1}. Posteriormente todas las suspensiones se almacenaron a -20 °C hasta su uso en laboratorio.

Fuente de los ovarios

Los ovarios se colectaron en un frigorífico de Fortaleza-Ceará, Brasil. Se extrajeron 20 ovarios completos de diez cerdas jóvenes prepúberes de raza Yorkshire (*Sus scrofa domestica*). Los ovarios se lavaron una vez en etanol al 70% y dos veces en un medio mínimo esencial (MEM) que contenía 100 µg.mL^{-1} de penicilina, 100 µg.mL^{-1} de estreptomicina. Para transportar los ovarios hasta el laboratorio se usó medio de cultivo MEM a 37 °C [30]. En el laboratorio el córtex ovariano fue separado y cortado en pequeñas piezas cuadradas que fueron dejadas luego en medio de cultivo. Los grupos estudiados se organizaron en: grupo control (sin adición de extractos), grupo tratado con extracto de *S. maxima* y grupo tratado con extracto de *Kéfir*; El tiempo de cultivo fue de 1 y 7 días.

Protocolo experimental

El córtex de tejido ovariano fue cultivado de acuerdo la metodología de Mao *et al.* [30]. El medio de cultivo usado fue Alpha MEM, con pH entre 7,2 y 7,4, con 100 mg.mL^{-1} de ácido ascórbico, 1000 mg.mL^{-1} BSA, 200 µg/mL hipoxantina, 10 µg.mL^{-1} transferrina, 1 mM piruvato, 100 µg.mL^{-1} penicilina y 100 µg.mL^{-1} de estreptomicina. De acuerdo con varios protocolos en la literatura [12, 31] el córtex ovariano luego de disectado debe ser dividido en piezas de un tamaño aproximado de 5 mm × 5 mm x 1 mm usando un bisturí y bajo condiciones estériles. En esta metodología se debe tener en cuenta que una muestra debe ir para análisis histológico (control en fresco) y las otras muestras del mismo par de ovarios se colocan en un grupo cultivo de 1 día y otro grupo cultivo de 7 días (cada muestra en pozo individual). Por último, las muestras de tejido cortical fueron transferidas a platos de cultivo de 24 pozos, los cuales contenían 1 mL de medio de cultivo y 10 µL de extractos de *S. maxima* o *Kéfir*. Se evaluaron cuatro concentraciones (10, 50, 100 y 200 µg.mL^{-1}) de cada extracto y posteriormente al término de los días de cultivo las muestras se analizaron por histología.

Análisis histológico

Las muestras se fijaron en una solución de paraformaldehído al 4% en PBS con pH 7,2 durante 12 h a 4 °C. Luego, se deshidrataron en concentraciones crecientes de etanol y se incluyeron en parafina. Las muestras histológicas se cortaron en secciones de 7 µm y se tiñeron con ácido periódico - Schiff (PAS) - hematoxilina. Cada sección fue evaluada con un microscopio óptico (Nikon, Tokio, Japón) en aumento de 400x.

Para realizar el análisis de las secciones histológicas, se evaluó en los tejidos ovarianos los folículos preantrales. Estos se clasificaron según su estado de desarrollo, el cual ya fue definido [6] como: 1. Folículos primordiales, los cuales tienen una capa de células de la granulosa de forma aplanada alrededor del ovocito. 2. Folículos en crecimiento, donde se incluyen los folículos primarios que poseen una capa de células de la granulosa de forma cuboidal y los secundarios que poseen dos o más capas de células de la granulosa.

Además de identificar el estado de desarrollo folicular, también los folículos preantrales se clasificaron en folículos sin alteraciones morfológicas y folículos con degeneraciones (no viables). Los folículos sin cambios en la morfología se evaluaron con base en la integridad de los ovocitos y las células de la granulosa, la presencia o ausencia de cuerpos picnóticos, la retracción ovoplásmica y la organización de las células de la granulosa (figura 1).

Los folículos con degeneraciones se identificaron como aquellos con un ovocito retraído, núcleo picnótico o células granulosas desorganizadas que se desprenden de la membrana basal. El porcentaje de folículos con cambios morfológicos, antes (día 0) y después del cultivo, indicó el porcentaje de supervivencia folicular (figura 1).

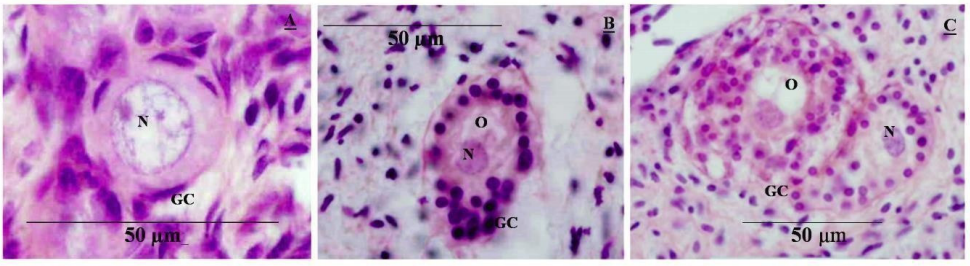

Figura 1. A) Folículos preantrales: folículo primordial sin cambios morfológicos. B) Folículo primario sin cambios morfológicos luego de 7 días de cultivo *in vitro*. C) Folículo preantral con cambios morfológicos que indican degeneración. (GC) células de la granulosa, (O) ovocito, (N) núcleo. Escala: 50 µm.

Análisis estadístico

Para cada uno de los extractos, los datos analizados contemplan una muestra control más cuatro grupos de concentraciones. De cada muestra se contaron 30 folículos (100%) y se dividió la población en tres grupos: folículos primordiales, folículos en desarrollo y folículos no viables. Luego de obtener un promedio para cada grupo, los valores fueron usados para el análisis estadístico. Las muestras control de los días de cultivo 0, 1 y 7 se analizaron sólo para establecer valores de referencia que pudieron ser

comparados con los valores de los grupos tratados. Todos los datos fueron analizados en el programa R Commander y la normalidad de las muestras se evaluó mediante el teste de Shapiro-Wilk. Para evaluar la homogeneidad de los datos se utilizó el teste de Bartlett. El porcentaje de folículos primordiales y la supervivencia folicular, así como los diámetros de ovocitos y folículos fueron sometidos a análisis de varianza (Anova) realizando la prueba *post hoc* de Tukey para la comparación entre grupos [31].

Resultados y discusión

Los avances en salud en los últimos años han intentado disminuir el número de animales usados en experimentación. Para esto fueron creadas las 3R, reducir, refinar y reemplazar. En este contexto la técnica MFP puede reemplazar los animales de laboratorio y disminuir el número de repeticiones en un estudio, contribuyendo así con el bienestar animal y con el desarrollo de un posible algoritmo para tener en cuenta en el estudio de sustancias naturales (figura 2). Este algoritmo representa a MFP como una técnica para evaluar los extractos naturales y diferentes sustancias obtenidas por nuevos procesos biotecnológicos. En el caso de sustancias tóxicas ayudaría a ampliar la identificación de las moléculas citotóxicas y por el contrario si las sustancias son seguras, la técnica MFP puede ayudar a dirigir los estudios hacia la caracterización de moléculas para uso medicinal.

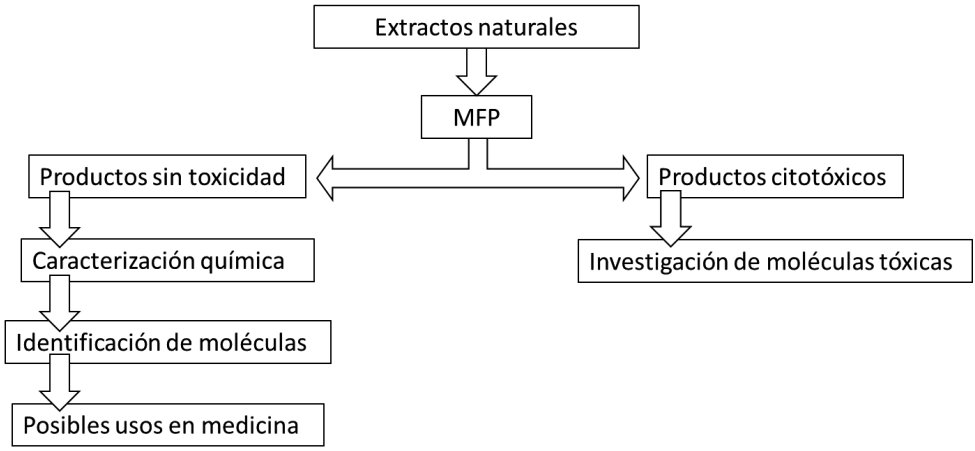

Figura 2. Algoritmo para la investigación de toxicidad y seguridad en sustancias naturales o las obtenidas por medio de biotecnología.

Análisis folicular

En el análisis realizado por la técnica MFP se encontró una disminución en el número de folículos preantrales durante la adición de los extractos de *S. maxima* y *Kéfir*. Esta

baja en la población folicular se observó durante el día 1 y 7 de cultivo *in vitro*. A pesar de que la reducción en el número de folículos del grupo control es un parámetro esperado [32], en los extractos estudiados esta pérdida fue más marcada (tabla 1). Teniendo en cuenta las concentraciones ascendentes evaluadas de los extractos, 10, 50, 100 y 200 μg.mL^{-1}, para el extracto de *S. maxima* los valores en la sobrevivencia folicular fueron entre: 63,33 ± 0,08 % a 48,66 ± 0,05 % en el día 1 de cultivo y para *Kéfir* estuvieron entre: 63,33 ± 0,08 a 50,00 ± 0,07 %. Los resultados para el día 7 de cultivo *in vitro* para el extracto de *S. maxima* fueron los más bajos variando entre: 47,33 ± 0,11% a 6,66 ± 0,07 % y para el extracto de *Kéfir* fueron entre: 43,33 ± 0,08 a 20,00 ± 0,03 %. Entre las dos sustancias naturales *S. maxima* fue el extracto con más toxicidad sobre la sobrevivencia folicular ($p > 0,05$), mientras que el extracto de *Kéfir* solo fue significativo en la concentración de 200 μg.mL^{-1} (tabla 1).

Tabla 1. Porcentaje de sobrevivencia del folículo preantral en las cerdas jóvenes en los días 0 y 7 con diferentes concentraciones de extractos de *S. maxima, kéfir* y grupos control.

Morfología folicular normal (%)			
***Spirulina* (μg.mL^{-1})**	**Día 0**	**Día 1**	**Día 7**
0	84,66±0,01^{A}	63,33±00,08^{B*}	47,33±00,11^{C*}
10		62,00±00,08^{B*}	34,67±00,05^{C**}
50		55,33±00,09^{B**}	33,33±00,07^{C**}
100		48,66±00,05^{B***}	29,33±00,04^{C**}
200		56,66±00,10^{B**}	06,66±00,07^{C***}
***Kéfir* (μg.mL^{-1})**	Día 0	Día 1	Día 7
0	73,33±00,06^{A}	63,33±00,08^{B***}	43,33±00,08^{C*}
10		48,66±00,10^{B*}	36,66±00,06^{C*}
50		52,00±00,08^{B**}	32,66±00,12^{C**}
100		50,66±00,07^{B*}	34,66±00,08^{C**}
200		50,00±00,07^{B*}	20,00±00,03^{C***}

(*) El asterisco representa la igualdad entre las concentraciones de los extractos evaluados y las mayúsculas representan la similitud estadística entre los días de cultivo ($p < 0,05$).

Para analizar la activación y el desarrollo de los folículos preantrales se tuvo en cuenta la población de folículos en desarrollo a partir de su estado primario hasta antes de la formación del antro folicular (tabla 2). Para el extracto *S. maxima* se presentaron varios efectos adversos que indican toxicidad, el primer efecto negativo fue la baja activación

folicular vista en las concentraciones de 50, 100 y 200 μg.mL^{-1} y el segundo efecto negativo fue la disminución del desarrollo folicular en la concentración de 200 μg.mL^{-1}. Por otro lado, las concentraciones del extracto de *Kéfir* no influyeron de forma negativa sobre la activación y el desarrollo folicular porque no tuvieron diferencia con el grupo control (tabla 2).

Tabla 2. El porcentaje de activación de los folículos primordiales y el desarrollo de los folículos en los días cero, uno y siete con diferentes suspensiones de *S. maxima* y extracto de *Kéfir*.

	Activación de folículos primordiales (%)			**Desarrollo folicular (%)**		
Spirulina **(μg.mL^{-1})**	**Día 0**	**Día 1**	**Día 7**	**Día 0**	**Día 1**	**Día 7**
0	57,50±09,56^{A}	39,27±15,99^{A*}	04,38±07,23^{B*}	42,49±09,56^{A}	60,72±15,99^{A*}	95,61±07,23^{B*}
10		24,78±03,52^{B*}	19,27±08,93^{B*}		75,21±03,52^{B*}	80,72±08,93^{B*}
50		36,99±12,06^{AB*}	22,19±12,82^{B**}		63,00±12,06^{A*}	77,80±12,82^{AB*}
100		32,33±10,81^{B*}	25,30±16,22^{B**}		67,66±10,81^{B*}	74,69±16,22^{B*}
200		43,01±12,22^{A*}	15,00±33,54^{B*}		56,98±12,22^{A*}	45,00±51,23^{A**}
Kéfir **(μg.mL^{-1})**	**Día 0**	**Día 1**	**Día 7**	**Día 0**	**Día 1**	**Día 7**
0	58,46 ±14,86^{A}	46,91±09,69^{A*}	07,04±12,37^{B*}	41,53±14,86^{A}	53,08±09,69^{A*}	92,95±12,37^{B*}
10		41,66±23,38^{B*}	17,26±07,52^{C*}		58,33±23,38^{B*}	82,73±07,52^{C*}
50		25,71±14,94^{B**}	19,67±17,30^{B*}		74,28±14,94^{B**}	80,32±17,30^{B*}
100		31,44±15,26^{B*}	16,79±05,24^{B*}		68,55±15,26^{B*}	83,20±05,24^{B*}
200		06,72±10,21^{B***}	02,85±06,38^{B*}		93,27±10,21^{B***}	97,14±06,38^{B*}

(*) El asterisco representa la igualdad entre las concentraciones de los extractos evaluados y las mayúsculas representan la similitud estadística entre los días de cultivo ($p < 0,05$).

El diámetro folicular y ovocitario fueron analizados porque permiten evaluar el crecimiento y la maduración de los folículos preantrales. El tamaño promedio para el grupo control fue un diámetro folicular de 40,5 ± 7,3 μm y para el diámetro ovocitario de 22,01 ± 2,8 μm luego de los 7 días de cultivo. Teniendo como referencia los anteriores diámetros, el extracto de *S. maxima* disminuyó significativamente el diámetro folicular ($P<0,05$) mientras que en el diámetro ovocitario no hubo diferencias estadísticas. Para el extracto de *Kéfir* no se encontraron diferencias para ninguna de las concentraciones evaluadas porque las concentraciones de 10, 50, 100 y 200 μg fueron estadísticamente igual a los grupos control (tabla 3).

Tabla 3. Diámetro de los folículos preantrales de las cerdas después del cultivo *in vitro* de 1 y 7 días con diferentes concentraciones (μg.mL^{-1}) de *S. máximas, Kéfir* y grupo control.

	Diámetro folicular (μm)			**Diámetro *ovocitario* (μm)**		
***Spirulina* (μg.mL^{-1})**	**Día 0**	**Día 1**	**Día 7**	**Día 0**	**Día 1**	**Día 7**
0	39,80±6,81^{A}	33,22±8,12^{A*}	40,53±7,31^{A*}	24,19±3,02^{A}	20,40±3,53^{A*}	22,01±2,86^{A*}
10		30,80±6,91^{AB*}	28,75±7,16^{B***}		19,38±2,48^{AB*}	17,86±4,71^{B*}
50		36,27±8,74^{A*}	30,41±8,03^{A***}		17,75±1,81^{B*}	18,41±3,10^{AB*}
100		32,96±8,87^{A*}	36,33±9,90^{A**}		19,20±2,30^{A*}	19,66±4,34^{A*}
200		31,81±4,44^{A*}	3,64±8,14^{B***}		19,12±2,64^{A*}	2,46±5,51^{B**}
***Kéfir* (μg.mL^{-1})**	**Día 0**	**Día 1**	**Día 7**	**Día 0**	**Día 1**	**Día 7**
0	28,94±6,08^{A}	32,81±4,24^{AB*}	38,05±8,30^{B*}	22,29±3,73^{A}	20,38±1,93^{A*}	22,06±2,26^{A*}
10		25,52±2,49^{A***}	36,66±7,56^{B*}		17,66±1,49^{B*}	20,91±2,55^{A*}
50		35,14±7,36^{AB*}	42,12±4,96^{B*}		20,50±3,19^{A*}	21,45±0,90^{A*}
100		30,33±5,39^{A**}	34,31±7,35^{A*}		18,40±2,67^{B*}	18,60±2,97^{B*}
200		35,85±4,81^{A*}	34,09±8,40^{A*}		19,98±1,08^{A*}	19,60±3,21^{A*}

(*) El asterisco representa la igualdad entre las concentraciones de los extractos evaluados y las mayúsculas representan la similitud estadística entre los días de cultivo ($p < 0,05$).

El análisis estadístico muestra que a mayor concentración de extracto de *S. maxima* mayor toxicidad sobre la sobrevivencia y desarrollo folicular. Para el extracto de *Kéfir* solo se presenta toxicidad sobre la sobrevivencia folicular con la adición de 200 μg.mL^{-1}.

Aunque no hay reportes de toxicidad para *Spirulina spp.,* en varias investigaciones realizadas no se describe toxicidad sobre los tejidos como riñón, hígado, cerebro, bazo y eritrocitos [33]. En análisis practicados en peces *zebrafish* que fueron alimentados con *S. platensis* el número de huevos por desove disminuyó y la calidad de los huevos fue superior a los huevos del grupo control [34]. Sin embargo, en estos artículos no se evalúa la influencia de *Spirulina spp.* sobre la foliculogénesis. En este caso la técnica MFP muestra que hay toxicidad sobre sobrevivencia y el desarrollo folicular, evidenciando de esta manera la importancia de continuar ampliando los estudios de varios extractos naturales y sustancias obtenidas por bioprocesos. La toxicidad encontrada también se refuerza en los bajos diámetros ovocitarios encontrados (22,0 ± 2,8 μm y 2,46 ± 5,5 μm, tabla 3) y el pobre crecimiento de las células de la granulosa (entre 36,3 ± 9,9 μm y 3,6 ± 8,1 μm).

En relación al extracto de *Kéfir*, algunos estudios describen toxicidad subcrónica sin cambios histopatológicos [3, 35]. Esto puede confirmarse por la disminución de la sobrevivencia folicular con la concentración de 200 μg.mL^{-1} y la ausencia de crecimiento del ovocito durante la evaluación de los diámetros. El óptimo desarrollo del ovocito y sus estructuras anexas son importantes para que una vez maduro el óvulo, este pueda ser fértil y también permita un desarrollo adecuado del embrión [36-38]. En este caso la falta de crecimiento ovocitario se evidencia en los diámetros descritos por Silva *et al.* [39], donde el valor de referencia fue de 26,0 ± 2,5 μm y 27,3 ± 2,8 μm. Estos diámetros ovocitarios fueron superiores a los presentados en esta investigación y a pesar de que el diámetro folicular muestra un mayor crecimiento en células de la granulosa, este comportamiento no justifica que los ovocitos puedan ser fértiles posteriormente, (crecimiento folicular fue de 42,1 ± 4.9 μm a 34,1 ± 8,4 μm y el ovocitário de 22,1 ± 2,2 μm a 18,6 ± 2,9 μm).

Los resultados del extracto de *S. maxima* muestran importantes efectos tóxicos sobre la foliculogénesis en todas las concentraciones evaluadas, mientras que para el extracto de *Kéfir* la concentración tóxica encontrada fue sobre los 200 μg.mL^{-1}. Además de este resultado también se encontró alta variabilidad entre las repeticiones experimentales. Este fenómeno se puede explicar por las diferencias individuales relacionadas a la dieta y al estado fisiológico reproductivo [40, 41]. Este punto se debe tener en cuenta porque la mayoría de las muestras colectadas provienen de animales que son sacrificados en frigorífico y de diferentes sistemas de cría. También se debe resaltar que en tratamientos de superovulación, el estado fisiológico de cada hembra es altamente variable [42]. Por tanto, se debe tener en cuenta que es normal la alta variabilidad entre muestras durante los días de cultivo y que aun así la técnica MFP continúa siendo útil para la evaluación de la toxicidad.

Buenas prácticas de laboratorio

En la actualidad los modelos animales son usados en estudios de fármacos y diferentes sustancias porque su fisiología es similar a la de los humanos [1]. Debido a las nuevas políticas de protección animal, varias organizaciones en todo el mundo impulsan los estudios basados en metodologías diferentes al uso de animales, un ejemplo de esto son las técnicas *in vitro* [28, 29]. Por tanto, es necesario estudiar técnicas como el MFP, técnicas predictivas computarizadas [1] ,otras técnicas como el uso de bacterias y el cultivo de células de mamíferos *in vitro* [28] que podrían ofrecer alternativas.

A partir de este punto, se propone usar la técnica MFP en extractos de origen natural y durante los procesos de separación de moléculas para evaluar la seguridad y evitar el uso de animales. La técnica MFP puede ser auxiliada con otras técnicas como el test de Chopper, el cultivo de folículos aislados, la electroforesis para evaluar la fragmentación

del ADN y la inmunohistoquímica (TUNEL). Este tipo de pruebas complementan los análisis de marcadores celulares apoptóticos y la integridad del folículo ovárico [31, 43-46].

Hoy en día los requisitos éticos en el uso de animales de laboratorio se han resumido en: reducir, refinar y reemplazar (3R) a través de la armonización de la declaración de Helsinki y las buenas prácticas de laboratorio. Todo esto en un intento de controlar el uso de animales en la investigación de acuerdo con las recomendaciones de varias organizaciones y leyes internacionales como: la directiva 2001/83/EC de la Agencia Europea de Medicamentos (EMA 2008), el Comité de Medicamentos para el Hombre (CHMP,) la regulación 1394/2007/EC, la Administración de Alimentos y Medicamentos (FDA), el Comité Coordinador Interinstitucional para la Validación de Métodos Alternativos (ICCVAM), el NTP Centro Interinstitucional de Evaluación de Métodos Toxicológicos Alternativos (NICEATM), la Organización Mundial de la Salud (WHO) y la Organización de Cooperación y Desarrollo Económicos (OECD). Sin embargo, a pesar de que varias de las anteriores organizaciones presentan nuevas alternativas y regulan el uso de animales, las metodologías alternativas al uso de animales aún son limitadas.

Se puede decir que la técnica MFP abraza la política de las 3R, porque reduce el número de animales sacrificados en los experimentos y aprovecha al máximo la unidad experimental [47], ya que con cada unidad se evaluaron todas las concentraciones de cada uno de los extractos. La técnica MFP también permitió refinar el uso de animales porque es una técnica menos invasiva, mejora las condiciones de bien estar animal y sustituye las microtécnicas de análisis de fluidos animales. La MFP es una técnica sensible en la experimentación, debido a que las células donadas con las que se trabajan no han son modificadas y porque este ensayo requiere siete días de cultivo, lo que es tiempo suficiente para analizar y autorizar su uso en los ensayos clínicos (Directiva 2001/83/EC) [48]. Finalmente, reemplaza la tradicional prueba con animales, por una prueba basada en células donadas de los animales.

Agradecimientos

Los autores agradece al equipo de LAMOFOPA de la Universidad Estadual do Ceará por el entrenamiento en la técnica MFP y al programa de postgrado en Ingeniería de Bioprocesos y Biotecnología de la Universidad Federal do Paraná por el apoyo con el desarrollo de la investigación.

Conflicto de intereses

Los autores declaran que no hay conflicto de intereses.

Referencias

1. S.K. Doke, S.C. Dhawale, Alternatives to animal testing: A review, *Saudi Pharm. J.*. **23**, 223-229 (2015).

2. M.S. Miranda, R.G. Cintra, S.B.M. Barros, J. Mancini-Filho, Antioxidant activity of the microalga *Spirulina maxima*, *Braz. J. Med. Biol. Res.*, **31**, 1075-1079 (1998).

3. D. Diniz-Rosa, M.D.C. Gouveia-Peluzio, T. Pérez-Bueno, E. Vega-Cañizares, L. Sánchez-Miranda, B. Mancebo-Dorbignyi, D. Chong-Dubí, I. Espinosa-Castaño, L. Marcin-Grześkowiak, C.LD.L. Fortes-Ferreira, Evaluation of the subchronic toxicity of *Kéfir* by oral administration in *Wistar* rats, *Nutr. Hosp.*, **29**, 1352-1359 (2014).

4. K.V.O. O'Brien, L.K. Stewart, L.A. Forney, K.J. Aryana, W. Prinyawiwatkul, C.A. Boeneke, The effects of postexercise consumption of a *Kéfir* beverage on performance and recovery during intensive endurance training, *J. Dairy Sci.*, **98**, 7446-7449 (2015).

5. J.J. Eppig, M. O'Brien, K. Wigglesworth, Mammalian oocyte growth and development *in vitro*, *Mol. Reprod. Dev.*, **44**, 260-273 (1996).

6. E.E. Telfer, The development of methods for isolation and culture of preantral follicles from bovine and porcine ovaries, *Theriogenology*, **45**, 101-110 (1996).

7. N. Songsasen, O. Comizzoli, J. Nagashima, M. Fujihara, D.E. Wildt, The domestic dog and cat as models for understanding the regulation of ovarian follicles development *in vitro*, *Reprod. Domest. Anim*., **47**, 13-18 (2012).

8. V.R. Araújo, M.O. Gastal, J.R. Figueiredo, E.L. Gastal, *In vitro* culture of bovine preantral follicles: a review, *Reprod. Biol. Endocrinol*., **12**, 78:1-14 (2014).

9. N. Mochida, A. Akatani-Hasegawa, K. Saka, M. Ogino, Y. Hosoda, R. Wada, H. Sawai, H. Shibahara, Live births from isolated primary/early secondary follicles following a multistep culture without organ culture in mice, *Reproduction*, **146**, 37-47 (2013).

10. C.J. Mark-Kappeler, P.B. Hoyer, P.J. Devine, Xenobiotic effects on ovarian preantral follicles, *Biol. Reprod.*, **85**, 871-883 (2011).

11. S. Scholz, E. Sela, L. Blaha, T. Braunbeck, M. Galay-Burgos, M. García-Franco, J. Guinea, N Klüver, K. Schirmer, K. Tanneberger, M. Tobor-Kapłon, H. Witters, S. Belanger, E. Benfenati, S. Creton, M.T.D. Cronin, R.I.L. Eggen, M. Embry, D. Ekman, A. Gourmelon, M. Halder, B. Hardy, T. Hartung, B. Hubesch, D. Jungmann, M.A. Lampi, L. Lee, M. Léonard, E. Küster, A. Lillicrap, T. Luckenbach, A.J. Murk, J.M. Navas, W. Peijnenburg, G. Repetto, E. Salinas, G. Schüürmann, H. Spielmann, K.E. Tollefsen, S. Walter-Rohde, G. Whale, J.R. Wheeler, M.J. Winter, A European perspective on alternatives to animal testing for environmental hazard identification and risk assessment, *Regul. Toxicol. Pharmacol.*, **67**, 506-530 (2013).

12. J.J.H. Celestino, J.B. Bruno, I.B. Lima-Verde, M.H.T Matos, M.V.A Saraiva, R.N. Chaves, F.S. Martins, L.F. Lima, K.P.O. Name, C.C. Campello, J.R.V. Silva, S.N. Bao, J.R. Figueiredo, Recombinant epidermal growth factor maintains follicular ultrastructure and promotes the transition to primary follicles in caprine ovarian tissue cultured *in vitro*, *Reprod. Sci.*, **16**, 239-246 (2009).

13. A. Abedelahi, M. Salehnia, A.A. Allameh, D. Davoodi, Sodium selenite improves the *in vitro* follicular development by reducing the reactive oxygen species level and increasing the total antioxidant capacity and glutathione peroxide activity, *Hum. Reprod.*, **25**, 977-985 (2010).

14. R.H. Elmazoudy, A.A. Attia, Efficacy of *Ginkgo biloba* on vaginal estrous and ovarian histological alterations for evaluating anti-implantation and abortifacient potentials in albino female mice, *Birth Defects Res. B, Dev. Reprod. Toxicol.*, **95**, 444-459 (2012).

15. G.A. Gutiérrez-Rebolledo, M. Galar-Martínez, R.V. García-Rodríguez, G.A. Chamorro-Cevallos, A.G. Hernández-Reyes, E. Martínez-Galero, Antioxidant effect of *Spirulina* (*Arthrospira*) *maxima* on chronic inflammation induced by Freund's complete adjuvant in rats, *J. Med. Food*, **18**, 865-871 (2015).

16. H.C. Lee, M. Lee, W. Den, *Spirulina maxima* for phenol removal: study on its tolerance, biodegradability and phenol-carbon assimilability, *Water, Air, Soil Pollut.*, **226**, 395 (2015).

17. T.M. Saber, S.A. Elgaml, H.A. Ali, A.A., Saleh, Protective effect of *Spirulina platensis* against aluminium-induced nephrotoxicity and DNA damage in rats, *Toxicol. Environ. Chem.*, **97**, 1113-1123 (2015).

18. R.J. Marles, M.L. Barrett, J. Barnes, M.L. Chavez, P. Gardiner, R. Ko, G.B. Mahady, T.L. Dog, N.D. Sarma, G.I. Giancaspro, M. Sharaf, J. Griffiths, United States Pharmacopeia safety evaluation of *Spirulina*, *Crit. Rev. Food Sci. Nutr.*, **51**, 593-604 (2011).

19. S. Arslan, A review: chemical, microbiological and nutritional characteristics of *Kéfir*, *CyTA - J. Food*, **13**, 340-345 (2015).

20. J.R. Liu, S.Y. Wang, M.J. Chen, H.L. Chen, P.Y. Yueh, C.W. Lin, Hypocholesterolaemic effects of milk-*Kéfir* and soyamilk-*Kéfir* in cholesterol-fed hamsters, *Br. J. Nutr.*, **95**, 939-946 (2006).

21. T. Furuno, M. Nakanishi, Kefiran suppresses antigen-induced mast cell activation, *Biol. Pharm. Bull.*, **35**, 178-183 (2012).

22. C. Iraporda, D.E. Romanin, M. Rumbo, G.L. Garrote, A.G. Abraham, The role of lactate on the immunomodulatory properties of the nonbacterial fraction of *Kéfir*, *Food Res. Int.*, **62**, 247-253 (2014).

23. P. Carasi, S.M. Racedo, C. Jacquot, D.E. Romanin, M.A. Serradell, M.C. Urdaci, Impact of *Kéfir* derived *Lactobacillus Kéfir* on the mucosal immune response and gut microbiota, *J. Immunol. Res.*, **2015**, 361604:1-12 (2015).

24. A. Londero, C. Iraporda, G.L. Garrote, A.G. Abraham, Cheese whey fermented with *Kéfir* micro-organisms: Antagonism against Salmonella and immunomodulatory capacity, *Int. J. Dairy Technol.*, **68**, 118-126 (2015).

25. J. Gao, F. Gu, H. Ruan, Q. Chen, J. He, G. He, Induction of apoptosis of gastric cancer cells SGC7901 *in vitro* by a cell-free fraction of Tibetan *Kéfir*, Int. Dairy J., **30**, 14-18 (2013).

26. P.P. McCue, K. Shetty, Phenolic antioxidant mobilization during yogurt production from soymilk using *Kéfir* cultures, *Process Biochem.*, **40**, 1791-1797 (2005).

27. M.R. Prado, L.M. Blandón, L.P.S. Vandenberghe, C. Rodrigues, G.R. Castro, V. Thomaz-Soccol, C.R. Soccol, Milk *Kéfir*: composition, microbial cultures, biological activities, and related products, *Front. Microbiol.*, **6**, 1177,1-10 (2015).

28. I.C.H., *Preclinical safety evaluation of biotechnology-derived pharmaceuticals S6(R1)*, Guideline, 1997.

29. J. Lehmann, M.R. Schulz, R. Sanzenbacher, Strategic considerations on the design and choice of animal models for non-clinical investigations of cell-based medicinal products, *Bundesgesundheitsblatt - Gesundheitsforsch. - Gesundheitsschutz*, **58**, 1215-1224 (2015).

30. J. Mao, M.F. Smith, E.B. Rucker, G.M. Wu, T.C. McCauley, T.C. Cantley, R.S. Prather, B.A. Didion, B.N. Day, Effect of epidermal growth factor and insulin-like growth factor I on porcine preantral follicular growth, antrum formation, and stimulation of granulosal cell proliferation and suppression of apoptosis *in vitro*, *J. Anim. Sci.*, **82**, 1967-1975 (2004).

31. D.M. Magalhães-Padilha, P.M. Andrade, E.T. Sales, V.R. Araujo, I.M.T. Lima, S.V. Castro, L.R. Faustino, C.A.P. Lopes, C.C. Campello, S.N. Báo, M.O. Gastal, E.L. Gastal, J.R. Figueiredo, Effect of sequential medium on *in vitro* culture of goat ovarian cortical tissue, *Anim. Reprod. Sci.*, **132**, 159-168 (2012).

32. P.S.P. Gupta, S. Nandi, B.M. Ravindranatha, P.V. Sarma, *In vitro* culture of buffalo (*Bubalus bubalis*) preantral follicles, *Theriogenology*, **57**, 1839-1854 (2002).

33. G. Chamorro, S. Salazar, L. Favila-Castillo, C. Steele, M. Salazar, Reproductive and peri- and postnatal evaluation of *Spirulina maxima* in mice, *J. Appl. Phycol.*, **9**, 107-112 (1997).

34. B. Geffroy, O. Simon, Effects of a *Spirulina platensis*-based diet on zebrafish female reproductive performance and larval survival rate, *Cybium, Int. J. Ichthyol.*, **37**, 31-38 (2013).

35. E.E. Owaga, M.J. Chen, W.Y. Chen, C.W. Chen, R.H. Hsieh, Oral toxicity evaluation of *Kéfir*-isolated *Lactobacillus Kéfiranofaciens* M1 in Sprague-Dawley rats, *Food Chem. Toxicol.*, **70**, 157-162 (2014).

36. K.P. Xu, T. Greve, A detailed analysis of early events during *in vitro* fertilization of bovine follicular oocytes, *J. Reprod. Fertil.*, **82**, 127-134 (1988).

37. B. Anguita, A.R. Jimenez-Macedo, D. Izquierdo, T. Mogas, M.T. Paramio, Effect of oocyte diameter on meiotic competence, embryo development, p34 (cdc2) expression and MFP activity in prepubertal goat oocytes, *Theriogenology*, **67**, 526-536 (2007).

38. F.P. Gottardi, G.Z. Mingoti, Bovine oocyte maturation and influence on subsequent embryonic developmental competence, *Rev. Bras. Reprodução Anim.*, **33**, 82-94 (2009).

39. R.C. Silva, S.N. Báo, J.L.P.R. Jivago, C.M. Lucci, Ultrastructural characterization of porcine oocytes and adjacent follicular cells during follicles development: lipid component evolution, *Theriogenology*, **76**, 1647-1657 (2011).

40. B.D. Murphy, R.J. Mapletoft, J. Manns, W.D. Humphrey, Variability in gonadotrophin preparations as a factor in the superovulatory response, *Theriogenology*, **21**, 117-125 (1984).

41. M.A. Driancourt, Regulation of ovarian follicular dynamics in farm animals, Implications for manipulation of reproduction, *Theriogenology*, **55**, 1211-1239 (2001).

42. P.S. Baruselli, M.F. De Sá Filho, C.M. Martins, L.F. Nasser, M.F.G. Nogueira, C.M. Barros, G.A. Bó, Superovulation and embryo transfer in *Bos indicus* cattle, *Theriogenology*, **65**, 77-88 (2006).

43. F.M.J. Hughes, W.C. Gorospe, Biochemical identification of apoptosis (programmed cell death) in granulosa cells: evidence for a potential mechanism underlying follicular atresia, *Endocrinology*, **129**, 2415-2422 (1991).

44. W.J. Murdoch, Programmed cell death in preovulatory ovine follicles, *Biol. Reprod.*, **53**, 8-12 (1995).

45. Q. Wang, Q. Sun, Evaluation of oocyte quality: morphological, cellular and molecular predictors, *Reprod. Fertil. Dev.*, **19**, 1-12 (2007).

46. R.J.S, Gonçalves, A.Y.P. Cavalcante, B.B. Gouveia, T.L.B. Lins, R.S. Barberino, V.G. Menezes, , V.R.P. Barros, T.J.S. Macedo, J.R. Figueiredo, M.H.T. Matos, Lower apoptosis rate in ovine preantral follicles from ovaries stored in supplemented preservation media, *Zygote*, **23**, 943-950 (2015).

47. J.R. Figueiredo, J.J. De H. Celestino, L.R. Faustino, A.P.R. Rodrígues, Advances in artificial ovary in goats, *Acta Sci. Vet.*, **38**, S417-S424 (2010).

48. W.H. Nah, I.K. Koh, H.S. Ahn, M.J. Kim, H.G. Kang, J.H. Jun, M.C. Gye, Effect of *Spirulina maxima* on spermatogenesis and steroidogenesis in streptozotocin-induced type I diabetic male rats, *Food Chem.*, **134**, 173-179 (2012).

Como citar este artículo

D.C. Saavedra-Plazas, R. Petterle, C.A. Piechnik, El modelo de ovario artificial como prueba celular para evaluar la seguridad de los extractos de *Spirulina maxima* y *Kéfir*: un estudio preliminar, *Rev. Colomb. Cienc. Quím. Farm.*, **49**(3), 759-775 (2020).

Artículo de investigación clínica / *http://dx.doi.org/10.15446/rcciquifa.v49n3.91344*

Conocimiento preventivo y su práctica entre la población de Colombia hacia la enfermedad por Coronavirus (COVID-19): una perspectiva de género

Paola A. Rivera Diaz[1], Henry Rubiano Daza[2], Juan Camilo Quintero Quimbaya[3], Diana Patricia Hoyos Armero[3], Carolina Herrera Ramírez[3], Sandra Milena Rivera Ospitia[3], Claudia Patricia Ortiz[3]*

[1]Universidad Santiago de Cali, Facultad de Salud, Instituto de Investigaciones Biomédicas, Cali, Colombia.

[2]Universidad Cooperativa de Colombia, Campus Neiva, Programa Derecho, Grupo de Investigación Comdehuila, Neiva, Huila, Colombia.

[3]Corporación Universitaria Minuto de Dios-UNIMINUTO, Programa de Administración en Seguridad y Salud en el Trabajo, Semillero de Investigación en Seguridad y Salud en el Trabajo, Neiva, Huila, Colombia.

*Autor de correspondencia: claudia.ortiz.de@uniminuto.edu.co

Recibido: 13 de julio de 2020

Revisado: 24 de julio de 2020

Aceptado: 27 de julio 2020

Resumen

Este estudio investiga el conocimiento existente de la COVID-19 en ambos sexos y propone una práctica para prevenir la COVID-19. Se realizó un estudio transversal con una encuesta en línea recopilando datos en diferentes regiones de Colombia, a través de un cuestionario validado estructurado y de diseño propio basado en el asesoramiento público general de la Organización Mundial de la Salud (OMS) sobre la prevención de la COVID-19. Este estudio ha empleado la técnica de muestreo de bola de nieve, y contó con 445 participantes (46,5% hombres y 53,5% mujeres). Se identificó que las mujeres no solo tienen un mejor conocimiento, sino que su comportamiento en la práctica es mucho mejor que sus contrapartes masculinas. Aunque los resultados entre hombres y mujeres son muy similares, la pregunta de quedarse en casa es bastante concluyente a favor de las mujeres, quienes son más responsables. Finalmente, el estudio demuestra que las mujeres corren menos riesgo en comparación con los hombres, porque estas tienen mejores prácticas de prevención, como lo indican las estadísticas. Este estudio destaca aún más la idea de que las mujeres son menos propicias para contraer la infección de covid-19 debido a su mejor comportamiento de práctica que los hombres.

Palabras clave: COVID-19, conocimiento preventivo, práctica, Colombia, género, coronavirus.

Summary

Preventive knowledge and its practice among Colombian population towards coronavirus disease (COVID-19): A Gender-Based Perspective

This study investigates the existing knowledge of covid-19 among both genders and a likely use of it in practice to combat COVID-19. Cross sectional study with an online survey and data was collected from Colombia, through a structured, self-design validated questionnaire was created based on the World Health Organization (WHO) general public advice towards COVID-19 prevention. This study has employed snow-ball sampling technique, counted on 445 participants (46.5% male and 53.5% female). This study has found out that women not only carry better knowledge, but their practicing behavior is far better than their male counterparts. Although the results between men and women are very similar, the question about staying at home is quite conclusive in favor of women, who are more responsible. Finally his study proves that women are on a less risk in comparison to men on the basis of prevention practices exercised better as the prevailing statistics indicate. This study highlighted the notion further that women are less conducive to infection of COVID-19 due to their better practicing behavior than men.

Key words: COVID-19, preventive knowledge, practice, Colombia, gender based, coronavirus.

Introducción

El coronavirus SARS-CoV-2, es un nuevo virus zoonótico de la familia coronaviridae que genera la enfermedad por coronavirus 2019 (COVID-19), este virus fue detectado por primera vez en diciembre de 2019 en la ciudad de Wuhan (China) [1], y desde entonces hasta la fecha se han registrado 12 476 028 casos de personas contagiadas en el mundo y 559 998 muertes a causa del mismo, así el coronavirus 2019 en una amenaza importante para la salud pública mundial [2]. La Organización Mundial de la Salud (OMS) lo declara pandemia el 11 de marzo de 2020 y estableció que el coronavirus 2019 causa infecciones respiratorias que pueden ir desde un resfriado común, hasta enfermedades más graves como el síndrome respiratorio agudo grave. Los síntomas de esta patología se han relacionado con los generados por el síndrome respiratorio agudo severo (SARS) y con el síndrome respiratorio del oriente medio (MERS) [3], enfermedades respiratorias causadas por especies de Coronavirus que se transmiten de

persona a persona. Debido a que cuenta con un nivel alto de propagación la OMS hace un llamamiento a todos los países en acoger medidas preventivas urgentes y agresivas ante la pandemia [4].

Desde entonces organizaciones gubernamentales y no gubernamentales han iniciado e incentivado la investigación científica desde diferentes enfoques, pero con un único objetivo: desarrollar la solución que contrarreste la pandemia. La comunidad científica ha generado diversos estudios que han proporcionado información importante, la cual ha permitido identificar las variables directas e indirectas en la propagación del virus, además de avanzar en el desarrollo de un tratamiento antiviral efectivo o una vacuna [5]. Esta solución aún está lejana, por ello, actualmente, varios países han adoptado medidas preventivas que permitan disminuir los contagios por COVID-19 de persona a persona. En Colombia se ha acogido la técnica preventiva basada en el conocimiento y la importancia de la práctica de medidas de prevención como el uso de mascarilla, lavado frecuente de las manos y mantener el distanciamiento social, medidas preventivas recomendadas por organizaciones como el Centros para el Control y la Prevención de Enfermedades [6], la Organización Mundial de la Salud [4] y el Ministerio de Salud de Colombia [7], entre otras.

De acuerdo con la Asociación Europea de Editores de Ciencia, la editorial de la revista *The Lancet* y *GlobalHealth50/50* es necesario investigar las enfermedades desde la perspectiva de género, debido a que en brotes pasados como el SARS, MERS, ébola, zika, se ha evidenciado la mortalidad en hombres y la vulnerabilidad de la enfermedad en mujeres [8]. Los expertos coinciden que es necesario contar con información más detallada que incluyan variables como sexo y edad para generar estrategias que aporten al mejoramiento de atención primaria y secundaria en emergencias sanitarias por brotes. Según López [9] "La experiencia de brotes pasados muestra la importancia de incorporar un análisis de género en los esfuerzos de preparación y respuesta para mejorar la efectividad de las intervenciones de salud y promover objetivos de equidad de género y salud", a su vez, según la información suministrada por algunos entes, se identifica que actualmente la COVID-19 registra mayor mortalidad en hombres, debido a hábitos no saludables como el tabaquismo, la ingesta de bebidas alcohólicas, que propenden a que los hombres sufran de hipertensión, enfermedades cardiovasculares y enfermedades respiratorias lo cual aumenta la probabilidad de mortalidad en el mismo, por otro lado aunque no se establece qué género es el más vulnerable ante la COVID-19 [10], estudios relacionados entre conocimiento y aplicación de este, evidencian que las personas con un conocimiento claro y amplio sobre enfermedades, ejecutan prácticas adecuadas. Generalmente, las mujeres están más informadas y adoptan comportamientos más favorables, que ayudan a la prevención de enfermedades [11].

Metodología

Este un estudio observacional cuantitativo de corte trasversal basado en encuestas diligenciadas en internet. Los datos para este estudio se obtuvieron de 17 departamentos de Colombia: Antioquia, Atlántico, Boyacá, Caldas, Caquetá, Cauca, Cundinamarca, Huila, Magdalena, Meta, Quindío, Risaralda, Santander, Sucre, Tolima y Valle del Cauca y Bogotá D.C., utilizado la técnica de muestreo de bola de nieve no probabilístico.

Se desarrolló un cuestionario para el público basado en la recomendaciones de la Organización Mundial de la Salud [4], estipulando medidas preventivas básicas contra el COVID-19 como lavarse las manos frecuentemente, adoptar medidas de higiene respiratoria, mantener un distanciamiento social de mínimo un metro, cuidados al toser, permanecer en los hogares, entre otras.

La herramienta de recolección de datos esta divida en tres partes. La primera estaba relacionada con la información sociodemográfica como sexo, edad, formación académica y estrato socioeconómico. La segunda parte contenía preguntas relacionadas con el conocimiento de la prevención de COVID-19 y su práctica en la vida cotidiana; este apartado está constituido por un total de 14 preguntas, de las cuales 7 eran para conocimiento y otras 7 para medir la apropiación de ese conocimiento en la vida cotidiana. La última parte del cuestionario contiene 7 preguntas basadas en el conocimiento de la persona, relacionado con la protección contra COVID-19 de acuerdo con las recomendaciones de la OMS. Estas preguntas están relacionadas con el tiempo de cuarentena de personas que llegan del extranjero y las llamadas al número de emergencia 192 en caso de síntomas relacionadas con la infección.

Todas las respuestas se registraron como "Sí" o "No". Los datos se recopilaron mediante un formulario en línea de Google Drive®. El objetivo del estudio se describió a los encuestados antes del consentimiento y la participación fue completamente voluntaria. Se registraron un total de 445 respuestas (considerando una población de 50 100 000 habitantes y, de acuerdo con los parámetros de la fórmula para calcular el tamaño de la muestra sobre una población finita, con un nivel de confianza del 95 % se establece un numero de muestra de 383). Los datos fueron recopilados desde el 8 hasta el 10 de julio de 2020. Todos los datos se codificaron y transfirieron a Microsoft Excel®, y luego se transfirieron a el programa RStudio versión libre para su análisis. Se utilizó la prueba de chi-cuadrado de Pearson para verificar la significación estadística. El valor de $p < 0{,}05$ se consideró significativo.

Resultados y discusión

Se encuestaron a un total de 445 personas (hombres: 46,5%; mujeres: 53,5%), los rangos de edad se establecieron de acuerdo con ciclo propuesto por el Ministerios de Salud [12] que define que el 18% son jóvenes de entre 18 y 26 años de edad, el 77,1% son personas adultas de entre 27 y 59 años de edad y el 4,9% son mayores de edad (>60 años). En cuanto a la formación académica la mayor proporción son profesionales (49,7) seguido de profesionales con maestría (24%) y educación media (20,2). Finalmente, en cuanto a información sociodemográfica, la población encuestada en su mayoría pertenece a los estratos 2 y 3 (41,8% y 31,5%) (tabla 1).

Tabla 1. Información sociodemográfica de la población encuestada.

Variables	Masculino (n= 207; 46,5%)	Femenino (n=238; 53,5%)	Total (n =445)
	n (%)	n (%)	n (%)
Edad en años			
18-26	31 (7,0)	49 (11,0)	80 (18,0)
27-59	164 (36,9)	179 (40,2)	343 (77,1)
>60	12 (2,7)	10 (2,2)	22 (4,9)
Formación académica			
Primaria	4 (0,9)	4 (0,9)	8 (1,8)
Secundaria	32 (7,2)	58 (13,0)	90 (20,2)
Profesional	100 (22,3)	121 (27,2)	221 (49,7)
Maestría	60 (13,5)	47 (10,6)	107 (24)
Doctorado	11 (2,5)	8 (1,8)	19 (4,3)
Estrato socioeconómico			
1	6 (1,3)	25 (5,6)	31 (7,0)
2	94 (21,1)	92 (20,7)	186 (41,8)
3	69 (15,5)	71 (16,0)	140 (31,5)
4	28 (6,3)	33 (7,4)	61 (13,7)
5	8 (1,8)	11 (2,5)	19 (4,3)
6	2 (0,4)	6 (1,4)	8 (1,8)

En general, la población está informada y respondió de manera correcta las preguntas basadas en el conocimiento relacionadas con la propagación de COVID-19, incluido, el uso de mascarilla o tapabocas (P1. 96,9%) lavarse las manos durante 20 segundos (P2. 96,6%), estornudar o toser en el brazo/codo (P3. 85,9%) , el coronavirus se puede transferir dándose la mano (P4. 90,8%), manteniendo una distancia segura de al menos 1 metro (88,1%), tocando la cara puede transferir el coronavirus (P5. 95,1%), quedarse en casa puede disminuir las posibilidades de contraer una infección (P6. 98,0%). Los encuestados informaron el menor conocimiento acerca de la pregunta que refiere que el coronavirus puede permanecer en los objetos durante algunas semanas o días (P10. 83,6%) y de la llamada al 192 para buscar atención médica para el coronavirus (P8. 79,5%). Pese a que los porcentajes sobre aciertos en general son altos, preguntas como la P1, P3 y P4 que implican interacción social, presentan entre el 4% al 15 % de desconocimiento, lo que pone en alto riesgo la población.

Realizado un análisis en función del género (tablas 2 y 3), los resultados muestran lo siguiente: con respecto al "uso de mascarilla o tapabocas (P1)", las mujeres tienen un mejor conocimiento respecto a los hombres (F: 98%; M: 96%; p>0,05). En respuesta al "lavado de manos durante mínimo 20 segundo (P2)", de nuevo las mujeres muestran tener un mejor conocimiento respecto a los hombres (F: 98%; M: 95%; p>0,05). En respuesta al conocimiento sobre "estornudar o toser en el brazo / codo (P3)", las mujeres estaban mejor informadas que los hombres y el valor "p" fue estadísticamente significativo (F: 92%; M: 79%; p<0,05), indicando una relación entre la respuesta y el género. Frente al conocimiento "sobre el contagio de COVID-19 por darse la mano (P4)" las mujeres presentaron mayores aciertos (F: 93%; M: 88%; p>0,05). A la pregunta sobre "distanciamiento social (P5)" las mujeres muestran un mejor conocimiento que los hombres (F: 90%; M: 86%; p>0,05). En cuanto a la pregunta sobre "tocar la cara puede transferir el coronavirus (P6)" las mujeres continúan estando mejor informadas que los hombres (F: 97%; M: 93%; p>0,05). El conocimiento sobre "quedarse en casa puede disminuir las posibilidades de contraer una infección (P7)", (F: 98%; M: 99%; p>0,05) ambos géneros son conscientes del tema con un leve repunte en los hombres. En respuesta a la pregunta sobre "puede llamar al 192 para buscar atención médica para el coronavirus (P8)", de nuevo además de no haber una diferencia marcada entre géneros ambos presentan un buen conocimiento sobre la línea telefónica (F: 79%; M: 80%; p>0,05). El conocimiento sobre "las personas mayores tienen un mayor riesgo de desarrollar coronavirus (P9) "continua la similitud en las respuestas entre hombres y mujeres (F: 98%; M: 97%; p>0,05). En respuesta a "el coronavirus puede permanecer en los objetos durante algunas semanas o días (P10)", ambos sexos, ofrecen respuestas similares (F: 84%; M: 83%; p>0,05). Del mismo modo, para la pregunta "las personas que han viajado desde el extranjero no deben conocer a otras personas durante 2

semanas (P11)", la respuesta de ambos sexos es prácticamente la misma (F: 100%; M: 99%; p>0,05), y es la pregunta de mayor acierto por parte de los encuestados. Respondiendo a "evitar el contacto con personas que tienen tos/fiebre (P12)", vuelve a presentarse el consenso entre hombres y mujeres, con un alto grado de acierto de todas las personas (F: 99%; M: 98%; p>0,05). En respuesta a la pregunta "debe buscar atención médica si tiene tos, fiebre y dificultad para respirar (P13)" la tendencia es la misma entre sexos (F: 98%; M: 97%; p>0,05).

Tabla 2. Preguntas sobre el conocimiento de algunas medidas preventivas contra la COVID-19, propuestas por la OMS.

P	Pregunta		Masculino n (%)	Femenino n (%)	Total n (%)	Valor-p
1	¿El uso de mascarilla o tapaboca ayuda a prevenir el contagio de coronavirus?	Sí	198 (95,6)	233 (97,9)	431 (96,9)	0,2792
		No	9 (4,3)	5 (2,1)	14 (3,1)	
2	¿Lavarse las manos durante 20 segundos, puede ayudar a prevenir el coronavirus?	Sí	196 (94,7)	234 (98,3)	430 (96,6)	0,0636
		No	11 (5,3)	4 (1,7)	15 (3,4)	
3	¿Toser o estornudar en el brazo/ codo puede evitar la propagación del coronavirus?	Sí	164 (79,2)	218 (91,6)	382 (85,9)	**0,0003**
		No	43 (20,8)	20 (8.4)	63 (14.1)	
4	¿El coronavirus puede transferirse por darse la mano?	Sí	183(88.4)	221(92,8)	404 (90,8)	0,1456
		No	24 (11,6)	17 (7,2)	41 (9,2)	
5	¿Mantener una distancia mínima de 1 metro con otras personas ayuda al no contagio del coronavirus?	Sí	177 (85,5)	215 (90,3)	392 (88,1)	0,155
		No	30 (14,5)	23 (9,7)	53 (11,9)	
6	¿Tocarse la cara puede transferir el coronavirus?	Sí	193(93,2)	230 (96,6)	423 (95,1)	0,1521
		No	14 (6,8)	8 (3,4)	22 (4,9)	
7	¿Permanecer en cuarentena (estar en casa) disminuye la probabilidad de contraer el coronavirus?	Sí	204(98,6)	232 (97,5)	436 (98,0)	0,643
		No	3 (1,4)	6 (2,5)	9 (2,0)	
8	¿El gobierno nacional dispone de la línea gratuita 192 para orientación sobre COVID-19?	Sí	166(80,2)	188 (79,0)	354 (79.5)	0,8449
		No	41 (19,8)	50 (21,0)	91 (20,4)	
9	¿Las personas de la tercera edad son más vulnerables ante el COVID-19?	Sí	201(97,1)	234 (98,3)	435 (97,8)	0,5865
		No	6 (2,9)	4 (1,7)	10 (2,2)	

(*Continúa*)

Tabla 2. Preguntas sobre el conocimiento de algunas medidas preventivas contra la COVID-19, propuestas por la OMS.

P	Pregunta		Masculino n (%)	Femenino n (%)	Total n (%)	Valor-p
10	¿El virus puede permanecer en los objetos durante días o semanas?	Sí	171(82,6)	201 (84,4)	372 (83,6)	0,6922
		No	36 (17,4)	37 (15,6)	73 (16,4)	
11	¿Las personas que llegan del extranjero deben permanecer aisladas durante un periodo mínimo de 14 días?	Sí	205(99,0)	237 (99,6)	442 (99,4)	0,9034
		No	2 (1,0)	1 (0,4)	3 (0,6)	
12	¿Se debe evitar el contacto con personas que presentan tos o fiebre?	Sí	203 (98,1)	236 (99,2)	439 (98,6)	0,5591
		No	4 (1,9)	2 (0,8)	6 (1,3)	
13	¿Se debe buscar atención médica si se presentan síntomas de tos, fiebre, problemas para respirar?	Sí	201 (97,1)	234 (98,3)	435 (97,8)	0,5865
		No	6 (2,9)	4 (1,7)	10 (2,2)	

Tabla 3. Preguntas sobre la práctica de algunas medidas preventivas contra la COVID-19, propuestas por la OMS.

P	Pregunta		Masculino n (%)	Femenino (%)	Total n (%)	Valor-p
14	¿Usted utiliza siempre mascarilla o tapaboca al salir de su casa?	Sí	203 (98,1)	235 (98,7)	438 (98,4)	0,8523
		No	4 (1,9)	3 (1,3)	7 (1,6)	
15	¿Usted lava sus manos frecuentemente y mínimo por 20 segundos?	Sí	182 (87,9)	217 (91,2)	399 (89,7)	0,3328
		No	25 (12,1)	21 (8,8)	46 (10,3)	
16	¿Usted se cubre la cara con el brazo/codo al toser o estornudar?	Sí	183 (88,4)	219 (92,1)	402 (90,3)	0,2605
		No	24 (11,6)	19 (7,9)	43 (9,7)	
17	¿Usted al saludar a otra persona da la mano o beso?	Sí	20 (9,7)	22 (9,2)	42 (9,4)	1,0
		No	187 (90,3)	216 (90,8)	403 (90,5)	
18	¿Usted mantiene una distancia mínima de 1 metro mientras se encuentra con otras personas en estos días de pandemia?	Sí	183 (88,4)	228 (95,8)	411 (92.3)	**0,0060**
		No	24 (11,6)	10 (4,2)	34 (7,6)	

(*Continued*)

Tabla 3. Preguntas sobre la práctica de algunas medidas preventivas contra la COVID-19, propuestas por la OMS.

P	Pregunta		Masculino n (%)	Femenino (%)	Total n (%)	Valor-p
19	¿Usted evita tocarse la cara?	Sí	180 (87,0)	221 (92,8)	401 (90,1)	0,0548
		No	27 (13,0)	17 (7,2)	44 (9,9)	
20	¿Usted permanece en casa a menudo?	Sí	181 (87,4)	219 (92,0)	400 (89,9)	0,1499
		No	26 (12,6)	19 (8,0)	45 (10,1)	

En cuanto a las respuestas sobre preguntas que pretenden evaluar la apropiación del conocimiento (P14-P20) (tabla 3) la práctica de usar mascarilla o tapabocas (P14) y saludar a personas dándoles la mano o un beso (P17), no hay diferencia significativa entre las respuestas dadas por hombres y mujeres. Aunque P14 presenta un grado de apropiación, P17 muestra que un 10% de las personas continúan saludando, dando la mano/beso, lo que se constituye en un factor de riego alto para la propagación de la pandemia. En cuanto a lavase las manos por mínimo 20 segundos (P15), las mujeres practicaban más esta acción que los hombres (F: 91%; M: 88%; $p>0,05$). Respeto a cubrirse la cara con el codo/brazo al estornudar o toser, de nuevo las mujeres son más consientes al realizar esta práctica (F: 92%; M: 88%; $p>0,05$). Al indagar sobre el distanciamiento social de mínimo 1 metro, las mujeres practican más esta acción que los hombres y presenta un p menor a 0,05 indicando una relación entre el sexo del individuo y la práctica (F: 96%; M: 88%; $p<0,05$); finalmente, a las preguntas "evita tocarse la cara (P19)" y "permanece en casa a menudo (P20)" las mujeres vuelven a tener un mayor grado de concienciación (F: 93%; M: 87%; $p<0,05$) y (F: 92%; M: 87%; $p<0,05$).

En la tabla 4 se presentan los porcentajes de aplicación del conocimiento en la práctica, y se identificó un fenómeno que, aunque no se podría calificar como atípico, puede llegar a ser interesante. Si bien las personas registran no tener conocimiento sobre una práctica, sus acciones son correctas, por lo que se obtienen porcentajes mayores al 100% como es el caso de las relaciones (R) 1, 3, 4 y 5. Lo anterior, podría deberse a que, si bien las personas no tienen el conocimiento, o creen que estas prácticas no contribuyen al control de la pandemia, la obligación de cumplir una norma jurídica o social obliga a los individuos a actuar de forma correcta.

Ahora bien, con respecto al uso de mascarillas (R1) o tapabocas los hombres practican más sus conocimientos que las mujeres (102,5 vs. 100,9), los hombres también practican más sus conocimientos respecto a poner su brazo o codo al estornudar (R3) (111,6 vs 100,4) y no estrechar la mano o dar besos (R4) (102,2 vs 97,7). Con relación a

Tabla 4. Apropiación del conocimiento relacionado con prácticas recomendadas por la OMS para contrarrestar la pandemia de la COVID-19.

R	Apropiación del conocimiento	Masculino %	Femenino %	Valor-p
1.	Influencia del conocimiento del uso de la mascarilla o tapaboca al salir de su casa	102,5	100,9	0,9582
2.	Influencia del conocimiento de lavarse las manos en la práctica	92,9	92,7	0,9519
3.	Influencia del conocimiento de estornudos/ tos en la práctica	111,6	100,4	0,5105
4.	Influencia del conocimiento de no estrechar la mano en la práctica	102,2	97,7	0,8070
5.	Influencia del conocimiento de la distancia social en la práctica	103,4	106,0	0,9142
6.	Influencia del conocimiento sobre la propagación de la infección al tocar la cara en la práctica	93,26	96.01	0,8864
7.	Influencia del conocimiento de quedarse en casa para prevenir infecciones en la práctica	88,7	94,39	0,7065

practicar su conocimiento del lavado de manos durante al menos 20 minutos (R2) tanto hombres como mujeres presentan una apropiación del 93%. En cuanto a las relaciones 5 (distanciamiento social), 6 (tocarse la cara) y 7 (permanecer en casa), las mujeres adoptaron más estas prácticas que los hombres.

El objetivo del presente estudio fue medir las diferencias específicas de género en el conocimiento y la práctica para prevenir COVID-19 en la población colombiana. Actualmente, no hay una vacuna contra este virus y las opciones de tratamiento no tienen respuesta efectiva. Las organizaciones mundiales de salud pública, incluida la OMS [4], los ministerios de salud de diferentes países y el Centro para el Control y la Prevención de Enfermedades de Estados Unidos [13] han recomendado al público adoptar medidas preventivas simples para limitar la exposición y la propagación del virus. Estas recomendaciones son prácticas de higiene, aislamiento y distanciamiento social como la forma más efectiva de detener la propagación del virus. El Ministerio de Salud de Colombia ha implementado programas de sensibilización pública y medidas de prevención y mitigación. Estos programas contribuyeron con un papel integral para concienciar al público sobre los síntomas, la propagación y las recomendaciones para la prevención mediante diferentes medios de comunicación.

En general, este estudio reveló que la mayoría de los encuestados tenían un nivel significativo de conocimiento y también seguían las instrucciones de prevención recomendadas

por la OMS. Sin embargo, las mujeres están mejor informadas sobre las preguntas basadas en el conocimiento y también asimilaban mejor los conocimientos relacionados con la prevención del virus en comparación con los hombres. La significativa apropiación del conocimiento (tabla 4) puede ser consecuencia de varios factores como, el impacto de las campañas de sensibilización, la exigencia en la aplicación de normas tendientes al control de la pandemia, entre otros. Esto muestra, que las mayorías de las personas presentan un alto grado de sensibilización, además de permanecer bien informadas pese al gran número de noticias falsas presentadas en redes sociales [14,15] que pueden llevar a la población a automedicarse, esto podría implicar mayores complicaciones en los sistemas de salud [16, 17].

Otro hallazgo interesante de este estudio es que las mujeres también presentaban una mayor aplicación de sus conocimientos en comparación con sus homólogos masculinos. La mortalidad e infección por COVID-19 entre hombres es mayor en comparación con las mujeres. Los datos de los 39 países más afectados no presentan un informe contúndete sobre quien padece más la infección entre hombres y mujeres, sin embargo, la mortalidad de los hombres es mayor en comparación con las mujeres [18]. Los resultados adversos en los hombres están relacionados con comorbilidades, que incluyen enfermedades pulmonares, hipertensión y problemas cardiovasculares, que están relacionados con el tabaquismo y el consumo de alcohol, en comparación con las mujeres (4,7% frente a 2,8%) [19]. Estudios anteriores sobre el SARS, la gripe, el ébola y el VIH han mostrado diferentes relaciones entre la infección, hombres y mujeres, demostrando que los hombres corren mayor riesgo de infección [18].

La falta de conocimiento y prácticas para prevenir la COVID-19, sumado a la tendencia presentada por los estudios desarrollados por De Loyola Filho *et al*, y Ortiz *et al*, en Brasil y Colombia respectivamente [16, 20], los cuales documentan que los hombres presentan mayor tendencia por prácticas riesgosas como la automedicación, aumentan el riesgo de contagio. Como se constata en las últimas recomendaciones de funcionarios como el presidente de los Estados Unidos, Donald Trump y el alcalde la Ciudad de Santiago de Cali, sobre consumo de hidroxicloroquina, ivermectina y desinfectantes, además del uso del dióxido de cloro [21, 22]. Estas prácticas pueden transformarse en otro factor de riesgo que podría sumarse a la razón por la cual se presenta un mayor potencial de tasa de muertes entre los hombres, por lo que una mayor concienciación hacia los hombres podría disminuir la mortalidad de los mismos. Así mismo, estos estudios sustentan la mayor responsabilidad por parte de las mujeres frente al cuidado de su salud, lo que concuerda con los resultados obtenidos en el presente estudio.

Conclusiones

A partir de los hallazgos se puede observar que las mujeres no solo poseen un mejor conocimiento que los hombres para la mayoría de los ítems, sino que también aplican mejor las medidas prácticas que ellos. Las mujeres que se quedan en casa están menos expuestas al virus en comparación con los hombres, lo que puede ser un argumento de consideración válida para futuros estudios. En general, este estudio es un esfuerzo por contribuir con la comprensión de la noción de por qué los hombres son más propensos para la infección que las mujeres. Además, este estudio, aunque con todas sus limitaciones de solo enfocarse en la población colombiana es una contribución sustancial para que los responsables de políticas públicas lo incluyan como una guía en la emisión de medidas prácticas basadas en el conocimiento con perspectiva de género en la prevención la infección de COVID-19.

Conflicto de intereses

Los autores no declaran conflicto de intereses.

Agradecimientos

Nos gustaría expresar nuestro agradecimiento al señor Milcíades Ortiz D. por su colaboración en la recolección de la información para la presente investigación.

Referencias

1. P. Amariles, J. Granados, M. Ceballos, C.J. Montoya, COVID-19 in Colombia endpoints. Are we different, like Europe?, *Research in Social and Administrative Pharmacy*, **16**, 267-436 (2020).

2. M. Zhou, X. Zhang, J. Qu, Coronavirus disease 2019 (COVID-19): a clinical update, *Frontiers of Medicine*, **14**, 126-135 (2020).

3. C. Ramos, Covid-19: la nueva enfermedad causada por un coronavirus, *Salud Pública de México*, **62**, 225-227 (2020).

4. Organización Mundial de la Salud, *Brote de enfermedad por coronavirus (COVID-19): orientaciones para el público*, 2019, URL: https://www.who.int/es/emergencies/diseases/novel-coronavirus-2019/advice-for-public, accesado el 10 de julio de 2020.

5. R. Trejo-González, M.S. Ramiro-Mendoza, H.G. Hernández-Orozco, ¿Cuáles son las medidas de prevención contra el Novel Coronavirus (COVID-19)?, *Revista Latinoamericana de Infectología Pediátrica*, **33**, 4-6 (2020).

6. M.Y. Yen, J. Schwartz, C.C. King, C.M. Lee, P.R. Hsueh, Recommendations for protecting against and mitigating the COVID-19 pandemic in long-term care facilities, *Journal of Microbiology, Immunology and Infection*, **53**, 447-453 (2020).

7. Ministerio de Salud de Colombia, *Coronavirus (COVID-19)*, (n.d.)., URL: https://www.minsalud.gov.co/salud/publica/PET/Paginas/Covid-19_copia.aspx, accesado el 10 de julio de 2020.

8. The Lancet Editorial, The gendered dimensions of COVID-19, *The Lancet*, **395**(10231), 1168 (2020).

9. C.M. Lopez, ¿Afecta por igual el COVID-19 a hombres y mujeres?, *Gaceta Médica*, (n.d.). URL: https://gacetamedica.com/investigacion/afecta-por-igual-el-covid-19-a-hombres-y-mujeres/, accesado el 10 de julio de 2020.

10. C. Wenham, J. Smith, R. Morgan, COVID-19: the gendered impacts of the outbreak, *The Lancet*, **395**, 846-848 (2020).

11. L.K.P. Suen, Z.Y.Y. So, S.K.W. Yeung, K.Y.K. Lo, S.C. Lam, Epidemiological investigation on hand hygiene knowledge and behaviour: A cross-sectional study on gender disparity, *BMC Public Health*, **19**, 401 (2019).

12. Ministerio de Salud de Colombia, *Ciclo de vida*, URL: https://www.minsalud.gov.co/proteccionsocial/Paginas/cicloVida.aspx, accesado el 10 de julio de 2020.

13. Centers for Disease Control and Prevention, *How to protect yourself and others*, URL: https://espanol.cdc.gov/coronavirus/2019-ncov/prevent-getting-sick/prevention.html, accesado el 10 de julio de 2020.

14. J.-M. Manus, Fake news: et si moustiques et tiques transmettaient le Covid-19?, *RFL - Revue Francophone des Laboratoires*, **2020**(524), 12 (2020).

15. S. Talwar, A. Dhir, D. Singh, G.S. Virk, J. Salo, Sharing of fake news on social media: Application of the honeycomb framework and the third-person effect hypothesis, *Journal of Retailing and Consumer Services*, **57**, 102197 (2020).

16. C.P. Ortiz, O.D. Fúnez-David, H. Rubiano-Daza, C.L. García-Rojas, C.A. Calderón-Ospina, D.R. Delgado, Automedicación en estudiantes de la Sede Neiva de la Universidad Cooperativa de Colombia, *Revista Colombiana de Ciencias Químico-Farmacéuticas*, **48**, 128-144 (2019).

17. C.A. Calderón, F. Soler, A.M. Pérez-Acosta, El observatorio del comportamiento de automedicación de la Universidad del Rosario y su rol en la pandemia de COVID-19, *Revista Ciencias de la Salud*, **18**, 1-8 (2020).

18. S. Rozenberg, J. Vandromme, M. Charlotte, Are we equal in adversity? Does Covid-19 affect women and men differently?, *Maturitas*, **138**, 62-68 (2020).

19. J. Kuriansky, *The Psychosocial Aspects of a Deadly Epidemic: What Ebola Has Taught Us about Holistic Healing*, ABC-CLIO, Westport, 2016, vol. 1, p. 428.

20. A.I. Loyola-Filho, E. Uchoa, H.L. Guerra, J.O.A. Firmo, M.F. Lima-Costa, Prevalence and factors associated with self-medication: The Bambuí health survey, *Revista Saude Publica*, **36**, 55-62 (2002).

21. British Broadcasting Corporation (BBC), *Trump drug hydroxychloroquine raises death risk in Covid patients, study says* - BBC News, (n.d.), URL: https://www.bbc.com/news/world-52779309, accesado el 24 de julio de 2020.

22. Organización Mundial de la Salud, *Consejos para la población acerca de los rumores sobre el nuevo coronavirus (2019-nCoV)*, (n.d.), URL: https://www.who.int/es/emergencies/diseases/novel-coronavirus-2019/advice-for-public/myth-busters?gclid=EAIaIQobChMInr2_0PXl6gIVAeDICh3RzgNjEAAYASAAEgKDDfD_BwE, accesado el 24 de julio de 2020.

Como citar este artículo

P.A. Rivera-Diaz, H. Rubiano-Daza, J.C. Quintero-Quimbaya, D.P. Hoyos-Armero, C. Herrera-Ramírez, S.M. Rivera-Ospitia, C.P. Ortiz, Conocimiento preventivo y su práctica entre la población de Colombia hacia la enfermedad por Coronavirus (COVID-19): una perspectiva de género, *Rev. Colomb. Cienc. Quím. Farm.*, **49**(3), 776-789 (2020).

Technological research article / *http://dx.doi.org/10.15446/rcciquifa.v49n3.91345*

Aloe gel: manipulation and characterization of physical-chemical quality adjustment

Italy Heibe Mendes Aciole[1], Francisco Patricio de Andrade Júnior[2], Laísa Vilar Cordeiro[3], Júlia Beatriz Pereira de Souza[4]

[1]Academic Unit of Health, Education and Health Center, Universidade Federal de Campina Grande, 58175-000, Cuité, Paraíba, Brazil. E-mail: italymendes@hotmail.com

[2]PhD student of Programa de Pós-Graduação em Produtos Naturais e Sintéticos Bioativos at Universidade Federal da Paraíba, 58033-455, João Pessoa, Paraíba, Brazil. E-mail: juniorfarmacia.ufcg@outlook.com

[3]PhD student of Programa de Pós-Graduação em Produtos Naturais e Sintéticos Bioativos at Universidade Federal da Paraíba, 58033-455, João Pessoa, Paraíba, Brazil. E-mail: laisavilar@gmail.com

[4]Professor PhD at Universidade Federal de Campina Grande, 58429-900, Cuité, Paraíba, Brazil. E-mail: juliabtriz@gmail.com

Received: 14 July 2019

Revised: 24 July 2020

Accepted: 27 July 2020

Summary

The objective of the study was to develop and characterize the gel based on *Aloe vera* for the Manoel Casado de Almeida Pharmacy School. The research was done at the Education and Health Center off the Federal University of Campina Grande, located in the city of Cuité (PB). For the quality control, chemical physical tests were carried out as determine pH, apparent density, viscosity, spreadability and centrifugation test. The gel demonstrated acceptable physicochemical characteristics exhibiting pH 5, bulk density 0.1018 (± 0.0008), viscosity above 10 000 cP, and adequate stability. Complementary studies on microbiological quality are suggested, to give safety on their therapeutic potential in wound management.

Key words: *Aloe*, phytotherapy, medicinal plants, complementary therapies.

Resumen

Gel de aloe: manipulación y caracterización del ajuste de la calidad físico-química

El estudio tuvo como objetivo desarrollar y caracterizar el gel a base de *Aloe vera* para la Escuela de Farmacia Manoel Casado de Almeida. La investigación se llevó a cabo en el Centro de Educación y Salud, Universidad Federal de Campina Grande, ubicada en la ciudad de Cuité (PB). Para el control de calidad, se realizaron las siguientes pruebas físico-químicas: determinación de pH, densidad aparente, viscosidad, capacidad de propagación y prueba de centrifugación. El gel mostró características fisicoquímicas aceptables, con pH 5, densidad aparente 0,1018 (± 0,0008), viscosidad superior a 10 000 cP y estabilidad adecuada. Por lo tanto, se sugieren estudios complementarios con respecto a la calidad microbiológica, lo que garantiza la seguridad dado su potencial terapéutico en el tratamiento de heridas.

Palabras clave: *Aloe*, fitoterapia, plantas medicinales, terapias complementarias.

Resumo

Gel de babosa: manipulação e caracterização de parâmetros físico-químicos de qualidade

O estudo teve como objetivo desenvolver e caracterizar o gel a base de *Aloe vera* para Farmácia Escola Manoel Casado de Almeida. A pesquisa foi realizada no Centro de Educação e Saúde, da Universidade Federal de Campina Grande, situado na cidade de Cuité (PB). Para o controle de qualidade foram realizados os seguintes ensaios físico-químicos: determinação de pH, densidade aparente, viscosidade, espalhabilidade e teste de centrifugação. O gel demonstrou características físico-químicas aceitáveis apresentando pH 5, densidade aparente 0,1018 (± 0,0008), viscosidade acima de 10 000 cP e estabilidade adequada. Assim, sugere-se estudos complementares no tocante a qualidade microbiológica, garantindo a segurança dado seu potencial terapêutico no manejo de feridas.

Palavras-chave: *Aloe*; fitoterapia; plantas medicinais; terapias complementarias.

Introduction

Phytotherapy is an ancient practice that uses plants to treat diseases, being an alternative that does not use isolated active substances, preserving the original composition of the original plant [1, 2]. It is still possible to notice a certain resistance from prescribing professionals to the use of medicinal plants and herbal medicines. This low adherence occurs, often, due to the discredit in therapy and the lack of technical-scientific knowledge [3, 4].

Due to the high consumption of medicinal plants/herbal medicines and insecurity about their quality controls, on June 22, 2006, the National Policy on Medicinal Plants and Herbal Medicines [5] was created in Brazil, through a decree of the presidential republic. This measure is of great importance for SUS, which aims in its guidelines to ensure the effectiveness, quality and safety of these products, in addition to easy access for treatment. It is also the aim of SUS that these treatments be a less costly alternative, especially for poor communities.

Currently, the phytotherapy is experiencing a new level with recent publications, bringing credibility and security to patients and health professionals. Thus, transforming it not only in an alternative therapy, but in a possibility that the herbal medicines, in some cases, are considered as treatment of first choice [4].

Skin lesions, burns, skin infections and chronic wounds, have a greater difficulty in healing, impair the functions of the skin, and in more severe cases can lead to death. Thus, they require greater care in the long term, increasing costs for health systems worldwide [6].

In order to minimize costs, the use of medicinal plants and natural products is being a new alternative for the treatment of wounds, especially in developing countries [7]. The search for alternative therapies to promote wound healing has been intensified, while modern therapies with antibiotics and corticosteroids have been neglected due to the side effects that conventional drugs can cause [8].

Aloe vera L. or *Aloe barbadensis*, popularly known as "babosa", is one of the most important medicinal plants in the treatment of wounds, considering that countless studies report its healing and anti-inflammatory properties [9].

Considering the high consumption of medicinal plants and natural products as low-cost treatments by the low-income population, and understanding that the lack of uniformity of the chemical composition, together with the presence of contaminants, cause deficiency in the safety of these products, it is important to develop formulations

that ensure the quality of medicinal products of plant origin, since it directly interferes with efficacy and may offer risks to consumer health.

In this context, the present study aimed to develop and characterize a formulation of aloe gel as an alternative for the treatment of wounds, as well as to compose the portfolio of formulations of the Pharmacy School Manuel Casado de Almeida of the Federal University of Campina Grande, Education Center and Health, Campus Cuité (PB).

Material and methods

The research was carried out at the Federal University of Campina Grande, campus Cuité (CES), in the teaching laboratories of the Pharmacy course and in the Pharmacy School Manoel Casado de Almeida.

Plant material

Initially, *Aloe vera* leaves were collected from the medicinal plant garden at the Education and Health Center (CES), and then the material was prepared, which included: washing, removing mucilage and crushing to prepare the glycolic extract.

Preparation of glycolic extract

The extract was prepared according to the steps shown in figure 1. After crushing, the material was weighed and added in a wide-mouthed bottle. Separately, in a beaker, a solution of 50% Ethanol and 5% Propylene Glycol was prepared, and then added to the flask containing the mucilage, which was left to soak for eight days with daily stirring. After this period, the material was filtered, stored in amber glass, in a dry place and protected from light [10].

Preparation of *Aloe vera* gel

Table 1 shows the components present in the formulation of the *Aloe vera* gel, with their respective quantities specified for 100 g.

To produce the *Aloe vera* gel, the carbopol 940 gel shown in figure 2 was prepared.

Chemical physical analysis

pH determination

The pH was determined directly in a calibrated pH meter, as described in the Brazilian Pharmacopeia [12].

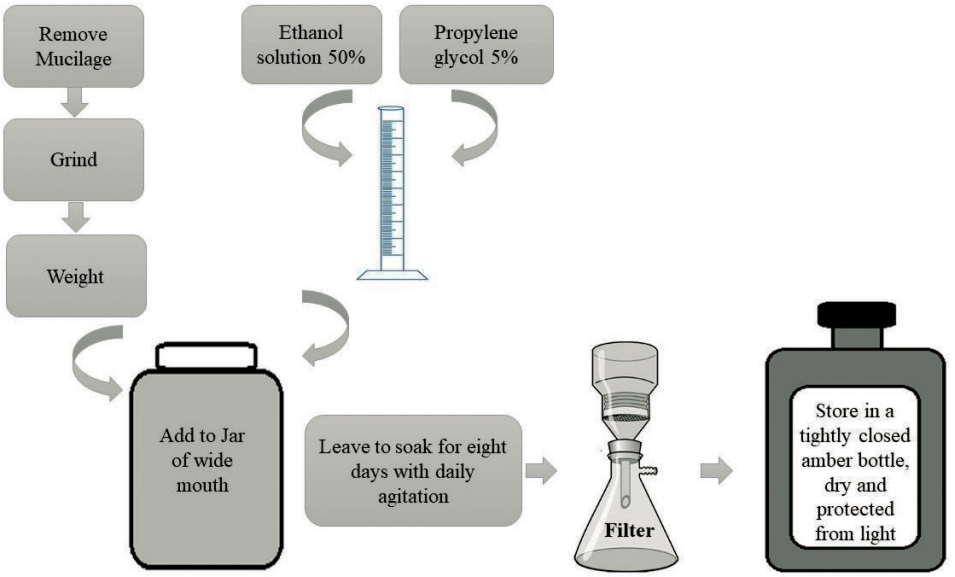

Figure 1. Flowchart of preparation of the glycolic extract of *Aloe vera.* Source: Own authorship.

Table 1. Composition of *Aloe vera* gel.

Components	Quantities
Carbopol 940	1 g
Glycerin	5 g
EDTA	0.10 g
Propylene glycol	2.70 g
Methylparaben	0.20 g
Triethanolamine	1.15 g
Glycolic extract	10 mL
Water	q.s.p 100 g

Source: Adapted from *Formulário Nacional da Farmacopéia Brasileira* [11].

Determination of apparent density

The apparent density was determined in triplicate using 10 g of gel in heavy empty and filled beakers on an analytical balance and calculated from the formula [13]:

$$d = \frac{m}{v}$$

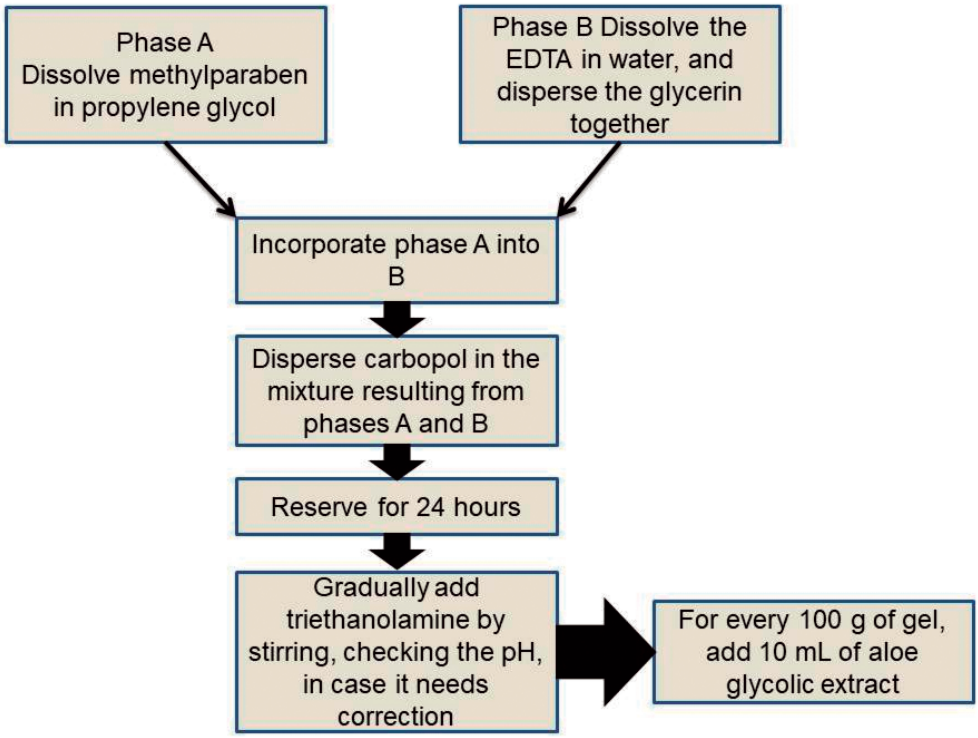

Figure 2. Flow chart of *Aloe vera* gel development. Source: Own authorship.

Determination of viscosity

The viscosity of the gel was evaluated by measuring the resistance to the rotation movement of metal axes when immersed in the liquid in a Brookfield rheometer [12]. Rotors 2, 3 and 4 were used, with a speed of 6 rpm and the calculation was performed using the following equation:

$$\eta = \kappa.\alpha$$

where, η is the absolute viscosity, κ is the coefficient, α is the reading indicated by the pointer.

Determination of spreadability

To determine the spreadability, the technique proposed by Knorst [14] was used, which uses glass plates on a scale of graph paper to determine the surface that the sample covers by measuring perpendicular diameters, with subsequent calculation of the area obtained in mm^2. 1 g of the sample was deposited in the central space of the plate

(20 x 20 cm), after which a glass plate of known mass was placed on the sample. After three minutes, the diameters covered by the sample were read in a horizontal position, using the graph paper and then the spreadability was calculated. This procedure was repeated by successively adding 250 g, 500 g, and 750 g weights in intervals of three minutes from one weight to another, the procedure was performed in triplicate. The spreadability of the samples was determined according to the added weight, according to the equation below [15].

$$Ei = d^2 \times \pi/4$$

where, *Ei:* Sample spreadability for a given weight in square millimeter (mm^2), *d*: Average diameter in millimeter (mm).

The spreadability factor (FE) was also calculated by:

$$FE = Ei/P$$

where, *Ei* = maximum spreading area (mm^2) and P = total added weight (g).

Centrifugation test

The centrifugation test produces stress in the sample, anticipating possible instabilities of the product, through a simulation in the increase in the force of gravity, and increasing the mobility of the particles [13]. 5 g of gel was weighed and placed in the centrifuge at three different rotations, respectively, 1000 rpm, 2500 rpm, 3000 rpm. For 15 minutes [16].

Organoleptic characteristics

The obtained gel was observed visually, in terms of appearance, color and odor [13].

Results and discussion

Organoleptic characteristics

Considering the suitability for the treatment of wounds by topical application, the gel obtained was evaluated for its physical-chemical properties. Such a semi-solid formulation is characterized as an aqueous vehicle with pleasant sensory and easy application on the skin. The gel containing glycolic extract of *Aloe vera* obtained, was homogeneous, translucent, shiny, odorless and without lumps as observed in figure 3.

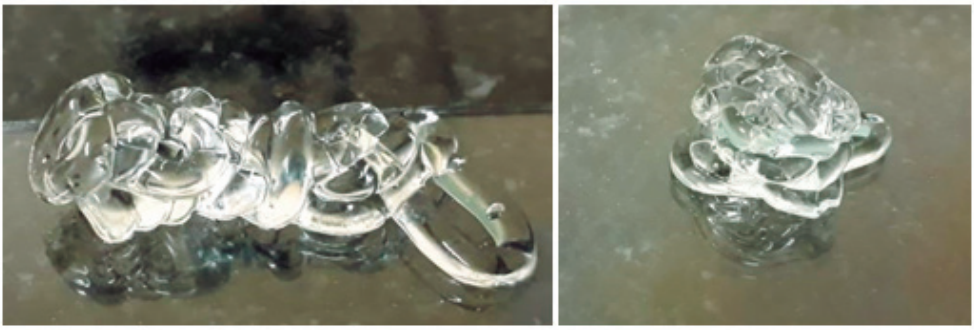

Figure 3. Visual aspect of the obtained gel. Source: Research archives, 2019.

The gel formulation is the choice, among topical semi-solid manipulation options, because in addition to ease of administration, it has high viscosity, good permanence, moisturizing effect on scaly skin, greater bio-adhesion and less potential for irritation [17].

Physical-chemical characteristics

The physical-chemical characteristics of the gel obtained are shown in table 2.

Table 2. Physicochemical characteristics of *Aloe vera* Gel (n = 3).

Test				
pH	**Apparent density (g/mL)**	**Viscosity (Cp)**	**Centrifugation**	**FE Spreadability (mm^2/g)**
5.44 ± 0.00	0.1018 ± 0.0008	> 10 000	No change	8.40 ± 3.6

Source: Research data, 2019.

pH

The pH value (5.44) was similar to that found by Borella *et al.* [18], in which he highlights small pH variations using Carbopol 940 in papain gels. The gel showed values according to the cutaneous pH which is slightly acid varying from 4.6 to 5.8, this acidity is a way of protecting the skin against microorganisms [19, 20]. The pH is an important parameter with regard to acute wounds since they have an alkaline pH, which predisposes to less healing, while acidic conditions help in this process [21, 22].

Apparent density

The apparent density of the aloe gel was 0.1018 ± 0.0008 (g/mL) and represents the relationship between the mass and the volume occupied by the sample. In liquids or

semi-solids this parameter may indicate the incorporation of air or the loss of volatile ingredients in the sample [13]. According to Pedrazzi *et al.* [23] the measure of the product density is dependent on the characteristics of the components present in its formulation, and also on the existence or not of incorporated air during the mixing process.

Viscosity

It was not possible to obtain an accurate viscosity value because it exceeded the maximum reading limit of the equipment used. Following the proposed formula and considering the maximum possible reading value (100), it can be said that the sample has viscosity above 10 000 cP. In addition, it is important to highlight that this finding is expected, since, according to Handbook of Pharmaceutical Excipients, carbomers such as Carbopol 940 have viscosity that can vary between 40 000 to 60 000 cP [24, 25].

The present study corroborates the research by De Aguiar [24] who tested gels based on Carbopol at different temperatures, including body temperature, in which it had a high viscosity, reinforcing that this group of gels has high consistency and good adherence. The evaluation of this component helps to define whether a product indicates the appropriate consistency or fluidity and can show whether the stability is adequate [13]. Thixotropy is a rheological characteristic referring to changes in viscosity with time of application [26].

Topically applied formulations should preferably be viscous when inert and become more fluid when administered to the skin [27]. The rheological characteristic referring to the change in viscosity with the application time is thixotropy [26], and according to Mateus *et al.* [22], an increase in the viscosity of the gel prolongs the release of the drug causing it to improve patient compliance with treatment as it will reduce the number of applications.

The type of polymer and its concentration influence the thixotropic characteristic of the gel. Base formulation with Carbopol presents a higher thixotropy, which is desirable together with its high viscosity, due to deformation in the application and soon after resuming its initial viscosity [28].

Spreadability

The expansion capacity of the semi-solid formulation against a given force (weight) for a time is defined as spreadability. Its determination is essential, as it is related to the ease of topical application of the product [29]. Spreadability is based on resistance to forced movement. The results correspond to the relationship between the spreading area, which will be caused by a force applied on the gel [30].

The graphical representation of the spreadability as a function of the applied mass (figure 4) revealed rheological behavior ranging from 1994.65 mm^2, when subjected to the weight of the glass plate, to 4042.97 mm^2 with the additional mass of 750 g.

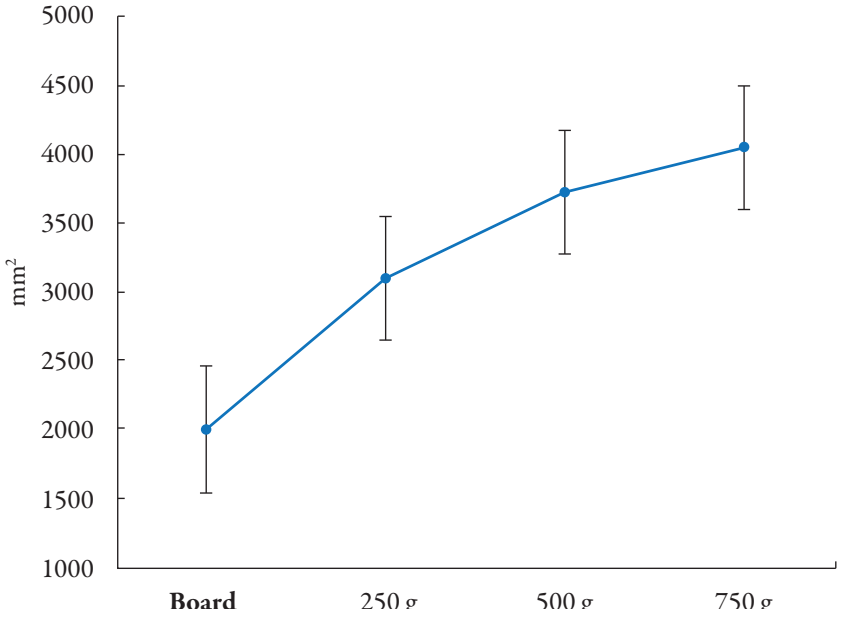

Figure 4. Representative graph of *Aloe vera* gel spreadability (n = 3). Source: Research Archives, 2019.

The spreadability factor of the aloe gel obtained with 1% carbopol was 8.40 ± 3.6 mm^2/g. Carbopol Ultrez hydrogels obtained by Paines *et al.* [31] containing clotrimazole and tea tree oil showed spreadability factors around 4.6 mm^2/g, but it is not clear the percentage of the polymer in the formulation.

Cordeiro *et al.* [30], in a technological development study and evaluation of the stability of dermatological gel based on ginger essential oil, showed that gel based on Carbopol 940 maintains its spreadability without the product draining during administration, even in the face of changes of temperatures, since it was exposed to a preliminary and accelerated stability study showing good physical stability of the formulation which contains Carbopol.

The uniform application of the gel on the skin depends on the spreadability, a good gel will spread easily, the spreadability will help the patient's adherence to the treatment as well as an easier application [32]. A good criterion for the gel to meet the qualities recommended by Organs regulatory bodies is the propagation capacity, which would be the extension of the area where the gel spreads easily at the time of use [33].

Centrifugation test

The centrifugation test represents a preliminary stability test, since, with increased gravity, it is demonstrated in advance if the product will show any type of instability [34]. After centrifugation in all conditions established for the test, the sample remained stable and without change in coalescence, phase changes, color, or odor, showing itself stable as seen in figure 5.

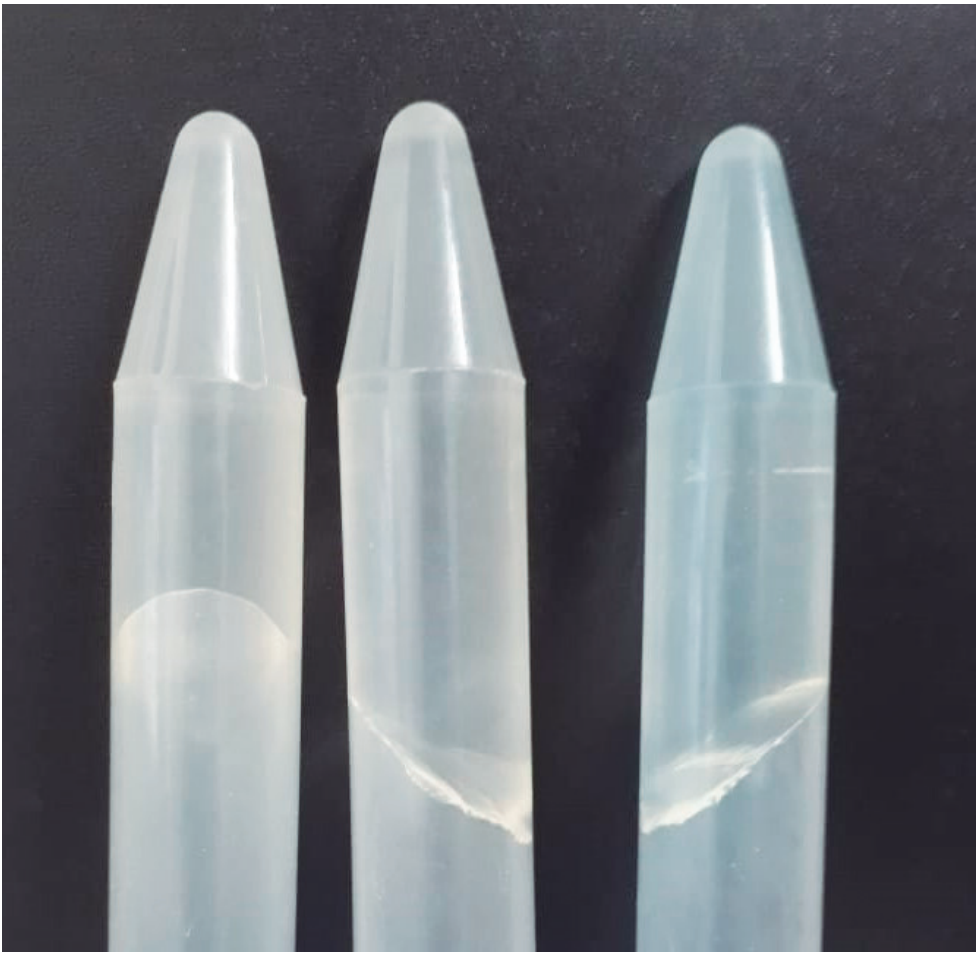

Figure 5. Visual aspect of the gel after the centrifugation test. Source: Research Archives, 2019.

Cordeiro *et al.* [30], and Coelho *et al.* [34] obtained similar results in preliminary stability in dermatological gel from ginger essential oil and gel containing guava leaf extract, respectively. The stability research contributes to: Guide the development of

the formulation and packaging material, serve as alternatives for improving the formulations, help to also determine the expiration date and control of organoleptic, physical-chemical and microbiological stability, producing information on the quality of the product. On the other hand, rheology represents the study of the flow and deformation properties of matter under the action of forces, whose behavior helps in the early detection of signs of instability in formulations, assuming paramount importance for the evaluation of semi-solid formulations [35, 36].

Conclusions

The gel formulated from glycolic extract of *Aloe vera* showed satisfactory organoleptic characteristics, with a homogeneous and shiny appearance, with no apparent odor and translucent color, without altering these characteristics; slightly acid pH, compatible with the skin, which favors wound healing; adequate rheological aspects with good viscosity and spreadability; no changes related to stability, under the conditions evaluated. The development of gels must be carried out consistently and taking into account the therapeutic potential of the present formulation for the treatment of wounds, it is suggested complementary studies regarding the microbiological quality, guaranteeing the safety of a product that presented a pleasant appearance and rheological characteristics, and promising stability.

Disclosure statement

No potential conflict of interest was reported by the authors.

References

1. C.C. Falzon, A. Balabanova, Phytotherapy: An introduction to herbal medicine, *Prim. Care*, **44**, 217-227 (2017).

2. E.C.M. Dias, D.D. Trevisan, S.C. Nagai, N.A, Ramos, E.M. Silva, Uso de fitoterápicos e potenciais riscos de interações medicamentosas: reflexões para prática segura, *Rev. Baiana Saúde Pública*, **41**, 297-307 (2017).

3. T.M. Souza-Moreira, H.R.N. Salgado, R.C.L.R. Pietro, O Brasil no contexto de controle de qualidade de plantas medicinais, *Rev. Bras. Farmacogn.*, **20**, 435-440 (2010).

4. M. Oshiro, M. Miguel, J. Dias, E. Gomes, O. Miguel, A evolução do registro e prescrição de fitoterápicos no Brasil sob a perspectiva legal e sanitária, *Vigilância Sanitária em Debate: Sociedade, Ciência & Tecnologia*, **4**, 116-122 (2016).

5. Ministério da Saúde do Brasil, *Política Nacional de Plantas Medicinais e Fitoterápicos*, 2006.

6. H.S. Kim, S. Xiaoyan, J.H. Lee, H.W. Kim, X. Fu, K.W. Leong, Advanced drug delivery systems and artificial skin grafts for skin wound healing, *Advanced Drug Delivery Reviews*, **146**, 209-239 (2019).

7. P.K. Ghosh, A. Gaba, Phyto-extracts in wound healing, *J. Pharm. Pharmaeut. Sci.*, **16**, 760-820 (2013).

8. L.L. Silva, P.F. Lopes, M.H.D.A. Monteiro, H.W. Macedo, Importância do uso de plantas medicinais nos processos de xerose, fissuras e cicatrização na diabetes mellitus, *Rev. Bras. Plant. Med.*, **17**, 827-835 (2015).

9. P.L. Mercês, L.A. Araújo, A.C.V. Araújo, M.H.A.S. Santos, S.R. Lemos, P.R. Melo-Reis, Avaliação da atividade cicatricial do *Aloe vera* em feridas em dorso de ratos, *Estima*, **15**, 35-42 (2017).

10. Ministério da Saúde do Brasil, Anvisa, Agência Nacional de Vigilância Sanitária, *Formulário de Fitoterápicos da Farmacopéia Brasileira*, Brasília, 2011, v. 1, p. 125.

11. Ministério da Saúde do Brasil, Anvisa, Agência Nacional de Vigilância Sanitária, *Formulário Nacional da Farmacopéia Brasileira*, Brasília, 2012, v. 2.

12. Ministério da Saúde do Brasil, Anvisa, Agência Nacional de Vigilância Sanitária, *Farmacopeia Brasileira*, Brasília, 2019, v. 1, p. 873.

13. Ministério da Saúde do Brasil, Anvisa, *Agência Nacional de Vigilância Sanitária, Guia de Controle de Qualidade de Produtos Cosméticos: uma abordagem sobre os ensaios físicos e químicos*, Brasília, 2008, v. 1, p. 123.

14. M.T. Knorst, *Desenvolvimento tecnológico de forma farmacêutica plástica contendo extrato concentrado de Achyrocline satureioides. (Lam). DC. Compositae. (Marcela)*, M. Sc. thesis, Universidade Federal do Rio Grande do Sul, Porto Alegre, 1991, p. 257.

15. G.S. Borghetti, M.T. Knorst, Desenvolvimento e avaliação da estabilidade física de loções O/A contendo filtros solares, *Rev. Bras. Ciênc. Farm.*, **42**, 532-537 (2006).

16. C.G. Lima, A.F.G. Vilela, A.A. Silva, A.R. Painnovski, K.K. Silva, V.F.M. Carvalho, C.R. Musis, S.R. Machado, M. Ferrari, Desenvolvimento e avaliação da estabilidade física de emulsões O/A contendo óleo de babaçu *(Orbignya oleifera)*, *Rev. Bras. Farm.*, **89**, 239-245 (2008).

17. R. Aiyalu, A. Govindarjan, A. Ramasamy, Formulation and evaluation of topical herbal gel for the treatment of arthritis in animal model, *Braz. J. Pharm. Sci.*, **52**, 493-507 (2016).

18. J.C. Borella, J.C.L. Teixeira, R.L.A. Puga, M.C.B. Stevenato, Semi-solid pharmaceutical forms based on papain - Preliminary evaluation of stability, microbiological contamination and enzymatic activity, *Visão Acadêmica*, **19**, 24-43 (2018).

19. G.R. Leonardi, L.R. Gaspar, P.M.B.G.M. Campos, Estudo da variação do pH da pele humana exposta à formulação cosmética acrescida ou não das vitaminas A, E ou de ceramida, por metodologia não invasiva, *An. Bras. Dermatol.*, 77, 563-569 (2002).

20. B.R. Mendes, D.M. Shimabukuro, M. Uber, K.T. Abagge, Critical assessment of the pH of children's soap, *J. Pediatr.*, **92**, 290-295 (2016).

21. E.M. Jones, C.A. Cochrane, S.L. Percival, The effect of pH on the extracellular matrix and biofilms, *Advances in Wound Care*, **4**, 431-439 (2015).

22. D. Mateus, J. Marto, P. Trindade, H. Gonçalves, A. Salgado, P. Machado, A. Melo-Gouveia, H.M. Ribeiro, A.J. Almeida, Improved morphine-loaded hydrogels for wound-related pain relief, *Pharmaceutics*, **11**, 76:1-16 (2019).

23. V. Pedrazzi, M.S. Pita, C. Nascimento, F.H.C.N. Fernandes, J.M. Oliveira-Neto, P.L. Calefi, Avaliação da densidade e do pH de géis fluoretados disponíveis no mercado nacional, *Revista da Faculdade de Odontologia de Lins*, **22**, 21-26 (2012).

24. M.M.G.B. de Aguiar, *Obtenção de gel mucoadesivo de nistatina para o tratamento da candidíase oral. Desenvolvimento e caracterização de dispersões sólidas de nistatina*, Ph. D. thesis, Universidade de São Paulo, 2016, p. 231.

25. R.C. Roew, P.J. Sheskey, S.C. Owen, *Handbook of Pharmaceutical Excipients*, Pharmaceutical Press, London/Chicago, 2006, p. 918.

26. R.A. Moura, A.M. Moraes, A. Domingues, S.P. Alcântara, M.F. Naccache, A.S. Sirqueira, *Avaliação reológica de tintas acrílicas aditivadas com carga condutora*, URL: http://www.proceedings.blucher.com.br/article-details/28662, accessed June 2020.

27. S.-F. Ng, N.-A. Anuwi, T. Tengku-Ahmad, Topical lyogel containing corticosteroid decreases ige expression and enhances the therapeutic efficacy against atopic eczema, *AAPS PharmSciTech*, **16**, 656-663 (2015).

28. N.M. Corrêa, F.B. Camargo Júnior, R.F. Ignácio, G.R. Leonardi, Avaliação do comportamento reológico de diferentes géis hidrofílicos, *Rev. Bras. Cienc. Farm.*, **41**, 73-78 (2005).

29. N.C. Ngwuluka, Y.E. Choonara, P. Kumar, G. Modi, L.C. Toit, V. Pillay, A hybrid methacrylate-sodium carboxymethylcellulose interpolyelectrolyte complex: rheometry and in silico disposition for controlled drug release, *Materials*, **6**, 4284-4308 (2013).

30. M.S.F. Cordeiro, J.K.B. Costa, C.G. Lima, J.D.C. Campelo Júnior, A.F.M. Melo, Desenvolvimento tecnológico e avaliação de estabilidade de gel dermatológico a partir do óleo essencial de gengibre (*Zingiber officinalle Roscoe*), *Rev. Bras. Farm.*, **94**, 148-153 (2013).

31. T.C. Paines, J.A. Lima, J. Weber, F.C. Flores, C.B. Silva, Desenvolvimento tecnológico de hidrogéis a partir de nanoemulsão contendo clotrimazol em associação com o óleo de melaleuca, *Ciência e Natura*, **37**, 106-115 (2015).

32. R.F. El-Kased, R.I. Amer, D. Attia, M.M. Elmazar, Honey-based hydrogel: *In vitro* and comparative *in vivo* evaluation for burn wound healing, *Sci. Rep.*, **7**, 9692:1-11 (2017).

33. A.S. Zakaria, S.A. Afifi, K.A. Elkhodairy, Newly developed topical cefotaxime sodium hydrogels: Antibacterial activity and *in vivo* evaluation, *BioMed Res. Int.*, **2016**, ID 6525163:1-15 (2016).

34. K.D. Coelho, C.S. Paim, R.A.N. Deuschle, J.W. Bortolotto, V.C.K.N. Deuschle, Desenvolvimento e avaliação da estabilidade e capacidade antioxidante de uma formulação em gel contendo o extrato das folhas de goiabeira (*Psidiumguajava L.*), *Biomotriz*, **10**, 136-155 (2016).

35. L. Mazzarino, M.T. Knorst, Desenvolvimento e caracterização farmacotécnica de formas farmacêuticas semi-sólidas contendo nimesulida, *Lat. Am. J. Pharm.*, **26**, 415-419 (2007).

36. V.L.B. Isaac, L.C. Cefali, B.G. Chiari, C.C.L.G. Oliveira, H.R.N. Salgado, M.A. Corrêa, Protocolo para ensaios físico-químicos de estabilidade de fitocosméticos, *Rev. Ciênc. Farm. Básica Apl.*, **29**, 81-96 (2009).

How to cite this article

I.H. Mendes-Aciole, F.P. de Andrade-Júnior, L. Vilar-Cordeiro, J.B. Pereira de Souza, Aloe gel: manipulation and characterization of physical-chemical quality adjustment, *Rev. Colomb. Cienc. Quím. Farm.*, **49**(3), 790-805 (2020).

Scientific research article / *http://dx.doi.org/10.15446/rcciquifa.v49n3.91346*

In silico approach of antiviral compounds potentials for SARS-CoV-2 and SARS-CoV and drug-like property predictions

Nerlis Pájaro-Castro[1]*, Cristhian Ibañez-Bersinger[2], Glicerio León-Méndez[3]

[1]Medical and Pharmaceutical Sciences Group, School of Health Sciences, Department of Medicine, University of Sucre, Sincelejo, 700003, Sucre, Colombia. ORCID: https://orcid.org/0000-0002-9831-9663.

[2]Medical and Pharmaceutical Sciences Group, School of Health Sciences, Department of Medicine, University of Sucre, Sincelejo, 700003, Sucre, Colombia.

[3]Faculty of Health Sciences. Corporación Universitaria Rafael Núñez. Programa de Tecnología en Estética y Cosmetología. GITEC, Cartagena, Colombia. University of Cartagena, Cartagena, Bolívar 130015, Colombia. ORCID: https://orcid.org/0000-0002-9899-5872.

*Author to whom correspondence should be addressed: nerlis.pajaro@unisucre.edu.co

Received: 4 October 2019

Revised: 29 August 2020

Accepted: 31 August 2020

Summary

Introduction: SARS-CoV-2 (Coronavirus 2 of the severe acute respiratory syndrome; previously 2019-nCoV) and SARS-CoV (coronavirus of the severe acute respiratory syndrome) are closely related viruses, which have no treatment so far. Therefore, the search for new molecules is essential. *Objectives*: the objective of this study is to use *in silico* approach to propose antiviral compounds potential for SARS-CoV-2 and SARS-CoV and drug-like properties predictions. *Materials and methods*: Molecular docking were performed using AutoDock Vina with the molecules that had previously demonstrated drug-like properties. Subsequently, amino acids and the type of interaction involved in the protein-ligand complex were identified. *Results*: It was possible to identify six potential candidates available in the PubChem database capable of interacting with the 6U7 and 2GTB proteases, which bind to the same active site that lopinavir and remdesivir. *Conclusion*: Small molecules with drug-like properties could be used as antivirals, after experimental evaluations.

Key words: Coronavirus, small molecules, molecular docking, pandemic, antiviral treatments.

Resumen

Enfoque *in silico* de potenciales compuestos antivirales para SARS-CoV-2 Y SARS-CoV y predicción de propiedades *drug-like*

Introducción: los coronavirus SARS-CoV-2 (coronavirus del síndrome respiratorio agudo grave de tipo 2; previamente identificado como 2019-nCoV) y SARS-CoV (coronavirus del síndrome respiratorio agudo grave) son virus estrechamente relacionados, que no tienen tratamiento hasta el momento. Por lo tanto, la búsqueda de nuevas moléculas es esencial. *Objetivos*: el objetivo de este estudio es utilizar un enfoque *in silico* para proponer potenciales compuestos antivirales para el SARS-CoV-2 y el SARS-CoV y predicciones de propiedades "drug-like". *Materiales y métodos*: el acoplamiento molecular se realizó utilizando "AutoDock Vina" con las moléculas que previamente habían demostrado propiedades similares a los fármacos. Posteriormente, se identificaron los aminoácidos y el tipo de interacción involucrada en el complejo proteína-ligando. *Resultados*: fue posible identificar seis candidatos potenciales disponibles en la base de datos PubChem capaces de interactuar con las proteasas 6U7 y 2GTB, que se unen al mismo sitio activo al que se unen lopinavir y remdesivir. *Conclusiones*: moléculas pequeñas con propiedades similares a los fármacos podrían usarse como antivirales, después de evaluaciones experimentales.

Palabras clave: Coronavirus, pequeñas moléculas, acoplamiento molecular, pandemia, tratamientos antivirales.

Introduction

Coronaviruses are enveloped positive single-stranded large RNA viruses that infect humans, but also a wide range of animals [1]. According to their morphology as spherical virions with a central nucleus and surface projections that resemble a solar corona, they were called coronaviruses [2]. There are four subfamilies, namely alpha, beta, gamma, and delta coronavirus [1]. The size of the genome varies between 26 kb and 32 kb [3]. Among the coronavirus subtypes that can infect humans, beta-coronaviruses can cause serious illness and death, while alpha-coronaviruses cause asymptomatic or mildly symptomatic infections [1]. Severe acute respiratory syndrome coronavirus 2 (SARS-CoV-2) belongs to the B-lineage of beta-coronaviruses and is closely related to the SARS-CoV virus [1]. There are four major structural proteins encoded by the coronaviral genome in the envelope, one of which is the spike protein (S) that binds to the angiotensin-converting enzyme 2 (ACE2) receptor and mediates subsequent fusion between the envelope and host cell membranes to aid viral entry into the host cell [2].

The world is currently facing a SARS-CoV-2 pandemic, declared by the World Health Organization (WHO) Emergency Committee on March 11, 2020, based on rising case notification rates in different countries. This virus has spread to 188 countries as of August 10 and has infected more than 19.995.057 people. The case detection rate changes daily and can be tracked in near real-time on the website provided by Johns Hopkins University and other forums [4]. Most worrying is that the disease has posed a serious threat to global public health, by requiring the development of safe and effective prophylactic and therapeutic drugs against the infection of its causative agent, SARS-CoV-2, also known as the new coronavirus 2019 (2019-nCoV) [3]. Therefore, the lack of specific medications to prevent and treat an attack is an important need at the present time, considering that the available treatment is clearly symptomatic [5]. Drug discovery can also be accelerated by applying new detection techniques, including computational approaches, to identify antivirals that could be ready for large-scale clinical trials in a matter of weeks [6].

The main pharmacological targets for coronavirus (CoV) are spike protein, envelope protein, membrane protein, protease, nucleocapsid protein, hemagglutinin esterase, and helicase, for which drug design can be considered. There are 16 other non-structural proteins (NSP) that can also be considered from the perspective of drug design including RNA-dependent RNA polymerase (RdRp), coronavirus main protease (3CLpro), and papain-like protease (PLpro). These proteins are important because upon entering host cells, the viral genome is released as a single-stranded positive RNA. Subsequently, it is translated into viral polyproteins using host cell protein translation machinery, which is then cleaved into effector proteins by viral proteins 3CLpro and PLpro. PLpro also behaves like a deubiquitinase that can de-position certain proteins from the host cell, including interferon factor 3 and NF-κB, resulting in immune suppression. RdRp synthesizes a full-length negative-strand RNA template to be used by RdRp to produce more viral genomic RNA [7]. 3CLpro is a key CoV enzyme, which plays a key role in mediating viral replication and transcription, making it an attractive drug target for this virus [7-8]. This protein was selected to be used as a pharmacological target in this study. Lopinavir is an antiretroviral drug used in patients with HIV and Remdesivir is an antiviral prodrug used to treat Ebola virus disease, currently these two drugs have been proposed as antivirals for SAR-CoV-2. Lopinavir and remdesivir are antiviral agents [7].

Therefore, the main structural proteins and NSP can play an important role in the perspective of drug design. However, the occurrence of frequent recombination events is an important deterrent towards the development of vaccines and medications specific to CoV [9]. The objective of this study is to use *in silico* approach to propose antiviral compounds potential for SARS-CoV-2 and SARS-CoV and drug-like properties predictions.

Methods

Equipment and Software

Drug Likeness Tool (DruLiTo 1) was used to detect molecules with ADME properties. AutoDock Vina was the primary docking programs used in this work [10]. The preparation of the PDBQT files and determination of the grid box size was carried out using Auto-Dock Tools version 1.1. Chimera was utilized to prepare protein structures. PyMol (DeLano Scientific LLC, USA) was employed to visualize protein-ligand complex structures. The identification of protein residues that interact with small molecules was carried out employing LigandScout. Computational studies were carried out using a machine running on Inter Core i7 4.0GHZ, a processor with 8GB RAM and 1TB hard disk.

Selection of molecules with properties drug-likeness

The database PubChem was used to download 3 million molecules deposited during 2015 and 2016. These chemicals were filtered considering those having characteristics of drugs-like, to filter molecules were used free software Drug Likeness Tool (DruLiTo 1). The rules Lipinski that predict if a compound is more likely to be membrane-permeable and easily absorbed by the body [11]. Veber rule, to predict good oral bioavailability [12]. Ghose filter that defines drug-likeness constraints [13]. The molecules that passed these filters were selected for molecular docking. The criteria that were taken into account were: molecular weight ≤ 500, Log *P* ≤ 5, H-Bond donor ≤ 5, H-bond acceptor ≤ 10, rotatable bond ≤ 10, polar surface area ≤ 140, Atom-Count from 20 to 70 and refractivity from 40 to 130. Of the three million molecules discharged in PubChem, only 997 passed the drug-like filters, that is, they possess drug-like properties.

Protein structure preparation

The 3D structure of proteins: COVID-19 main protease and SARS coronavirus main peptidase were downloaded from Protein Data Bank (PDB: 6LU7 and 2GTB, respectively), both obtained by x-ray diffraction, and prepared with Chimera. The water molecules and other ligands present in the proteins were eliminated. Proteins were minimized using atomic partial charges by Kollman method, which describes the potential of the system in terms of the energy positions of the atoms and is parameterized for proteins and nucleic acids [14]. MGLTools 1.5.0 software was utilized to convert structures from PDB to PDBQT format, adding polar hydrogens and assigning Kollman partial charges [14].

Protein-ligand docking

Molecular docking was performed using AutoDock Vina is a virtual molecular docking and screening program. Vina uses a sophisticated gradient optimization method in his local optimization procedure. The gradient calculation effectively provides the optimization algorithm with a "sense of direction" from a single evaluation. By using multithreading, Vina can further speed up execution by leveraging multiple CPUs or CPU cores. The docking site for ligands on evaluated proteins was defined by establishing a cube with a sufficient dimension to cover the complete protein, with a grid point spacing of 1 Å for the proteins. Three runs were carried out by ligand, and for each run the best pose was saved. Finally, the average binding affinity for best poses was accepted as the binding affinity value for a particular complex [14]. The three-best protein-ligand complexes were selected, those that showed the highest affinity value.

Identifying interactions

Three ligand structures were selected and coupled with proteins to identify residues of proteins that interact with small molecules, using Ligand scout software. This program proposes the number and type of primary existing ligand–residue interactions on the protein active site. For this, the coordinates generated during molecular coupling are used, to identify the amino acids participating in the protein-ligand interaction.

Results

In this study of the 3 million new molecules selected, only 997 met drug-like properties (rules Lipinski, Veber rule, and Ghose filter), which were used to make molecular docking. These molecules possess ADME properties and also have a high affinity for all proteins (molecules with scores below -7.8 kcal/mol) (table 1 and figure 1), this value represents the affinity of a protein for a ligand as a semi-quantitative parameter related to the inverse of the dissociation constant. Therefore, only the three molecules for each protein with higher affinity values were selected as possible candidates.

The three-best protein-ligand complexes were selected and are shown in figures 2 and 3 for each protein, SARS coronavirus main peptidase (2GTB), and COVID-19 main protease (6LU7). 6LU7 is the main protease (M^{pro}) found in SARS-CoV-2 and 2GTB is the main protease found in the SARS-CoV [15]. With both proteins, blind molecular docking was carried out, that is, docking over the entire surface of the protein. Furthermore, molecular docking was performed using the same protocol with two antiviral drugs, in order to validate the binding site of the ligands evaluated by comparison with lopinavir and remdesivir.

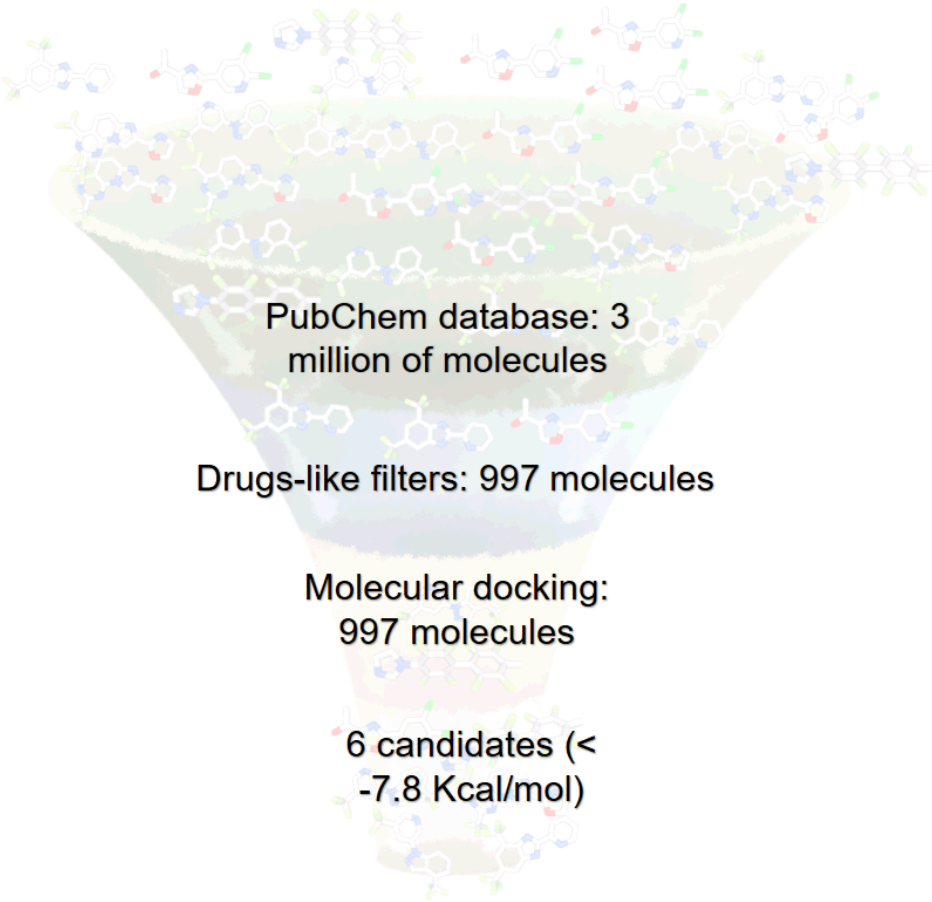

Figure 1. Flowchart for selecting the best protein-ligand complexes. Source: Own elaboration.

Table 2 shows the amino acids found in the active site pockets of 6LU7 and 2GTB in the complex with two reported inhibitors (lopinavir and remdesivir) and the selected new molecules selected.

The affinity values and three-dimensional view of the complexes with lopinavir and remdesivir are shown in figure 4. Lopinavir and remdesivir are two antiviral drugs against a clinical isolate of SARS-CoV-2 *in vitro* (7). In this study, we have used them to check the ability of the proposed new molecules to bind to the same active site of the proteins evaluated to which these two antiviral agents used in the treatment of SARS-CoV-2 and SARS-CoV bind. Being able to identify that the amino acid residues that participate in the formation of the protein-ligand complex were also identified in the protein-ligand complexes of the molecules with the best affinity values (table 1 and 2). The predominant type of interaction was the hydrophobic type interaction.

Table 1. Drug-like properties and AutoDock-calculated affinities obtained for docking of best molecules on proteins of COVID-19 (< -7.8 kcal/mol).

Compounds	Drug-like properties					Protein affinity (kcal/mol)
	MW (g/mol)	Log *P*	LRV	GFV	VRV	2GTB
CID 90252773 (4-(Trifluoromethyl)-1-[5-(trifluoromethyl)pyridin-3-yl]indazole)	331.22	2.578	0*	0	0	-8,2
CID 90381721 (2-[10,12-Bis(trifluoromethyl)-2,5,11,13-tetrazatricyclo[7.4.0.02,6] trideca-1(13),3,5,7,9,11-hexaen-4-yl]-1,3-oxazole)	373.21	1.963	0	0	0	-8,6
CID 90380837 (1-[2-(5,6-Dichloropyridin-3-yl) -1,3-oxazol-4-yl]ethanone)	257.07	1.384	0	0	0	-8.5
Lopinavir	628.35	3.688	1	1	1	-8.4
Remdesivir	602.23	0.336	1	1	1	
						6LU7
CID 90178936 (1-[2,3,5,6-Tetrafluoro-4-(2,3,5,6-tetrafluoro-4-methylphenyl) phenyl]imidazole)	378.22	2.63	0	0	0	-8,0
CID 90364642 (2-Pyridin-2-yl-4,6-bis(trifluoromethyl) -1H-benzimidazole)	331.22	2.735	0	0	0	-8,1
CID 90380837 (1-[2-(5,6-Dichloropyridin-3-yl) -1,3-oxazol-4-yl]ethanone)	257.07	1.384	0	0	0	-7.8
Lopinavir	628.35	3.688	1	1	1	-8.3
Remdesivir	602.23	0.336	1	1	1	

MW: Molecular weight

Log *P*: Logarithm of octanol/water partition coefficient

LRV: Lipinski rule of 5 violations: Maximum is 4 violations

GF: Ghose Filter violation

VR: Vebers Rule violation

*This value refers to the number of violations found for each drug-like filter evaluated.

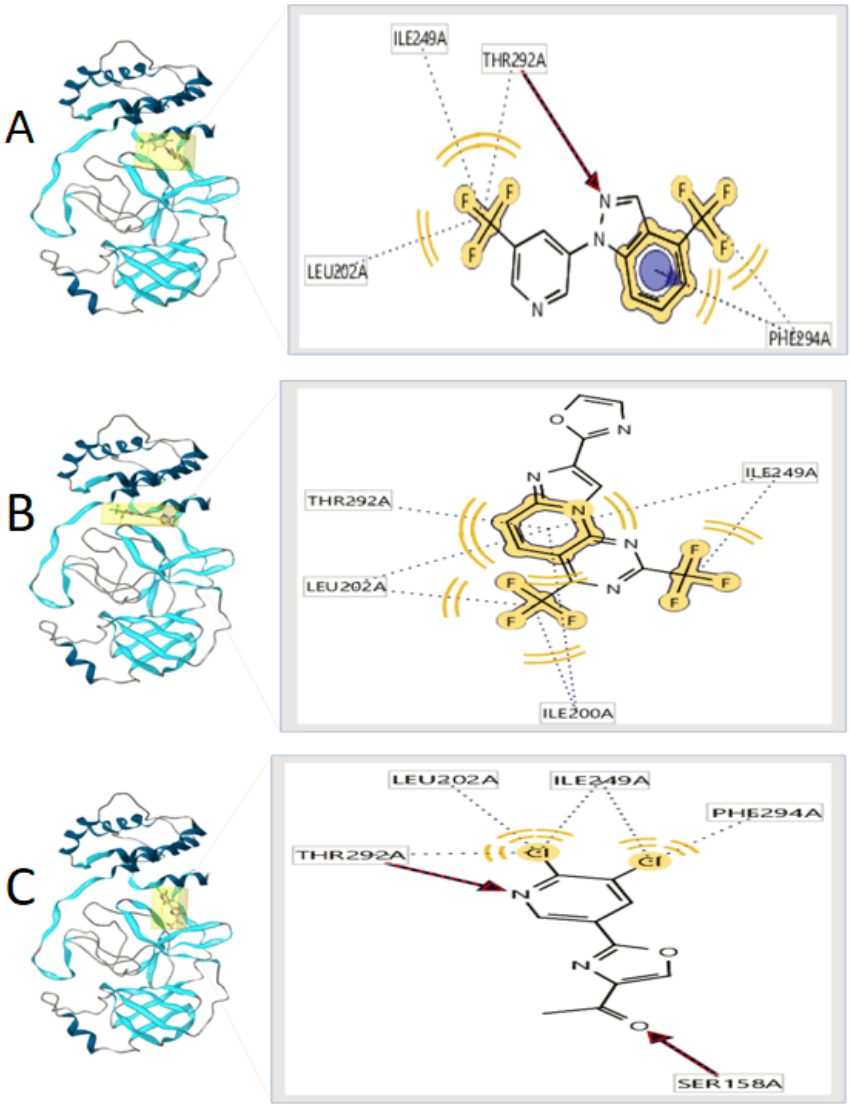

Figure 2. 3D view and interacting residues present in proteins 2GTB. A: 2GTB -90252773, B: 2GTB -90381721, C: 2GTB -90380837. Source: Own elaboration.

Discussion

SARS-CoV-2 represents a pandemic threat to public health because there is no treatment to counteract the virus [16]. So the search for new molecules with antiviral properties is imperative [7]. The present study focused on the main proteases

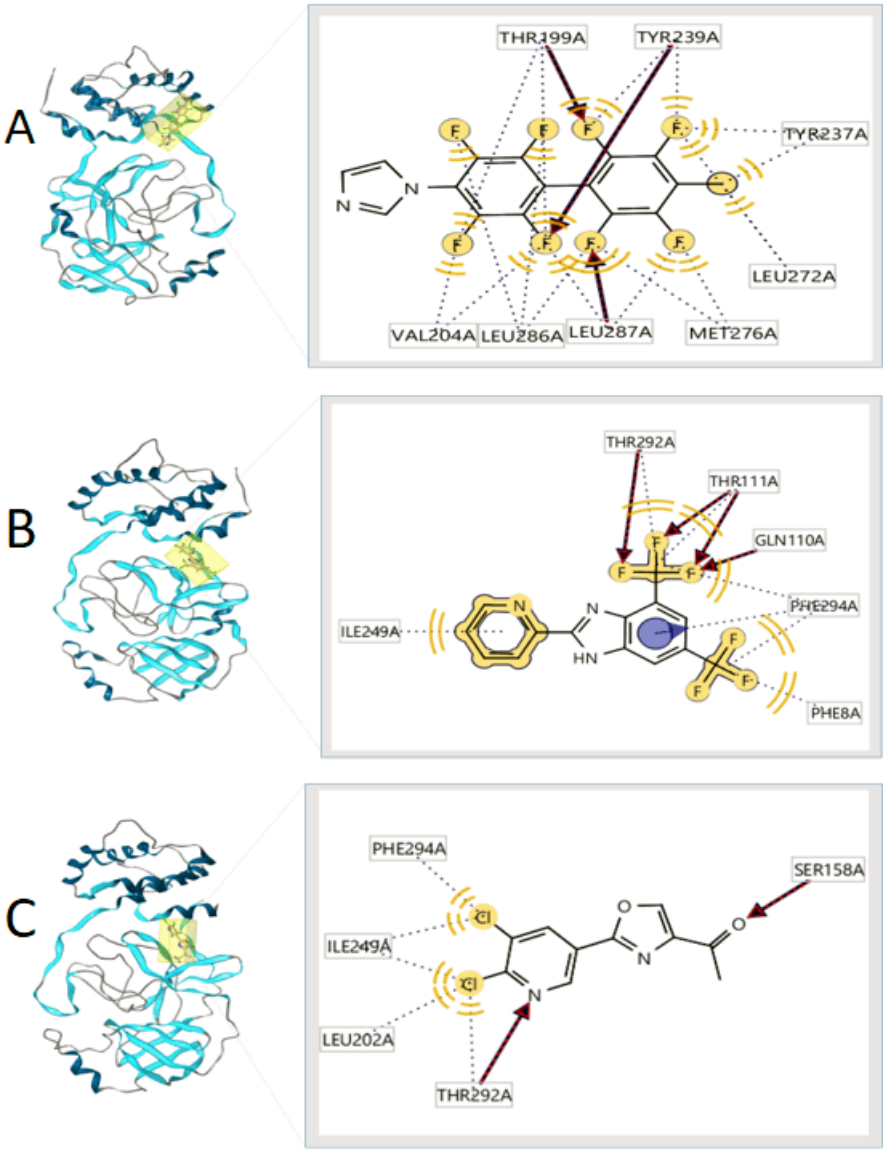

Figure 3. 3D view and interacting residues present in proteins 6LU7. A: 6LU7 -90178936, B: 6LU7 -90364642, C: 6LU7 -90380837. Source: Own elaboration.

in CoVs (3CLpro/M^{pro}), especially PDB ID 6LU7, as potential target proteins for SARS-CoV-2 treatment [15] and is the main peptidase of the SARS coronavirus (SARS-CoV M (pro)), which plays an essential role in the life cycle of the virus and is a main target for the development of anti-SARS agents [17]. Xu *et al.* [18] mentioned

Table 2. Interacting residues 2GTB and 6LU7 protein - inhibitor complex in comparison with ligands studied.

Interaction 2GTB in complex with inhibitor					
Name	**Amino acid**	**Type of interaction**	**Interaction identified in the protein - ligand complexes**		
			90252773	**90381721**	**90380837**
Lopinavir	Phe294	Aromatic ring	X	-*	X
	Thr292	Hydrophobic	X	X	X
	Leu202	Hydrophobic	X	X	X
	Ile249	Hydrophobic	X	X	X
	Val297	Hydrophobic	-	-	-
	Ile106	Hydrophobic	-	-	-
	Val104	Hydrophobic			
Remdesivir	Phe294	Hydrophobic	X	-	X
	Val297	Hydrophobic	-	-	-
	Leu253	Hydrophobic	-	-	-
	Ile249	Hydrophobic	X	X	X
	Thr292	Hydrophobic	X	X	X
	Leu202	Hydrophobic	X	X	X
	Gln110	H bond acceptor	-	-	-
	Asn151	H bond donor	-	-	-
	Thr111	H bond donor	-	-	-
	Ile106	Hydrophobic	-	-	-
Interaction 6LU7 in complex with inhibitor					
			90178936	**90364642**	**90380837**
Lopinavir	Val202	Hydrophobic	-	-	-
	Ile249	Hydrophobic	-	X	X
	Phe294	Aromatic ring	-	X	X
	Val104	Hydrophobic	-	-	-
	Ile106	Hydrophobic	-	-	-

(*Continued*)

Table 2. Interacting residues 2GTB and 6LU7 protein - inhibitor complex in comparison with ligands studied.

Interaction 6LU7 in complex with inhibitor					
Remdesivir	Thr199	H bond acceptor	X	-	-
	Tyr239	H bond acceptor	X	-	-
	Leu286	Hydrophobic	X	-	-
	Leu271	Hydrophobic	-	-	-
	Met276	Hydrophobic	X	-	-
	Leu272	Hydrophobic	-	-	-
	Tyr237	Hydrophobic	X	-	-
	Leu287	H bond acceptor	X	-	-
	Asp289	H bond donor	-	-	-

*The presence of the amino acid in the protein-ligand complex of the proposed candidates was not identified.

that the main protease in 2019-nCoV shares 96% similarity with that in SARS0 [14]. To make comparisons, these two proteins were used.

In the search for new molecules that can be used as antivirals, it is important to predict the similarity of the drugs, as well as the intestinal absorption capacity and bioavailability requirements [19]. In this study, the selected chemical compounds meet these. As for the affinities obtained, they are comparable with those obtained for lopinavir and remdesivir. Khaerunnisa *et al.*, [15] reported that the binding energies obtained from the docking of 6LU7 with native ligand, nelfinavir, lopinavir, kaempferol, quercetin, luteolin-7-glucoside, demethoxycurcumin, naringenin, apigenin-7-glucoside, oleuropein, curcumin, catechin, epicatechin-gallate, zingerol, gingerol, and allicin were -8.37, -10.72, -9.41, -8.58, -8.47, -8.17, -7.99, -7.89, -7.83, -7.31, -7.05, -7.24, -6.67, -5.40, -5.38, and -4.03 kcal/mol, respectively. As can be seen, the affinity values reported using AutoDock and the same protein are comparable with those obtained in this study.

Several authors [15, 20, 21] have reported new molecules with antiviral properties against SARS-CoV-2 through molecular docking with affinity values comparable to those obtained in this study. For the main peptidase of the SARS coronavirus, the protein-ligand complex (2GTB -90252773, B. 2GTB -90381721, C. 2GTB -90380837) show that all bind to the same active site including lopinavir and remdesivir, involving the same amino acids and the same type of interactions, being the interactions of hydrophobic type the main ones found. The protein complexes binding to the 6LU7

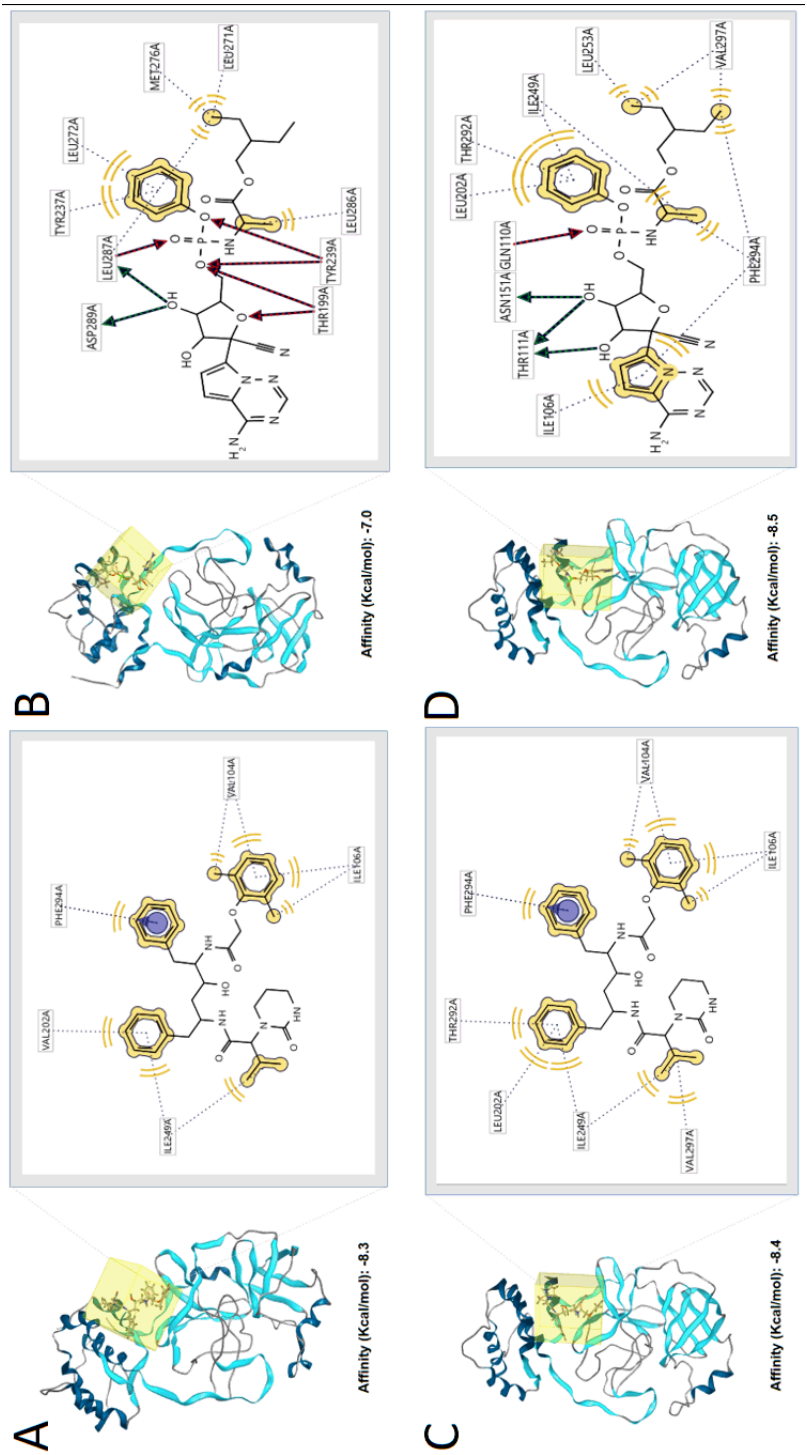

Figure 4. 3D view and interacting residues present 2GTB and 6LU7 protein - inhibitor complex. A: 6LU7 -Lopinavir, B: 6LU7 -Remdesivir, C: 2GTB – Lopinavir, D: 2GTB – Remdesivir. Source: Own elaboration.

protein show that the 6LU7-90364642 and 6LU7-90380837 complexes bind to the same site as lopinavir, but the 6LU7-90178936 complex interacts at a different site together with remdenavir, which leads us to think of a possible allosteric site of interaction, in which other amino acids with predominantly hydrophobic interactions are involved. Chauhan [21], reported that remdesivir couples with 6LU7 with an affinity value of -13.1. Khalifa *et al.* [22], reported that tellimagradin interacts within the protease binding pocket with the amino acids Phe294, Thr292, Ile249, among others, which were also identified in our protein-ligand complexes. These results suggest that small molecules identified by *in silico* approaches and with drug-like properties may be useful candidates for the development of new antiviral drugs. These molecules are available in the PubChem database and can be used to carry out experimental studies.

The results obtained are of great importance because they allow us to identify potential molecules with antiviral characteristics using an *in silico* approach, which reduces the time and budget required in the laborious search for a treatment to stop the progression of this disease that is affecting millions of people in the world. In this study, it is recommended to continue to a next phase in drug development, which consists of conducting in vitro and in vivo evaluation with the proposed candidates, to develop new drugs against SARS-CoV-2 and SARS-CoV.

Conclusions

The protein-ligand complexes 2GTB -90252773, 2GTB -90381721, 2GTB -90380837, 6LU7-90364642, 6LU7-90380837 and 6LU7-90178936 were those that showed the highest affinity values (< -7.8), with the ability to interact in the same binding sites for lopinavir and remdenavir, being potential candidates with drug-like properties to act as antivirals against SARS-COV and SARS-CoV-2. These molecules can be evaluated by pharmacological experimentation.

Acknowledgements

The authors want to thank the University of Sucre.

Disclosure statement

No potential conflict of interest was reported by the authors.

References

1. T.P. Velavan, C.G. Meyer, The COVID-19 epidemic, *Trop. Med. Int. Health*, **25**, 278-280 (2020).

2. Z.Y. Zu, M.D. Jiang, P.P. Xu, W. Chen, Q.Q. Ni, G.M. Lu, L.J. Zhang, Coronavirus disease 2019 (COVID-19): A perspective from China, *Radiology*, **296,** E15-E25 (2020).

3. W. Tai, L. He, X. Zhang, J. Pu, D. Voronin, S. Jiang, Y. Zhou, L. Du, Characterization of the receptor-binding domain (RBD) of 2019 novel coronavirus: implication for development of RBD protein as a viral attachment inhibitor and vaccine, *Cell. Mol. Immunol.*, **17**, 613-620 (2020).

4. E. Dong, H. Du, L. Gardner, An interactive web-based dashboard to track COVID-19 in real time, *Lancet Inf. Dis.*, **20**, 533-534 (2020).

5. L.S. Wang, Y.R. Wang, D.W. Ye, Q.Q. Liu, Review of the 2019 Novel Coronavirus (COVID-19) based on current evidence, *Int. J. Antimicrob. Agents*, **55**(6), 105948 (2020).

6. B. Gates, Responding to Covid-19. A Once-in-a-century pandemic?, *N. Engl. J. Med.*, **382**, 1677-1679 (2020).

7. C. Liu, Q. Zhou, Y. Li, L. Garner, S.Watkins, L. Carter, J. Smoot, A. Gregg, A. Daniels, S. Jervey, D. Albaiu, Research and development on therapeutic agents and vaccines for COVID-19 and related human coronavirus diseases, *ACS Central Science*, **6**, 315-331 (2020).

8. Z. Jin, X. Du, Y. Xu, Y. Deng, M. Liu, Y. Zhao, B. Zhang, X. Li, L. Zhang, C. Peng, Y. Duan, J. Yu, L. Wang, K. Yang, F. Liu, R. Jiang, X. Yang, T. You, X. Liu, X. Yang, F. Bai, H. Liu, X. Liu, H. Yang, Structure of M^{pro} from COVID-19 virus and discovery of its inhibitors, *Nature*, **582**, 289-293 (2020).

9. M. Prajapat, P. Sarma, N. Shekhar, P. Avti, S. Sinha, H. Kaur, S. Kumar, A. Bhattacharyya, H. Kumar, S. Bansal, B. Medhi, Drug targets for corona virus: A systematic review, *Indian J. Pharmacol.*, **52**, 56-65 (2020).

10. O. Trott, A.J. Olson, AutoDock Vina: improving the speed and accuracy of docking with a new scoring function, efficient optimization and multithreading, *J. Comput. Chem.*, **31,** 455-461 (2010).

11. P. Leeson, Drug discovery: Chemical beauty contest, *Nature,* **481**, 455-456 (2012).

12. D.F. Veber, S.R. Johnson, H.Y. Cheng, B.R. Smith, K.W. Ward, K.D. Kopple, Molecular properties that influence the oral bioavailability of drug candidates, *J. Med. Chem.*, **45,** 2615-2623 (2002).

13. A.K. Ghose, V.N. Viswanadhan, J.J. Wendoloski, A knowledge-based approach in designing combinatorial or medicinal chemistry libraries for drug discovery. 1. A qualitative and quantitative characterization of known drug databases, *J. Comb. Chem.*, **1,** 55-68 (1999).

14. N. Pájaro-Castro, M.C. Flechas, R. Ocazionez, E. Stashenko, J.T. Olivero-Verbel, Potential interaction of components from essential oils with dengue virus proteins, *Bol. Latinoamer. Caribe Plant. Med. Aromát.*, **14,** 141-155 (2015).

15. S. Khaerunnisa, H. Kurniawan, R. Awaluddin, S. Suhartati, S. Soetjipto. Potential inhibitor of COVID-19 main protease (M^{pro}) from several medicinal plant compounds by molecular docking study, *Preprints* (2020). URL: https://www.preprints.org/manuscript/202003.0226/v1, accessed March 2020.

16. K. Dhama, K. Sharun, R. Tiwari, S. Sircar, S. Bhat, Y.S. Malik, K.P. Singh, W. Chaicumpa, D.K. Bonilla-Aldana, A.J. Rodriguez-Morales, Coronavirus disease 2019 – COVID-19, *Clin. Microbiol. Rev.*, **33**, e00028-20 (2020).

17. T.W. Lee, M.M. Cherney, J. Liu, K.E. James, J.C. Powers, L.D. Eltis, M.N. James, Crystal structures reveal an induced-fit binding of a substrate-like Aza-peptide epoxide to SARS coronavirus main peptidase, *J. Mol. Biol.*, **366**, 916-932 (2007).

18. Z. Xu, C. Peng, Y. Shi, Z. Zhu, X. Mu, X. Wang, Nelfinavir was predicted to be a potential inhibitor of 2019-nCov main protease by an integrative approach combining homology modelling, molecular docking and binding free energy calculation, *BioRxiv* (2020). URL: https://www.biorxiv.org/content/10.1101/2020.01.27.921627v1, accessed March 2020.

19. H. Matter, K.H. Barighaus, T. Naumann, T. Klabunde, B. Pirard, Computational approaches towards the rational design of drug-like compound libraries, *Comb. Chem. High Throughput Screen*, **4**, 453-475 (2001).

20. Z. Haider, M.M. Subhani, M.A. Farooq, M. Ishaq, M. Khalid, R.S.A. Khan, A.K. Niazi, *In silico* discovery of novel inhibitors against main protease (M^{pro}) of SARS-CoV-2 using pharmacophore and molecular docking based virtual screening from ZINC database, *Preprints* (2020). URL: https://europepmc.org/article/ppr/ppr117373, accessed March 2020.

21. N. Chauhan, Possible drug candidates for COVID-19, (2020), URL: https://sweetcitruswhispers.files.wordpress.com/2020/03/possible-drug-candidates-for-covid-19.pdf, accessed March 2020.

22. I. Khalifa, W. Zhu, M.S. Nafie, K. Dutta, C. Li, Anti-Covid-19 effects of ten structurally different hydrolysable tannins through binding with the catalytic-closed sites of COVID-19 main protease: An *in-silico* approach, *Preprints* (2020), URL: https://www.preprints.org/manuscript/202003.0277/v1, accessed March 2020.

How to cite this article

N. Pajaro-Castro, C. Ibañez-Bersinger, G. Leon-Mendez, *In silico* approach of antiviral compounds potentials for SARS-CoV-2 and SARS-CoV and drug-like property predictions, *Rev. Colomb. Cienc. Quím. Farm.*, **49**(3), 806-821 (2020).

Scientific research article / *http://dx.doi.org/10.15446/rcciquifa.v49n3.91347*

Prediction of sulfadiazine solubility in some cosolvent mixtures using non-ideal solution models

Rossember E. Cardenas*, Luz Elena Tinoco, Diana M. Galindres, Alejandro Beltrán, Carlos D. Oviedo, Jhonny Osorio

Grupo de Fisicoquímica y análisis matemático, Facultad de Ciencias y Humanidades, Fundación Universidad de América, Avenida Circunvalar No. 20-53, Bogotá D.C., Colombia.

*Corresponding author: rossember.cardenas@profesores.uamerica.edu.co

Received: 19 September 2020

Revised: 28 September 2020

Accepted: 30 September 2020

Summary

The experimental data of sulfadiazine in (methanol + water), (ethanol + water) and (1-propanol + water) cosolvent mixtures at some temperatures were correlated using non-ideal solution models, namely, the modified Apelblat and Buchowski-Ksiazaczak equations and the van't Hoff equation. The calculated results agreed well with the experimental data. According to the Buchowski equation, the solubility of sulfadiazine in the three co-solvent mixtures shows important deviations from ideality, which is consistent with the literature.

Key words: Sulfadiazine, solubility, van't Hoff model, Buchowski-Ksiazaczak λh model, Apelblat model.

Resumen

Predicción de la solubilidad de la sulfadiazina en algunas mezclas cosolventes utilizando modelos de solución no ideales

Los datos experimentales de sulfadiazina en mezclas de cosolvente de (metanol + agua), (etanol + agua) y (1-propanol + agua) a algunas temperaturas se correlacionaron utilizando modelos de solución no ideales, a saber, las ecuaciones modificadas de Apelblat y Buchowski y la ecuación de van't Hoff. Los resultados calculados coincidieron bien con los datos experimentales. Según la ecuación de Buchowski, la solubilidad de la sulfadiazina en las tres mezclas de cosolventes muestra importantes desviaciones de la idealidad, lo que concuerda con la literatura.

Palabras clave: Sulfadiazina, solubilidad, modelo de van't Hoff, modelo de Buchowski-Ksiazaczak λh, modelo de Apelblat.

Introduction

Sulfadiazine (N^1-2-pyrimidinylsulfanilamide) (figure 1) is a member of the sulfonamide family [1]. As one of the earliest antibacterial drugs used in the prevention and treatment of bacterial infections, sulfonamides are widely used in the medical and livestock industries due to their broad antibacterial spectrum, stability and low-cost [2-4], however, sulfadiazine solubility in ambient water is very low and it is considered as practically insoluble [5-8]. Although the solid dosage form of sulfadiazine has been widely used in therapeutics, the development of liquid dosage forms is important to administer the drug to special groups of patients. To increase the solubility of sulfadiazine some cosolvents have been added to water [9, 10]. The analysis of sulfadiazine in the pharmaceutical industry typically involves high-performance liquid chromatograph that consumes a large quantity of hazardous organic solvents and its waste needs to be properly disposed of [11, 12].

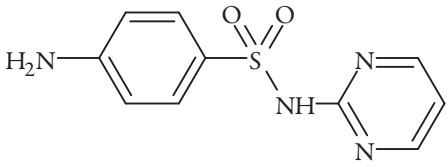

Figure 1. Molecular structure of sulfadiazine.

However, solubility measurement and optimization of the solvent composition for dissolving a desired amount of a drug in a given volume of the solution in most of the cases is a laborious and time consuming procedure which may cause some limitations in discovering and development of new drugs [13, 14]. Mathematical model, as an alternative method, could be used to estimate drug's solubility especially when the solid–liquid equilibrium measurements become impractical. Various numerical models proposed for the estimation of the solubility of drug and/or drug like compounds in the cosolvency systems which in order of appearance include van't Hoff equation [15], Yalkowsky model [5, 16, 17], the mixture response surface model, the double log-log model, the modified Wilson model[18], the Jouyban-Acree model [19-21], the Jouyban-Acree-van't Hoff model, and modified Jouyban-Acree-van't Hoff model. Van't Hoff equation predicts solubility at different temperatures in each solvent composition [22, 23], whereas Yalkowsky model, the modified Wilson model [18], the double log-log model and mixture response surface model predict solubility at different solvent mixtures. Whereas, the Jouyban-Acree [24] and Jouyban-Acree-van't Hoff models [25] predict the solubility in various solvent composition at different temperatures.

The objective of the present work is to evaluate the application of the van't Hoff, Buchowski-Ksiazaczak λh, and modified Apelblat models to the solubility of sulfadiazine in three cosolvent systems.

Theoretical

Modified Apelblat equation

From the Williamson equation, the solubility of non-electrolytes is expressed as [26]:

$$\frac{\partial \ln\left(m/m^{o}\right)}{\partial T^{-1}} = \frac{\Delta_{\text{soln}} H(T)}{R\left[1-0.001hM_1 m\right] f}, f = 1 + \left\{ \frac{\partial \ln \gamma_3}{\partial \ln\left(m/m^{o}\right)} \right\}_T, \tag{1}$$

where h denotes a number of water molecules in the hydrate, $\Delta_{\text{soln}}H(T)$ is the molar enthalpy of solution, γ_3 is the activity coefficient of the solute, M_1 is the molar mass of solvent, R is the gas constant and $m^{\circ} = 1$ mol.kg^{-1}.

If it is assumed that the enthalpy of solution depends linearly on the temperature, the integral form of equation (1) is [27]:

$$\ln\left(m/m^{\circ}\right) = A + BT^{-1} + C\ln T \tag{2}$$

So, expressing the solubility in mole fraction, the modified Apelblat equation, which is a semi-empirical model derived from solid-liquid equilibrium is [28]:

$$\ln x_3 = A + BT^{-1} + C\ln T \tag{3}$$

x_1 refers to measured mole fraction solubility of drug in selected solvent at absolute temperature T; A and B reflect the variation in the solution activity coefficient; C represents the influence of temperature on enthalpy of fusion [29, 30]; The above three parameters and experimental prediction values can be obtained by the nonlinear regression method in Python.

Van't Hoff equation

The van't Hoff equation is also a semi-empirical equation, which reveals the relationship between the mole fraction solubility and the temperature in an ideal solution by taking the solvent effect into account. The formula is shown as equation (4).

$$\ln x_3 = A + \frac{B}{T} \tag{4}$$

A and B are parameters, which can be related to thermodynamic parameters such as dissolution enthalpy and dissolution entropy [22]. The above can be shown from the two mathematical expressions for the Gibbs energy [31-34]:

$$\Delta_{soln} G^\circ = -RT \ln x_3 \tag{5}$$

$$\Delta_{soln} G^\circ = \Delta_{soln} H^\circ - T\Delta_{soln} S^\circ \tag{6}$$

Solving for $\Delta_{soln} G^\circ$ from equation (5), subsequently replacing $\Delta_{soln} G^\circ$ from equation (6), we obtain,

$$\ln x_3 = -\frac{\Delta_{soln} G^\circ}{RT} = \frac{\Delta_{soln} H^\circ - T\Delta_{soln} S^\circ}{RT} \tag{7}$$

$$\ln x_3 = -\frac{\Delta_{soln} H^\circ}{RT} + \frac{\Delta_{soln} S^\circ}{R} \tag{8}$$

So,

$$A = -\frac{\Delta_{soln} H^\circ}{RT}; B = \frac{\Delta_{soln} S^\circ}{R} \tag{9}$$

Buchowski-Ksiazaczak λh model

In 1980, based on the generalized relationship, the Buchowski-Ksiazaczak λh equation was first proposed, which contains two parameters and is widely used to correlate solubility data. The Buchowski-Ksiazaczak λh equation is shown in equation (10).

$$\ln\left[1 + \frac{\lambda(1 - x_3)}{x_3}\right] = \lambda h\left(\frac{1}{T} - \frac{1}{T_f}\right) \tag{10}$$

where λ and h are the two parameters of the λh model, and T_f represents the melting point of drug [35-37]. The model can be tested starting from the following identity [38]:

$$\frac{\partial \ln(1 - a_1)}{\partial \ln a_1} = \frac{-a_1}{1 - a_1} \tag{11}$$

Integrating the identity –equation (11)– into the equation of into the Gibbs-Duhem equation, we obtain,

$$\frac{-a_1}{1-a_1}\frac{x_3}{x_1}=\left(\frac{\partial \ln(1-a_1)}{\partial \ln a_3}\right)_T \equiv \lambda \tag{12}$$

In this way λ is related to activity and therefore to the concept of ideality.

Buchowski showed that when graphing $\ln(1-a)$ vs $1/T$, a linear function was obtained whose slope is λh

$$\frac{\partial \ln(1-a_3)}{\partial T^{-1}}=\lambda h \tag{13}$$

Integration of equation (13) from T_m to T gives equation (14).

$$-\ln(1-a_3)_{sat}=\lambda h\left(\frac{1}{T}-\frac{1}{T_m}\right) \tag{14}$$

where T_m is the melting temperature.

For the solubility curve, equation (14) is rearranged as:

$$\frac{\lambda(1-x_3)}{x_3}=\frac{a_1}{1-a_1} \tag{15}$$

Hence,

$$-\ln(1-a_1)=\ln\left[1+\lambda(1-x_3)/x_3\right] \tag{16}$$

So, equations (14) and (16) give the solubility curve:

$$\ln\left[1+\frac{\lambda(1-x_3)}{x_3}\right]_{sat}=\lambda h\left(\frac{1}{T}-\frac{1}{T_m}\right) \tag{17}$$

Equation (17) is equal to equation (10).

Results and discussion

The solubilities of sulfadiazine in mixtures of (methanol + water), (ethanol + water) and (1-propanol + water) were provided by Delgado and Martínez [6-8].

The experimental solubility data were correlated with the van't Hoff equation, Apelblat equation and Buchowski–Ksiazaczak λh equation, using the software with the Python version 3.8 using pandas and NumPy library, the parameters of the models were calculated with SciPy library and plots were made with Plotly library.

Table 1 shows the parameters of the equations of λh, van't Hoff and Apelblat, for the solubility of SD in (methanol + water) co-solvent mixtures. Although Delgado and Martínez implements the van't Hoff equation, the purpose is to calculate the thermodynamic functions as shown in other references [39-42], and not, to use the equation to calculate the solubility at different temperatures regarding the experimental ones [43, 44]. The melting temperature data, necessary for the development of the λh model, was taken from the literature (259.5 °C) [6].

Table 1. The λh, van't Hoff and Apelblat equations parameters for sulfadiazine in (methanol + water) cosolvent mixtures.

w_1	λh		van't Hoff		Apelblat		
	λ	h	a	b	A	B	C
0.0	0.012	453579.478	-5240.132	5.381	721.839	-37592.530	-106.700
0.1	0.024	231338.674	-5471.214	6.531	-450.653	15179.951	68.083
0.2	0.048	117837.137	-5637.581	7.547	-245.459	5818.116	37.662
0.3	0.102	55545.250	-5641.050	8.306	-873.483	34189.980	131.315
0.4	0.091	58195.968	-5271.480	7.499	127.882	-10687.332	-17.940
0.5	0.071	67026.233	-4794.893	6.372	-636.382	24238.424	95.718
0.6	0.065	68272.846	-4436.498	5.607	-453.188	16284.888	68.325
0.7	0.055	74423.661	-4130.908	4.883	-1134.337	47356.976	169.635
0.8	0.048	80928.039	-3886.460	4.284	-591.953	23047.998	88.790
0.9	0.042	87512.255	-3735.108	3.886	-461.868	17310.056	69.356
1.0	0.033	105595.312	-3502.490	3.205	44.861	-5385.482	-6.203

Table 2 shows the calculated solubility using each of the exposed models, and the relative deviation, calculated using equation (18) [45-48].

$$DR = 100\left(\left|x_3^{Exp} - x_3^{Cal}\right|\right)\left(x_3^{Exp}\right)^{-1} \quad (18)$$

Table 2. Calculated solubility of sulfadiazine in (methanol + water) mixtures expressed in mole fraction ($10^4 x_3$), from equations of λh, van't Hoff and Apelblat.

Buchowski–Ksiazaczak λh equation										
w_1	**293.15 K**	**RD**	**298.15 K**	**RD**	303.15 K	**RD**	**308.15 K**	**RD**	**313.15 K**	**RD**
0.0	0.375	1.326	0.506	5.195	0.676	4.788	0.895	1.771	1.174	2.988
0.1	0.538	1.459	0.736	0.185	0.996	2.230	1.335	1.045	1.772	1.603
0.2	0.843	0.841	1.163	1.791	1.589	0.202	2.149	2.153	2.878	0.960
0.3	1.780	6.404	2.457	4.582	3.357	4.038	4.540	0.833	6.082	2.702
0.4	2.801	1.866	3.786	2.549	5.068	0.200	6.720	0.015	8.831	0.557
0.5	4.613	2.671	6.068	0.347	7.911	3.472	10.226	1.072	13.111	2.139
0.6	7.291	2.672	9.396	0.525	12.008	4.118	15.227	0.660	19.165	1.223
0.7	10.019	3.404	12.686	1.356	15.940	4.728	19.883	4.183	24.632	3.907
0.8	12.674	2.996	15.824	1.819	19.617	1.607	24.153	1.704	29.547	2.066
0.9	14.267	0.861	17.659	1.638	21.708	2.939	26.513	1.268	32.183	1.657
1.0	15.960	1.356	19.493	1.955	23.657	0.316	28.538	1.515	34.229	0.633
van't Hoff equation										
0.0	0.375	1.328	0.506	5.199	0.676	4.784	0.895	1.769	1.174	2.980
0.1	0.538	1.464	0.736	0.185	0.996	2.234	1.335	1.049	1.772	1.605
0.2	0.843	0.838	1.163	1.790	1.589	0.199	2.149	2.155	2.878	0.962
0.3	1.779	6.410	2.457	4.582	3.357	4.041	4.540	0.836	6.082	2.701
0.4	2.800	1.862	3.786	2.546	5.068	0.204	6.720	0.013	8.831	0.551
0.5	4.613	2.684	6.068	0.347	7.912	3.479	10.227	1.079	13.111	2.140
0.6	7.290	2.689	9.396	0.526	12.010	4.129	15.228	0.650	19.164	1.226
0.7	10.015	3.438	12.685	1.360	15.942	4.742	19.887	4.201	24.633	3.902
0.8	12.670	3.028	15.825	1.820	19.620	1.625	24.157	1.721	29.546	2.070
0.9	14.262	0.893	17.659	1.635	21.713	2.960	26.518	1.285	32.180	1.665
1.0	15.955	1.384	19.495	1.965	23.663	0.341	28.542	1.501	34.221	0.610

(*Continued*)

Table 2. Calculated solubility of sulfadiazine in (methanol + water) mixtures expressed in mole fraction ($10^4 x_3$), from equations of λh, van't Hoff and Apelblat.

w_1	**293.15 K**	**RD**	**298.15 K**	**RD**	303.15 K	**RD**	**308.15 K**	**RD**	**313.15 K**	**RD**
Apelblat equation										
0.0	0.363	4.561	0.513	6.566	0.695	2.070	0.908	0.361	1.143	0.253
0.1	0.550	0.694	0.730	1.007	0.978	0.371	1.322	0.048	1.801	0.032
0.2	0.857	2.502	1.161	1.990	1.574	1.133	2.135	1.499	2.895	0.350
0.3	1.855	2.451	2.417	2.888	3.239	0.376	4.452	1.122	6.268	0.276
0.4	2.794	1.624	3.802	2.148	5.095	0.739	6.732	0.159	8.774	0.091
0.5	4.754	0.309	5.997	0.829	7.709	0.823	10.083	0.340	13.404	0.052
0.6	7.446	0.600	9.315	0.338	11.788	2.209	15.077	1.638	19.474	0.373
0.7	10.608	2.280	12.446	3.217	15.224	0.024	19.359	1.436	25.527	0.416
0.8	13.035	0.233	15.655	0.728	19.153	0.796	23.839	0.382	30.151	0.065
0.9	14.594	1.411	17.519	2.416	21.310	1.050	26.239	0.221	32.676	0.149
1.0	15.919	1.605	19.506	2.024	23.700	0.500	28.567	1.412	34.175	0.472

In all cases, the DR of the data calculated with respect to the experimental data is less than 7%. which indicates that the three models predict the solubility of SD in (methanol + water) cosolvent mixtures with good precision. When graphing the experimental data *vs.* the calculated data (figures 2, 3 y 4), linear holdings are obtained with correlation coefficients equal to 0.99, corroborating that these models show good agreement with the experimental solubility data.

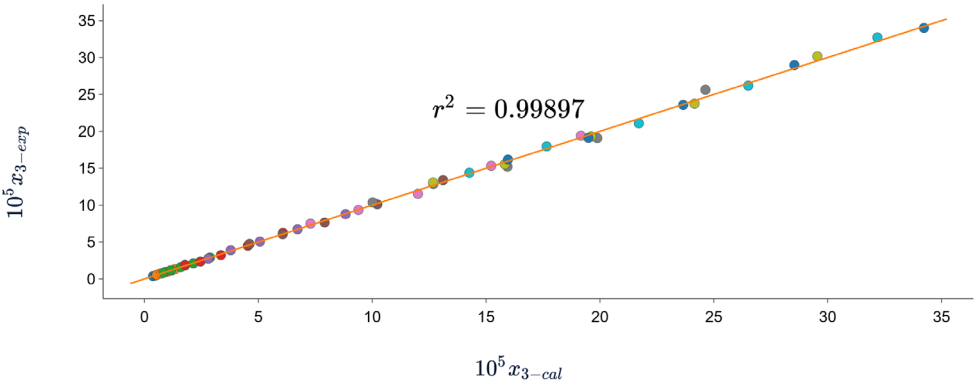

Figure 2. Experimental solubility *vs* calculated solubility by λh model of sulfadiazine in (methanol + water) mixtures.

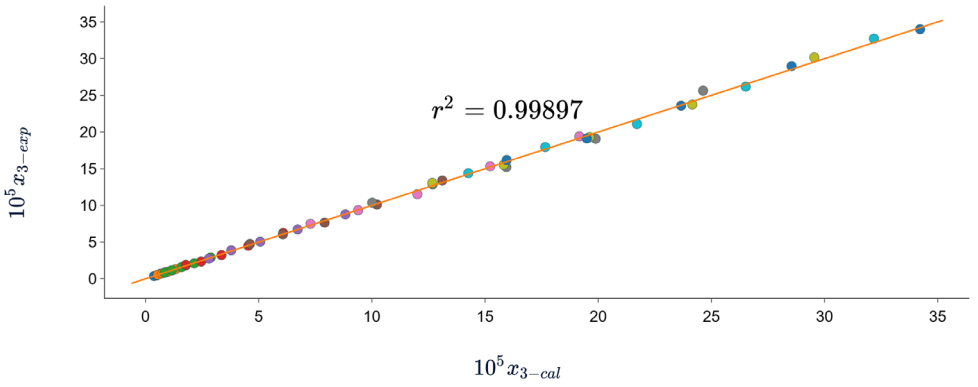

Figure 3. Experimental solubility *vs* calculated solubility by van't Hoff model of sulfadiazine in (methanol + water) mixtures.

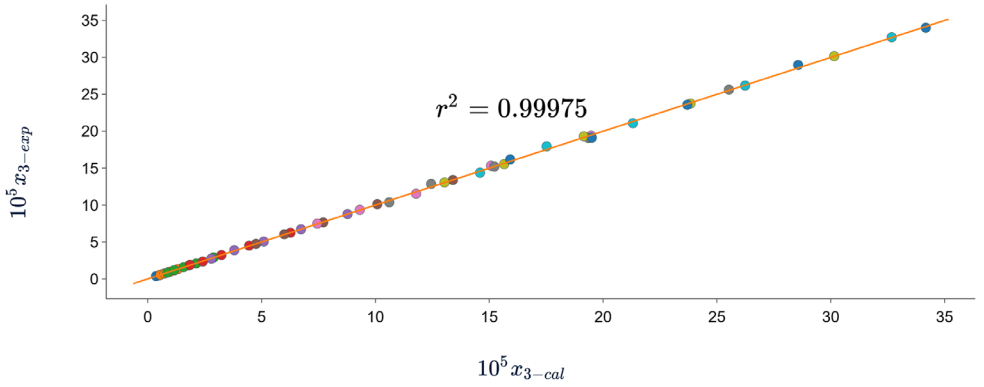

Figure 4. Experimental solubility *vs* calculated solubility by Apelblat model of sulfadiazine in (methanol + water) mixtures.

Table 3 shows the parameters of the equations of λh, van't Hoff and Apelblat, for the solubility of SD in (ethanol + water) cosolvent mixtures and table 4 shows the calculated solubility using each of the exposed models, and the relative deviation. As in the (methanol + water) cosolvent mixtures, the three models predict the solubility data of the SD, with good precision, in this case, the DR are less than 5%.

Table 3. The λh, van't Hoff and Apelblat equations parameters for sulfadiazine in (ethanol + water) cosolvent mixtures.

w_1	λh		van't Hoff		Apelblat		
	λ	h	a	b	A	B	C
0.0	0.012	452082.860	-5242.737	5.390	713.032	-37197.056	-105.387
0.1	0.017	298576.937	-5212.287	5.742	-48.821	-2742.779	8.123
0.2	0.052	105393.552	-5505.28	7.387	-459.017	15545.968	69.466
0.3	0.083	64173.623	-5324.945	7.512	-363.930	11469.983	55.305
0.4	0.041	108496.176	-4467.030	5.208	-203.729	4971.161	31.114
0.5	0.033	120784.624	-4031.583	4.188	-266.243	8182.280	40.273
0.6	0.035	110275.998	-3904.101	4.011	-190.160	4868.094	28.915
0.7	0.042	91475.436	-3893.641	4.175	312.345	-17810.217	-45.894
0.8	0.042	92808.419	-3869.417	4.110	-118.671	1681.403	18.282
0.9	0.031	123363.288	-3815.112	3.710	257.067	-15252.485	-37.734
1.0	0.016	220875.617	-3652.567	2.785	193.870	-12282.134	-28.457

Table 4. Calculated solubility of sulfadiazine in (ethanol + water) mixtures expressed in mole fraction ($10^4 x_3$), from equations of λh, van't Hoff and Apelblat.

	Buchowski–Ksiazaczak λh equation									
w_1	293.15 K	RD	298.15 K	RD	303.15 K	RD	308.15 K	RD	313.15 K	RD
0.0	0.375	1.341	0.506	5.196	0.676	4.771	0.895	1.736	1.175	2.948
0.1	0.592	0.462	0.797	1.131	1.063	1.363	1.405	1.017	1.841	0.305
0.2	1.128	4.139	1.545	2.761	2.095	3.675	2.814	0.790	3.742	1.354
0.3	2.364	0.262	3.205	0.558	4.303	0.203	5.722	2.533	7.541	1.481
0.4	4.406	0.515	5.687	1.153	7.281	2.692	9.248	0.449	11.658	0.544
0.5	7.022	0.893	8.841	0.464	11.048	2.141	13.710	0.087	16.898	0.855
0.6	9.082	0.400	11.351	0.003	14.086	0.039	17.360	1.221	21.258	0.854
0.7	11.087	0.162	13.849	0.058	17.177	0.968	21.159	2.789	25.896	1.773
0.8	11.285	0.351	14.077	1.180	17.435	0.594	21.449	0.785	26.218	0.540
0.9	9.107	0.090	11.325	1.677	13.985	2.169	17.155	0.429	20.911	1.058

(*Continued*)

Table 4. Calculated solubility of sulfadiazine in (ethanol + water) mixtures expressed in mole fraction ($10^4 x_3$), from equations of λh, van't Hoff and Apelblat.

w_1	**293.15 K**	**RD**	**298.15 K**	**RD**	303.15 K	**RD**	**308.15 K**	**RD**	**313.15 K**	**RD**
1.0	6.284	0.304	7.741	0.023	9.474	0.135	11.521	1.406	13.926	1.008
van't Hoff equation										
0.0	0.375	1.344	0.506	5.199	0.676	4.766	0.895	1.735	1.175	2.940
0.1	0.591	0.467	0.797	1.133	1.063	1.358	1.405	1.020	1.841	0.310
0.2	1.128	4.145	1.545	2.761	2.096	3.679	2.814	0.786	3.742	1.355
0.3	2.364	0.267	3.205	0.557	4.303	0.199	5.722	2.536	7.540	1.483
0.4	4.405	0.528	5.688	1.150	7.282	2.702	9.249	0.442	11.657	0.551
0.5	7.020	0.915	8.841	0.460	11.050	2.157	13.711	0.099	16.897	0.865
0.6	9.080	0.422	11.352	0.003	14.088	0.056	17.362	1.233	21.255	0.867
0.7	11.085	0.148	13.851	0.049	17.180	0.985	21.160	2.781	25.891	1.752
0.8	11.283	0.330	14.078	1.174	17.439	0.612	21.451	0.797	26.214	0.555
0.9	9.105	0.105	11.326	1.688	13.988	2.151	17.156	0.421	20.906	1.034
1.0	6.282	0.285	7.742	0.012	9.476	0.157	11.522	1.395	13.923	0.982
Apelblat equation										
0.0	0.363	4.561	0.513	6.566	0.695	2.070	0.908	0.361	1.143	0.253
0.1	0.550	0.694	0.730	1.007	0.978	0.371	1.322	0.048	1.801	0.032
0.2	0.857	2.502	1.161	1.990	1.574	1.133	2.135	1.499	2.895	0.350
0.3	1.855	2.451	2.417	2.888	3.239	0.376	4.452	1.122	6.268	0.276
0.4	2.794	1.624	3.802	2.148	5.095	0.739	6.732	0.159	8.774	0.091
0.5	4.754	0.309	5.997	0.829	7.709	0.823	10.083	0.340	13.404	0.052
0.6	7.446	0.600	9.315	0.338	11.788	2.209	15.077	1.638	19.474	0.373
0.7	10.608	2.280	12.446	3.217	15.224	0.024	19.359	1.436	25.527	0.416
0.8	13.035	0.233	15.655	0.728	19.153	0.796	23.839	0.382	30.151	0.065
0.9	14.594	1.411	17.519	2.416	21.310	1.050	26.239	0.221	32.676	0.149
1.0	15.919	1.605	19.506	2.024	23.700	0.500	28.567	1.412	34.175	0.472

Figures 5, 6 and 7 show the correlation between the experimental solubility data of SD in (ethanol + water) cosolvent mixtures and those calculated with the three models, in all cases the correlation coefficients are equal to or greater than 0.99.

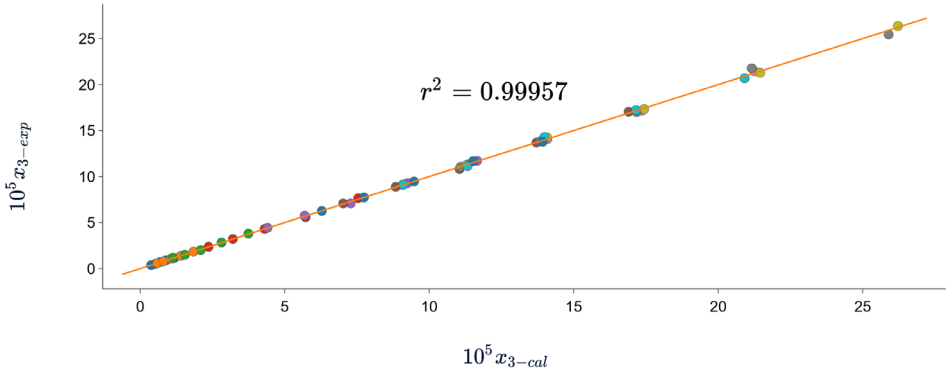

Figure 5. Experimental solubility *vs* calculated solubility by λh model of sulfadiazine in (ethanol + water) mixtures.

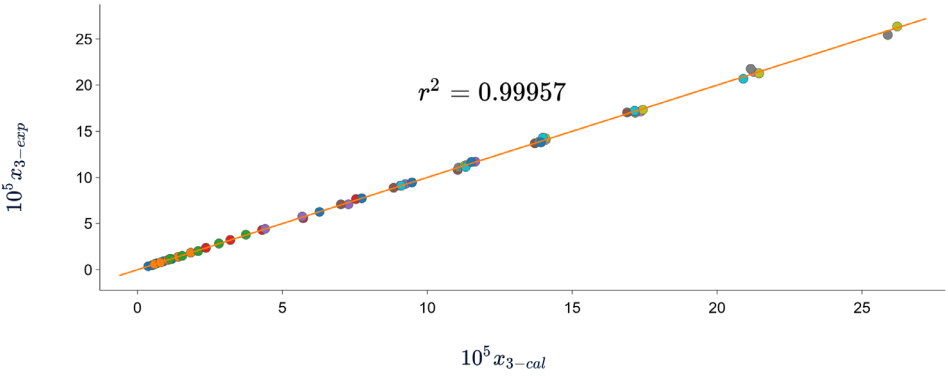

Figure 6. Experimental solubility *vs* calculated solubility by van't Hoff model of sulfadiazine in (ethanol + water) mixtures.

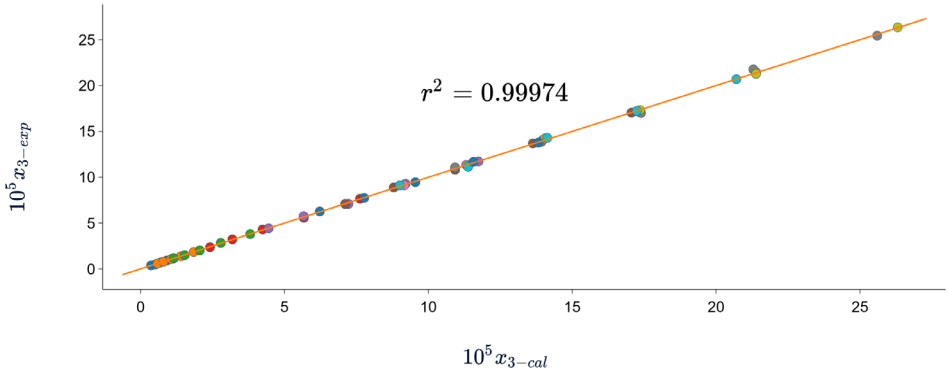

Figure 7. Experimental solubility *vs* calculated solubility by Apelblat model of sulfadiazine in (ethanol + water) mixtures.

Table 5 shows the parameters of the equations of λh, van't Hoff and Apelblat, for the solubility of SD in (1-propanol + water) cosolvent mixtures and table 6 shows the calculated solubility using each of the exposed models, and the relative deviation.

Table 5. The regression parameters of the Apelblat, van't Hoff, and λh model for sulfadiazine in (1-propanol + water) mixtures.

w_1	λh		van't Hoff		Apelblat		
	λ	h	a	b	A	B	C
0.0	0.012	451771.183	-5243.218	5.392	712.964	-37194.385	-105.377
0.1	0.016	314684.946	-4894.286	5.032	371.415	-21443.827	-54.561
0.2	0.022	214826.896	-4760.884	5.136	94.695	-8770.827	-13.357
0.3	0.043	107306.471	-4636.504	5.572	373.823	-21276.670	-54.836
0.4	0.055	83741.522	-4605.045	5.754	-172.781	3454.943	26.590
0.5	0.067	67398.827	-4537.686	5.831	-69.720	-1123.467	11.250
0.6	0.074	59687.244	-4436.373	5.741	166.048	-11686.808	-23.867
0.7	0.056	73997.588	-4171.041	4.970	-39.879	-2132.985	6.672
0.8	0.045	88738.406	-3996.161	4.422	-175.520	4134.765	26.795
0.9	0.029	132531.458	-3874.517	3.764	165.295	-11166.077	-24.058
1.0	0.016	248491.514	-3949.778	3.296	-427.185	15494.320	64.107

Table 6. Calculated solubility of sulfadiazine in (1-propanol + water) mixtures expressed in mole fraction ($10^4 x_3$), from equations of λh, van't Hoff and Apelblat.

	Buchowski–Ksiazaczak λh equation									
w_1	293.15 K	RD	298.15 K	RD	303.15 K	RD	308.15 K	RD	313.15 K	RD
0.0	0.375	1.342	0.506	5.197	0.676	4.770	0.895	1.736	1.175	2.948
0.1	0.860	0.856	1.138	0.643	1.491	0.373	1.938	2.213	2.498	1.678
0.2	1.505	1.653	1.976	1.035	2.572	3.044	3.318	2.431	4.247	0.091
0.3	3.556	0.135	4.635	0.915	5.990	0.090	7.678	2.591	9.764	1.774
0.4	4.753	1.420	6.184	1.561	7.978	0.055	10.208	0.461	12.961	0.645
0.5	6.455	2.143	8.368	3.534	10.754	1.629	13.711	0.533	17.348	0.214
0.6	8.334	1.577	10.740	2.261	13.726	0.651	17.406	2.347	21.908	1.072
0.7	9.537	0.496	12.105	1.541	15.245	2.492	19.059	1.882	23.662	0.382

(*Continued*)

Table 6. Calculated solubility of sulfadiazine in (1-propanol + water) mixtures expressed in mole fraction ($10^4 x_3$), from equations of λh, van't Hoff and Apelblat.

Buchowski–Ksiazaczak λh equation										
w_1	**293.15 K**	**RD**	**298.15 K**	**RD**	303.15 K	**RD**	**308.15 K**	**RD**	**313.15 K**	**RD**
0.8	10.006	1.358	12.573	1.946	15.681	1.178	19.422	1.384	23.896	0.761
0.9	7.849	1.704	9.795	3.547	12.135	1.733	14.933	1.002	18.258	0.980
1.0	3.801	1.935	4.764	1.137	5.926	0.934	7.321	1.486	8.986	1.596
van't Hoff equation										
0.0	0.375	1.344	0.506	5.200	0.676	4.766	0.895	1.735	1.175	2.940
0.1	0.860	0.851	1.138	0.640	1.492	0.380	1.938	2.210	2.498	1.669
0.2	1.505	1.648	1.976	1.031	2.572	3.037	3.318	2.435	4.247	0.082
0.3	3.555	0.142	4.635	0.919	5.991	0.098	7.678	2.587	9.763	1.764
0.4	4.752	1.431	6.184	1.563	7.979	0.064	10.209	0.468	12.960	0.651
0.5	6.455	2.154	8.368	3.537	10.755	1.620	13.712	0.539	17.347	0.221
0.6	8.333	1.587	10.740	2.265	13.728	0.661	17.407	2.341	21.906	1.063
0.7	9.536	0.510	12.105	1.546	15.247	2.479	19.061	1.890	23.659	0.394
0.8	10.004	1.378	12.573	1.951	15.684	1.162	19.424	1.395	23.893	0.772
0.9	7.848	1.721	9.795	3.556	12.137	1.716	14.934	0.993	18.254	0.960
1.0	3.800	1.962	4.764	1.140	5.927	0.952	7.322	1.500	8.985	1.603
Apelblat equation										
0.0	0.363	4.536	0.512	6.551	0.695	2.086	0.908	0.343	1.144	0.248
0.1	0.845	0.911	1.145	0.006	1.513	1.841	1.953	1.455	2.465	0.356
0.2	1.507	1.769	1.986	0.566	2.583	2.612	3.320	2.485	4.218	0.589
0.3	3.490	1.992	4.662	1.508	6.077	1.546	7.739	1.810	9.642	0.504
0.4	4.789	0.662	6.162	1.196	7.921	0.661	10.171	0.097	13.046	0.013
0.5	6.479	1.787	8.357	3.401	10.722	1.923	13.688	0.360	17.388	0.016
0.6	8.256	2.490	10.761	2.460	13.811	1.272	17.471	1.981	21.801	0.579
0.7	9.573	0.116	12.108	1.567	15.223	2.633	19.032	1.735	23.666	0.367
0.8	10.094	0.492	12.535	1.642	15.571	1.871	19.345	0.984	24.035	0.183
0.9	7.793	2.416	9.826	3.882	12.215	1.084	14.981	0.683	18.140	0.327
1.0	3.878	0.039	4.726	0.341	5.825	0.789	7.254	0.551	9.121	0.120

According to the results shown in table 6 and figures 8, 9 and 10, in which the experimental and calculated solubility are compared. the three solubility models, including Apelblat model, Buchowski-Ksiazaczak λh equation and van't Hoff model, were applied to fit with experimental data obtaining a good predictability of the experimental data, since the DR values do not exceed 5%.

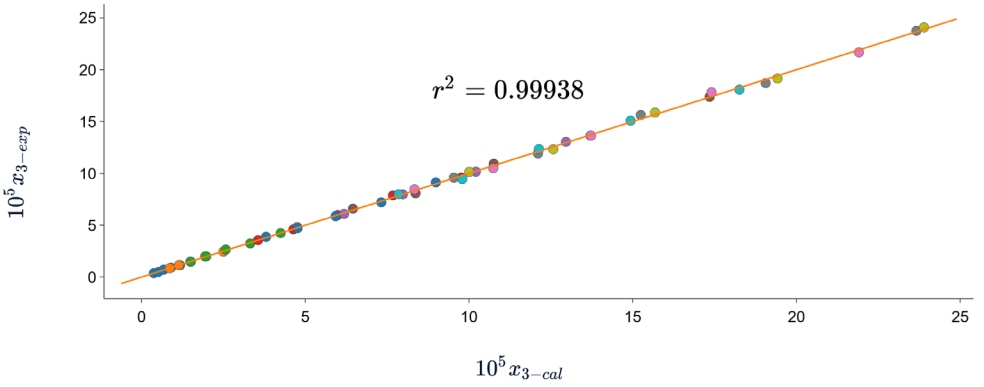

Figure 8. Experimental solubility *vs* calculated solubility by λh model of sulfadiazine in (1-propanol + water mixtures) mixtures.

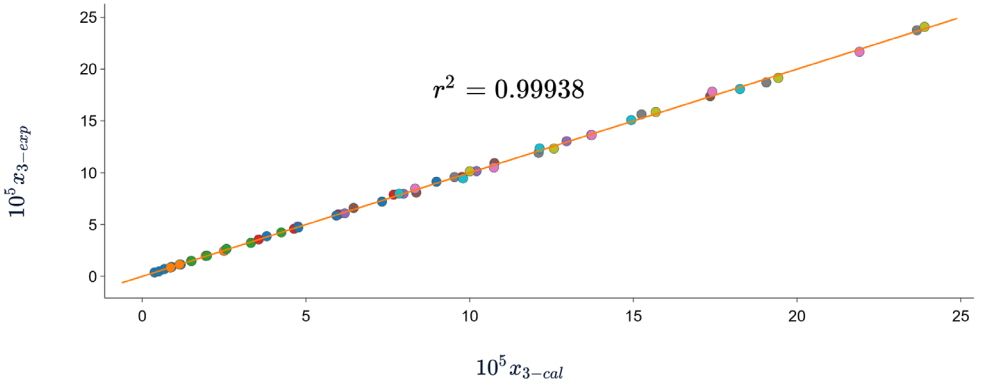

Figure 9. Experimental solubility *vs* calculated solubility by van't Hoff model of sulfadiazine in (1-propanol+ water) mixtures.

In general terms, from the results shown in tables 2, 4, 6 and figures 2-10, it can be observed that the Apelblat model, Buchowski-Ksiazaczak λh equation and van't Hoff model gave almost the same goodness of fit to the experimental data. Error percentages of the predicted solubility values obtained from calculations using both models were below 5%, except for one point of SD solubility in (methanol + water) mixtures

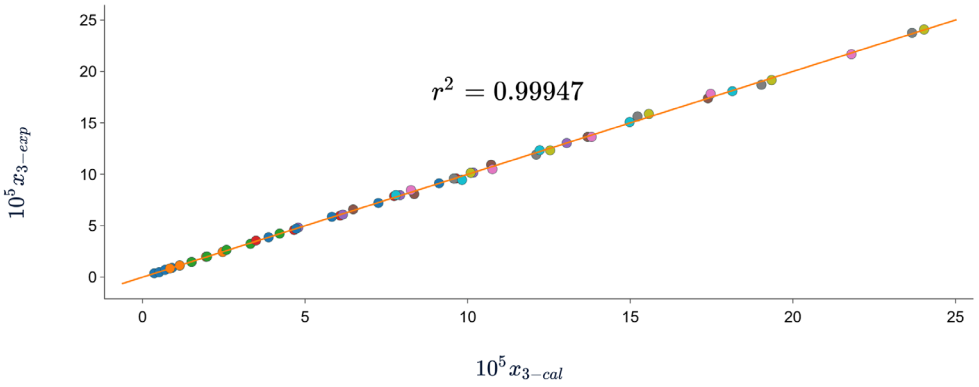

Figure 10. Experimental solubility *vs* calculated solubility by Apelblat model of sulfadiazine in (1-propanol+ water) mixtures.

(w_3 at 293.15 K). The goodness of fit of these equations can also be seen from the r^2 values listed in figures 2-10, which are almost unity. Buchowski *et al.* [38] stated that in an ideal solution, the value of λ equals to 1. The values of the obtained equation parameter (λ) in tables 2, 4 and 6 showed that the SD in (methanol + water), (ethanol + water) and (1-propanol + water) cosolvent mixtures, understandably were nonideal. This agrees with Delgado and Martínez [6-8], who reported that solution of SD in some cosolvent mixtures are highly non-ideal.

Acknowledgements

The authors gratefully acknowledge support from the Faculty of Science and Humanities and Research Direction of the Fundación Universidad de América.

Disclosure statement

No potential conflict of interest was reported by the authors.

References

1. R.S. Vardanyan, V.J. Hruby, *Synthesis of Essential Drugs*, Elsevier, Amsterdam (Netherlands), 2006, pp. 499-523.

2. H. Li, L. Duan, H. Wang, Y. Chen, F. Wang, S. Zhang, Photolysis of sulfadiazine under UV radiation: Effects of the initial sulfadiazine concentration, pH, NO^{3-} and Cd^{2+}, *Chem. Phys. Lett.*, **739**, 136949 (2020).

3. K. Kümmerer, A. Al-Ahmad, V. Mersch-Sundermann, Biodegradability of some antibiotics, elimination of the genotoxicity and affection of wastewater bacteria in a simple test, *Chemosphere*, **40**, 701-710 (2000).

4. D.R. Delgado, F. Martínez, Solubility and solution thermodynamics of sulfamerazine and sulfamethazine in some ethanol + water mixtures, *Fluid Phase Equilib.*, **360**, 88-96 (2013).

5. S.H. Yalkowsky, *Solubility and solubilization in aqueous media*, American Chemical Society and Oxford University Press, New York (NY), 1999.

6. D.R. Delgado, F. Martínez, Solution thermodynamics of sulfadiazine in some ethanol + water mixtures, *J. Mol. Liq.*, **187**, 99-105 (2013).

7. D.R. Delgado, F. Martínez, Solubility and solution thermodynamics of some sulfonamides in 1-propanol + water mixtures, *J. Solution Chem.*, **43**, 836-852 (2014).

8. D.R. Delgado, F. Martínez, Solubility and preferential solvation of sulfadiazine in methanol + water mixtures at several temperatures, *Fluid Phase Equilib.*, **379**, 128-138 (2014).

9. D.M. Jiménez, Z.J. Cárdenas, D.R. Delgado, M.A. Peña, F. Martínez, Solubility temperature dependence and preferential solvation of sulfadiazine in 1,4-dioxane + water co-solvent mixtures, *Fluid Phase Equilib.*, **397**, 26-36 (2015).

10. M.M. Muñoz, D.R. Delgado, M.Á. Peña, A. Jouyban, F. Martínez, Solubility and preferential solvation of sulfadiazine, sulfamerazine and sulfamethazine in propylene glycol + water mixtures at 298.15 K, *J. Mol. Liq.*, **204**, 132-136 (2015).

11. S. Akay, B. Kayan, D. Cunbin, J. Wang, Y. Yang, Research of sulfadiazine using subcritical water and water + alcohol mixtures as the solvent: Solubility and thermodynamic property, *J. Mol. Liq.*, **253**, 270-276 (2018).

12. D.R. Delgado, G.A. Rodríguez, J.A. Martínez, J.H. Rojas, F. Martínez, Validación de una metodología analítica empleando espectrofotometría ultravioleta para el estudio de la solubilidad de algunas sulfonamidas en mezclas cosolventes alcohol + agua, *Rev. Colomb. Quim.*, **42**, 31-40 (2013).

13. S. Zadaliasghar, E. Rahimpour, T. Ghafourian, F. Martínez, M. Barzegar-Jalali, A. Jouyban, Measurement and mathematical modeling of ketoconazole solubility in propylene glycol + water mixtures at various temperatures, *J. Mol. Liq.*, **291**, 111246 (2019).

14. H. Kishi, Y. Hashimoto, Evaluation of the procedures for the measurement of water solubility and n-octanol/water partition coefficient of chemicals results of a ring test in Japan, *Chemosphere*, **18**, 1749-1759 (1989).

15. A.Y. Lin, K.T. Cheng, S.C. Chen, H.W. Tsui, Effect of solvent composition on the van't Hoff enthalpic curve using amylose 3,5-dichlorophenylcarbamate-based sorbent, *J. Chromatogr. A*, **1515**, 179-186 (2017).

16. F. Shakeel, N. Haq, N.A. Siddiqui, F.K. Alanazi, I.A. Alsarra, Thermodynamics of the solubility of reserpine in {2-(2-ethoxyethoxy)ethanol + water} mixed solvent systems at different temperatures, *J. Chem. Thermodyn.*, **85**, 57-60 (2015).

17. M.A. Ruidiaz, D.R. Delgado, F. Martínez, Performance of the Jouyban-Acree and Yalkowsky-Roseman models for estimating the solubility of indomethacin in ethanol+ water mixtures, *Rev. Acad. Colomb. Cienc.*, **35**, 329-336 (2011).

18. X. Hu, Y. Tian, Z. Cao, J. Sha, Z. Huang, Y. Li, T. Li, B. Ren, Solubility measurement, Hansen solubility parameter and thermodynamic modeling of etodolac in four binary solvents from 278.15 K to 323.15 K, *J. Mol. Liq.*, **318**, 114155 (2020).

19. D.R. Delgado, G.A. Rodríguez, A.R. Holguín, F. Martínez, A. Jouyban, Solubility of sulfapyridine in propylene glycol + water mixtures and correlation with the Jouyban-Acree model, *Fluid Phase Equilib.*, **341**, 86-95 (2013).

20. G.A. Rodríguez, D.R. Delgado, F. Martínez, A. Jouyban, W.E. Acree Jr., Solubility of naproxen in ethyl acetate+ethanol mixtures at several temperatures and correlation with the Jouyban-Acree model, *Fluid Phase Equilib.*, **320**, 49-55 (2012).

21. I.P. Osorio, F. Martínez, D.R. Delgado, A. Jouyban, W.E. Acree Jr., Solubility of sulfacetamide in aqueous propylene glycol mixtures: Measurement, correlation, dissolution thermodynamics, preferential solvation and solute volumetric contribution at saturation, *J. Mol. Liq.*, **297**, 111889 (2020).

22. D.J.W. Grant, M. Mehdizadeh, A.H.L. Chow, J.E. Fairbrother, Non-linear van't Hoff solubility-temperature plots and their pharmaceutical interpretation, *Int. J. Pharm.*, **18**, 25-38 (1984).

23. G.A.M. Areiza-Aldana, A. Cuellar-Lozano, N.A. Peña-Carmona, D.I. Caviedes-Rubio, A. Mehrdad, A. Hossein-Miri, G.A. Rodríguez-Rodríguez, D.R. Delgado, Solution thermodynamics and preferential solvation of 3-chloro-*N*-phenylphthalimide in acetone + methanol mixtures, *Rev. Colomb. Cienc. Quím. Farm.*, **45**, 256-274 (2016).

24. D.R. Delgado, M.A. Peña, F. Martínez, A. Jouyban, W.E. Acree Jr., Further numerical analyses on the solubility of sulfapyridine in ethanol + water mixtures, *Pharm. Sci. (Tabriz)*, **22**, 143-152 (2016).

25. A.M. Romero-Nieto, N.E. Cerquera, D.R. Delgado, Measurement and correlation of solubility of ethylparaben in pure and binary solvents and thermodynamic properties of solution, *Rev. Colomb. Cienc. Quím. Farm.*, **48**, 332-347 (2019).

26. A.T. Williamson, The exact calculation of heats of solution from solubility data, *Trans. Faraday Soc.*, **40**, 421-436 (1944).

27. A. Apelblat, E. Manzurola, N.A. Balal, The solubilities of benzene polycarboxylic acids in water, *J. Chem. Thermodyn.*, **38**, 565-571 (2006).

28. A. Noubigh, M.H. Oueslati, Measurement and modeling of the solubility of vanillin constituent of olive mill wastewater in binary water + ethanol solvents mixtures between 278.15 K and 308.15 K, *Austr. J. Basic Appl. Sci.*, **8**, 396-403 (2014).

29. R. Heryanto, M. Hasan, E.C. Abdullah, A.C. Kumoro, Solubility of stearic acid in various organic solvents and its prediction using non-ideal solution models, *ScienceAsia*, **33**, 469-472 (2007).

30. J. Cuevas-Valenzuela, Á. González-Rojas, J. Wisniak, A. Apelblat, J.R. Pérez-Correa, Solubility of (+)-catechin in water and water-ethanol mixtures within the temperature range 277.6-331.2 K: Fundamental data to design polyphenol extraction processes, *Fluid Phase Equilib.*, **382**, 279-285 (2015).

31. A.M. Romero-Nieto, D.I. Caviedes-Rubio, J. Polania-Orozco, N.E. Cerquera, D.R. Delgado, Temperature and cosolvent composition effects in the solubility of methylparaben in acetonitrile + water mixtures, *Phys. Chem. Liq.*, Forthcoming 2020, doi: 10.1080/00319104.2019.1636379.

32. D.R. Delgado, A. Holguin, F. Martínez, Solution thermodynamics of triclosan and triclocarban in some volatile organic solvents, *Vitae, Rev. Fac. Quim. Farm.*, **19**, 79-92 (2012).

33. D.M. Jiménez, Z.J. Cárdenas, D.R. Delgado, A. Jouyban, F. Martínez, Solubility and solution thermodynamics of meloxicam in 1,4-dioxane and water mixtures, *Ind. Eng. Chem. Res.*, **53**, 16550-16558 (2014).

34. E.A. Ahumada, D.R. Delgado, F. Martínez, Solution thermodynamics of acetaminophen in some PEG 400 + water mixtures, *Fluid Phase Equilib.*, **332**, 120-127 (2012).

35. A. Ksiazczak, J.J. Kosinski, Vapour pressure of binary, three-phase (S-L-V) systems and solubility, *Fluid Phase Equilib.*, **44**, 211-236 (1988).

36. A. Ksiazczak, K. Moorthi, I. Nagata, Solid-solid transition and solubility of even n-alkanes, *Fluid Phase Equilib.*, **95**, 15-29 (1994).

37. S. Krajangsod, S. Chotikamas, A. Tawai, M. Sriariyanun, Measurement and thermodynamic modelling of erythritol solubility in aqueous solvents, *Oriental J. Chem.*, **34**, 265-275 (2018).

38. H. Buchowski, A. Ksiazczak, S. Pietrzyk, Solvent activity along a saturation line and solubility of hydrogen-bonding solids, *J. Phys. Chem.*, **84**, 975-979 (1980).

39. D.R. Delgado, M.A. Ruidiaz, S.M. Gómez, M. Gantiva, F. Martínez, Thermodynamic study of the solubility of sodium naproxen in some ethanol + water mixtures, *Quim. Nova*, **33**, 1923-1927 (2010).

40. A.R. Holguín, D.R. Delgado, F. Martínez, Thermodynamic study of the solubility of triclocarban in ethanol + propylene glycol mixtures, *Quim. Nova*, **35**, 280-285 (2012).

41. K.C. Mercado, G.A. Rodríguez, D.R. Delgado, F. Martínez, A. Romdhani, Solution thermodynamics of methocarbamol in some ethanol + water mixtures, *Quim. Nova*, **35**, 1967-1972 (2012).

42. J.H. Blanco-Márquez, Y.A. Quigua-Medina, J.D. García-Murillo, J.K. Castro-Camacho, C.P. Ortiz, N.E. Cerquera, D.R. Delgado, Thermodynamic analysis and applications of the Abraham solvation parameter model in the study of the solubility of some sulfonamides, *Rev. Colomb. Cienc. Quím. Farm.*, **49**, 234-255 (2020).

43. C. Holm, M. Zaman, Regulating audit quality: Restoring trust and legitimacy, *Account. Forum*, **36**, 51-61 (2012).

44. J. Tritschler, *Audit quality: Association between published reporting errors and audit firm characteristics*, (Ph. D. thesis, University of Innsbruck, 2013), Springer-Gabler, 2014.

45. M.A. Ruidiaz, D.R. Delgado, F. Martínez, Indomethacin solubility estimation in 1,4-dioxane + water mixtures by the extended Hildebrand solubility approach, *Quim. Nova*, **34**, 1569-1574 (2011).

46. D.R. Delgado, M.Á. Peña, F. Martínez, Extended Hildebrand solubility approach applied to sulphadiazine, sulphamerazine and sulphamethazine in some {1-propanol (1) + water (2)} mixtures at 298.15 K, *Phys. Chem. Liq.*, **57**, 388-400 (2019).

47. M. Ruidiaz, D.R. Delgado, F. Martínez, Correlating the solubility of indomethacin in 1,4-dioxane + water mixtures by means of the Jouyban-Acree model, *Rev. Colomb. Cienc. Quím. Farm.*, **39**, 211-226 (2010).

48. F. Almanza, A.R. Holguín, D.R. Delgado, F. Martínez, A. Jouyban, Solution thermodynamics of sodium diclofenac in ethanol + water mixtures and correlation with the Jouyban-Acree model, *Lat. Am. J. Pharm.*, **31**, 427-436 (2012).

How to cite this article

R.E. Cardenas, L.E. Tinoco, D.M. Galindres, A. Beltrán, C.D. Oviedo, J. Osorio, Prediction of sulfadiazine solubility in some cosolvent mixtures using non-ideal solution models, *Rev. Colomb. Cienc. Quím. Farm.*, **49**(3), 822-842 (2020).

Rev. Colomb. Cienc. Quím. Farm., Vol. 49, números 1 a 3, 2020.

Índice general por tipo de artículos

Artículos de investigación científica

Artículos de investigación tecnológica

Artículos de investigación clínica

Artículos de revisión

ÍNDICE GENERAL DE AUTORES

ÍNDICE ANALÍTICO DE TÉRMINOS

Español

Inglés

Portugués

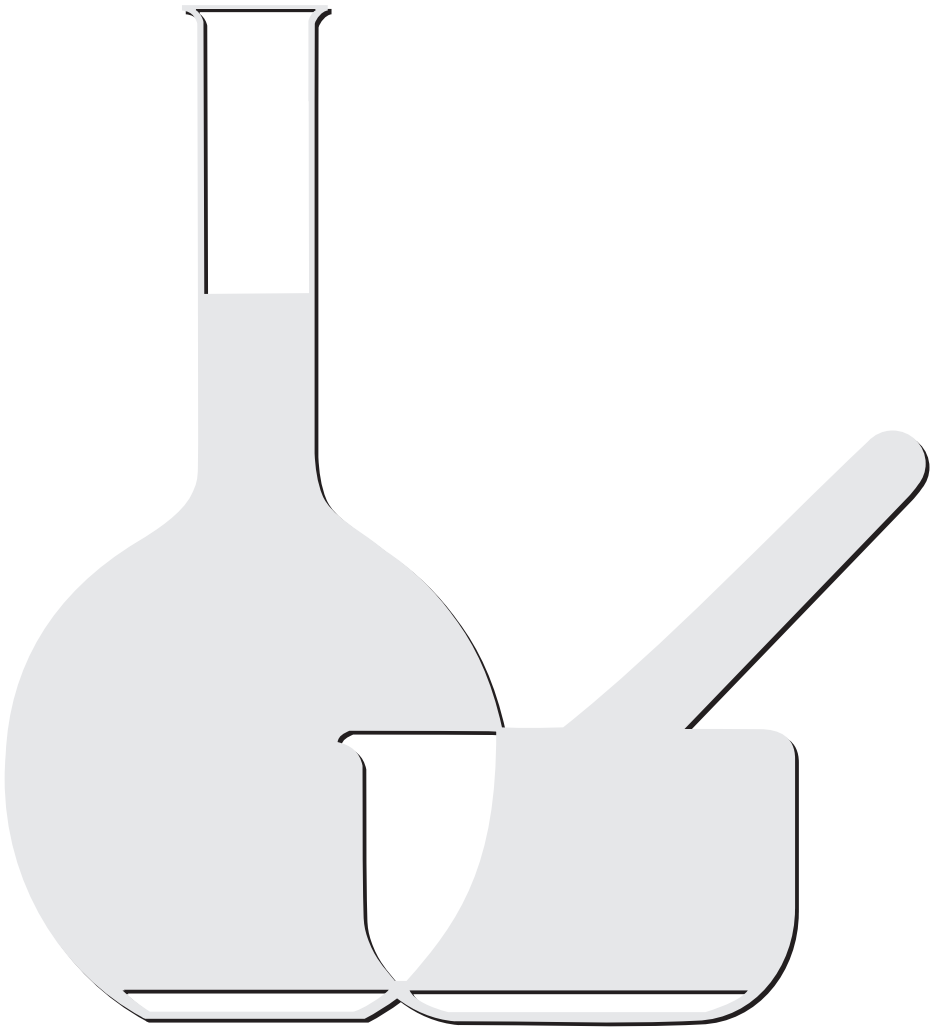

NORMAS PARA PUBLICACIÓN

La Revista Colombiana de Ciencias Químico Farmacéuticas es editada por el Departamento de Farmacia de la Universidad Nacional de Colombia (Sede Bogotá), con una periodicidad cuatrimestral y tiene como objetivo publicar artículos originales de diversos tópicos relacionados con las ciencias farmacéuticas como recursos naturales, atención farmacéutica, evaluación clínica y preclínica, y los relacionados con la industria farmacéutica, la salud y los medicamentos.

Además de artículos completos, la revista acepta revisiones, comunicaciones breves y cartas al Editor. Las contribuciones pueden enviarse en español, portugués o inglés, en letra Times New Roman, tamaño 12, al correo electrónico rccquifa_fcbog@.unal.edu.co o a través del sistema OJS en el sitio web: https://revistas.unal.edu.co/index.php/rccquifa.

Todo el material propuesto para publicación será revisado por el Comité Editorial, y luego de su aceptación para evaluación, será sometido a revisión por pares académicos. Las evaluaciones recibidas por el Comité Editorial serán remitidas al autor para que se realicen los ajustes sugeridos. Los autores tendrán un lapso de tres semanas para responder cada una de las observaciones, introducir en el texto las modificaciones del caso y retornar el documento corregido al Comité Editorial. Después de que los evaluadores o el Comité Editorial lleven a cabo una segunda revisión del manuscrito, la revista comunicará a los autores la decisión sobre la publicación o no del mismo. Los manuscritos deberán acompañarse de una carta firmada por todos los autores en la cual se declare que el trabajo es inédito; es decir, que el artículo ni parte de este ha sido publicado o está en vía de publicación en otra revista, y en la que se responsabilizan por la información publicada. Se entiende claramente que los trabajos enviados no están siendo considerados para su publicación en otros medios.

Criterios para la presentación de manuscritos

- La fuente de los manuscritos debe ser Times New Roman tamaño 12.
- No se admiten notas a pie de página.
- Título, centrado y en minúscula.
- Autor(es) con su respectiva filiación institucional y correo electrónico del autor principal.
- Resumen, *Summary* o Resumo. Incluye la justificación del estudio y los principales hallazgos y conclusiones, debe tener entre 50 y 200 palabras. Se debe incluir el título del artículo y el resumen en inglés (*Summary*) independiente del idioma del manuscrito.
- *Key words* (debajo de *Summary*) y Palabras clave (debajo del Resumen) o Palavras chave (debajo de Resumo). De tres a seis palabras en minúscula, excepto la primera, y separadas por coma y espacio. Preferiblemente tomadas del Index

Medicus (http://www.nlm.nih.gov/mesh/meshhome.htm).

- En los manuscritos en español y portugués se empleará la coma (,) como separador decimal, en inglés se utilizará el punto (.).

- Los artículos se dividirán en las siguientes secciones: Introducción, Metodología, Resultados y Discusión, Conclusiones (si las hay), Agradecimientos, Conflicto de intereses y Referencias. Los títulos deben estar separados por dos espacios en sus partes superior e inferior, centrados y en negrilla. Los detalles acerca de la metodología experimental utilizada deberán ser lo suficientemente claros como para repetir la experimentación.

- Las tablas deben llevar numeración arábiga de acuerdo con el orden de aparición en el texto. El título debe ir en su parte superior y las notas en la parte inferior. En los encabezamientos de las columnas se deben anotar los símbolos de las unidades utilizadas.

- Las fotografías, gráficas, dibujos y esquemas se denominan 'figuras' y deben llevar numeración arábiga de acuerdo con el orden de aparición en el texto. El título debe ir debajo de las figuras.

De otro lado, los artículos relacionados con experimentación con animales deben ajustarse plenamente a los lineamientos éticos trazados por la Organización Mundial de la Salud. Los extractos o fracciones evaluados *in vitro* o *in vivo* deben definirse químicamente, cuando menos en cuanto a la clase de constituyente. El material vegetal deberá estar clasificado botánicamente.

Las abreviaturas de pesos y medidas serán las indicadas por la Farmacopea de los Estados Unidos en su edición oficial o unidades SI. Los datos espectroscópicos se deben presentar de la siguiente manera:

UV λ max (solvente ε) nm (log ε). Ej.: UV λ max (MeOH) 275 (log ε 2,94).

IR ν max (medio) cm^{-1}. Ej.: IR ν max (KBr) 1740, 1720 cm^{-1}.

EM *m/z* (% intensidad relativa). Ej.: em *m/z* (%): 340 (M^+, 100), 295 (10), 134 (26) ...

RMN ^1H (solvente, frecuencia de registro) δ ppm (integración, multiplicidad, J en Hz, asignación). Ej.: RMN ^1H ($CDCl_3$, 400 MHz) 3,84 (1H, *d*, J = 10,3 Hz, H-30).

RMN ^{13}C (solvente, frecuencia de registro) δ ppm (multiplicidad, asignación). Ej.: RMN ^{13}C ($CDCl_3$, 600 MHz) 16,60 (t, C-12).

Las abreviaturas usadas para describir la multiplicidad de las señales en RMN son: *s* = singlete, *d* = doblete, *t* = triplete, *m* = multiplete, *dd* = doble de dobletes, *ddd* = doble de doble de dobletes.

Las abreviaturas para los solventes y reactivos más comúnmente usados son: EtOH= etanol, MeOH = metanol, $CHCl_3$ = cloroformo, C_6H_6 = benceno, AcOEt = acetato de etilo, EP = éter de petróleo, Me_2CO = acetona, DMSO = dimetilsulfóxido, AcOH = ácido acético.

Se evitará el uso excesivo de tablas y figuras que estarán numeradas y que se anexarán en hojas separadas con su respectiva descripción

Referencias de los manuscritos

Las referencias se citarán en el texto con su respectiva numeración. Solo se pueden citar tesis y libros o artículos que hayan sido publicados. Deben incluir: autor(es), título de la publicación, año, volumen y páginas, así:

Revistas: Iniciales del nombre y apellido completo de todos los autores, título completo del artículo, nombre abreviado o nombre completo de la revista dependiendo si aparece en el Chemical Abstract o en índices equivalentes. El nombre de la *revista debe ir en letra itálica*, **volumen en negrilla**, páginas inicial y final, y año entre paréntesis. Ej.:

1. H.P. Baden, L.A. Goldsmith, B. Fleming, A comparative study of the physicochemical properties of human keratinized tissues, *Bioch. Biophys. Acta*, **322**, 269-278 (1973).

Comunicaciones personales: Iniciales del nombre, apellido completo e institución, seguido por las palabras comunicación personal y el año. Ej.:

2. A.J.M. Leeuwenberg, Agricultural University, Wageningen, Holanda, comunicación personal, 1984.

Libros: Iniciales del nombre y apellido completo de los autores, título del libro entre comillas, editorial, ciudad, año, volumen y página. Ej.:

3. D.R. Morris, "The Biochemistry of Disease", Morris et Marton Eds., London, 1981, Vol. 8, p. 223.

Capítulos de libros escritos por varios autores: Iniciales del nombre y apellido completo del autor, título del capítulo, seguido de: En: título del libro entre comillas, editores, editorial, ciudad, año, volumen, páginas. Ej.:

4. A.D. Elbein, R.J. Molyneux, The chemistry and biochemistry of simple indolizidine and related polyhydroxy alkaloids. En: "Alkaloids: Chemical and Biological Perspectives", Ed. por S.W. Pelletier, Wiley, New York, 1987, Vol. 5, pp. 1-54.

Tesis: Iniciales del nombre y apellido completo de los autores, *título en cursiva*, Tesis de..., institución, ciudad, año, páginas. Ej.:

5. F. Salcedo, *Contribución al estudio de las Cinchonas colombianas*, Tesis de Grado, Universidad del Valle, Cali, 1983, pp. 14-16.

Referencias de Internet: Iniciales del nombre y apellido completo del autor, título del documento, dirección URL y fecha de revisión. Ej.:

6. Lipidat, Lipid thermotropic phase transition database, Ohio State University, URL: http://www.lipidat.chemistry.ohio-state.edu, consultado en septiembre de 2001.

La correspondencia puede enviarse a la siguiente dirección o al correo de la revista *rcciquifa_fcbog@unal.edu.co*

Comité Editorial

Revista Colombiana de Ciencias Químico-Farmacéuticas
Departamento de Farmacia
Facultad de Ciencias
Universidad Nacional de Colombia

Cra. 30 N.° 45-03
Fax: 57-1-3165060

Bogotá - Colombia
Correo electrónico:
rcciquifa_fcbog@unal.edu.co

Dirección WEB:
http://www.revistas.unal.edu.co/index.php/rccquifa

Revista Colombiana
de Ciencias Químico-Farmacéuticas, 49(3)
se terminó de editar, imprimir y encuadernar
en Proceditor, sobre papel bond de 90 gramos
Bogotá, D. C., Colombia.